Functional analysis of molecular mechanisms regulating vesicle trafficking pathways in *Arabidopsis thaliana*

Dissertation

der Mathematisch-Naturwissenschaftlichen Fakultät

der Eberhard Karls Universität Tübingen

zur Erlangung des Grades eines

Doktors der Naturwissenschaften

(Dr. rer. nat.)

vorgelegt von

Sabine Brumm

aus Adenau

Tübingen

2019

Gedruckt mit Genehmigung der Mathematisch-Naturwissenschaftlichen Fakultät der Eberhard Karls Universität Tübingen.

Tag der mündlichen Qualifikation:	24.05.2019
Dekan:	Prof. Dr. Wolfgang Rosenstiel
1. Berichterstatter:	Prof. Dr. Gerd Jürgens
2. Berichterstatter:	Prof. Dr. Klaus Harter
3. Berichterstatter:	Prof. Dr. Christian Hardtke

Danksagung

Die vorliegende Dissertation wurde am Lehrstuhl für Entwicklungsgenetik am Zentrum für Molekularbiologie der Pflanzen (ZMBP) unter der Leitung von Prof. Dr. Gerd Jürgens angefertigt.

Ich danke meinem Betreuer Prof. Dr. Gerd Jürgens und meinem Zweitgutachter Prof. Dr. Klaus Harter für das Lesen und die Korrektur dieser Arbeit. Des Weiteren danke ich Prof. Dr. Gerd Jürgens, Prof. Dr. Klaus Harter, Prof. Dr. Christopher Grefen und Dr. Sandra Richter für die Bereitschaft mein Thesis Advisory Committee (TAC) zu bilden und die Teilnahme an den begleitenden TAC Meetings. Prof. Dr. Claudia Oeking danke ich für die Teilnahme an meinem Prüfungsausschuss.

Ein großes Dankeschön geht an die Reinhold-und-Maria Teufel Stiftung in Tuttlingen, deren finanzielle Unterstützung mir die Teilnahme an vielen großartigen molekularbiologischen/pflanzenwissenschaftlichen Konferenzen ermöglicht hat.

Außerdem möchte ich mich bei Gerd sehr herzlich für jegliche Unterstützung in all den Jahren bedanken. Er ermöglichte mir nicht nur die Arbeit an spannenden Projekten sondern gab mir auch die Freiheit eigene Ideen zu entwickeln, mein Projekt auf diversen Konferenzen vorzustellen und ermutigte mich meine akademischen Karriere weiter zu verfolgen.

Neben Gerd möchte ich Sandra ein riesiges und herzliches Dankeschön aussprechen. Nicht nur für die Korrektur der Arbeit, das Durchgehen und Verbessern meiner Vorträge und aller endlos Schichten am Mikroskop: Ohne dich wäre vieles nicht möglich gewesen! Danke, dass du mich immer sowohl im Labor als auch privat unterstützt und mir geholfen hast mich weiter zu entwickeln.

Dieses Dankeschön möchte ich auch Marika aussprechen. Du hast immer ein offenes Ohr für mich gehabt und mich unterstützt wo es nur ging. Generell sind mir Sandra, Marika und Kerstin (meine Happy-Gnomicorn-Buddhis) immer zur Hilfe geeilt und haben für jede Menge Spaß und schöne Zeiten gesorgt. Gaaaaaaanz lieben Dank für so Vieles ihr Lieben! Dabei auch gleich ein Hoch auf die gesamte Blutgruppe Sekt, ohne die das Laborleben soviel weniger lustig und motivierend gewesen wäre!

Ich möchte mich darüber hinaus bei dem festen Kern der GNOM Gruppe (Sandra, Marika, Kerstin, Hauke und Manoj) und York für all die interessanten wissenschaftlichen Diskussionen, Anregungen zu meinen Projekten und Beiträge zu beiden Manuskripten bedanken. Das ARF-Dimer/Loop>J Projekt wäre ohne unseren ehemaligen und stets lustigen, dänischen PostDoc Mads niemals möglich gewesen: lieben Dank für deine tolle Vorarbeit. Vielen Dank auch an Uli und Misoon, die mir immer mit Rat (und Tat) zur Seite standen.

Es sollen auch all die Hiwis und Studenten nicht unerwähnt bleiben, die mir das Leben in den letzten Jahren um so vieles erleichtert haben und entscheidend zum Gelingen dieser Arbeit beigetragen haben: lieben Dank Angela, Tobi, Conner, Adrian, Eli und Mara! (falls ich jemanden vergesse habe, auch an den/diejenigen)

Der gesamten Entgen und allen ehemaligen Doktoranden danke ich für tolle 6 Jahre am Institut und viele “Happy Hours”, nicht nur nach dem Laboralltag. Ein großes Dankeschön auch an Brigitte, die, wie ein fleißiges Heinzelmännchen, ganz früh morgens das Labor für den Alltag bereitmacht.

Last but not least möchte ich meine Familie erwähnen, die mich schon immer auf meinen Wegen unterstützt und an mich glaubt hat. Danke Mama, Papa und Basti, ihr seid die Besten!

Table of contents

1. Summary

The spatiotemporal regulated distribution of proteins within cells is an essential process of eukaryotic organisms. Protein transport between different cellular compartments is enabled by the exchange of membranes via vesicle trafficking, maturation or compartment fusion. Major regulators are small GTPases, their guanine-nucleotide exchange factors (GEFs) and effectors.

Here, we identify the ARF-GEFs BIG1-4 as main post-Golgi vesicle trafficking regulators mediating late secretory and vacuolar transport in plants. In contrast, recycling relies only on GNOM function. During cytokinesis, recycling is counteracted by BIG1-4 mediated trafficking to the cell plate. Interestingly, PIN1 can be transported to the cell plate and be recycled at the same time which might ensure proper auxin flux during developmental processes with high cell proliferation rates.

In animals, maturation of early to late endosomes requires the conversion of RAB GTPases. Plant vacuolar trafficking also relies on late endosome maturation from the TGN. In this study we demonstrate the conserved role of the RAB-GEF subunit SAND/MON1 in RAB5 to RAB7-like GTPase conversion during vacuolar trafficking in Arabidopsis. However, RAB conversion in plants is rather required for fusion of late endosomes with the vacuole than for early to late endosome maturation.

Main regulators of vesicle budding are ARF GTPases and ARF-GEFs. It was not clear why ARF-GEF form dimers *in vivo*. Our analysis suggests that ARF-GEFs mediate ARF1 GTPase dimerization by cooperative binding of two ARF1•GDP molecules to a functional ARF-GEF dimer. ARF GTPase dimerization plays an important role in vesicle formation and may be a conserved feature across the eucaryotes.

The two ARF-GEF paralogues GNOM and GNL1 share high sequence similarity but are functionally diverged. Here we show the dual function of the GNOM DCB domain in promoting GNOM homodimerization but preventing heterodimerization with GNL1 at the same time. The separation of the two proteins may ensure proper secretory trafficking as well as efficient PIN1 recycling at developmental stages with high demands of protein transport.

1.1. Zusammenfassung

Die zeitlich und räumlich geordnete Verteilung von Proteinen ist ein essentieller Prozess eukaryotischer Zellen. Proteine werden entweder durch Vesikeltransport, Reifung oder Fusion von Membranen zwischen verschiedenen Zellkompartimenten ausgetauscht. Hauptregulatoren der Membranen-Transportprozesse sind kleine GTPasen, ihre Austauschfaktoren (GEFs) und Effektoren.

Die ARF-GEFs BIG1-4 werden in dieser Arbeit als Hauptregulatoren des post-Golgi sekretorischen und vakuolären Vesikeltransportweges in Pflanzen identifiziert. Das post-Golgi Proteinrecycling ist im Gegensatz dazu nur von der Funktion GNOMs abhängig. Während der Zytokinese wir das Recycling durch den von BIG1-4 vermittelten Proteintransport ersetzt. Interessanterweise kann der Auxin Efflux Transporter PIN1 gleichzeitig recycelt und zur Zellplatte transportiert werden. Dies stellt vermutlich die korrekte Verteilung des Hormons Auxin während biologischen Prozessen mit hohen Zellteilungsraten sicher.

In tierischen Zellen wird die Endosomenreifung über den Austausch verschiedener RAB-GTPasen an der Membran reguliert. Pflanzliche, vakuoläre Transportprozesse basieren ebenfalls auf Endosomenreifung. In dieser Studie analysieren wir die konservierte Funktion der RAB-GEF Untereinheit SAND/MON1 im Austausch von RAB5 zu RAB7-ähnlichen GTPasen während des vakuolären Transports in Arabidopsis. Der RAB GTPasen Austausch wird in Pflanzen jedoch eher für die Fusion später Endosomen mit der Vakuole als für Endosomenreifung benötigt.

ARF GTPasen und ARF-GEFs sind die Hautregulatoren der Vesikelknospung. Es war lange Zeit nicht bekannt warum ARF-GEFs *in vivo* dimerisieren. Unsere Daten legen nahe, dass ARF-GEFs die Dimerisierung der GTPase ARF1 durch die Bindung zweier ARF1•GDP Moleküle an ein funktionales ARF-GEF Dimer vermitteln. Die ARF Dimerisierung spielt eine wichtige Rolle für die Vesikelbildung und scheint eine konservierte Eigenschaft der Eukaryoten sein.

Die Proteinsequenzen der zwei ARF-GEF Paraloge GNOM und GNL1 sind sehr ähnlich, aber die Proteinfunktionen unterscheiden sich. Wir zeigen hier, dass die GNOM DCB-Domäne zwei Funktionen erfüllt: zum einen vermittelt sie die Homodimerisierung GNOMs, verhindert aber zum anderen die Heterodimerisirung mit GNL1. Das funktionale Auseinanderhalten der zwei Proteine stellt möglicherweise sowohl die geregelte Sekretion als auch effizientes PIN1 Recycling während Entwicklungsstadien mit erhöhtem Proteintransport sicher.

2. Introduction

2.1. Vesicle trafficking in plant cells

A fundamental, well conserved biological process is the temporal and spatial distribution of proteins within a cell. Protein delivery is accomplished by membrane exchanges between different compartments of the endomembrane system and the plasma membrane. Cellular compartments are confined reaction chambers with diverse functions in protein biogenesis, modification and sorting. Different modes are known for trading materials between the endomembrane system and the plasma membrane. The most prevailing way is the budding of vesicles from a donor compartment which traffic along the cytoskeleton and finally fuse with an acceptor compartment. However, compartments can also mature from one into another and thereby switch their identity or just fuse with each other (Niemes et al., 2010; Scheuring et al., 2011). Furthermore, the fusion of several vesicles with each other can lead to the formation of a new compartment (Jürgens, 2004). Despite remarkable scientific progress concerning the characterisation of the different endomembrane compartments and their connecting trafficking pathways over the years, the molecular regulation of these processes in detail is still being under investigation.

2.2. Trafficking pathways

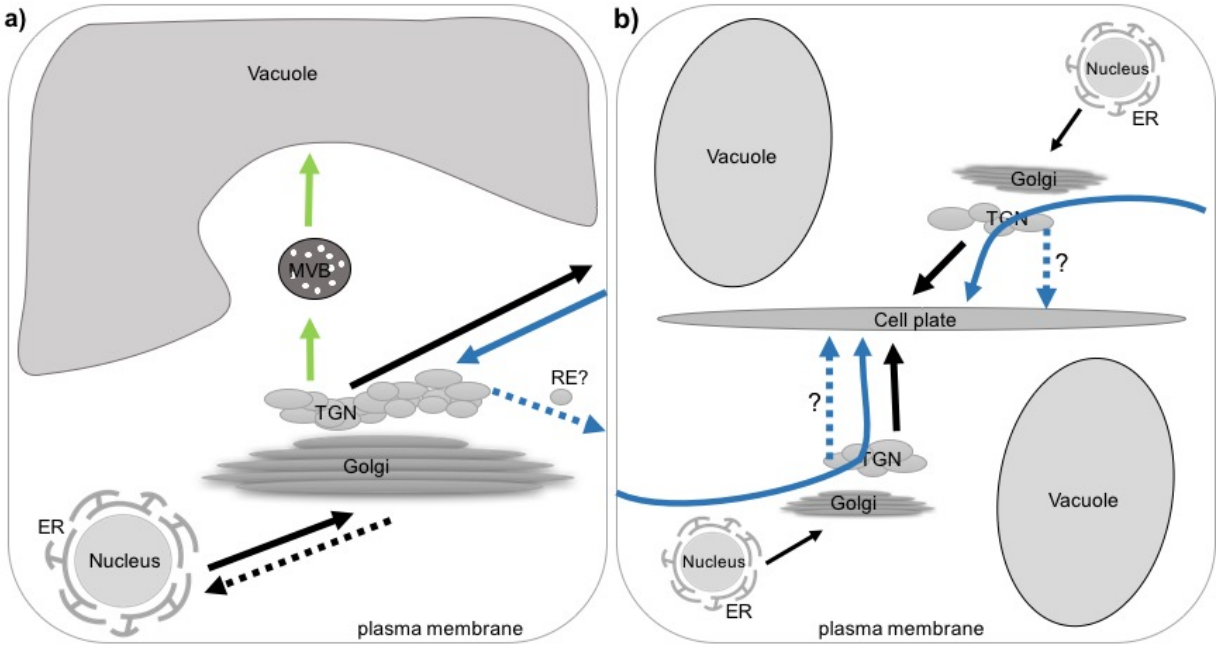

Figure 1. Simplified scheme of vesicle trafficking pathways in an interphase (a) and mitotic plant cell (b)

(a) Scheme of an interphase cell including the plant endomembrane system and the vesicle trafficking pathways between different compartments in an interphase cell. Newly synthetized proteins with ER uptake signals are transported from the ER via the Golgi and trans-Golgi network (TGN) to the plasma membrane on the secretory route (black arrow). Membrane material and proteins with an ER retrieval signal are transported back on the retrograde Golgi-ER trafficking pathway (dashed black arrow). From the TGN, vacuolar cargo and proteins destined for degradation reach the vacuole via multivesicular bodies (MVBs) (green arrows). The TGN serves as an early endosome in plants since also endocytosed proteins from the plasma membrane (PM) first reach the TGN (blue arrow) before they are either recycled back to the PM (dashed blue arrow) or degraded in the vacuole. (b) Scheme of a cell during cytokinesis. The cell plate of dividing cells receives endocytosed and newly synthetized material provided by the two descendants. It is not clear whether protein recycling and trafficking to the cell plate can occur simultaneously during cytokinesis or if all recycled proteins are transported to the cell plate by default.

2.2.1. Secretory route

The tightly controlled distribution of e.g. transporters, receptors and integral membrane proteins is not only crucial for preserving the functional organization of cells but also key to the development of whole organisms. In eukaryotes, the translation of proteins takes place at ribosomes attached to the endoplasmic reticulum (ER) which is the entry point for subsequent transport within the endomembrane system (Jürgens, 2004). On the secretory route proteins are loaded into COPII-coated vesicles which fuse with the *cis*-side site of the Golgi apparatus and subsequently proteins are processed in the different Golgi cisternae. Proteins with an ER retrieval signal are transported back from the Golgi to the ER in COP1-coated vesicles on the retrograde route (Nilsson and Warren, 1994) (Figure 1a; dashed, black arrow). After modification in the Golgi, proteins without a retention signal reach by maturation steps the main sorting hub of a plant cell: the trans-Golgi network (TGN). The default pathway for proteins lacking any internal signal peptide leads from the TGN via clathrin-coated vesicles to the plasma membrane (PM), where the soluble cargo (carrier content) is released into the apoplast (Figure 1a; black arrows). In contrast to animals, the plant TGN is a distinct compartment on the secretory route but also serves as early endosome (EE) for endocytosed material originating from the plasma membrane and as source for material destined for degradation in the vacuole (Dettmer et al., 2006) (Figure 1a; black, green and blue arrows). Therefore, the TGN can be seen as the main sorting hub in a plant cell. Up to date, the detailed analysis of newly synthetized and recycled or endocytosed cargo is obviously difficult because of the intersection of the different trafficking pathways at the TGN (Robinson et al., 2008; Viotti et al., 2010).

2.2.2. Endocytosis and Recycling

Plasma membrane-resident proteins and extracellular matrix material become mainly internalized via clathrin-coated vesicles (Chen et al., 2011). In contrast to animals, the regulation and composition of the endocytic machinery in plants is still not well

understood. The loss of lipids and proteins at the PM via endocytic uptake is compensated by the delivery of material from the TGN back to the PM, known as endocytic recycling (Figure 1a; dashed, blue arrow). The balance of the two pathways is of high importance as the composition of the PM needs to be tightly regulated for several cellular processes. Therefore, it is not surprising that the abundance and distribution of several receptors and transports is under the strict control of endocytic and/or recycling pathways. Famous examples are the auxin efflux carriers PIN-FORMED (PINs) (Geldner et al., 2003), the leucine-rich repeat-receptor like kinases (LRR-RLKs) flagellin sensing 2 (FLS2) (Robatzek et al., 2006) and brassinosteroid insensitive 1 (BRI1) (Russinova et al., 2004) and the boron transporter (BOR1) (Takano et al., 2010).

Rather than a single, specific signal, complex molecular networks including environmental cues, hormonal responses, receptor-ligand interactions and post-translational modifications seem to initiate the endocytosis of proteins (Fan et al., 2015). It is still not clear whether plants, like animals, have recycling endosomes (RE) like animals (van Ijzendoorn, 2006). Small GTPase members of the RAS-related in brains (RAB) family, RAB4 and RAB11, are known markers for REs in mammals (Rodman and Wandinger-Ness, 2000). Small GTPases in general are molecular switches that play an important role in the regulation of various cellular processes. In plants, the adenosine ribosylation factor guanine nucleotide exchange factor (ARF-GEF) GNOM localizes to a subpopulation of endosomes (Geldner et al., 2009) that could resemble REs but the existence and definition of distinct REs in plants is still under debate (Robinson et al., 2008; Valencia et al., 2016).

2.2.3. Vacuolar trafficking

Plants possess two functional distinct types of vacuoles: storage and lytic vacuoles (Pereira et al., 2014). Endocytosed or newly synthetized, soluble proteins destined for vacuolar degradation generally carry a short peptide motif which is recognised by vacuolar sorting receptors (VSRs). Based on data from animal and yeast field, it is believed that VSRs bind their cargo at the TGN. Upon a change of pH they release the cargo into multivesicular bodies (MVBs) which will eventually fuse with the vacuole but little direct evidences are given for that model in plants (Figure 1a; green arrows) (Robinson and Pimpl, 2014). In contrast, the degradation of membrane-associated proteins is initiated upon ubiquitination. On the way to the vacuole, ubiquitinated and

soluble cargos are sorted into MVBs with the help of the Endosomal Sorting Complexes Required for Transport (ESCRT) (MacDonald et al., 2012). MVBs resemble the late endosome (LE) of animal cells and enable the degradation of transmembrane proteins by formation of intraluminal vesicles via endosomal invagination (Reyes et al., 2011). In animals, early endosomes mature into late endosomes. The change of membrane identity involves the activation and inactivation of small GTPases of the RAB family (Rink et al., 2005). The RAB-GEF RABex-5 binds to ubiquitinated proteins at the EE (Mattera and Bonifacino, 2008; Huotari and Helenius, 2011) where it, together with Rabadaptin-5, activates RAB5 (Horiuchi et al., 1997; Huotari and Helenius, 2011). As Rabadaptin is an effector of RAB5•GTP, RAB5 recruits itself to the EE membrane via a positive feedback loop (Lippe et al., 2001). During maturation, RAB5•GTP also recruits RAB7 GTPases to the EE membrane. Subsequently, RAB7 activation by the RAB-GEF complex MON1/SAND + CCZ1 inactivates RAB5•GTP (Kinchen and Ravichandran, 2010; Nordmann et al., 2010; Poteryaev et al., 2010) in such a way that finally solely RAB7 marks the late endosome (Rink et al., 2005; Huotari and Helenius, 2011). Recent evidences suggest that in planta MVBs/LEs mature from the TGN but it is not clear whether the same regulatory molecular mechanism of RAB5 to RAB7 conversion applies here as well because RAB5 and other EE markers do mostly not localize to the plant TGN/EE (Vermeer et al., 2006; Stierhof and El Kasmi, 2010; Scheuring et al., 2011).

2.3. Vesicle trafficking during cytokinesis

Cytokinesis is the final process of cell division where the cytoplasm of two daughter cells is physically separated by the formation of a new plasma membrane stretch (Jürgens, 2005). The necessary membrane material is provided by a massive flow of AP1-coated vesicles from the TGN to the centre of the cell division plane (Figure 1b; black and blue arrows) (Reichardt et al., 2007; Park et al., 2013; Teh et al., 2013). A plant-specific array of microtubules, the so called phragmoplast, facilitates the formation of a transient endomembrane compartment, known as the cell plate, by conducting the arrival and homotypic fusion of vesicles across the division plane (Jürgens, 2005). After centrifugal expansion and fusion of the cell plate's margin with the parental plasma membranes, the cell plate will finally give rise to a new plasma membrane shared by the two descendants. If also recycling of plasma resident-proteins contributes to the formation of cell plates and which exact components of the

trafficking machinery are involved in the delivery process still needs to be determined (Figure 1b; dashed, blue arrow).

Homotypic fusion of arriving vesicles during cytokinesis requires activity of newly synthetized syntaxins (Reichardt et al., 2011). Syntaxins belong to the family of soluble N-ethylmaleimide-sensitive factor (NSF) attachment protein (SNAP) receptor (SNARE) proteins which are tail-anchored membrane proteins mediating membrane fusions (Jürgens, 2005). It was quite early discovered that the syntaxin KNOLLE (SYP111) plays an important role in vesicle fusion during cell division in Arabidopsis. In *knolle* mutants unfused vesicles accumulate at the cell division plane (Lukowitz et al., 1996; Lauber et al., 1997b). KNOLLE localizes mainly to the Golgi stacks and the cell plate during cytokinesis since its RNA transcription and protein turnover is highly regulated in a cell cycle-dependent manner and the protein is only expressed during M phase (Jürgens, 2005). Although cytokinesis is strongly impaired in *knolle*, embryonic cells are still able to divide and give rise to abnormally shaped seedlings eventually dying after a varying time (Lukowitz et al., 1996). This hints towards another syntaxin being involved in cytokinesis. Another member of the SYP1 family, PEN1 (SYP121) was shown to localize to the cell plate but also continually cycle between the PM and endosomes in interphase (Reichardt et al., 2011). Beside the cell plate localization, PEN1 seems not to play a major role in the regulation of cytokinesis. *pen1* (Collins et al., 2003) exhibits no cytokinesis-defective phenotype and the protein itself is not able to rescue *knolle* (Müller et al., 2003; Reichardt et al., 2011). PEN1 function seems rather specific for plant innate immunity (Collins et al., 2003; Kwon et al., 2008). Just recently, by double mutant analysis, SYP132, a mainly plasma membrane-localized SYP1 family member, was identified as KNOLLEs functionally overlapping SNARE counterpart in cytokinesis (Park et al., 2018).

2.4. Molecular regulators of vesicle budding and fusion

Vesicle trafficking is at several levels highly regulated in eukaryotic cells since protein mislocalization, abnormally low or high abundance or ill-timed distribution can cause fatal consequences for cellular processes. Already the formation of vesicles at a donor compartment is tightly controlled by the action of molecular switches and their up- and downstream interactors. Essential regulators of vesicle budding are small GTPases of the ADP-ribosylation factor (ARF) ARF/SAR1 family. Inactive, GDP-bound ARF (ARF•GDP) becomes recruited to a donor membrane (Figure 2). There the exchange

of GDP to GTP leads to a conformational change of the protein resulting in the insertion of a N-terminal myristoylated amphipathic helix into the membrane (Antonny et al., 1997; Goldberg, 1998). The exchange reaction is catalysed by the interaction of the ARF GTPase with an ARF-GEF whereby bound GDP dissociates and free GTP associates with the GTPase (Figure 2) (Anders and Jürgens, 2008). A conserved region in the catalytic SEC7 domain of ARF-GEFs encodes a so called glutamate finger which facilitates the GDP displacement (Beraud-Dufour et al., 1999; Anders and Jürgens, 2008). The reaction can be blocked by a fungal toxin, called Brefeldin A (BFA), which binds into a pocket between ARF•GDP and ARF-GEF and locks the inactive complex at the membrane (Mossessova et al., 2003; Renault et al., 2003). BFA treatment leads, via aggregation of endosomes and TGNs, to the formation of so called BFA compartments which are surrounded by Golgi stacks in *Arabidopsis thaliana* (Satiat-Jeunemaitre and Hawes, 1992; Satiat-Jeunemaitre et al., 1996; Geldner et al., 2001; Geldner et al., 2004; Teh and Moore, 2007). After successful GTPase activation, the membrane- associated ARF (ARF•GTP) recruits coat proteins to the membrane, subsequently causing membrane curvature and budding of a vesicle (Figure 2). Before fusion with an acceptor compartment, vesicles have to become uncoated to enable their tethering, which was long thought to be induced by ARF dissociation from the membrane (Trahey and Hay, 2010). The dissociation of ARF•GTP from the membrane is triggered by ADP-ribosylation factor GTPase-activating proteins (ARF-GAPs) (Figure 2). As ARF GTPases have a very low GTPase activity themselves (Kahn and Gilman, 1986), ARF-GAPs induce the hydrolysis of the bound GTP by stimulating ARF GTPase activity (Spang et al., 2010). The old model, of GTP hydrolysis triggering coat proteins to fall off the membrane directly after vesicle budding, gets challenged by recent data from animal and yeast systems (Trahey and Hay 2010). The data suggests that the vesicle coat is retained during travel through the cytosol and it may participate in the initiation of tethering. The tethering process includes the first contact between a vesicle and an acceptor membrane often established by the interaction of RAB GTPases with (multi-subunit) tethering complexes (Vukasinovic and Zarsky, 2016) (Figure 2). Once the vesicle is brought into close proximity to its acceptor compartment, SNARE proteins form complexes that mediate membrane fusion (Figure 2).

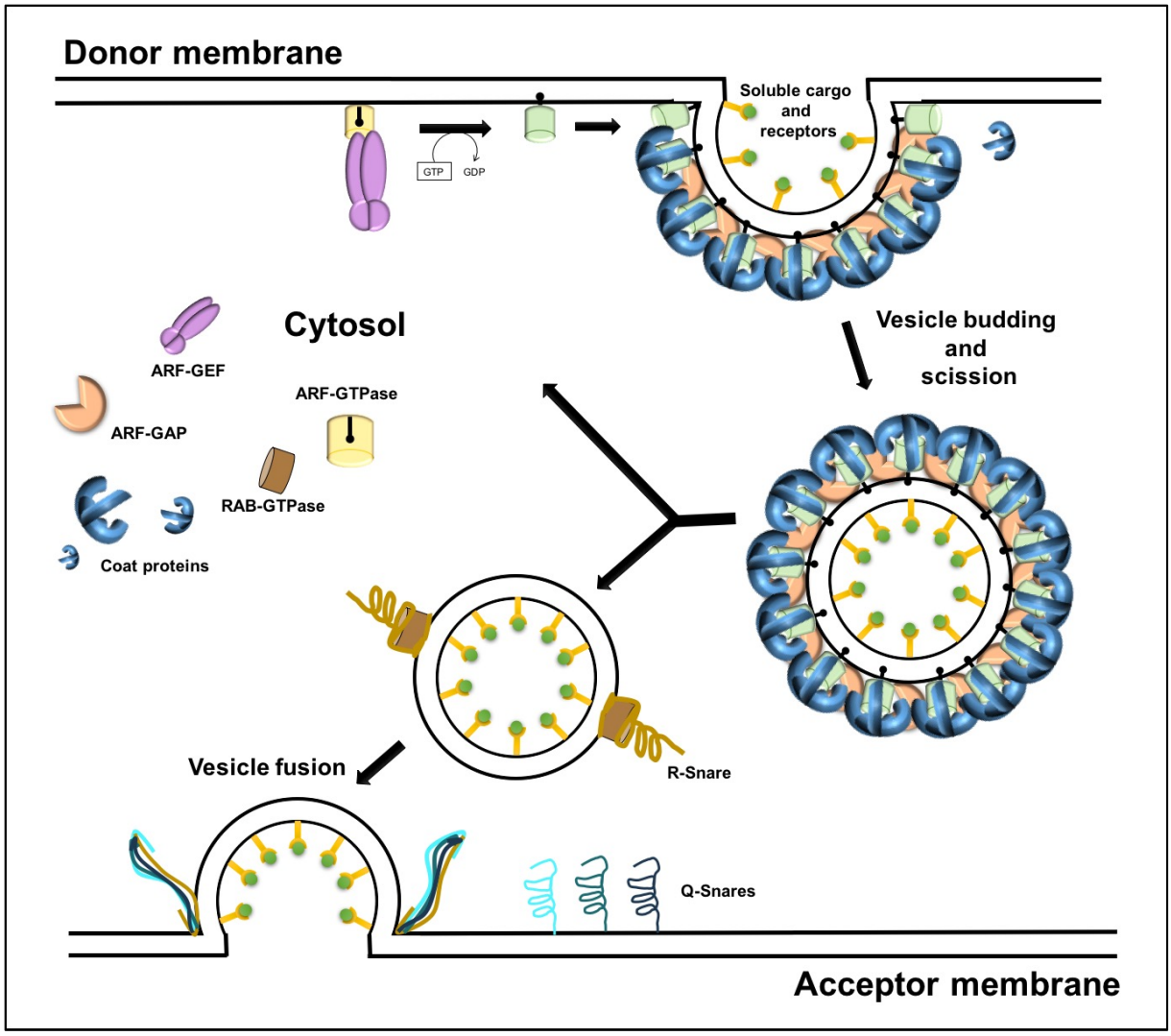

Figure 2. Simplified scheme of vesicle trafficking processes and major molecular regulators (modified according to Singh and Jürgens, 2018)

At a donor compartment vesicle formation is initiated by the recruitment of ARF-GEFs and ARF GTPases to the membrane. ARF-GEFs catalyse the exchange reaction of GDP to GTP on ARF-GTPase. The active ARF GTPase is inserted into the membrane via a N-terminal myristoylated amphipathic helix. While the ARF-GEF dissociates from the membrane and cargo proteins are sorted into the forming vesicle, active ARF GTPases recruit coat proteins leading to membrane curvature followed by vesicle bud formation. After vesicle scission, ARF-GAPs trigger the hydrolysis of GTP to GDP and inactive ARF GTPases, ARF-GAPs and coat proteins fall off the vesicle membrane. Subsequent vesicle fusion requires the activity of RAB-GTPases and the interaction of R-SNARE proteins on the vesicle membrane with Q-SNARE at the acceptor compartment. After fusion of uncoated vesicles with the acceptor membrane, cargo is released into the lumen of the acceptor compartment.

2.4.1. Vesicle Coats

Eukaryotic cells express three classes of conserved coat complexes: COPI, COPII and adaptor protein complexes with or without clathrin (Myers and Payne, 2013). In the anterograde trafficking between the ER and the *cis*-side of Golgi, vesicles are covered by COPII while COPI functions in the retrograde way between the two organelles. Adaptor protein/clathrin coats are involved in the regulation of post-Golgi trafficking steps like late secretion and endocytosis between the TGN and plasma membrane.

The three coat complexes form cage like structures which are comprised of an outer scaffold shell and inner cargo binding layer. In case of clathrin, the outer shell is assembled of three heavy and light chains which are connected to membranes and cargo by multiple different adaptor proteins or protein complexes. In mammalian and Arabidopsis genomes, monomeric and composite clathrin adaptors are encoded. Five types of complex forming adaptor proteins (AP) and a related ancient T-plate complex have been identified so far (Paul and Frigerio, 2007; Dacks and Robinson, 2017). AP complexes consist of two large, one medium and small subunit where one of the large subunits interacts with specific membrane lipids of distinct endomembrane compartments. In mammals, AP1 is found at the Golgi, AP2 at the PM, AP3 is present at lysosomes and AP4 at endosomes (Robinson, 2004). Coat complexes are recruited from the cytoplasm to the membrane via interaction with active ARF GTPases. However, the functional characterization of each of the Arabidopsis coat complexes and their involvement in specific vesicular trafficking pathways is still in progress.

2.4.2. ARF-GTPases

In general, the ARF/SAR1 family of GTPases is conserved within the eukaryotes but along evolution different subfamilies evolved in different kingdoms. Based on sequence homology, the mammalian ARF family is subdivided into three different classes: class-I containing ARF1, ARF2 and ARF3; class-II containing ARF4 and ARF5 and class-III consisting only of ARF6 (Jackson and Bouvet, 2014). Class-I ARFs are highly conserved within the eukaryotes whereas class-II and class-III are not present in plants (Singh and Richter et al., 2018). The *Arabidopsis thaliana* genome encodes six highly similar ARF1 similar proteins and three additional ARF1-related proteins (Gebbie et al., 2005). Two of the three genes are classified as class A, the other as class B. At the starting point of this thesis nothing was known about the biological function of the two plant-specific classes of ARF-GTPases. ARFB was shown to localize to the plasma membrane after transient expression in *Nicotiana benthamiana* leaves but its subcellular function and role in plant development remained unknown (Matheson et al., 2008).

In plants, members of class-I ARFs are implicated to be important regulators of various vesicular trafficking pathways (Lee et al., 2002; Pimpl et al., 2003; Xu and Scheres, 2005; Tanaka et al., 2014). Accordingly, ARF1 subfamily members were found to localize to the Golgi and TGN in Arabidopsis (Stierhof and El Kasmi, 2010). Strikingly,

data from various eukaryotic systems implies that different coat proteins play a role in the various ARF1-controlled trafficking pathways. For example, COPI was found as coat for retrograde Golgi-ER trafficking and clathrin seems to be the main coat-component of post-Golgi processes (Paul and Frigerio, 2007). So far it is not known how a single class of ARF1 GTPases is able to recruit a variety of coat proteins to distinct membrane sites at the same time. As mentioned above, the ARF activation through ARF-GEFs leads to the insertion of ARF-GTPases into a membrane and may therefore contribute to specificity of ARF1 localization. However, at the beginning of the thesis, it was not clear which specific ARF-GEFs activate ARF1 in Arabidopsis but it is likely that more than a single ARF-GEF has to be involved in the regulation of the different trafficking pathways.

ARF1 GTPases can be rendered activation-impaired or hydrolysis-defective variants by exchanging the amino acid threonine at position 31 to asparagine (T31N) or glutamine at position 71 to leucine (Q71L), respectively (Dascher and Balch, 1994). The ARF1-T31N variant is thought to be impaired in GDP to GTP exchange and therefore should be locked in an inactive complex with its interacting ARF-GEFs at the membrane (Takeuchi et al., 2002; Xu and Scheres, 2005). Overexpression of this variant should therefore titrate the interacting ARF-GEFs out, which could lead to interference with all other trafficking ways that need that particular ARF-GEF function. In contrast, the Q71L variant is thought to be slowed down in GTP hydrolysis. The hydrolysis-impaired ARF1 variant probably persists longer at the membrane, giving rise to problems with vesicle uncoating (Dascher and Balch, 1994). Furthermore, effector recruitment will probably be enhanced, which could lead to interference with other trafficking pathways where the effectors would be missing. Assuming structural similarities between the Arabidopsis GTPases, the T31N and Q71L motif could be a useful tool for the analysis of the so far uncharacterized ARFA and ARFB GTPase classes in Arabidopsis.

Two other single amino acid exchanges where shown to have strong influence on ARF1 function. The *bfa-visualized exocytosis defective 1 (bex1)* mutant has a single amino acid exchange from leucine to phenylalanine at position 34 (L34F) in the ARF1 isoform ARF1A1C (Tanaka et al., 2014). Overexpression of L34F causes strong developmental phenotypes and protein mislocalization but the molecular mechanism underlying these observations is not understood so far. Interestingly, if the tyrosine at position 35 is exchanged to an alanine (Y35A), the ARF1 variant is still able to perform

the classical ARF1 functions (GDP to GTP exchange followed by coat recruitment) but vesicle scission is strongly impaired (Beck et al., 2008; Beck et al., 2011). By chemical cross-linking experiments it was discovered that ARF1•GTP dimerizes *in vitro* whereas the Y35A mutation seems to change the protein structure in a way that dimerization is inhibited. Indeed, monomeric ARF1 is still able to recruit coat proteins to membranes and consequently vesicle buds will be formed but these buds are not able to pinch off. Probably the simultaneous insertion of two close amphipathic helices near the vesicle neck region is needed to enforce off budding (Beck et al., 2011). However, the mechanism by which ARF dimerization is accomplished *in vivo* still needs to be examined.

2.4.3. ARF-GEFs

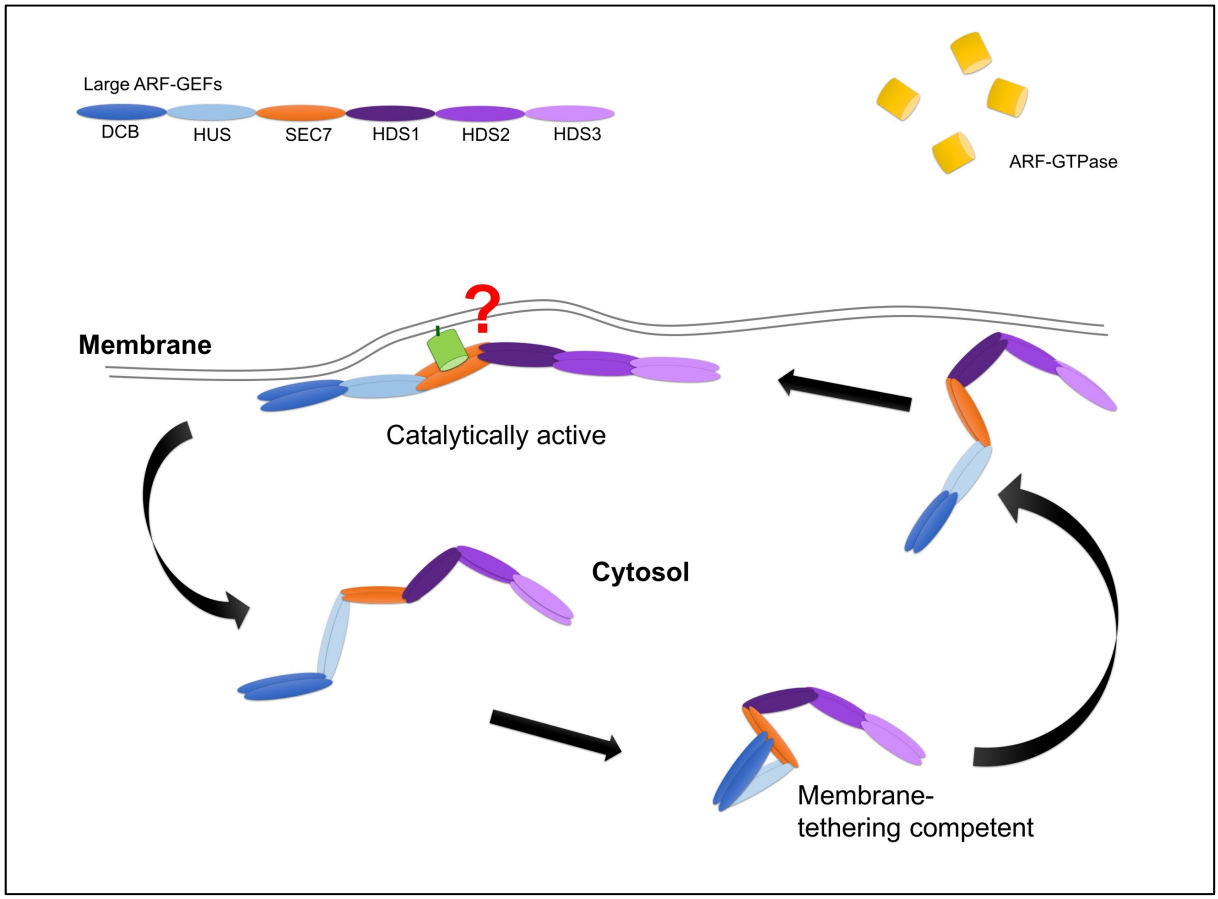

Figure 3. Simplified scheme of ARF-GEF domain architecture and membrane association (modified according to Anders et al., 2008)

Large ARF-GEFs consist of six conserved domains, named as DCB, HUS, SEC7, HDSI, HDSII and HDSIII. Eukaryotic ARF-GEFs form dimers in vivo. Plant ARF-GEFs were shown to associate with the membrane upon heterotypic interaction of the DCB domain with the HUS and SEC7 domain in the cytosol. At the membrane the folded ARF-GEF probably opens up to activate its ARF GTPase substrate. It is still not clear whether the ARF-GEF dimer interacts only with one ARF•GDP molecule at the membrane and how ARF-GEF are targeted to specific membranes (red question mark).

ARF-GEFs are classified according to their protein size and protein domains. Only large ARF-GEFs seem to be conserved across the eukaryotes (Anders and Jürgens, 2008). In contrast to mammals, no medium-sized or small ARF-GEFs were identified in plants. In general, all ARF-GEFs share one highly conserved protein feature, named SEC7 domain after the first identified ARF-GEF Sec7p from yeast *Saccaromyces cerevisiae* (Anders and Jürgens, 2008) (Figure 3). The SEC7 domain is catalytically active and facilitates the GDP to GTP exchange reaction (Beraud-Dufour et al., 1999). On an ultrastructural level, SEC7 domains are composed of several α-helices and a hydrophobic groove, building the interaction surface for the ARF GTPase (Betz et al., 1998; Cherfils et al., 1998; Mossessova et al., 1998). Later it was discovered that not only the hydrophobic groove but also the linker after helix J (Loop>J) plays a role in ARF binding, at least in mammalian ARF-GEFs (Lowery et al., 2011). The Loop>J mutated ARF-GEFs are still able to associate with the membrane suggesting that interaction with an ARF GTPase is not required for ARF-GEF membrane association. It is not clear at all which of the two trafficking regulators (ARFs and ARF-GEFs) reach the membrane first or if they meet independently at the membrane. The already mentioned fungal toxin BFA is able to bind to the ARF•GDP binding pocket of the SEC7 domain and inhibit the GDP to GTP exchange given that the ARF-GEF is BFA-sensitive. Specific combinations of residues in a 40-amino acid long region of the SEC7 domain determine whether an ARF-GEF is BFA-sensitive or -resistant (Peyroche et al., 1999; Sata et al., 1999) and reciprocal replacements can change the ARF-GEF to one or the other status (Geldner et al., 2003; Richter et al., 2007). In addition to the SEC7 domain, large ARF-GEFs harbor at their N-terminus a Dimerisation and Cyclophilin Binding (DCB) domain and a Homology Upstream of Sec7 (HUS) domain (Figure 3). At the C-terminus, three Homology Downstream of Sec7 domains (HDS1-3) domains with so far unknown function are present (Anders and Jürgens, 2008) (Figure 3). In contrast to small and medium-sized ARF-GEFs, large ARF-GEF do not harbor characterized membrane association domains like Pleckstrin Homolgy (PH) domain. So it remains enigmatic how large ARF-GEFs can cycle on and off specific endomembrane compartments (Figure 3). Interestingly, intramolecular interactions of DCB and HUS domain in case of animals or DCB with the HUS and SEC7 domains in plants were shown to be crucial for membrane association (Ramaen et al., 2007; Anders et al., 2008). If the ARF-GEF stays in a closed conformation at the membrane or opens up upon ARF binding is not clear, yet (Figure 3). However, in addition to the

intramolecular interaction, the DCB domain was shown to interact intermolecularly with a second DCB domain mediating dimerization of ARF-GEFs *in vitro* and *vivo* (Grebe et al., 2000; Ramaen et al., 2007; Anders et al., 2008) (Figure 3). Intriguingly, studies showed that a membrane association-defective ARF-GEF protein and a catalytically impaired one can complement each other by interacting with each other (Busch et al., 1996a; Geldner et al., 2004; Anders et al., 2008). Nevertheless, the actual biological significance of ARF-GEF dimerization has still to be revealed (Figure 3).

The Arabidopsis genome codes for eight large ARF-GEF proteins. They can be subdivided into two different clades: the GBF1 (GNOM, GNL1 and GNL2) and BIG (BIG1, BIG2, BIG3, BIG4 and BIG5) clade.

2.4.3.1 GBF1-related clade

A long time ago, several alleles of *GNOM* were discovered in an EMS screen for Arabidopsis mutants affected in embryo development. The mutants display a severe, ball-shaped, dwarf-like phenotype with no roots and fused cotyledons (hence the name *gnom*) (Mayer, 1991; Mayer, 1993; Busch et al., 1996a). The phenotype is caused by failure of establishing the apical-basal polarity axis during embryogenesis (Vroemen et al., 1996; Richter et al., 2010). The plant hormone auxin is a major player of embryo pattern formation and has to be distributed in a polar fashion (Gälweiler et al., 1998; Friml et al., 2003). Interestingly, polar distribution of the auxin efflux carrier PIN1 is defective in *gnom* (Steinmann et al., 1999). Subsequently, subcellular localization studies with GNOM rendered BFA-resistant (GNOM-ML) pointed out that the ARF-GEF actually regulates polar recycling of PIN1 to the basal plasma membrane in specific cell files (Geldner et al., 2003; Geldner et al., 2004). As *GNOM* was discovered in an EMS screen, all the known alleles carry single point mutations leading to defective full-length proteins or premature stop codons. The different alleles can be classified into three classes (A-C), depending on their ability to complement each other, where class C represents loss-of-function alleles (Richter et al., 2010). Two strong alleles, namely $gnom^{b4049}$ (G579R) and $gnom^{emb30}$ (E658K), representing allele classes A and B, respectively, were shown to nearly fully complement each other, giving rise to fertile plants (Busch et al., 1996a; Anders et al., 2008). Both point mutations are located in the SEC7 domain, interfering with two separate functions. The $GNOM^{b4049}$ protein is membrane association-deficient because the mutated SEC7 domain cannot interact

with the DCB domain anymore (Anders et al., 2008). In contrast, the GNOM^{emb30} protein is catalytically inactive since this mutation affects the glutamate finger that is important for GDP to GTP exchange. A rather weak GNOM allele is called *gnom*^{R5} (S1369Δ), giving rise to seedlings with short roots and fused cotyledons, eventually dying after a few weeks (Geldner et al., 2009). The premature stop codon leads to a truncated protein that seems to be unstable. Surprisingly, a *gnom*^{R5} suppressor screen revealed that the effect can be reversed by shortening the protein even more (Richter et al., 2010). Remarkably, the human and yeast GNOM paralogous GBF1 and Gea1/2 are essential for cell viability by regulating Golgi-ER trafficking (Spang et al., 2001; Zhao et al., 2006). In contrast to GBF1 and Gea1/2, GNOM seemed to be involved in endosomal recycling and a role in Golgi-ER trafficking was not obvious. However, further studies pointed out that GNOM acts redundantly together with its close paralogue GNL1 in the regulation of retrograde Golgi-ER transport (Richter et al., 2007). GNL1 was shown to localize to the Golgi where it is important for the recruitment of COPI coat. *gnl1* knockout plants show a dwarf, bushy phenotype but are in general still viable and fertile pointing towards a second GEF being involved in the pathway. In contrast to BFA-sensitive GNOM, GNL1 is naturally BFA-resistant and therefore the involvement of GNOM in retrograde trafficking was at first not obvious. However, when *gnl1* seeds are grown on BFA-containing media, the activity of BFA-sensitive GNOM is additionally blocked and therefore the retrograde trafficking pathway between Golgi and ER breaks down. As a consequence, early secretory trafficking in general collapses as there always has to be a balance between anterograde and retrograde pathways. Consistently, the *gnl1 gnom* double mutant is gametophytic lethal. Additionally, GNL1 seems to play a role in endocytosis since BFA-treated *gnl1* roots are impaired in the selective internalization of PIN2 (Teh and Moore, 2007). GNL1 acts together with a BFA-sensitive ARF-GEF in selective PIN2 endocytosis (Teh and Moore, 2007) but it is not clear weather GNOM or another BFA-sensitive ARF-GEF takes over this function. Interestingly, although GNOM and GNL1 act redundantly in Golgi-ER trafficking, GNL1 cannot take over the function of GNOM in endosomal recycling even though the proteins are highly similar at the amino acid level. Up to this time it is not clear how the various functions are kept separate and which molecular factors contribute to the differentiation between GNOM and GNL1.

The third, a bit more distantly related member of the GBF1 clade, GNL2, was demonstrated to essentially behave like GNOM (Richter et al., 2011). Yet, GNL2 is pollen-specifically expressed and acts in haploid pollen development.

2.4.3.2 BIG clade

While the ARF-GEFs of the GBF1 clade are already well characterized, far less information is available about the BIG clade (BIG1-5). The mammalian counterparts BIG1 and BIG2 were shown to localize to the TGN and to have distinct but also overlapping functions in secretory and endosomal trafficking (Ishizaki et al., 2008; Donaldson and Jackson, 2011). These data and the fact that the regulators of late secretory trafficking were not known at that time in Arabidopsis, raised the question whether the Arabidopsis BIG clade could be involved in post-Golgi trafficking processes. Several years ago, BIG5 was discovered as *Arabidopsis thaliana HopM1 interactor 7* (MIN7) being important for pathogen immunity (Nomura et al., 2006; Nomura et al., 2011). Later, in a fluorescence-based screen for PIN internalization-defective mutants, BIG5 *BFA-visualized endocytic trafficking defective 1 (BEN1*) was characterized as regulator of early endocytosis (Tanaka et al., 2009; Tanaka et al., 2013). Yet, *big5* has only a minor developmental phenotype I.) pointing towards other ARF-GEFs being redundantly involved in the regulation of endocytosis and II.) showing that BIG5 is at least not the main regulator of late secretory trafficking as the interference with it should be lethal. These raises the question if one (or more) of the remaining members of the Arabidopsis BIG clades do play a role in post-Golgi trafficking.

3. Aims of this thesis

The fine-tuned delivery of proteins within the endomembrane system is an essential process for eukaryotic cells. The presence or abundance of e.g. receptors, enzymes and transporters is spatially and temporally coordinated to meet the needs of multicellular systems. Several modes for membrane exchanges are known, like vesicle trafficking, maturation and fusion of compartments. Each mode of trafficking might involve specific regulatory mechanism, often requiring the action of molecular switches like small GTPases and their effectors.

Vesicle budding is regulated by small GTPases of the ARF/SAR1 family, their activating ARF-GEFs and specific coat proteins for different vesicle trafficking pathways. In plants, the regulators of late secretion are not known so far. In mammals, the large ARF-GEFs BIG1 and BIG2 are known to be important for late secretory trafficking (Donaldson and Jackson, 2011). The Arabidopsis genome encodes 5 related proteins but whereas BIG1-4 protein sequences are highly similar, BIG5 seems to be more distantly related and was shown to play a role in pathogen defense (Nomura et al., 2006; Nomura et al., 2011). Therefore, we focused on the analysis of BIG1-4 and explored their role in post-Golgi trafficking regulation. We examined phenotypes of single and multiple knockout mutants as well as subcellular localization of fusion proteins. In contrast to animal cells, the plant TGN functions as an early endosome where secretory, vacuolar, endocytic and recycling trafficking pathways merge with each other. This makes the analysis of post-Golgi trafficking processes quite difficult (Robinson et al., 2008). To dissect the diverse transport routes and examine which pathway is regulated by BIG1-4, we I.) generated Estradiol-inducible secretory, vacuolar, endocytic and recycling marker lines and II.) engineered BFA-resistant and -sensitive BIG1-4 variants.

Plant vacuoles can make up to 90% of a cell's volume and are not only important for degradation of proteins but also for regulating cell expansion via turgor pressure (Zhang et al., 2014). Newly synthetized and endocytosed proteins have to be transported from the TGN/EE via MVBs/LEs to the vacuole. In animal cells, early endosomes mature into late endosomes via RAB5 to RAB7 conversion before fusing with the vacuole (Rink et al., 2005). The conversion is facilitated by a RAB7 GEF-

complex consisting of MON1/SAND and CCZ1 which activates RAB7 and inactivates RAB5 (Kinchen and Ravichandran, 2010). Recent data suggested that MVBs in plants are also generated via maturation from the TGN (Scheuring et al., 2011). Surprisingly, established markers of animal EEs do not localize at TGNs but MVBs in plants (Vermeer et al., 2006; Stierhof and El Kasmi, 2010). This raises the question whether RAB5 to RAB7 conversions play a role for TGN to MVB maturation in plants and which role the so far uncharacterized Arabidopsis SAND protein might play. To address this question, *sand* knockout T-DNA lines were analysed with regard to phenotypic abnormalities and the subcellular localization of vacuolar trafficking markers as well as TGN/MVB markers. To clarify the role of SAND in RAB5 to RAB7 conversion, yeast two- and three-hybrid as well as coimmunoprecipitation interaction studies with SAND and RAB5 or RAB7 GTPase members were performed.

A major regulator of vesicle formation is the ARF-GTPase ARF1 which seems to be involved in the coordination of a multitude of trafficking pathways. The process of vesicle budding comprises the recruitment of coat proteins to a membrane, membrane curvature, bud formation and scission of the bud from the donor membrane. *In vitro* experiments have implicated the importance of ARF1 dimerization for the final vesicle scission step (Beck et al., 2008; Beck et al., 2011). Nevertheless, if ARF1 indeed dimerizes *in vivo* and how dimerization is mechanistically achieved remains to be elucidated. To investigate ARF1 dimerization *in vivo*, we tested the dimerization ability of different ARF1 variants in coimmunoprecipitation experiments and examined the biological relevance of ARF1 dimerization in plants. The already published finding that the ARF1 activator GNOM was shown to dimerize *in vivo (Anders et al., 2008)* might suggest that ARF-GEF dimers drive the formation of ARF1 dimers. To test this we mutated the Loop>J region of GNOM SEC7 domain (GNOM-Loop>J(3A)) which should impair the ARF1-binding capability of ARF-GEFs (Lowery et al., 2011). In the following, we investigated GNOM-Loop>J(3A) functionality and the ability of GNOM-Loop>J(3A)/GNOM heterodimers to interact with ARF1.

The two closely related ARF-GEFs GNOM and GNL1 are important regulators of retrograde Golgi-ER trafficking in Arabidopsis (Richter et al., 2007). Additionally, GNOM was shown to have a crucial function in polar recycling of the auxin efflux carrier PIN1 to the plasma membrane (Geldner et al., 2003). Interestingly, while GNOM is

able to replace GNL1 in the secretory pathway, GNL1 cannot take over PIN1 recycling from GNOM (Richter et al., 2007) even though the two proteins are highly similar by sequence. The finding that GNOM is able to from homodimers via its DCB domain *in vivo* (Grebe et al., 2000; Anders and Jürgens, 2008) led to the question if also GNL1 is able to form dimers *in vivo* and if the two closely related paralogues can heterodimerize with each other. Therefore, the hetero- and homodimerization abilities of GNOM and GNL1 were tested in co-immunoprecipiation experiments. Since the DCB domain of GNOM mediates homodimerization it was further analyzed whether the DCB domain of GNL1 acts in a similar way. Furthermore, the importance of the DCB domain for the functionality of GNOM was analyzed by truncation or swapping experiment

4. Results

4.1. The regulators of post-Golgi trafficking BIG1-4 change recycling of endocytosed proteins to secretion for cell plate formation during cytokinesis.

(Richter et al., 2014, eLIFE)

Eukaryotic cells developed a complex machinery to deliver proteins on specific vesicle trafficking routes to their destinations. In plants, the secretory pathway leads from the endoplasmic reticulum (ER) via the Golgi and TGN to the plasma membrane. On the opposing endocytic pathway, proteins are transported from the PM via the TGN to the vacuole or are recycled back to the PM. Hence, the plant TGN acts as an early endosome and is the main sorting station for in transiting proteins (Viotti et al., 2010). Since recycled, secreted and endocytosed cargoes intermixes in the TGN, the distinction of the different post-Golgi vesicle trafficking pathways is experimentally challenging (Robinson et al., 2008). Vesicle formation in general is initiated by GDP to GTP exchange on small ARF GTPases by their ARF-GEFs, subsequently followed by coat protein recruitment. The GDP to GTP exchange reaction can be blocked by the fungal toxin Brefeldin A which binds into a pocket between a sensitive ARF-GEF and ARF•GDP. Arabidopsis large ARF-GEFs are phylogenetically divided into two clades that are related to the human paralogues GBF1 and BIG1/2, respectively, and can be naturally BFA sensitive or resistant. The ARF-GEFs of the GBF1 related clade GNOM and GNL1 were shown to be important regulators of retrograde Golgi-ER trafficking (Richter et al., 2007) and GNOM additionally mediates the polar recycling of the auxin efflux carrier PIN1 from endosomes to the basal plasma membrane (Geldner et al., 2003). In contrast, the functions of the BIG ARF-GEFs remain elusive. While BIG5 was implicated to play a role in pathogen defence responses and endocytosis (Nomura et al., 2006; Nomura et al., 2011), nothing is known about the highly similar BIG1-4 proteins. Here we address the question of whether the ARF-GEFs BIG1-4 play a role in the regulation of post Golgi vesicle trafficking processes in Arabidopsis.

The phenotypic analysis of *big* knockout mutants demonstrated that BIG1-4 function redundantly in plant development. While single, double, and mostly also triple homozygous knockout mutants showed no phenotypic abnormalities, *big1,2,3* or triple

mutants with an additional heterozygous knockout for the remaining *BIG (*50% gene activity*)* resulted in growth retardation. *big1,2,3,4* quadruple mutants were male gametophytic lethal as BIG1-4 are required for pollen germination and pollen tube growth. Of the four proteins, only the SEC7 domain of BIG3 carries the amino acid combination required for BFA-resistance. Therefore, BFA treatment of *big3* enables the conditional, simultaneous knockout of all four BIGs, resulting in either seed germination or seedling root growth failure which can be rescued by BIG4 rendered BFA-resistant (M695L). Subcellular localization studies with Golgi (γCOP) and TGN (VHA-a1 and ARF1) markers as well as ultrastructural EM analysis in transgenic Arabidopsis root cells uncovered TGN localization of fluorescently tagged fusion proteins of BIG3 and BIG4. These results let us investigate whether BIG1-4 function in the regulation of post-Golgi trafficking pathways by analysing the localisation of secretory, vacuolar, endocytosis and recycling cargo markers in BFA-treated wildtype (WT) and *big3* mutant seedlings. As mentioned above, BFA treatment of *big3* enabled the conditional knockout of BIG1-4. The usage of heat shock or estradiol-inducible promoters for marker gene expression allowed us to specifically follow the trafficking of newly synthetized cargo after BIG1-4 knockout. Secretory trafficking was impaired in BFA-treated *big3* seedlings since secretory GFP (secGFP) destined for the apoplast and syntaxin SYP132 (YFP-SYP132), normally targeted to the plasma membrane, localized to BFA compartments in *big3* but not in WT. Similarly, proteins destined for the vacuole, like RFP fused to the vacuolar sorting sequence AFVY of phaseolin (AFVY-RFP) and endocytosed boron transporter 1 (BOR1), ended up in BFA compartments in *big3* but not in WT. Indeed, BIG1-4 seem to mediate secretory and vacuolar trafficking at the TGN which is further supported by the finding that the μB2-adaptin (AP1M2) protein is cytosolic in BFA-treated *big3* seedlings. AP1M2 is a subunit of the membrane- and cargo-binding adaptor protein complex AP-1 of clathrin coats, known to localize to the TGN in wildtype seedlings and to be important for late secretory and vacuolar trafficking (Mallet and Brodsky, 1996; Park et al., 2013). However, the COP1 subunit γCOP still associated with the Golgi in BFA-treated *big3* seedlings, pointing out that COP1 recruitment rather depends on the function of GBF1-related than BIG ARF-GEFs. Next, we examined the influence of BIG1-4 on trafficking of the auxin efflux carrier PIN1. In wildtype, newly synthetized PIN1 is transported from the ER via the TGN to the plasma membrane from where the stable protein is endocytosed and recycled back to the basal PM via the BFA-sensitive ARF-GEF

GNOM (Geldner et al., 2003). As in wildtype, steady-state populations of PIN1 localised to BFA compartments in BFA-treated *big3* root cells but were recycled back to the PM when the BFA-resistant GNOM variant (GNOM-ML) was co-expressed, indicating that BIG1-4 are not involved in endosomal recycling of PIN1. This pathway is only regulated by GNOM. In contrast, PIN1 that was newly synthesized after BFA treatment was not transported to the PM but accumulated in BFA compartments even with BFA-resistant GNOM-ML being present. These results demonstrate that BIG1-4 regulate late-secretory trafficking of newly synthetized proteins but PIN1 recycling solely relies on GNOM function. Strikingly, formation of lateral root primordia *of big3* were severely affected after simultaneous BFA and auxin (NAA) treatment, exhibiting cytokinesis defects with binucleate pericycle cells and proliferation arrest. As this effect could not be rescued by BFA-resistant GNOM, late-secretory trafficking rather than recycling seems to be required for cytokinesis during lateral root formation. During cytokinesis, a massive flow of endocytosed and secreted proteins is redirected from the TGN to the forming cell plate in a short time period. These trafficking processes require the activity of BIG1-4 as cell plates fail to form in BFA-treated meristematic root cells. In addition to binucleate cells, accumulation of secretory and endocytic markers, normally being transported to the cell plate, was observed in BFA compartments. Thorough analysis of PIN1 trafficking in mitotic cells revealed that PIN1 was also endocytosed and transported to the cell plate in BFA-treated wildtype seedlings but accumulated in BFA compartments of BFA-treated *big3* mutants. Surprisingly, PIN1 located back to the basal PM but not the cell plate when BFA-resistant GNOM was present in BFA-treated *big3* mitotic cells, suggesting that polar recycling and trafficking of PIN1 to the cell plate are simultaneous processes during cytokinesis.

Our study clearly identifies BIG1-4 as functionally redundant main regulators of specific post-Golgi trafficking pathways in *Arabidopsis thaliana*. While their activity is essential for late-secretory and vacuolar transport from the TGN to the PM and vacuole, respectively, recycling of e.g. auxin efflux carrier PIN1 from the TGN to the PM depends solely on the function of GNOM. During cytokinesis, BIG1-4 coordinate the massive flux of endocytosed and secretory cargo from the TGN to the division plane by changing the cell's transport status from recycling to secretion with one exception. Polar PIN1 recycling seems to be exempted from this rule to ensure proper auxin flux during developmental processes with high cell proliferation rates.

4.2. SAND-mediated RAB GTPase conversion is required for the fusion of late endosomes with the vacuole in *Arabidopsis thaliana*

(Singh et al., 2014, Current Biology)

The precise regulation of cargo trafficking to the vacuole is not only essential for protein degradation in plants but also required for protein storage and ion homeostasis (Marty, 1999). For degradation, membrane proteins have to be delivered via intraluminal vesicles in multivesicular bodies (MVBs) to the lumen of the vacuole. Recently, it was shown that cargo transport from the TGN to the vacuole is accomplished by maturation of late endosomes/MVBs from the TGN rather than vesicular trafficking (Scheuring et al., 2011). In animals, the maturation process involves membrane identity changes from early to late endosomes managed by the conversion of small GTPases of the RAB family (Rink et al., 2005). Active RAB5 GTPases on the early endosome recruit RAB7 GTPases to the maturing late endosome where RAB7 becomes activated and RAB5 in turn inactivated by the MON1/SAND + CCZ1 GEF complex (Kinchen and Ravichandran, 2010; Nordmann et al., 2010; Poteryaev et al., 2010). In plants, secretory and endocytic trafficking merge in the TGN which consequently functions as an early endosome (Viotti et al., 2010). In this study, we analysed whether the maturation process of MVBs in *Arabidopsis thaliana* also requires the conversion of RAB GTPases and if the SAND protein function is conserved in plants.

TGN to MVB maturation was examined by colocalization studies of the TGN marker VHA-a1, a subunit of the V-ATPase complex and the RAB5-like GTPase ARA7 (RABF2b) as well as the PI3P sensor YFP-2xFYVE in stably transformed Arabidopsis seedlings. Phosphatidylinositol-3-phosphate and RAB5-GTPases are characteristic components of early endosomal membranes in yeast and animal cells. While VHA-a1 and ARA7 showed low colocalization at the TGN, ARA7 and 2xFYVE greatly overlapped at the MVB but 2xFYVE marked additional endosomes lacking ARA7. Furthermore, ARA7 labelled a subdomain of the TGN lacking VHA-a1. BFA treatment of root cells supported these observations as VHA-a1 and ARA7 partly localised to the BFA compartment whereas 2x-FYVE remained exclusively at the MVBs together with ARA7. Hence, we concluded that during maturation ARA7 becomes recruited to a subdomain of the TGN whose membrane subsequently enriches in PI3P leading to a ARA7/PI3P-labelled late endosome/MVB. To determine the function of the Arabidopsis

SAND protein in vacuolar trafficking, we analysed the phenotype of *sand* T-DNA knockout mutants along with the subcellular localisation of vacuolar cargo. The two different knockout alleles showed impaired plant growth, cell shape and seed germination which could be rescued by SAND fluorescent fusion proteins under the control of ubiquitin10 or RPS5a promoter. However, gametophyte function and development were not affected. The *sand* phenotype was explainable by the mislocalisation of proteins destined for the vacuole. The analysis of the vacuolar trafficking pathway revealed that vacuolar cargo like GFP-CT24, AFVY-RFP and Aleurain-GFP was missorted to the apoplast in *sand* mutants. No effect was observed on the localisation of the cell plate marker KNOLLE for late-secretory trafficking or on recycling of the auxin efflux carrier PIN1 and PIN2. Accordingly, SAND function seems to be specifically required in vacuolar trafficking from the TGN to the vacuole but is probably not important for late secretion or recycling processes. Convincingly, subsequent ultrastructural EM analysis of *sand* root cells revealed changes of MVB morphology. *sand* MVBs were bloated in comparison to wildtype and as a consequence RAB5-like GTPases ARA6 (RABF1) and ARA7 labelled MVBs appeared as ring like structures in live-cell imaging. Consistent with a function of SAND at MVBs, SAND protein localised at MVBs in wildtype cells as shown by colocalization studies with ARA7, ARA6 and 2xFYVE as well as EM analysis. Interestingly, only in *sand* mutants and not in wildtype, ARA6 and 2xFYVE were observed at the tonoplast and upon overexpression of a hydrolysis-defective ARA6 variant (ARA6-Q69L) in wildtype cells, SAND also localised to the tonoplast. These findings raised the question if SAND is an effector of RAB5-like GTPases. Indeed, following yeast-two-hybrid and co-immunoprecipitation experiments confirmed an interaction between SAND and ARA6•GTP. As SAND together with CCZ1 acts as an GEF of RAB7-like GTPases on late endosomes in yeast, we next examined the localisation of the RAB7-like GTPase RABG3f in transgenic wildtype and *sand* Arabidopsis root cells. While RABG3f colocalised with SAND on MVBs and was additionally present at the tonoplast in wildtype, the tonoplast signal was gone in *sand* root cells. Instead, RABG3f appeared in the cytosol and in punctae that were no MVBs as they were not responsive to the PI3-kinase inhibitor Wortmannin. Thus, SAND seems to be required for RABG3f localisation to MVBs and the tonoplast. Subsequent co-immunoprecipitation analysis positively confirmed an interaction between SAND and RABG3f. As SAND was not able to directly interact with RABG3f•GDP in a yeast two-hybrid screen, we further

investigated the interaction of the SAND and CCZ1 GEF-complex with RABG3f in a yeast three-hybrid experiment. With CCZ1 as bridge, strong interaction of RABG3f•GDP and weak interaction of RABG3f•GTP with SAND was detected. Hence, SAND is important for the activation of RAB7-like GTPases in Arabidopsis.

These data confirm the previous observations that endosomal maturation from early endosomes to late endosome takes place in plants as in other eukaryotes. Furthermore, our results clearly demonstrate a role of SAND in the conversion of RAB5- and RAB7-like GTPases in Arabidopsis. Ergo, SAND function seems to be evolutionary conserved. However, unlike in non-plant organisms, plant RAB conversion is not required for MVB biogenesis but rather important for subsequent fusion of MVBs with the vacuole.

4.3. How to pair up: dimerization of ARF1-GTPases is mediated by cooperative high-affinity binding of ARF-GEF molecule pairs

(Brumm et al., manuscript)

A large number of proteins form dimers within a cell to be able to fulfil a biological function (Xu et al., 1998; Mei et al., 2005). ARF-GEFs, the activators of ARF GTPases, dimerize via their N-terminal DCB domain *in vivo* (Anders et al., 2008). Although the ability for dimerization seems to be a conserved ARF-GEF feature (Ramaen et al., 2007), the biological significance of dimer formation is still unknown. ARF-GEFs interact on membranes with ARF•GDP, catalyze GDP to GTP exchange and return into the cytosol after conformational changes of the ARF GTPase. The ARF and ARF-GEF interaction can be steadied by expression of the GDP-stabilized and therefore activation-impaired ARF-T31N variant. Upon nucleotide exchange, active ARF•GTP becomes inserted into membranes and recruits coat proteins in the course of the vesicle formation process. After GTP hydrolysis, the membrane insertion hasp becomes retracted and ARF•GDP is released into the cytosol. The ARF1-Q71L variant is impaired in GTP hydrolysis and therefore stabilized at membranes in the GTP-bound form. While function of ARF GTPases in coat recruitment was long known, it was only recently discovered that ARF1 dimerization plays a role in vesicle scission *in vitro* (Beck et al., 2008; Beck et al., 2011). Even though the monomeric ARF1 variant Y35A

was still able to recruit coat proteins to a membrane which led to the formation of vesicle buds, these vesicles were not able to separate themselves from the membrane anymore. However, it remains unclear if ARF GTPases indeed dimerize *in vivo* and how dimerization is achieved on a molecular level. Here, we not only analyse the ability of ARF1 to form dimers *in vivo* but also ask the question whether there is a molecular link between ARF1 and ARF-GEF dimerization.

To test ARF1 dimerization *in vivo,* we performed co-immunoprecipitation analysis on stably transgenic Arabidopsis seedlings expressing different, mostly cell-lethal ARF1 variants in an estradiol-inducible manner. Interestingly, both, activation-impaired ARF1-T31N and hydrolysis-defective ARF1-Q71L, interacted with endogenous ARF1 while only ARF1-T31N showed interaction with ARF-GEF GNOM, as expected. Since GDP-stabilized ARF1-T31N interacted with the ARF-GEF, we suggested that ARF1•GDP dimers are bridged by interacting ARF-GEFs but after conformational changes upon ARF1 activation, ARF1•GTP molecules might directly interact with each other. Indeed, FRET-FLIM analyses revealed a direct interaction of two ARF1-Q71L molecules. When the putatively dimer-disrupting Y35A mutation was introduced into ARF1-Q71L, no homodimerization of ARF1-Q71L-Y35A was measurable. To analyse the biological relevance of ARF1 dimerization, the rescue ability of ARF1-Y35A was tested in tobacco protoplast secretion assays in which α-amylase secretion was inhibited by ARF1-T31N expression. While co-expression of ARF1-WT with ARF1-T31N resulted in restored α-Amylase secretion, rescue ability of ARF1 was diminished by the Y35A mutation. Strikingly, expressing ARF1-Y35A alone resulted in reduced α-amylase secretion as well. Furthermore, EM analysis of Arabidopsis seedlings expressing ARF1-Y35A only for several hours already revealed changes of Golgi morphology, pointing towards an importance of ARF1 dimer formation for cell viability. It was recently shown, that ARF binding by ARF-GEFs requires the functionality of a specific region of the ARF-GEF SEC7 domain, called Loop>J region (Lowery et al., 2011). To first test if the function of Loop>J region in ARF1 binding is conserved, we introduced three alanine substitutions into the Loop>J region of the SEC7 domain of ARF-GEF GNOM. Indeed, in co-immunoprecipitation analysis ARF1-binding capability of GNOM-Loop>J(3A) was weakened to such an extent that an interaction was only detectable if the activation-impaired and therefore GDP-stabilized ARF1-T31N variant was expressed along with GNOM-Loop>J(3A). We additionally expressed the

transgene in *gnom* knockout background *sgt*. Here, for the first time we characterized the *sgt* allele in which 9 genes, including *GNOM*, were deleted upon Ds-induced transposon translocation. While *sgt* can be rescued by a tagged GNOM transgene, GNOM-Loop>J(3A) was only partially capable to rescue *sgt* giving rise to seedlings with fused cotyledons and short roots, eventually dying after a few weeks. The phenotype greatly resembled the one of weak mutant *gnom* allele R5 whose activity is decreased due to the instability of a truncated GNOM protein. However, as the interaction of ARF GTPases and ARF-GEFs is supposed to take place at the membrane, we next checked membrane association of GNOM-Loop>J(3A) in BFA-treated Arabidopsis root cells. BFA is known to stabilise ARF•GDP and ARF-GEF complexes at the membrane, resulting in the localisation of GNOM in BFA compartments. As GNOM-Loop>J(3A) does not efficiently bind to ARF1, BFA-treatment did not stabilize GNOM-Loop>J(3A) at the membrane. To test whether this effect is not caused by the inability of GNOM-Loop>J(3A) to bind to membranes, we fractionated seedling cells and observed the same amounts of GNOM and GNOM-Loop>J(3A) in membrane and cytosolic fractions. It was shown that membrane association of ARF-GEFs depends on the heterotypic interaction of the DCB with the rest of the protein (ΔDCB) (Anders et al., 2008). Yeast two-hybrid analysis revealed that ΔDCB-Loop>J(3A) was still able to interact with the DCB domain of GNOM, suggesting that GNOM-Loop>J(3A) is not defective in proper protein folding. In contrast, in $gnom^{b4049}$ heterotypic DCB-ΔDCB interaction is impaired. As GNOM in general forms dimers, $gnom^{b4049}$ can be complemented by a catalytically impaired but otherwise functional GNOM protein ($GNOM^{emb30}$), we wondered whether GNOM-Loop>J(3A) would rescue $gnom^{b4049}$. Surprisingly, GNOM-Loop>J(3A) neither complemented $gnom^{b4049}$ nor $gnom^{emb30}$ fully but rather partially rescued *gnom* seedlings like in *sgt*. These results suggest that heterodimers of GNOM-Loop>J(3A) and other mutated GNOM proteins are still impaired in ARF1 binding. To verify our hypothesis, we crossed GNOM-GFP into GNOM-Loop>J(3A) *sgt* transgenic Arabidopsis plants and performed co-immunoprecipitation experiments. Heterodimers of GNOM-GFP and GNOM-Loop>J(3A) showed no interaction with ARF1, implying that two functional molecules in a GNOM dimer are required for ARF1 binding.

In summary, our results suggest that ARF1 GTPases form dimers *in vivo* by cooperative binding of two ARF1•GDP molecules to a functional ARF-GEF dimer.

Once, the ARF-GEF dimer catalyses GDP to GTP exchange, the conformational change of the activated GTPase probably allows direct interaction of two ARF1•GTP molecules. We propose that this mechanism could be conserved across the eukaryotes as ARF-GEF dimers are found in all kingdoms and dimerization of human ARF1 was shown *in vitro* before (Beck et al., 2011).

4.4. The contradictory function of the DCB domain: its role in mediating and preventing dimerization of closely related ARF-GEFs GNOM and GNL1 (Brumm et al., manuscript)

Important regulators of vesicle formation are ARF-GTPases and their activating GEFs. Large ARF-GEFs are found in the genomes of all eukaryotes and their protein domain organization is conserved (Anders and Jürgens, 2008). The so far best characterized domain is the catalytically active SEC7 domain in the middle of the protein flanked by a Homology Upstream of SEC7 (HUS) domain N-terminally and three Homology Downstream of SEC7 (HSDI-III) domains C-terminally. The very N-terminal Dimerisation and Cyclophilin Binding (DCB) domain is not only important for ARF-GEF dimerization but also contributes to its membrane-association capability by interacting with at least one of the other domains (Ramaen et al., 2007; Anders et al., 2008). Biochemical, molecular as well as genetic studies showed that the Arabidopsis ARF-GEF GNOM forms dimers via its DCB domain *in vivo* (Busch et al., 1996a; Grebe et al., 2000; Anders et al., 2008). GNOM mediates polar recycling of the auxin efflux carrier PIN1 (Steinmann et al., 1999; Geldner et al., 2003). Moreover, GNOM is able to take over the function of its close paralog GNL1 in retrograde Golgi to ER trafficking (Richter et al., 2007). However, GNL1 is not able to take over the function of GNOM in endosomal recycling. Here, we analyze how GNOM and GNL1 functions are kept separate, although they share high sequence similarity. Therefore, we take a deeper look into the function of the DCB domains of the two closely related paralogues.

To test the homo- and heterodimerization ability of GNOM and GNL1, co-immunoprecipitation analysis on stably transgenic Arabidopsis seedlings was performed. GNL1 interacted with itself like the positive control GNOM. However, no heterodimers of GNOM and GNL1 were detectable. Since GNOM can dimerize via the

DCB domain, we next analyzed in a yeast two-hybrid assay whether DCB domains of GNL1 and GNOM in general show the same features. As expected from the co-immunoprecipitation results, the two DCBs did not interact with each other but surprisingly, the DCB(GNL1) also did not interact with itself. However, the DCB domain of GNL1 was able to interact with the rest of the GNL1 protein (ΔDCB of GNL1). Unexpectedly, DCB(GNL1) also interacted with ΔDCB(GNOM), and DCB(GNOM) interacted with ΔDCB(GNL1). These results made us wonder how a chimeric protein, consisting of the DCB domain of GNL1 and ΔDCB fragment of GNOM (further on abbreviated as DCB swap), would behave in plants. Interestingly, the DCB swap was able to fully rescue not only *gnom* knockout mutant *sgt* and *gnl1* single mutant but also the *sgt gnl1* double mutant. Furthermore, the DCB swap showed interaction with GNOM and GNL1 in co-immunoprecitation analysis. However, the DCB domain of GNL1 did not interact with itself in the yeast two-hybrid assay. Therefore it is likely that the interaction of DCB swap with GNL1 in co-immunoprecipitation can be explained by an heterotypic interaction of the GNL1 DCB domain of the chimeric swap protein with the ΔDCB(GNL1) fragment of the wildtype GNL1 full length protein. Furthermore, as no interaction between the DCB domains of GNOM and GNL1 was observed in yeast two-hybrid assay, we attributed the interaction of the DCB swap with GNOM to heterotypic interaction ΔDCB(GNOM) fragment of the chimeric swap protein with the DCB domain of the wildtype GNOM full length protein. As the DCB domain in general is required for membrane association, we next asked if a ΔDCB(GNOM) fragment would be able to rescue *sgt* allele. Surprisingly, ΔDCB(GNOM) nearly fully rescued the post embryonic phenotype of *sgt,* although lateral root development was still impaired. To test whether the rescue is due to a heterodimerization of ΔDCB(GNOM) with endogenous GNL1, co-immunoprecipitation analysis was performed on stably transgenic Arabidopsis seedlings. Indeed, the two proteins interacted with each other. Furthermore, ΔDCB(GNOM) failed to rescue the *sgt gnl1* double mutant, which strongly suggests that GNL1 is required for *sgt*-rescuing activity of ΔDCB(GNOM). Since GNOM normally localizes to endosomes represented by the BFA compartments in BFA-treated Arabidopsis root cells whereas GNL1 associates with Golgi stacks, we wondered where the heterodimer of ΔDCB(GNOM) and GNL1 would localize. Strikingly, GNL1 localized not only to the Golgi in ΔDCB(GNOM) *sgt* but was also found in the BFA compartment after treating seedlings with BFA. The DCB domain of GNL1

was not able to interact with ΔDCB(GNOM^{b4049}) in yeast two-hybrid assay. As the interaction of DCB(GNL1) with ΔDCB(GNOM) is required for heterodimerisation and endosomal membrane association, it was not surprising that ΔDCB(GNOM ^{b4049}) was not able to rescue the *sgt* knockout mutant.

Taken together, our data suggests that the DCB domain of the ARF-GEF GNOM performs a dual function. On one hand it is required for homodimerization of GNOM and on the other hand it prevents heterodimerization of GNOM with the closely related paralogue GNL1. However, while GNOM dimerization seems to be mediated by DCB-DCB and DCB-ΔDCB interaction, GNL1 dimerization rather seems to rely solely on the interaction of the DCB domain with the rest of the protein. The strict separation of the two paralogues is presumably necessary for efficient polar recycling of the auxin efflux carrier PIN1 in growth responses upon changing environmental conditions

5. Discussion

The coordinated transport of proteins is essential for eukaryotic organisms. The ability to vary membrane identities and cellular contents by spatiotemporal regulated distribution of proteins enables not only the incorporation of environmental cues into developmental contexts but also ensures cell to cell communication and cell homeostasis. Protein transport to different destinations is accomplished by membrane exchanges between cellular compartments. The prevailing way of membrane exchange is the formation and delivery of small carrier vesicles between donor and acceptor compartments (Singh and Jürgens, 2018). Yet, other possibilities are that membrane compartments themselves fuse with each other or mature from one into the other (Singh and Jürgens, 2018). Whichever way, all transport steps have to be highly regulated to keep the system balanced. Major regulators of membrane trafficking are well conserved small GTP-binding proteins which act as molecular switches (Vernoud et al., 2003). Upon activation with the help of accessory GEF proteins, GTPases interact with downstream effectors performing diverse cellular functions. In our studies, we mainly focused on members of the RAB and ARF GTPase subfamilies.

5.1. RAB-GTPase conversion plays a role in membrane fusion between late endosomes and the vacuole in *Arabidopsis thaliana*

RABs comprise with 57 genes the largest and most diverse subfamily of Arabidopsis small GTPases and are implicated to function in the coordination of various trafficking steps (Rutherford and Moore, 2002). Based on sequence similarities to yeast and human orthologues, Arabidopsis RAB GTPases are divided into 8 subgroups (RABA-H, corresponding to mammalian subclasses 11, 2, 18, 1, 8, 5, 7 and 6). The Arabidopsis genome encodes three RAB5-related members (plant specific RABF1; RABF2a and RABF2b) but the RAB7 related subclass RABG is with eight putative members more diverse (Rutherford and Moore, 2002). Proteins of both clades were shown to mediate protein transport steps towards the vacuole. Therefore, it was suggested that the greater diversification within the RABG clade may reflect the higher complexity of vacuolar function in plants (Rutherford and Moore, 2002). Plant vacuoles are not only essential for proteolysis but also contribute to storage, cellular stability and homeostasis. For that reason, the investigation of trafficking pathways to vacuoles and the involved regulatory machinery is of high interest. Since multiple combinations of

RABG T-DNA insertions lines (up to quadruple mutants) show no obvious phenotype, high redundancy between the different RABG members is assumed (Nielsen et al., 2008). In animal cells, the maturation of the early endosome to late endosome is characterized by the conversion of RAB5 to RAB7 GTPases on the membrane (Rink et al., 2005). The process is regulated by a RAB7 GEF complex consisting of MON1/SAND and CCZ1 proteins (Nordmann et al., 2010; Poteryaev et al., 2010). Even though RAB5 and RAB7-related GTPases were identified in plants, it was not clear if maturation of early to late endosomes also takes place in plant vacuolar trafficking. However, a major difference between the endosomal composition of plant and animal cells is that the plant TGN serves as an early endosome where secretory, endosomal and vacuolar trafficking merge (Viotti et al., 2010). The classical model of vacuolar protein transport in plant cells anticipated clathrin-coated vesicles to pinch off from the TGN and fuse with the MVBs where for example transmembrane proteins are internalized by subsequent invagination of the MVB membrane (Robinson and Pimpl, 2014). However, a recent ultrastructural study of the origin of MVBs in plants revealed that MVBs mature from the TGN (Scheuring et al., 2011) (Figure 4a). In accordance with their results, we found that the RAB5-like GTPase ARA7 (RABF2b), which in general labels MVBs, localizes to a subdomain of the TGN in live-cell imaging studies (Figure 4a). The dual localization pattern was also observed in previous ultrastructural root analysis (Stierhof and El Kasmi, 2010). Once the subdomain becomes enriched with RAB5-like GTPases, the maturation of MVBs goes along with the recruitment of PI3 kinases. As the maturation of MVBs includes the formation of intraluminal vesicles, it fits quite well that early components of the ESCRT machinery localize to the TGN as well (Scheuring et al., 2011). Interestingly, on matured MVBs, RABF (RAB5) and RABG (RAB7) GTPases colocalize with each other but only RABGs subsequently label the tonoplast (Figure 4a). In *sand,* RABG3f does no longer localize to MVBs and the tonoplast, although MVBs in general seem to be structurally intact as large membrane containers with intraluminal vesicles can still be observed. As in *sand* vacuolar markers do not reach the vacuole anymore but are rather secreted to the apoplast, we concluded that the activity of RABG3f is required for fusion of MVBs with the vacuole. Here we show that the role of SAND in RAB5 to RAB7 like GTPase conversion in plants is conserved but the event happens at a later time point. In contrast to animal cells, the change of plant RAB5 to RAB7-like GTPases is rather required for fusion of late endosomes with the vacuole than for early to late endosome maturation (Figure

4a). In the future it would be interesting to see with which downstream effectors RABG3f is interacting upon activation to mediate endosome and vacuolar fusion. It seems likely that the HOPS tethering complex would belong to RABG effectors because the yeast RAB7- related GTPase Ypt7 binds HOPS during late endosome to vacuole fusion (Kinchen and Ravichandran, 2010; Nordmann et al., 2010; Vukasinovic and Zarsky, 2016).

Our results concerning the role of SAND/CCZ1 in RAB conversion at late endosomes are supported by the finding of two other groups which analyzed the function of SAND and CCZ1 orthologues in plants (Cui et al., 2014; Ebine et al., 2014). The overexpression of an activation-impaired, Dexamethasone-inducible variant of RABG3f (RABG3f-T22N) in Arabidopsis seedlings resulted ultimately in cell death as MVBs were not able to fuse with the vacuole anymore (Cui et al., 2014). Both research teams were able to show direct GEF activity of the SAND/CCZ1 complex on RABG3f. In contrast to SAND, CCZ1 did not interact with ARA7 in yeast two-hybrid assays hinting towards SAND being the interaction platform of the SAND/CCZ1 complex for RABF interactions (Cui et al., 2014). While SAND is a single copy gene in Arabidopsis, CCZ1 is encoded by two highly similar genes (Ebine et al., 2014). Convincingly, the *ccz1a ccz1b* double mutant has a similar but slightly weaker phenotype than *sand*. Interestingly, Ebine et al. observed phenotypic differences between the *ccz1* double mutant (subunit of RABG-GEF) and a *vps9a* mutant (subunit of RABF-GEF) which implicates that RAB5 and RAB7-related GTPases in Arabidopsis have at least partially different functions. This notion was supported by additional crosses of *rabf* and *rabg* mutants with *zig1,* a mutant of the vacuolar/MVB-localized Qb-SNARE VTI11. Before fusion of two membranes, RAB GTPases in general interact with tethering complexes which in turn interact with SNARE proteins that mediate membrane fusion by complex formation. While *rabf* mutants synergistically exaggerated the *zig1* phenotype, a *rabg* (RABG3b,c,d,e,f) quintuple mutant partially suppressed it. In summary, beside their successive function in MVB to the vacuole trafficking after SAND/CCZ1 interaction, RAB5 and RAB7-related GTPases in Arabidopsis seem to fulfill different and probably counteracting functions in other vacuolar pathways.

5.2. Many paths can lead to the same destination: vacuolar trafficking in plants

The vacuole in plants has multiple functions and proteins have to be transported from various cellular compartments to it. The classical view of vacuolar trafficking of soluble cargo predicted that proteins are recognized by vacuolar sorting receptors (VSRs) at the TGN, then packed into clathrin-coated vesicles which fuse with the MVB where a low pH leads to dissociation of the cargo from the receptors (Cui et al., 2014; Robinson and Pimpl, 2014). While vacuolar cargo would be sent further to the vacuole, VSRs would be recycled back to the TGN or Golgi. This model altered over the last years. We and others showed that MVBs mature from the TGN (Scheuring et al., 2011; Singh et al., 2014) (Figure 4a and b). This does not exclude the possibility of additional vesicle trafficking between the TGN and MVBs but since transmembrane proteins can only be degraded if they reach the intraluminal vesicles of the MVBs by ESCRT- mediated invagination and ESCRT components were found to localize to the TGN (Scheuring et al., 2011), it seems quite likely that MVB maturation is the main source for degradable transmembrane proteins. Additionally, recent studies showed that the TGN rather than than the MVB is the most acidic endomembrane compartment on the way to the vacuole (Martiniere et al., 2013; Shen et al., 2013; Luo et al., 2015). Studies in tobacco leaf protoplasts suggest that VSRs already bind their cargo in the ER and Golgi and release it due to the pH shift in the TGN from where VSRs are recycled back to the Golgi (Künzl et al., 2016; Früholz et al., 2018). VSRs were proposed to be recycled via the retromer complex, a protein complex consisting of three vacuolar protein sorting (VPS) subunits which interact with sortin nexin (SNX) heterodimers. While SNX subunits were found to associate with the TGN in Arabidopsis root cells (Stierhof et al., 2013), retromer subunits where controversially localized to the TGN (Niemes et al., 2010) or MVBs (Munch et al., 2015). Retromer recruitment is normally triggered by RAB5 to RAB7 GTPase conversion in animal cells (Rojas et al., 2008) which would speak for MVB-localized retromer in plants as we and others showed that RAB GTPase conversion takes place at the late rather than the early endosome in plants (Cui et al., 2014; Ebine et al., 2014; Singh et al., 2014). Yet, taking the data about VSR unloading and recycling from the TGN to the Golgi into account, the proposed TGN localization of retromer also seems logical. The confusing data about retromer localization in plants and new studies on retromer/sorting nexin function in animal cells raised the question of whether retromer takes part in VSR recycling at all or if rather

clathrin-coated vesicles play a role in retrograde transport steps from the TGN (Robinson and Neuhaus, 2016; Robinson, 2018). Actually, we found evidences for a vesicle trafficking machinery including the ARF-GEFs BIG1-4 and the clathrin adaptor protein AP1 being involved in vacuolar transport (Richter et al., 2014). When BIG1-4 are conditionally knocked out by BFA-treatment of *big3* mutants, the soluble vacuolar cargo marker AFVY-RFP is no longer transported to the vacuole but gets stuck in BFA compartments. Interestingly, BIG1-4 mediate the recruitment of the clathrin-coat adaptor subunit mμB2-Adaptin (AP1M2) to the TGN in Arabidopsis (Richter et al., 2014) and a loss of AP1 was also shown to interfere with vacuolar trafficking (Park et al., 2013; Wang et al., 2013). These data suggest that vesicle trafficking plays a role in TGN-MVB-vacuole trafficking and contradict the TGN-MVB maturation model described before. However, maturation might also require the vesicle trafficking machinery since membrane material has to be retrieved from further maturing MVB and has to be recycled back to the TGN (Figure 4b). A similar model already exists for the maturation of the Golgi cisternae. Here, COPI-coated vesicles retrieve membrane material that is recycled back to the *cis*-side of the Golgi (Malhotra and Mayor, 2006) (Figure 4b). In the last years, several studies showed that multiple vesicle trafficking pathways lead to plant vacuoles (Viotti, 2014). One example is the Golgi-independent transport of some vacuolar storage proteins directly from the ER to the vacuole but the underlying regulatory machinery is still unknown (Hara-Nishimura et al., 1998; Uemura and Ueda, 2014) (Figure 4b). Furthermore, in addition to MVB maturation several other differently regulated transport ways from the Golgi to the vacuole seem to exist (Uemura and Ueda, 2014; Viotti, 2014). Beside the already mentioned opposing effects of *rabf x zig1* and *rabg x zig*1 crosses, other observations suggest distinct, RABF (RAB5) and RABG (RAB7) member-specific regulated pathways. The styryl dye FM4-64 still reaches the tonoplast in the *ccz1* double mutant, indicating an RAB7-independent trafficking pathway (Ebine et al., 2014). Moreover, in AP3 adaptor complex (*ap3*) and *sand* mutants, the SNARE protein SYP22 reaches RABF (RAB5) dependently still the tonoplast. In contrast, trafficking of the tonoplast-localized SNARE VAMP713 is disturbed in *ap3* but not in *sand* or *ccz1* mutants. Therefore, another explanation for the vacuolar trafficking defects in BFA-treated *big3* mutants could be that there is either a vesicle trafficking step from the TGN to the MVB or a direct connection between TGN and vacuole which is regulated by an ARF GTPase, ARF-GEF and clathrin regulatory network (Figure 4b).

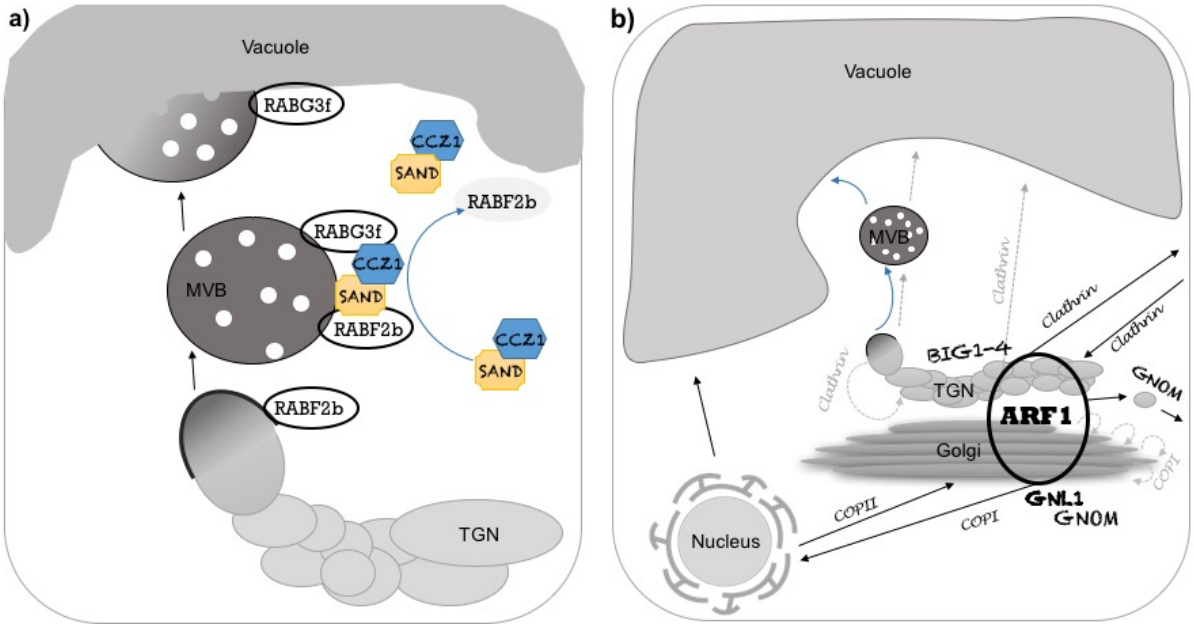

Figure 4. Overview of the molecular machineries regulating intracellular trafficking routes

(a) *Detailed scheme of late endosome maturation in Arabidopsis cells. A subdomain of the TGN membrane becomes enriched with RAB5-like GTPases like RABF2b. After maturation from the TGN, active RABF2b recruits the RAB7-GEF complex SAND/CCZ1 to the MVB membrane where SAND/CCZ1 activates the RAB7-like GTPase RABG3f. After RAB conversion the activity of RABG3f is required for MVB and vacuole fusion. Black encircled RAB GTPases stand for RAB•GTP while light grey backgrounds resemble RAB•GDP. (b) Scheme of ARF1 mediated vesicle trafficking pathways. ARF1 is a central regulator of vesicle trafficking within the Arabidopsis endomembrane system. Newly synthetized proteins are transported from the ER via COPII coated vesicles to the Golgi. For retrograde trafficking the GTPase ARF1 is activated by GNL1 and GNOM resulting in the recruitment of COPI coat proteins to the cis Golgi side. COPI may also play a role in retrograde vesicle trafficking between maturing Golgi cisternae. Activation of ARF1 at the TGN by BIG1-4 leads to AP1 and clathrin recruitment required for late secretory or vacuolar trafficking. It is not clear how BIG1-4 exactly contribute to vacuolar protein transport, as they may either regulate vesicle trafficking from a subdomain of the TGN back to the core of the compartment or from the TGN via, or without the MVB, to the vacuole. However, most proteins seem to reach the vacuole by MVB maturation from a subdomain of the TGN followed by fusion with the vacuole. Recycling of endocytosed PIN1 auxin efflux carrier is mediated by ARF1 activation upon interaction with GNOM at the putative recycling endosome. Black arrows indicate known vesicular trafficking routes, dashed grey arrows highlight possible but not proven vesicular trafficking ways and blue arrows mark protein transport directions by maturation and fusion steps.*

5.3. The ARF GTPase ARF1 regulates all essential trafficking pathways in *Arabidopsis thaliana*

Molecular switches of the ARF GTPase subfamily are main regulators of vesicle formation steps. Upon activation by ARF-GEFs, ARF GTPases recruit coat proteins to membranes, which ultimately leads to vesicle budding. In Arabidopsis, beside ARF-Like proteins (ARLs), three subclasses of ARF GTPases were identified and named ARF1, ARFA and ARFB (Singh and Richter et al., 2018). While ARF1 GTPases are conserved between all eukaryotes, ARFA and ARFB seem to be plant-specific subclasses with largely unknown function. A recent study of our group that analyzed ARF GTPases in plants showed that ARFA and ARFB are no essential regulators of main vesicle trafficking pathways in *Arabidopsis thaliana* (Singh and Richter et al.,

2018). However, it is still possible that ARFA and ARFB regulate specific transports steps required during special developmental processes or as a response to environmental cues. In contrast, the ARF GTPase ARF1 was shown to be involved in the regulation of all essential trafficking processes at the Golgi and TGN (Singh and Richter et al., 2018) (Figure 4b). Considering that ARF1 then was shown to interact with all known Arabidopsis ARF-GEFs in co-immunoprecipitation studies, it doesn't surprise that subsequent studies with ARF1-TN and markers for secretory, endocytic, recycling and vacuolar trafficking basically mimicked all observed defects of *gnom*, *gnl1, big5* or BFA-treated *big3* mutants (Singh and Richter et al., 2018). ARF1 recruits COPI coat proteins to the Golgi upon GNL1 and GNOM activation (Richter et al., 2007) as well as clathrin coat components to the TGN upon BIG1-4 activation (Richter et al., 2014) (Figure 4b). How a single class of ARF GTPases is able to recruit specific coat complexes to different membrane sites leads to the question of how the temporal and spatial activation of ARF1 is regulated.

5.4. How could specificity of ARF1-mediated vesicle trafficking be achieved?

The differently localizing ARF-GEFs seem to be good candidates for conferring specificity to ARF1-mediated trafficking. However, this assumption leaves a lot of questions open as it is still not known how ARF-GEFs like GNOM or GBF1 can activate ARF1 at distinct endomembrane compartments in the context of different cargo and trafficking routes. Strikingly, it was shown that the catalytic SEC7 domains of Golgi-localized GNL1 and TGN-localized BIG3 can be swapped with each other (GNL1::GNL1-$^{BIG3\text{-}SEC7}$:MYC in *gnl1* and UBQ::BIG3-$^{GNL1\text{-}SEC7}$:YFP in *big3*) without interfering with COPI or clathrin recruitment (Singh and Richter et al., 2018). Therefore, the catalytic activity of the ARF-GEF SEC7 domain does not confer any kind of specificity to ARF1 activation. A possible mechanism to ensure specific recruitment of coat proteins was suggested by the study of Deng et al. Here, an interaction of specific ARF-GEFs with distinct coat proteins independent of ARF1 activation was demonstrated for COPI and GBF1/GEA1 in animal cells (Deng et al., 2009). Yet, in plants it is not known whether ARF-GEFs and coats are able to directly interact with each other and where and when the interaction would take place.

5.5. Requirement of the DCB domain for ARF-GEF membrane association

Up to date it is still enigmatic how different ARF-GEFs are able to associate with distinct membranes or even how membrane association in general is accomplished. The domain architecture of large ARF-GEFs in general is quite conserved across the eukaryotes. Between the GBF1-related and BIG-related ARF-GEFs only the number of HDS domains at the C-terminus may vary a little. Several years ago, it was discovered that the interaction of the DCB domain with at least one of the C-terminally adjacent domains (HUS and SEC7) is important for membrane association of human and plant ARF-GEFs (Ramaen et al., 2007; Anders et al., 2008) (Figure 3). Single amino acid exchanges in the N-terminal part of the SEC7-domain of GNOM (G579R → *b4049*) and in the HUS-domain (D468G → HUS box motif) each interfere with the intramolecular interaction of the DCB domain with ΔDCB(GNOM) (Anders and Jürgens, 2008) (Figure 6a). Interestingly, when specific amino acid residues in the HDSI domain of GNOM were recently mutated, DCB(GNOM) did not interact with the rest of the protein (ΔDCB(GNOM)) anymore in yeast two-hybrid assays (Hauke Beckmann, personal communication) (Figure 5 and 6a). Therefore, it seems likely that the HUS, SEC7 and HDSI domains of GBF1-related plant ARF-GEFs together form an interaction platform for the DCB domain (Figure 5 and 6a). Upon intramolecular interaction of the DCB domain with the HUS-SEC7-HDS1 interaction surface, the folded ARF-GEF is able to associate with the membrane where it probably opens up to be able to bind ARF1 (Anders et al., 2008) (Figure 5). A similar model of conformational changes within the ARF-GEF protein was recently proposed for the regulation of the yeast ARF-GEF Sec7p (Halaby and Fromme, 2018). In this model, a structural unit of the DCB and HUS domain interacts with the C-terminal HDSI, II and III domains, leading to a closed conformation of Sec7p in the cytosol. After binding to the RAB11-like GTPase Ypt31 at the TGN, Sec7p changes to an open state, resulting in allosteric activation of GEF activity. It remains unclear whether the Sec7p-related Arabidopsis ARF-GEFs BIG1-5 require HDSI and HDSII for membrane association. However, not only the conformational state of ARF-GEFs seems to be important for membrane association in general but also interactions with potential adaptor proteins or the lipid composition at endomembrane compartments may determine the specific localization of particular ARF-GEF members. As *in vitro* studies can often only reveal some but not all of the required factors, one *in vivo* approach for a deeper understanding of the Arabidopsis ARF-GEF spatial regulation could be to perform

domain-swapping experiments between members of the same subfamily (e.g. GNOM and GNL1, BIG3 and BIG5) or even between different subfamilies (e.g. GNL1 and BIG3). Rescue experiments and subcellular localization studies with several domain chimeras could narrow down which domains have a central function in mediating ARF-GEF membrane association *in vivo*.

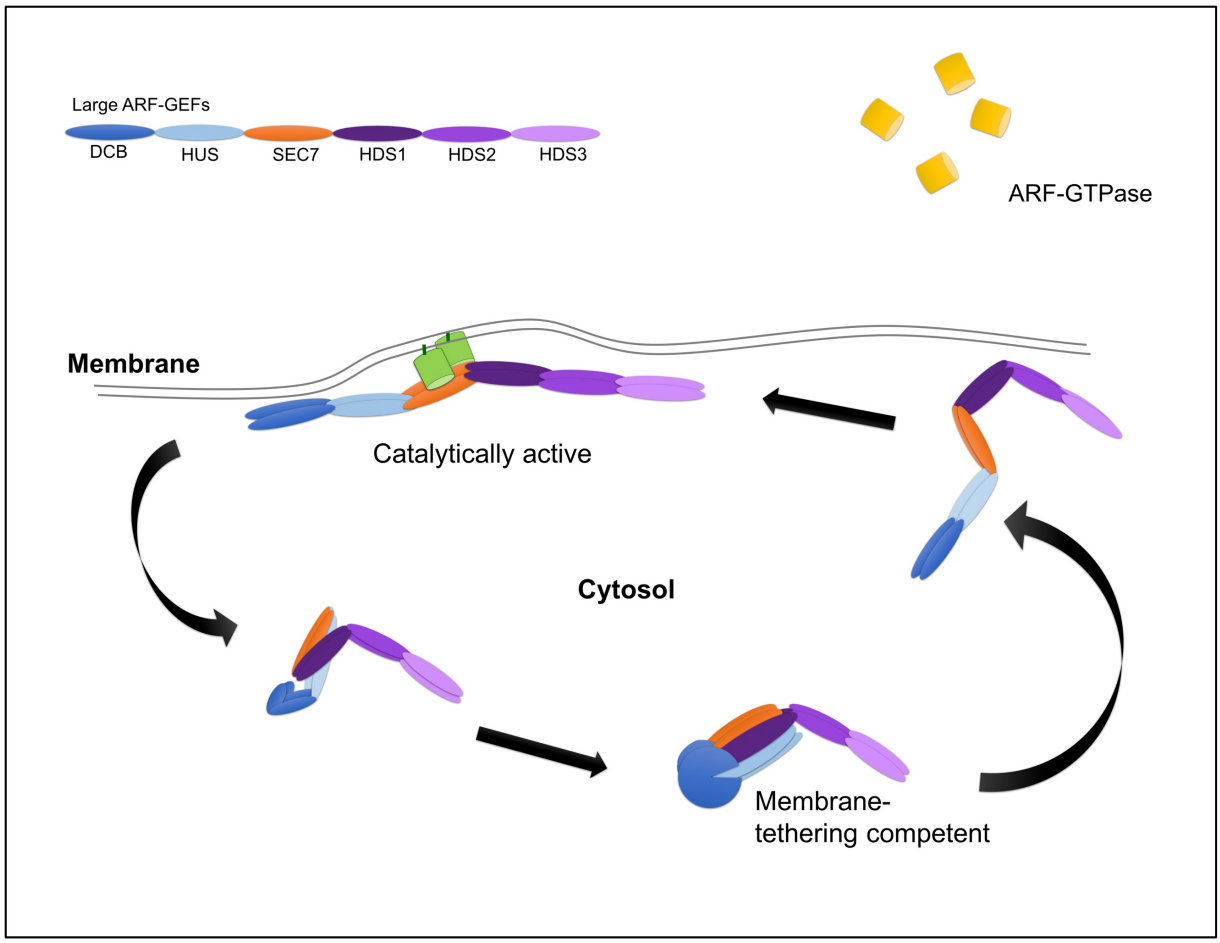

Figure 5. Simplified scheme of ARF-GEF intra- and intermolecular interactions required for membrane association (modified according to Anders et al., 2008)

The GNOM DCB domain interacts in addition to the already published finding of HUS and SEC7 domain also with the HDSI domain. HUS, SEC7 and HDSI domain together might form a "cup-shaped" interaction platform for the DCB domain. Upon association with the membrane, the ARF-GEF dimer interacts with two ARF1•GDP molecules. The conformational change upon GDP to GTP exchange probably leads to the direct interaction of two ARF1•GTP molecules at the membrane.

5.6. The dual function of the DCB domain in promoting and preventing dimerization of particular ARF-GEFs

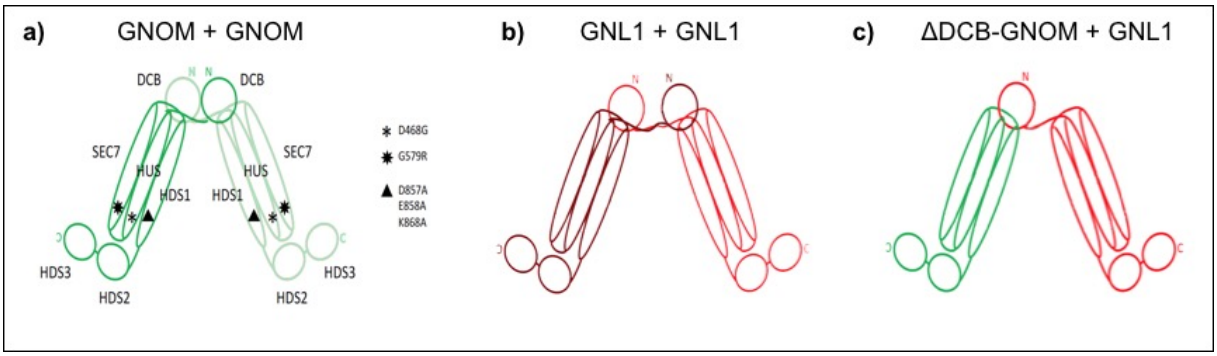

Figure 6. Simplified scheme of DCB-mediated ARF-GEF dimerization

(a) GNOM DCBs interact with each other and in addition heterotypically with the HUS-SEC7-HDSI. The interaction surface can be disrupted by D468G (HUS box), G579R (b4049) or D857A, E858A and K868A (HDSI motif) amino acid exchanges. (b) The DCB-domain of one GNL1 molecule interacts with the HUS-SEC7-HDSI interaction surface of another GNL1 molecule leading to a functional dimer even though the DCB domains themselves do not interact with each other. (c) GNOM lacking the DCB-domain (ΔDCB-GNOM) is able to interact with full length GNL1 protein because GNL1 DCB-domain can fold onto the HUS-SEC7-HDSI interaction surface of GNOM. In summary, ARF-GEFs can dimerize in two different ways: either via DCB-DCB interaction or intermolecular interaction of the DCB-domain with the SEC7-HUS-HDSI interaction surface of a second molecule.

Besides its role in ARF-GEF membrane association, actually the N-terminal DCB domain was first characterized as facilitating dimerization of Arabidopsis GNOM *in vitro* and *in vivo* (Grebe et al., 2000; Anders et al., 2008). Further studies revealed the evolutionary conservation of DCB-DCB interaction of mammalian GBF1 and BIG1/2 in yeast two-hybrid analysis (Ramaen et al., 2007). Yet, while also the yeast Gea1p and Gea2p homodimerize via their N-terminal domains, the yeast ARF-GEF Sec7p undergoes mechanistically different dimerization via the C-terminal HDSIIII domain (Richardson et al., 2016). Interestingly, we recently discovered that the DCB-DCB dimerization mechanism is not conserved between the two highly similar Arabidopsis GBF1-related ARF-GEFs GNOM and GNL1 (Brumm et al., manuscript in preparation). In contrast to DCB(GNOM), DCB domains of GNL1 do not dimerize in yeast two-hybrid analysis. However, in co-immunoprecipitation an interaction of two full- length GNL1 proteins can be detected *in vivo*. Although no DCB DCB interaction was detectable in yeast two-hybrid assays, the DCB domain of GNL1 was able to interact with the rest of the protein (ΔDCB(GNL1)) suggesting the dimerization of GNL1 dimerization via an interaction of the DCB domain with the HUS-SEC7-HDSI interface of a second GNL1 protein *in vivo* (Figure 2b). Interestingly, although the DCB domains of both GNOM and GNL1 are able to interact with both ΔDCB(GNL1) and ΔDCB(GNOM) in yeast two-hybrid analysis, no heterodimers of full-length GNOM and GNL1 can be detected *in vivo*. GNL1 and GNOM localize to the Golgi and mediate retrograde vesicle trafficking

between Golgi and ER via interaction with ARF1 followed by COPI coat recruitment (Richter et ak., 2007; Singh and Richter et al., 2018). Additionally, GNOM- mediated ARF1 activation is required for polar recycling of the auxin efflux carrier PIN1 (Steinmann et al., 1999; Geldner et al., 2003). Surprisingly, genetic complementation assays clearly showed that the close homologue GNL1 is not able to replace GNOM function in PIN1 recycling (Richter et al., 2007), raising the question of how the two proteins and functions are kept separate. To address this question we introduced ΔDCB(GNOM) into *gnom* knockout *sgt* (Brumm et al., manuscript in preparation). In the *sgt* allele, *GNOM* and flanking genes are missing due to a large deletion caused by transposon insertion (Brumm et al., manuscript in preparation). Surprisingly, ΔDCB(GNOM) was able to rescue *sgt* except for some post-embryonic defects (Brumm et al., manuscript in preparation). Initially, no rescue was expected since the missing DCB should be required for membrane association of the ARF-GEF via interaction with the HUS and SEC7 domains (Anders et al., 2008). One idea, how ΔDCB(GNOM) could still reach the membrane and therefore rescue *sgt,* was the involvement of a DCB domain of another Arabidopsis ARF-GEF molecule. GNL1 seemed to be a good candidate because of the high sequence similarity to GNOM and the ability of DCB(GNL1) to interact with ΔDCB(GNOM) in yeast two-hybrid analysis. Indeed, subsequent co-immunoprecipitation analysis revealed interaction of ΔDCB(GNOM) with full-length GNL1 (Brumm et al., manuscript in preparation). Moreover, ΔDCB(GNOM) was unable to rescue the *sgt gnl1* double mutant, confirming the requirement of GNL1 for ΔDCB(GNOM) functionality. Interaction with ΔDCB(GNOM) also shifted the localization of GNL1 from Golgi stacks to the endosomal BFA compartment in BFA-treated root cells. These findings imply that the DCB domain is required for dimerization and membrane association of ARF-GEFs in general but does not confer compartment-specific localization. As mentioned above, swapping experiments between other GNOM and GNL1 domains may help to answer the question how the localization and function of the two proteins are kept separate within a plant cell.

In summary, these results suggest that the DCB domain of GNOM normally prevents heterodimerization of GNOM and GNL1, probably to ensure effective PIN1 recycling but also efficient secretory trafficking during developmental processes where both trafficking pathways are needed at the same time. Similarly, efficient PIN1 recycling mediated by GNOM is ensured while most endocytosed proteins are redirected to the

plane of cell division by BIG1-4 during cytokinesis (Richter et al., 2007). In the future, it would be exciting to find specific amino-acid motifs in the DCB domain of GNL1 that inhibit its homotypic interaction. An EMS screen or computational analysis of the DCB domain of GNL1 in combination with further yeast two-hybrid studies could be useful for the identification. If Arabidopsis ARF-GEFs of the BIG subfamily also dimerize *in vivo* and if DCB-DCB interaction or rather DCB with the HUS-SEC7-HDSI domains would be required for dimerization is not known so far. It would be interesting to investigate if for example the two different subclades of BIGs (BIG1-4 and BIG5) might be kept separate by DCB-DCB-mediated homodimerization. Nevertheless, beside keeping the different members of specific ARF-GEF families separate, it is still not clear why ARF-GEFs form dimers *in vivo* at all and not rather act as monomeric proteins.

5.7. The biological relevance of ARF and ARF-GEF dimerization in ARF1-mediated vesicle trafficking events

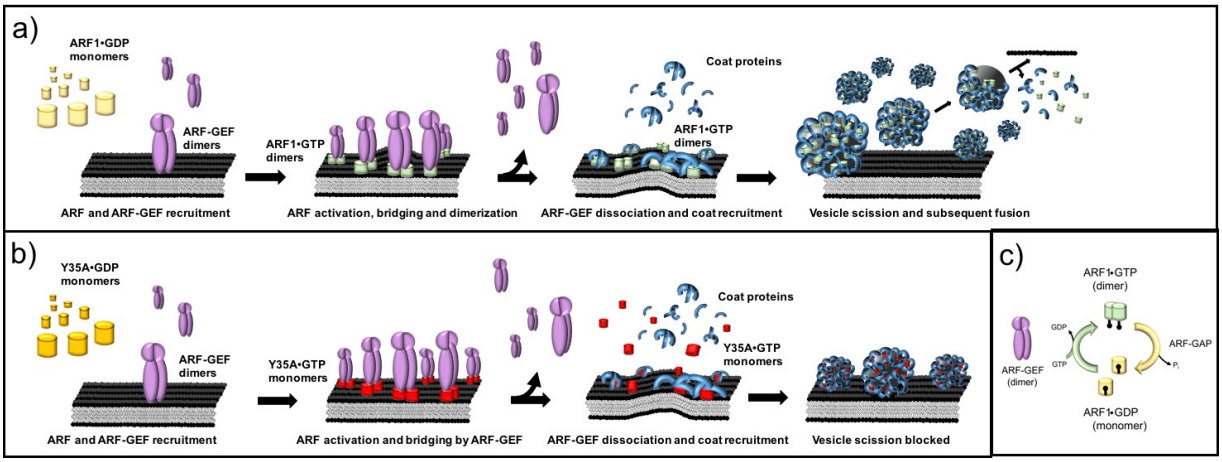

Figure 7: Simplified scheme of vesicle budding processes requiring ARF1 activation and dimerisation mediated by ARF-GEFs

(a) Vesicle formation is initiated by the recruitment of monomeric ARF1•GDP and ARF-GEFs dimers to the membrane. At the membrane two ARF1•GDP molecules are bridged by an ARF-GEF dimer. Upon GDP to GTP exchange catalyzed by the ARF-GEF dimer, the conformational change of the ARF proteins leads to stable insertion into the membrane and direct interaction of two ARF1 molecules. After ARF1 activation, the ARF-GEF dimer dissociates from the membrane. The active ARF1 dimer recruits coat proteins to the membrane which leads to membrane curving and vesicle bud formation. ARF1 dimerization is important for vesicle scission as the stable insertion of the dimer may create local strains at the vesicle neck region (Beck et al., 2011). Before vesicle fusion, inactive ARF1•GDP monomers and coat proteins are released into the cytosol. (b) The ARF1-variant Y35A in the GDP state is recruited to the membrane and bridged by an ARF-GEF dimer. Upon GDP to GTP exchange, Y35A does not dimerize but still recruits coat proteins to the membrane subsequentially leading to vesicle bud formation. The membrane insertion of monomeric Y35A at the vesicle neck region may not create the for vesicle scission required mechanical forces and as a consequence, vesicles cannot bud off. (c) Simplified scheme of ARF GTPase dimerization cycle. Monomeric ARF1•GDP is activated by ARF-GEF dimers which catalyze the GDP to GTP exchange reaction. Upon the conformational change ARF1•GTP molecules form dimers at the membrane. ARF-GAPs trigger the hydrolysis of GTP to GDP and the inactive ARF1•GDP monomers return to the cytosol.

One possible explanation for ARF-GEF dimerization could simply be an enhancement of protein stability by amino-acid interactions within the dimer as it is suggested by data from a oligomerization-deficient GBF1 mutant (Bhatt et al., 2016). When amino acids K91 and E130 were substituted with alanine residues within the DCB domain of full-length GBF1 protein, oligomerization of GBF1 was compromised but otherwise the protein was still functional, although its degradation was enhanced compared to wildtype. Nevertheless, our latest data offers a different explanation and assigns ARF-GEF dimers an essential role in Arabidopsis vesicle formation. In co-immunoprecipitation experiments, a GNOM variant impaired in ARF1 binding (GNOM-Loop>J(3A)) was able to heterodimerize with wildtype GNOM but the heterodimer did not interact with ARF1 (Brumm et al., manuscript in preparation). The Loop>J region of the SEC7 domain is conserved among eukaryotic ARF-GEFs and was first discovered to play a role in ARF1 binding and catalytic ARF-GEF activity in mammals (Lowery et al., 2011). Our result implies that coordinated and simultaneous interaction with two ARF-GEF molecules is required for high-affinity ARF binding which may lead to the dimerization of two ARF1•GTP molecules upon conformational changes during the ARF activation process (Figure 5 and 7a). Consistently, by further co-immunoprecipitation experiments we were able to show that also the ARF1 GTPase forms dimers *in vivo* at the membrane (Brumm et al., manuscript in preparation). As the activation-impaired ARF1-TN variant is able to interact with both endogenous ARF1 protein and the ARF-GEF GNOM, we hypothesize that the ARF-GEF dimer bridges two ARF1•GDP molecules at the membrane. Once, the catalytic reaction takes place and the conformation of ARF1 changes, probably the two ARF1•GTP molecules are able to directly interact with each other by intermolecular forces. This is supported by the finding that the hydrolysis-impaired ARF1-QL variant interacts with endogenous ARF1 but almost not with GNOM anymore. Previous studies with mammalian ARF1 protein already pointed out ARF1 dimerization *in vitro (Beck et al., 2008)*. However, their experiments required chemical crosslinking of the two ARF1 molecules and dimerization was only observed for ARF1•GTP. Furthermore, it was shown that a Y35A mutation in ARF1 inhibits dimerization of ARF1. We tested the Arabidopsis ARF1-Y35A variant in a protein secretion assay. The assay allows the quantification of protein transport through the endomembrane system by determining the activity of secreted α-amylase enzyme in transformed protoplasts and medium (Pimpl et al., 2003). Recently, it was shown that the inhibitory effect of ARFA-QL on secretory

trafficking can be suppressed by overexpression of ARFA-WT (Singh and Richter et al., 2018). Since the activation-impaired ARF1-T31N variant was shown to inhibit secretion of α-amylase in tobacco protoplasts as well (Pimpl et al., 2003), we tested whether overexpression of ARF1-Y35A would restore secretory trafficking like it would be expected of ARF1-WT. Expression of ARF1-T31N in tobacco protoplast leads to a competition for interacting ARF-GEFs between activation-impaired ARF1-T31N and endogenous ARF1. As ARF1-T31N is not able to get its GDP exchanged by GTP, the ARF-GEF will not dissociate anymore and therefore the activators for endogenous ARF1 will lack over the time. However, concurrent overexpression of ARF1-WT should counteract the titration effect as more ARF1-WT than ARF1-T31N molecules are likely to encounter an ARF-GEF molecule. Indeed, overexpression of ARF1-WT rescued the ARF1-T31N-caused secretion block of α-amylase whereas ARF1-Y35A rescue ability was impaired. Interestingly, overexpression of ARF1-Y35A alone impaired secretory transport of α-amylase as well. Since ARF1-Y35A is still able to slightly rescue ARF1-T31N impaired secretion, it is likely that ARF1-Y35A is defective in a function required at later stages of ARF1 activation (Brumm et al., manuscript in preparation). Assuming that ARF1-Y35A is actually monomeric, these results imply that dimerization of ARF1 GTPases is essential for vesicle formation in Arabidopsis (Figure 7b). Beck et al. proposed a molecular model in a second study which offers an explanation for the requirement of ARF1 dimerization in the scission of vesicles (Beck et al., 2011). The interaction of coat complexes with dimeric ARFs would lead to specific arrangement of the ARF1 amphipathic helices in the membrane, resulting in mechanical forces required for vesicle off-pinching (Figure 7b). Interestingly in an EMS screen for altered PIN1-GFP trafficking mutants, the *bfa-visualized exocytosis defective* mutant *bex1* was discovered. The mutant has a single amino acid exchange from leucine to phenylalanine at position 34 (L34F) in the ARF1 isoform ARF1A1C (Tanaka et al., 2014). However, the molecular mechanisms causing the observed phenotypic differences of *bex1* in comparison to wildtype are still unknown. It would be interesting to know, if the BEX1 protein is also impaired in ARF1 dimer formation as the ARF1-Y35A variant. Furthermore, a monomeric ARF-GEF variant should be generated in the future to prove the necessity of ARF-GEF dimerization for vesicle trafficking events. However, this project could turn out to be quite challenging for several reasons. First, it is not clear whether amino acid replacements according to the previously mentioned K91 and E130 amino acids in the DCB domain would inhibit GNOM dimerization

mediated by DCB-DCB interaction. Furthermore, the heterotypic interaction of DCB domain with HUS, SEC7 and HDSI domains is required for ARF-GEF membrane association and can hence not be disrupted as demonstrated by the failed rescue of ΔDCB(GNOM) in the *sgt gnl1* double mutant. Nevertheless, it would be interesting to see if the proposed mechanism of ARF-GEF-mediated ARF dimerization is not only true for GNOM but also for the other Arabidopsis ARF-GEFs. As not only Arabidopsis but also mammalian and yeast large ARF-GEFs dimerize *in vivo,* ARF-GEF-mediated ARF1 dimerization may be a conserved mechanism across the eukaryotes.

5.8. Conclusions

Vital processes of eukaryotic organism rely on the ability to exchange material between different cellular compartments. The transport of proteins is accomplished by the exchange of membranes via vesicle trafficking, maturation or fusion within the system. In the last years, research focused on the investigation of maturation processes being important for vacuolar trafficking. In accordance to the high diversification of plant vacuolar function, multiple vacuolar trafficking pathways seem to exist and a future goal will be the identification of the underlying regulatory machineries. Complex networks of interactions between several small GTPases, effector proteins and upstream regulators form the basis of regulatory machineries required for spatially and temporally coordinated protein transport. Inducible expression systems, multiple knockout-mutants and target-specific inhibitors allowed just recently the functional characterization of large Arabidopsis ARF-GEFs BIG1-4. However, many molecular features of ARF-GEF-specific functions are still not understood. Even though, the dimerization ability of ARF-GEFs was long time known, the biological relevance remained elusive. Our model suggests that cooperative binding of ARF-GEF dimers mediates the dimerization of two ARF-GTPase molecules *in vivo*. The dimerization ability of vesicle trafficking regulators may on one hand broaden the functional spectrum of single molecules and on the other hand enable the separation of architectural highly similar proteins. Future research focus should lay on the identification of factors adding specificity to the regulatory network of ARF1 and its interactors.

6. Publications

6.1. Richter et al., 2014

Delivery of endocytosed proteins to the cell–division plane requires change of pathway from recycling to secretion

Sandra Richter, Marika Kientz, **Sabine Brumm,** Mads Eggert Nielsen, Misoon Park, Richard Gavidia, Cornelia Krause, Ute Voss, Hauke Beckmann, Ulrike Mayer, York-Dieter Stierhof and Gerd Jürgens

Elife *3*, e02131

2014

eLIFE elifesciences.org

RESEARCH ARTICLE

Delivery of endocytosed proteins to the cell–division plane requires change of pathway from recycling to secretion

Sandra Richter[1], Marika Kientz[1], Sabine Brumm[1], Mads Eggert Nielsen[1†], Misoon Park[1], Richard Gavidia[1], Cornelia Krause[1], Ute Voss[1‡], Hauke Beckmann[1], Ulrike Mayer[2], York-Dieter Stierhof[2], Gerd Jürgens[1*]

[1]Department of Developmental Genetics, The Center for Plant Molecular Biology (ZMBP), University of Tübingen, Tübingen, Germany; [2]Microscopy, The Center for Plant Molecular Biology (ZMBP), University of Tübingen, Tübingen, Germany

Abstract Membrane trafficking is essential to fundamental processes in eukaryotic life, including cell growth and division. In plant cytokinesis, post-Golgi trafficking mediates a massive flow of vesicles that form the partitioning membrane but its regulation remains poorly understood. Here, we identify functionally redundant Arabidopsis ARF guanine-nucleotide exchange factors (ARF-GEFs) BIG1–BIG4 as regulators of post-Golgi trafficking, mediating late secretion from the trans-Golgi network but not recycling of endocytosed proteins to the plasma membrane, although the TGN also functions as an early endosome in plants. In contrast, BIG1-4 are absolutely required for trafficking of both endocytosed and newly synthesized proteins to the cell–division plane during cytokinesis, counteracting recycling to the plasma membrane. This change from recycling to secretory trafficking pathway mediated by ARF-GEFs confers specificity of cargo delivery to the division plane and might thus ensure that the partitioning membrane is completed on time in the absence of a cytokinesis-interphase checkpoint.
DOI: 10.7554/eLife.02131.001

***For correspondence:** gerd.juergens@zmbp.uni-tuebingen.de

Present address: †Department of Plant and Environmental Sciences, University of Copenhagen, Copenhagen, Denmark; ‡Plant Sciences Division, School of Biosciences, University of Nottingham, Nottingham, United Kingdom

Competing interests: The authors declare that no competing interests exist.

Funding: See page 14

Received: 19 December 2013
Accepted: 27 February 2014
Published: 08 April 2014

Reviewing editor: Christian S Hardtke, University of Lausanne, Switzerland

Introduction

In post-Golgi membrane trafficking, cargo proteins are dynamically distributed between trans-Golgi network (TGN), various endosomes, lysosome/vacuole and plasma membrane (***Surpin and Raikhel, 2004***). In contrast to animals, the TGN also functions as an early endosome in plants and is a major trafficking hub where secretory, endocytic, recycling and vacuolar pathways intersect (***Viotti et al., 2010***; ***Reyes et al., 2011***). Therefore, it has been notoriously difficult to functionally delineate the recycling vs secretory pathways in plants. Sorting of cargo proteins occurs during the formation of transport vesicles, involving activation of small ARF GTPases by ARF guanine-nucleotide exchange factors (ARF-GEFs) and recruitment of specific coat proteins (***Casanova, 2007***). Arabidopsis ARF-GEFs are related to human large ARF-GEFs, GBF1 or BIG1. Whereas the three GBF1-related members GNOM, GNL1 and GNL2 have been characterised in detail (***Geldner et al., 2003***; ***Richter et al., 2007***, ***2012***), of the 5 BIG1-related ARF-GEFs only BIG5 has been analysed so far and implicated in pathogen response (MIN7) and endocytic traffic (BEN1) (***Nomura et al., 2006***, ***2011***; ***Tanaka et al., 2009***; ***Tanaka et al., 2013***). Here, we show that ARF-GEFs BIG1-4 play a crucial role in post-Golgi traffic, which enables us to dissect the regulation of secretory and recycling pathways in interphase and cytokinesis.

eLife digest Cells are surrounded by a plasma membrane, and when a cell divides to create two new cells, it must grow a new membrane to keep the two new cells apart. Animal cells and plant cells tackle this challenge in different ways: in animal cells the new membrane grows inwards from the surface of the cell, whereas the new membrane grows outwards from the centre of the cell in plant cells.

The materials needed to make the plasma membrane are delivered in packages called vesicles: most of these materials arrive from a structure within the cell called the trans-Golgi network, but some materials are recycled from the existing plasma membrane. In plants the formation of the new cell membrane is orchestrated by scaffold-like structure that forms in the plant cell called the 'phragmoplast'. It is widely thought that this structure guides the vesicles bringing materials from the trans-Golgi network, but the details of this process are not fully understood.

Now, Richter et al. have discovered four proteins, called BIG1 to BIG4, that control the formation of the new cell membrane in the flowering plant *Arabidopsis thaliana*, a species that is routinely studied by plant biologists. These four proteins belong to a larger family of proteins that control the trafficking of vesicles within a cell. Richter et al show that a plant cell can lose up to three of these four proteins and still divide, as the plant can still grow and develop as normal. Thus, BIG1 to BIG4 appear to perform essentially the same role in the plant.

Richter et al. also show that, when a plant cell is not dividing, these proteins are involved in controlling the delivery of new materials to surface membrane, and not the recycling of material. However, when a cell is dividing, these proteins switch to regulate both processes, but direct all the material to a new destination—the newly forming membrane, instead of the established surface membrane. Richter et al. suggest that this switch is important to stop any recycling to the plasma membrane that might move material away from the new membrane. The next challenge will be to identify the molecular signals and mechanisms that enable the proteins BIG1 to BIG4 to re-route the recycling of membrane material during cell division.

DOI: 10.7554/eLife.02131.002

Results

ARF-GEFs BIG1 to BIG4 are redundantly required in development

Up to three of ARF-GEFs BIG1 to BIG4 (BIG1-4) were knocked out without recognisable phenotypic effect except for *big1,2,3*, which was retarded in growth because BIG4 is predominantly expressed in root and pollen (***Figure 1A***, ***Figure 1—figure supplement 1A***). Other triple mutants were growth-retarded only if the activity of the respective fourth gene was reduced to 50%. No quadruple mutants were recovered because BIG1-4 were essential in male reproduction, sustaining pollen tube growth (***Figure 1B***, ***Figure 1—figure supplement 1B***). BIG1-4 functional redundancy would be consistent with the occurrence of *BIG1-4*-like single-copy or closely related sister genes in lower plants (***Figure 1—figure supplement 1C***). Although large ARF-GEFs are often inhibited by the fungal toxin brefeldin A (BFA), the SEC7 domain of BIG3 (At1g01960; formerly named BIG2 in ***Nielsen et al., 2006***; see nomenclature used by ***Cox et al., 2004***) displayed BFA-insensitive GDP/GTP exchange activity in vitro (***Nielsen et al., 2006***). BFA treatment of *big3* mutants impaired seed germination and seedling root growth, in contrast to wild-type (***Figure 1D,E***). We engineered a BFA-resistant variant of the naturally BFA-sensitive ARF-GEF BIG4 by replacing amino acid residue methionine at position 695 with leucine, as previously described for the recycling ARF-GEF GNOM (***Geldner et al., 2003***). Engineered BFA-resistant BIG4-YFP rescued BFA-inhibited seed germination of *big3* (***Figure 1F***). The rescue activity of BFA-resistant BIG4 was comparable to that of BIG3 when both were expressed from the ubiquitin 10 (*UBQ10*) promoter whereas BFA-sensitive BIG4 did not at all rescue BFA-inhibited primary root growth of *big3* mutant seedlings (***Figure 1—figure supplement 1D,E***). Thus, BFA treatment of *big3* single mutants effectively causes conditional inactivation of BIG1-4 ARF-GEF function, providing us with a unique tool for studying BIG1-4-dependent trafficking in an organismic context.

BIG1 to BIG4 regulate membrane trafficking at the TGN

BIG4-YFP co-localized with TGN markers vacuolar H^+-ATPase (VHA) subunit a1 and ARF1 GTPase (***Figure 1I–L***, ***Figure 1—figure supplement 2O–R***; ***Dettmer et al., 2006***; ***Stierhof and El Kasmi,***

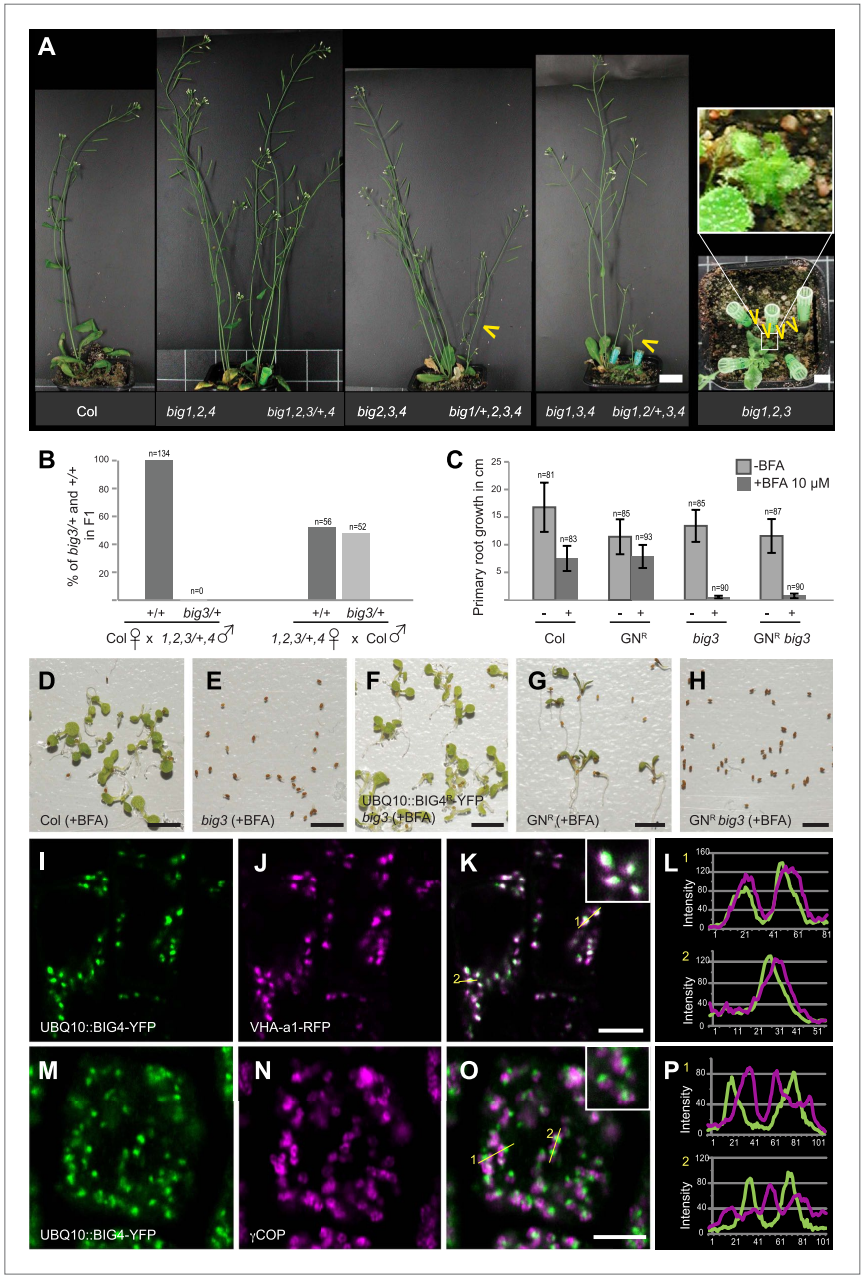

Figure 1. BIG1 – BIG4 act redundantly at TGN and are involved in several physiological processes. (**A**) *big1,2,4 (big1 big2 big4), big2,3,4 (big2 big3 big4), big1,3,4 (big1 big3 big4)* and *big1,2,3/+,4 (big1 big2 big3/BIG3 big4)* mutant plants without obvious phenotype but *big1/+,2,3,4 (big1/BIG1 big2*

Figure 1. Continued on next page

Figure 1. Continued

big3 big4), big1,2/+,3,4 (big1 big2/BIG2 big3 big4) and *big1,2,3 (big1 big2 big3)* were dwarfed (yellow arrowheads). Scale bar, 2 cm. (**B**) F1 of reciprocal crosses between wild-type (Col) and *big1 big2 big3/BIG3 big4* (*1,2,3/+,4*) mutants: 0% or 48% *big3* heterozygous seedlings derived from mutant male or female gamete, respectively. (**C**) BFA inhibited primary root growth of *big3* mutant seedlings with or without BFA-resistant GNOM (GN^R *big3*). Numbers of analysed seedlings are indicated (**B** and **C**). (**D**-**H**) BFA treatment did not prevent seed germination in wild-type (Col; **D**) and BFA-resistant GN (GN^R; **G**) but did so in *big3* mutants without (**E**) or with BFA-resistant GNOM (GN^R *big3*; **H**). This defect was suppressed by BFA-resistant BIG4 (UBQ10::BIG4R-YFP *big3*; **F**). Scale bar, 5 mm. (**I**-**L**) Live imaging of BIG4-YFP (**I**) and TGN marker VHA-a1-RFP (**J**) revealed co- localization (**K**; **L**, intensity–line profile). (**M**–**P**) Immunolocalization of BIG4 (UBQ10::BIG4-YFP; M) and Golgi-marker γCOP (**N**) indicated no co-localization (**O**; **P**, intensity–line profile). (**I**–**K**, **M**–**O**) Scale bar, 5 μm.

DOI: 10.7554/eLife.02131.003

The following figure supplements are available for figure 1:

Figure supplement 1. Expression and phylogeny of BIG ARF-GEFs.

DOI: 10.7554/eLife.02131.004

Figure supplement 2. BIG3 and BIG4 localize at the TGN.

DOI: 10.7554/eLife.02131.005

Figure supplement 3. Ultrastructural localization of BIG4-YFP and ultrastructural abnormalities in BFA-treated *big3* mutant seedling root cells.

DOI: 10.7554/eLife.02131.006

2010) but not with Golgi marker COPI subunit γCOP (***Figure 1M–P***; ***Movafeghi et al., 1999***). TGN localization of BIG4-YFP was confirmed by immunogold labeling on EM sections (***Figure 1—figure supplement 3A,B***). BIG3-YFP and BIG4-YFP co-localized with endocytic tracer FM4-64, labeling TGN after brief uptake (***Figure 1—figure supplement 2A–H***; ***Ueda et al., 2001***; ***Dettmer et al., 2006***). BIG3 and BIG4 also accumulated together with FM4-64 in BFA-induced post-Golgi membrane vesicle aggregates ('BFA compartments'), consistent with ultrastructural abnormalities in these aggregates and Golgi stacks in BFA-treated *big3* mutant (***Figure 1—figure supplement 2I–N, 3C–F***). Together, these data suggest a role for BIG1-4 in post-Golgi membrane trafficking.

Secretory and vacuolar trafficking depend on BIG1 to BIG4 function

To identify trafficking routes regulated by BIG1-4, pathway-specific soluble and membrane-associated cargo proteins were analysed in BFA-treated wild-type and *big3* mutant seedlings (for a list of markers used, see ***Supplementary file 1***; ***Figure 2—figure supplement 1S,T***). Secretory GFP (secGFP) (***Viotti et al., 2010***), which is normally secreted from the cell, and plasma membrane (PM)-targeted syntaxin SYP132 were trapped in BFA compartments and did not reach the plasma membrane of *big3* seedlings, in contrast to wild-type, suggesting a role for BIG1-4 in late secretory traffic, that is from the TGN to the plasma membrane (***Figure 2A–D***). There was a slight retention of SYP132 in the BFA compartments of wild-type seedling roots, which probably reflects slowed-down passage of newly-synthesized proteins through the TGN. This becomes apparent upon BFA treatment because of TGN aggregation into BFA compartments, as has been reported earlier for *HS::secGFP* (***Viotti et al., 2010***). Vacuolar cargo proteins also pass through the TGN via multivesicular bodies (MVBs) to the vacuole (***Reyes et al., 2011***). Soluble RFP fused to phaseolin vacuolar sorting sequence AFVY accumulated in BFA compartments in *big3* mutant, in contrast to wild-type (***Scheuring et al., 2011***; ***Figure 2E–J***, ***Figure 2—figure supplement 1A–F***). Endocytosed PM proteins are delivered to the vacuole for degradation, for example boron transporter BOR1 in response to high external boron concentration (***Takano et al., 2005***; ***Figure 2K–N***). BFA treatment prevented boron-induced trafficking of BOR1 to the vacuole in *big3* mutant, but not in wild-type (***Figure 2L,N***). BOR1 was rapidly turned over in the vacuole of wild-type, leaving no trace of GFP (***Figure 2L***). As expected, ARF-GEF BIG4 and its putative cargo BOR1 co-localized in BFA compartments (***Figure 2—figure supplement 1G–I***). Thus, BIG1-4 mediate both late secretory and vacuolar trafficking from the TGN.

Recruitment of clathrin adaptor complex AP-1 to the TGN requires BIG1 to BIG4 function

ARF-GEFs activate ARF GTPases, resulting in recruitment of vesicular coat proteins to the respective endomembrane compartment, such as COPI complex to Golgi stacks or adaptor protein (AP) complexes to post-Golgi compartments (***Robinson, 2004***). Like BIG1-4, AP-1 complex subunit muB2-adaptin (AP1M2) localizes to SYP61-labeled TGN and is required for late secretory and vacuolar trafficking (***Park et al., 2013***; ***Teh et al., 2013***; ***Wang et al., 2013***; ***Figure 2—figure supplement 1P–R***).

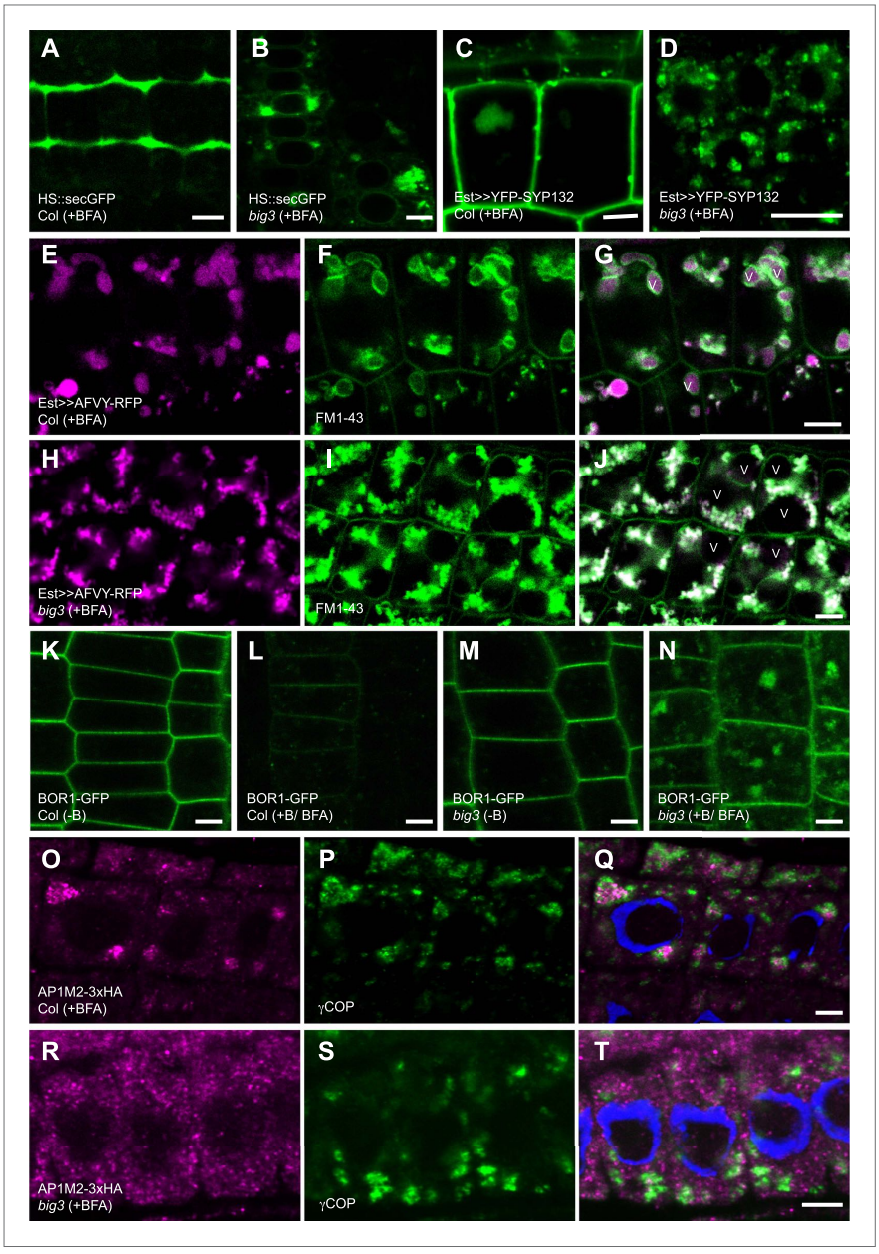

Figure 2. BIG1 – BIG4 regulate secretory and vacuolar trafficking by recruiting AP-1 adaptor complex. (**A** and **B**) BFA inhibited secretion of heat shock (HS)-induced secGFP in *big3* mutants (**B**) but not in wild-type (Col; **A**). (**C** and **D**) BFA inhibited trafficking of estradiol (Est)-induced YFP-SYP132 to the plasma membrane in *big3* mutants (**D**) but not in wild-type (Col; **C**). (**E**–**J**) BFA inhibited trafficking of soluble cargo AFVY-RFP to the vacuole (v), labeled by FM1-43 (**F** and **I**), in *big3* mutants (**H**–**J**) but not in wild-type (Col, **E**–**G**). (**K**–**N**) Live imaging of BOR1-GFP

Figure 2. Continued on next page

Figure 2. Continued

localization. Without boron (−B), BOR1-GFP localized at the plasma membrane in wild-type (**K**) and *big3* mutants (**M**). After BFA and boron treatment (+B), BOR1-GFP was degraded in the vacuole of wild-type (**L**) but accumulated in BFA compartments of *big3* mutants (**N**). (**O**–**T**) Immunostaining of 3xHA-tagged muB2 subunit of AP-1 complex (AP1M2; **O**, **R**) and COPI subunit γCOP (**P** and **S**) in BFA-treated seedlings. AP1M2 accumulated in BFA compartments surrounded by γCOP in wild-type (Col; **Q**). In *big3* mutants, γCOP was still recruited to Golgi membranes whereas AP1M2 was cytosolic (**R**–**T**). Blue, DAPI-stained nuclei. Scale bars, 5 μm.

DOI: 10.7554/eLife.02131.007

The following figure supplements are available for figure 2:

Figure supplement 1. BIG1 – BIG4 regulate trafficking of secretory and vacuolar cargo by recruiting AP-1 complex.

DOI: 10.7554/eLife.02131.008

AP1M2 also co-localized with TGN marker SYP61 in BFA compartments (***Figure 2—figure supplement 1J–L***). In BFA-treated *big3* mutant, however, AP1M2 was cytosolic whereas SYP61 was still TGN-associated (***Figure 2O,R***; ***Figure 2—figure supplement 1J–O***). In contrast to AP1M2, Golgi association of COPI subunit γCOP, which is mediated by BFA-resistant ARF-GEF GNL1 (***Richter et al., 2007***), was not affected in BFA-treated *big3* mutant (***Figure 2O–T***). Thus, BIG1-4 specifically mediate AP-1 recruitment to the TGN.

Secretion and recycling to the plasma membrane are independently regulated trafficking pathways

Another ARF-GEF in post-Golgi traffic, GNOM regulates polar recycling of auxin-efflux carrier PIN1 to the basal plasma membrane (***Geldner et al., 2003***). BFA treatment of wild-type and *big3* mutant seedlings inhibited recycling of PIN1, which accumulated in BFA compartments, and this defect was suppressed by engineered BFA-resistant GNOM (***Figure 3A–D***). Thus, BIG1-4 did not play any obvious role in PIN1 recycling. PIN1 is a stable protein such that most protein detectable at the plasma membrane is delivered via the recycling but not the secretory pathway (***Geldner et al., 2001***). In order to analyse the behavior of newly-synthesized PIN1 protein, we generated transgenic plants expressing estradiol-inducible PIN1. In contrast to recycling PIN1, newly-synthesized PIN1 protein was trapped in BFA compartments of *big3* mutant, regardless of BFA-resistant GNOM (***Figure 3E–H***). In conclusion, secretory ARF-GEFs BIG1-4 and recycling ARF-GEF GNOM regulate different post-Golgi trafficking pathways to the plasma membrane that function independently of each other.

Gravitropic growth response of the seedling root relies on GNOM-mediated PIN1 recycling (***Geldner et al., 2003***). We tested whether BIG1-4 are also required, using *DR5::NLS-3xGFP* expression to visualise auxin response (***Weijers et al., 2006***). BFA-induced inhibition of auxin response in wild-type and *big3* mutant was overcome by BFA-resistant GNOM, suggesting that BIG1-4 mediated secretion plays no role in gravitropic growth response (***Figure 4A–D***). GNOM-dependent PIN1 recycling is also required for lateral root initiation (***Geldner et al., 2003***). Surprisingly, BFA-resistant GNOM failed to initiate lateral root primordia in BFA-treated *big3* mutant in spite of stimulation by NAA, in contrast to seedlings that expressed both BIG3 and BFA-resistant GNOM (***Figure 4E–L***). *big3* mutants displayed binucleate cells, suggesting an essential role for secretory traffic in cytokinesis required for lateral root initiation (***Figure 4M–T***). For comparison, the BFA-induced defects in seed germination and primary root growth of *big3* were not rescued by engineered BFA-resistant GNOM, thus depending on secretory traffic rather than recycling (***Figure 1C,E,H***).

Trafficking of both endocytosed and newly-synthesized proteins to the plane of cell division is regulated by secretory ARF-GEFs BIG1 to BIG4

In plant cytokinesis, which is assisted by a dynamic microtubule array named phragmoplast, both newly-synthesized and endocytosed proteins traffic to the plane of cell division on post-Golgi membrane vesicles that fuse with one another to form the partitioning cell plate (***Samuels et al., 1995***). This raises the problem of coordinating different trafficking routes in the brief period of mitotic division (***Reichardt et al., 2011***). Cell-plate formation requires cytokinesis-specific syntaxin KNOLLE, newly synthesized during late G2/M phase (***Lauber et al., 1997***; ***Reichardt et al., 2007***). In contrast to wild-type, KNOLLE targeting to the division plane was inhibited in BFA-treated *big3* mutants, with KNOLLE accumulating in BFA compartments together with BIG4-YFP (***Figure 5A–F***, ***Figure 5—figure supplement 1A–D***). Cell-plate formation was disrupted, resulting in binucleate cells, which sometimes

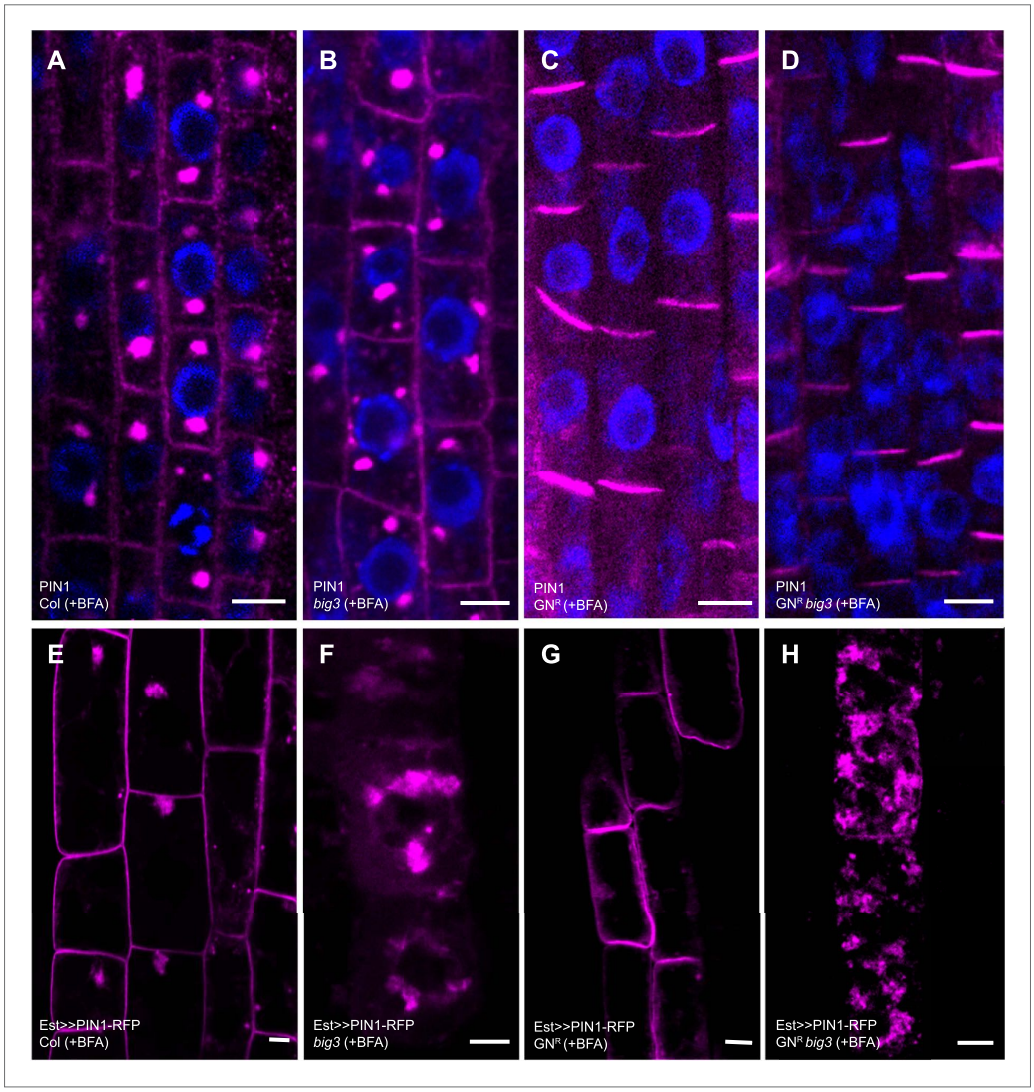

Figure 3. Secretion and recycling to the plasma membrane are regulated by different ARF-GEFs. (**A**–**D**) PIN1 localization in interphase cells of BFA-treated seedlings; apolar at the plasma membrane (PM) and in BFA compartments in wild-type (Col; **A**) and *big3* mutants (**B**); at the basal PM in BFA-resistant GN in wild-type (GN^R, **C**) or *big3* mutant background (GN^R *big3*, **D**). Blue, DAPI-stained nuclei. (**E**–**H**) After BFA treatment, estradiol (Est)-induced PIN1-RFP was trafficked to the PM in wild-type (**E**) and BFA-resistant GN seedlings (GN^R, **G**) but not in *big3* mutants without (**F**) or with expression of BFA-resistant GN (GN^R *big3*; **H**). Scale bars, 5 μm.
DOI: 10.7554/eLife.02131.009

displayed cell-wall stubs (***Figure 5—figure supplement 2A–C***). We used the non-cycling plasma-membrane syntaxin SYP132 expressed from the strong mitosis-specific *KN* promoter as another secretory marker for trafficking to the cell–division plane (***Reichardt et al., 2011***). SYP132 also accumulated, together with KN, in BFA compartments of BFA-treated *big3* mutants, in contrast to BFA-treated wild-type (***Figure 5—figure supplement 1E–J***). We also analysed endocytosed plasma-membrane proteins PEN1 and PIN1 for BFA-sensitive trafficking to the cell plate in *big3* mutants. PEN1 syntaxin involved

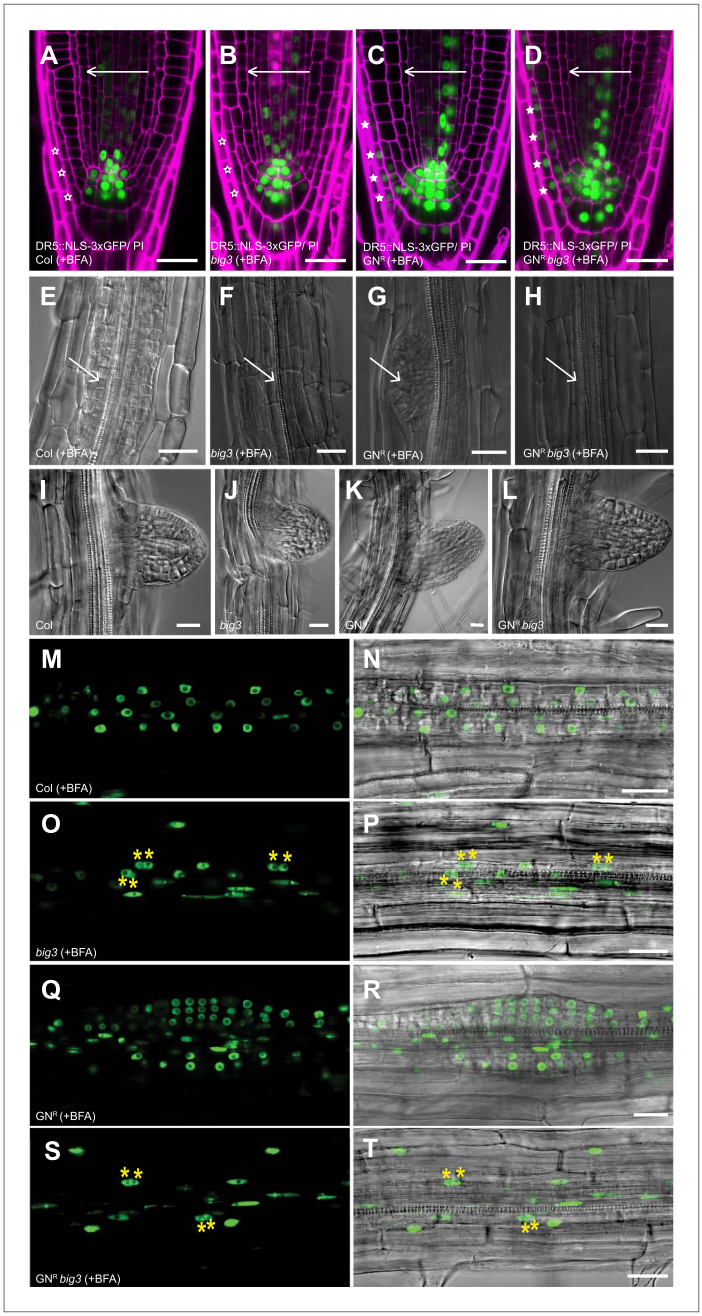

Figure 4. BIG1-4 in response to auxin application. (**A**–**D**) Visualization of auxin distribution by DR5::NLS-3xGFP (green) in BFA-treated seedlings after gravistimulation. Arrows, gravity vector. Cell walls were stained by propidium iodide (PI; magenta). Wild-type (**A**) and *big3* mutant seedling roots (**B**) did not respond to gravity (open asterisks),

Figure 4. Continued on next page

Figure 4. Continued

in contrast to BFA-resistant GN either in wild-type (GN^R, **C**) or *big3* mutant background (GN^R *big3*, **D**). Asterisks, auxin response in epidermal cell layer on lower side (**C** and **D**). (**E**–**H**) NAA and BFA treatment led to proliferation of pericycle cells (arrows) in wild-type (**E**) but not *big3* mutants without (**F**) or with BFA-resistant GN (**H**). Normal lateral root primordia only formed in BFA-resistant GN (GN^R, **G**). Scale bars, 25 μm. (**I**–**L**) Bright-field microcopy of developing lateral root primordia in NAA-treated seedlings; genotypes: wild-type (Col; **I**), *big3* (**J**), BFA-resistant GN (GN^R; **K**) and BFA-resistant GN in *big3* mutant background (GN^R *big3*; **L**). (**M**–**T**) Live imaging of DR5::NLS-3xGFP of seedling roots after NAA and BFA treatment. DR5::NLS-3xGFP signals (left panels **M**, **O**, **Q**, **S**) overlaid with Nomarski images (right panels **N**, **P**, **R**, **T**). Pericycle cells proliferated in wild-type (**M** and **N**) but became binucleate (asterisks) in *big3* (**O** and **P**) and GN^R *big3* (**S** and **T**) mutants. Normal lateral root primordia were only formed in BFA-resistant GN (GN^R; **Q**, **R**) mutant. Scale bars, 25 μm.

DOI: 10.7554/eLife.02131.010

in non-host immunity accumulates at the pathogen entry site by GNOM-dependent relocation following endocytosis from other regions of the plasma membrane (***Collins et al., 2003***; ***Nielsen et al., 2012***). PEN1 continually cycles between plasma membrane and endosomes in interphase and accumulates at the cell plate in cytokinesis (***Reichardt et al., 2011***). To make sure that we were only looking at endocytosed PEN1, PEN1 was expressed from a histone H4 expression cassette that limits protein synthesis to S phase (***Reichardt et al., 2011***). In wild-type, BFA treatment inhibited PEN1 recycling to the plasma membrane but not its trafficking to the cell plate (***Reichardt et al., 2011***; ***Figure 5G–I***). In contrast, in BFA-treated *big3* mutants, endocytosed PEN1 was not trafficked to the cell division plane but accumulated, together with KNOLLE, in BFA compartments (***Figure 5J–L***, asterisks). Endocytosed PIN1 trafficked, like KNOLLE, to the cell plate in BFA-treated wild-type but both PIN1 and KNOLLE were trapped in BFA compartments of *big3* mutants (***Figure 5M–R***). Expression of engineered BFA-resistant GNOM did not overcome the trafficking block to the division plane but rather diverted PIN1 to the basal plasma membrane (***Figure 5S–X***; compare ***Figure 5X*** with ***Figure 5R***). Careful analysis of mitotic cells revealed polar accumulation of PIN1 at the plasma membrane of BFA-resistant GNOM seedling roots throughout mitosis while additional PIN1 accumulates at the forming and expanding cell plate, suggesting that trafficking to the plane of division and polar recycling to the plasma membrane occur simultaneously (***Figure 5—figure supplement 3***). Thus, both endocytosed and newly-synthesized plasma-membrane proteins require secretory ARF-GEF function BIG1-4 for trafficking to the plane of cell division.

Discussion

It is a particularity of Arabidopsis and some other flowering-plant species that the secretory pathway of membrane traffic is comparatively insensitive to BFA treatment whereas endosomal recycling of endocytosed plasma-membrane proteins is rather sensitive (***Geldner et al., 2001***, ***2003***; ***Teh and Moore, 2007***; ***Richter et al., 2007***). The BFA insensitivity of the secretory pathway depends on the BFA resistance of ARF-GEF GNL1, which mediates COPI-vesicle formation in retrograde Golgi-ER traffic (***Teh and Moore, 2007***; ***Richter et al., 2007***), and also requires another BFA-resistant ARF-GEF acting in post-Golgi traffic to the plasma membrane. Here we show that ARF-GEFs BIG1-4 act at the TGN to mediate secretion of newly synthesized proteins to the plasma membrane in interphase but not recycling of endocytosed plasma-membrane proteins, and that BIG3 is BFA-resistant, unlike GNOM involved in recycling to the plasma membrane. Thus, there are two distinct trafficking pathways from the TGN to the plasma membrane in interphase. This is best illustrated by the trafficking of auxin-efflux carrier PIN1 - whereas newly synthesized PIN1 requires BIG1-4 on the late secretory pathway for non-polar delivery to the plasma membrane, polar PIN1 recycling to the basal plasma membrane solely depends on ARF-GEF GNOM (see model in ***Figure 5—figure supplement 4***).

Like newly synthesized proteins, endocytosed proteins are targeted to the division plane during cytokinesis (***Reichardt et al., 2011***). Proteins that cycle between endosomes and the plasma membrane in interphase accumulate, preferentially or even exclusively, at the cell plate (***Reichardt et al., 2011***). In general, recycling to the plasma membrane appears to be switched off during cytokinesis. Here we show that secretory ARF-GEFs BIG1-4 are essential for protein trafficking to the plane of cell division, regardless of proteins being newly synthesized or endocytosed from the plasma membrane (see model in ***Figure 5—figure supplement 4***).

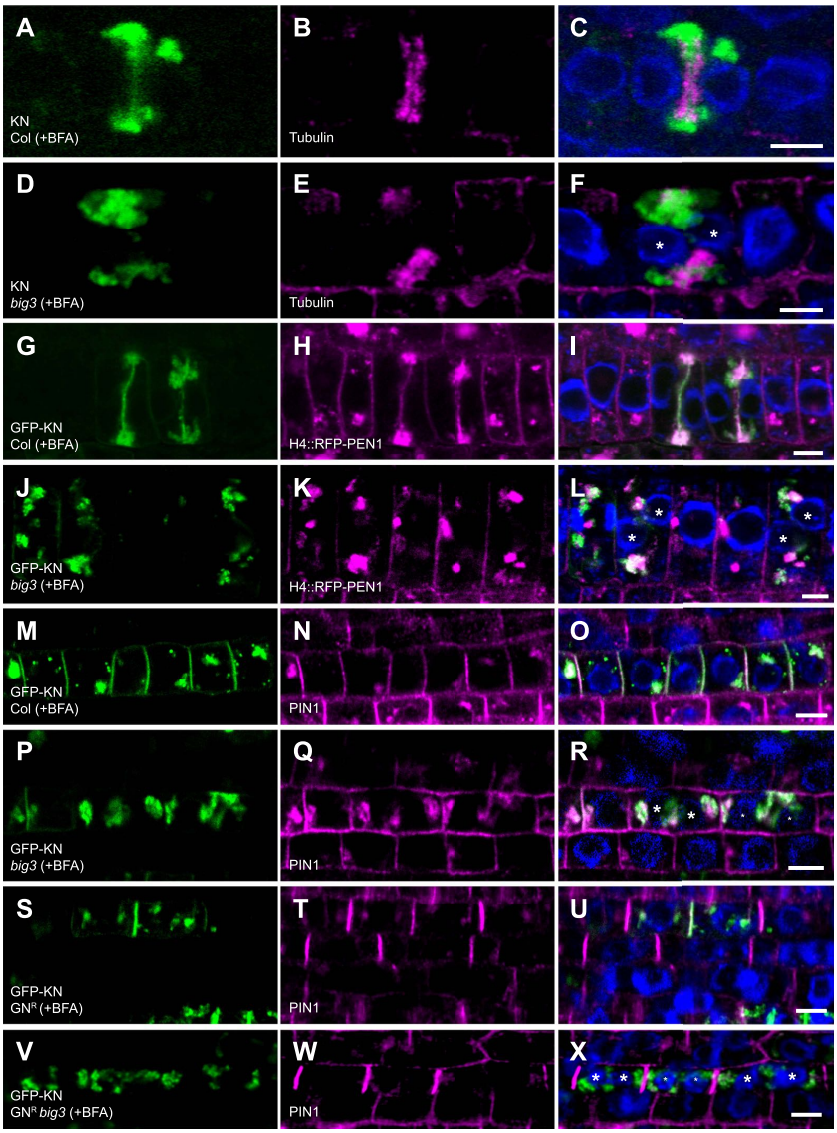

Figure 5. Trafficking to the plane of cell division is mediated by BIG1 – BIG4. (**A**–**F**) Immunolocalization of KNOLLE (KN; **A**, **D**) and tubulin (**B** and **E**) in cytokinetic root cells of BFA-treated seedlings (50 μM for 3 hr). (**A**–**C**) KN was located at the cell plate (**A**) flanked by tubulin-positive phragmoplast (**B**) in wild-type. (**D**–**F**) In *big3* mutants, KN accumulated in BFA compartments separated from tubulin-positive phragmoplast, resulting in a binucleate cell. (**G**–**L**) Co-localization of GFP-tagged KN and endocytosed RFP-PEN1 (H4::RFP-PEN1) in BFA-treated seedlings. KN and PEN1 co-localized at the cell plate and in BFA compartments of wild-type (**G**–**I**) but only in BFA compartments in *big3* mutants (**J**–**L**). (**M**–**X**) Immunostaining of GFP-KN and PIN1 in cytokinetic root cells of BFA-treated seedlings. (**M**–**R**) PIN1 localized apolarly at the plasma membrane (PM) and co-localized with KN in BFA compartments and at the cell plate in wild-type (**M**–**O**) but only in BFA-compartments in *big3* mutants (**P**–**R**). (**S**–**U**) In GN^R, PIN1 localized

Figure 5. Continued on next page

Figure 5. Continued

polarly at the plasma membrane (**T**) and co-localized with KN (**S**) at the cell plate (**U**). (**V**–**X**) Although PIN1 localized polarly at the PM (**W**) in GN^R *big3*, neither PIN1 (**W**) nor KN (**V**) was located at the cell plate. Blue, DAPI-stained nuclei. Asterisks label nuclei of binucleate cells (**F**, **L**, **R**, **X**). Scale bars, 5 μm.

DOI: 10.7554/eLife.02131.011

The following figure supplements are available for figure 5:

Figure supplement 1. BIG4 and cargo proteins trapped in BFA compartments of dividing cells in BFA-treated *big3* mutant seedlings.

DOI: 10.7554/eLife.02131.012

Figure supplement 2. Ultrastructural appearance of cryofixed, freeze-substituted and resin-embedded *big3* seedling root tips treated with BFA.

DOI: 10.7554/eLife.02131.013

Figure supplement 3. PIN1 recycling in mitotic cells.

DOI: 10.7554/eLife.02131.014

Figure supplement 4. Highly schematic model of secretory and recycling trafficking pathways in interphase and cytokinesis.

DOI: 10.7554/eLife.02131.015

Although trafficking to the plane of cell division appears to override recycling of endocytosed proteins to the plasma membrane, we noticed one clear exception—auxin-efflux carrier PIN1, which accumulates polarly at the plasma membrane in interphase and during cell division when both BFA-resistant BIG3 and engineered BFA-resistant GNOM were expressed. Rather than substituting for BIG1-4 in traffic to the plane of cell division, recycling ARF-GEF GNOM appeared to counteract that process by promoting PIN1 recycling to the basal plasma membrane. Of course, the critical question is whether both processes occur at the same time or whether GNOM-dependent PIN1 recycling only sets in after trafficking to the cell plate has come to an end. Although there are no time-course studies, which would be difficult to perform because the process is very fast, detailed analysis of dividing cells at different mitotic stages revealed that polar recycling mediated by BFA-resistant GNOM occurs throughout mitosis and cytokinesis. Furthermore, only in the absence of both BFA-resistant BIG3 and BFA-resistant GNOM is PIN1 trapped in BFA compartments. If then BFA-resistant GNOM is expressed PIN1 is not delivered to the plane of division but rather polarly recycled to the plasma membrane, again suggesting that the latter pathway is a direct route bypassing the cell plate. PIN1 might be exceptional because continuous recycling of PIN1 is required for maintaining the polar transport of auxin across tissues (***Geldner et al., 2003***). If PIN1 recycling were shut down during cytokinesis this would disrupt the polar auxin transport required in specific developmental situations such as forming lateral root primordia when essentially all cells proliferate (***Geldner et al., 2004***). Another problem in auxin flow arises from cell division when the partitioning membrane has physically separated the two daughter cells: one daughter suddenly has PIN1 located at opposite ends. Obviously, PIN1 has to be removed from the wrong end in order to sustain polar auxin transport. This seems to be a fast process and has been studied for the related auxin-efflux carrier PIN2 in detail (***Men et al., 2008***).

Animal and plant cytokinesis differ in the way the partitioning membrane is laid down. In animals, secretory and recycling pathways contribute to the ingrowth of the plasma membrane mediated by a contractile actomyosin ring and to the subsequent abscission of the daughter cells (***Schiel and Prekeris, 2013***). In plants, a massive flow of membrane vesicles from TGN/early endosome to the plane of cell division sustains, by fusion, the rapid formation and outward expansion of the partitioning cell plate (***Samuels et al., 1995***). This process is orchestrated by a specialised cytoskeletal array termed phragmoplast that delivers those membrane vesicles to the division plane. Phragmoplast-assisted trafficking might be required for completing the partitioning membrane on time, in the absence of a cytokinesis-interphase checkpoint, and would thus effectively rule out recycling of endocytosed proteins to the plasma membrane. However, our results make clear that this is not the case because recycling to the plasma membrane is not switched off during cytokinesis. Rather, endocytosed proteins enter the late-secretory pathway to reach the division plane at the expense of being recycled to the plasma membrane, which requires the late-secretory ARF-GEFs BIG1-4. In conclusion, our results raise the possibility that in general, different ARF-GEFs have different specificity of action during vesicle formation such that the same cargo protein can be delivered to different destinations.

Materials and methods

Plant material and growth conditions

Plants were grown on soil or agar plates in growth chambers under continuous light conditions at 23°C. *big* mutant lines: *big1* (GK-452B06) and *big2* (GK-074F08) T-DNA lines were from GABI-KAT (http://www.gabi-kat.de), *big3* (SALK_044617) and *big4* (SALK_069870) T-DNA lines from the SALK collection (http://signal.salk.edu/cgi-bin/tdnaexpress). *big3* mutant lines were selected on MS plates using kanamycin.

The following transgenic marker lines were used: H4::RFP-PEN1 (**Reichardt et al., 2011**) (expressed from *HISTONE4* (*H4*) promoter during S phase), KN::Myc-SYP132 (**Reichardt et al., 2011**) (expressed during lateG2/M phase), HS::secGFP (**Viotti et al., 2010**) (expressed from heat shock promoter), GFP-KN (**Reichardt et al., 2007**), BOR1-GFP (**Takano et al., 2005**), DR5::NLS-3xGFP (**Weijers et al., 2006**), VHA-a1-RFP (**Viotti et al., 2010**), AP1M2-3xHA (**Park et al., 2013**).

T-DNA genotyping of *big* mutant lines

Primers used to test for *big1* heterozygosity:
5′GCAAGATCAGGGAAGACG 3′ and 5′ACCAGAGGAAGGTGCTTCTTC 3′
Primers used to test for *big1* homozygosity:
5′TCGTCCCATCTTCTTCATTTG 3′ and 5′ACCAGAGGAAGGTGCTTCTTC 3
Primers used to test for *big2* heterozygosity:
5′GCAAGATCAGGGAAGACG 3′ and 5′TTGAGGGGTTCATATGACAGC 3′
Primers used to test for *big2* homozygosity:
5′TTTCCCACTTTTTCCACTGTG 3′ and 5′TTGAGGGGTTCATATGACAGC 3′
Primers used to test for *big3* heterozygosity:
5′AAACTCTCCACTGGCTAAGCC 3′ and 5′ATTTTGCCGATTTCGGAAC 3′
Primers used to test for *big3* homozygosity:
5′AAACTCTCCACTGGCTAAGCC 3′ and 5′GCAAGTTTTCTTGCGCAATAC 3′
Primers used to test for *big4* heterozygosity:
5′ATTTTGCCGATTTCGGAAC 3′ and 5′CTATCTTGCGCTGGAGACAAC 3′
Primers used to test for *big4* homozygosity:
5′TCCTCTTCAAACTCGTCAACG 3′ and 5′CTATCTTGCGCTGGAGACAAC 3′

Generating transgenic plants

Genomic BIG4 was amplified and introduced into pDONR221 (Invitrogen, Darmstadt, Germany) and afterwards into *UBQ10::YFP* destination vector (**Grefen et al., 2010**). For generation of BFA-resistant *UBQ10::BIG4^R-YFP*, methionine at position 695 was exchanged with leucine by site-directed mutagenesis. *BIG3* promoter was amplified and introduced into pUC57L4 via *Kpn*I and *Sma*I restriction sites. Multistep gateway cloning was performed using pUC57L4-*BIG3*-promoter, pEntry221-*BIG4* and R4pGWB553 (**Nakagawa et al., 2008**) yielding *BIG3::BIG4-RFP*. Cloning the CDS from *BIG3* into pGREENII via A*pal* and *Sma*I restriction sites generated pGII-*BIG3*. The 1 kb *BIG3* promoter was amplified and introduced into pGII-*BIG3* via *Apa*I. 1 kb of 3′UTR was amplified and introduced into pGII-*BIG3::BIG3* via *Sma*I and *Spe*I. C-terminal YFP was inserted via *Sma*I and *Spe*I. *AFVY-RFP* was amplified from *35S::AFVY-RFP* (**Scheuring et al., 2011**) and introduced into pDONR221 (Invitrogen) generating a pEntry clone. Afterwards, LR reaction was performed introducing *AFVY-RFP* into the estradiol-inducible destination vector pMDC7 (**Curtis and Grossniklaus, 2003**). *PIN1* cDNA was cloned into pGem-T (Promega, Mannheim, Germany). *RFP* was inserted in *PIN1* via the *Xho*I site. *PIN1-RFP* was amplified and introduced first into pDONR221 and then into pMDC7. *YFP-SYP132* was amplified and introduced into pDONR221 and then into pMDC7.

All constructs were transformed into *big3* mutants and BFA-resistant GN (GN^R) in *big3* mutant background. T1 plants of *UBQ10::BIG4-YFP*, *UBQ10::BIG4^R-YFP* and *BIG3-YFP* were selected by spraying with Basta. T1 seeds of estradiol-inducible lines and *BIG3::BIG4-RFP* were selected with hygromycin. Experiments were performed using T2 or T3 seedlings. At least three independent lines were analysed.

Immunofluorescence localization and live imaging in seedling roots

5 days old seedlings were incubated in 1 ml liquid growth medium (0.5x MS medium, 1% sucrose, pH 5.8) containing 50 μM BFA (Invitrogen, Molecular Probes) for 1 hr or 3 hr at room temperature in 24-well

cell-culture plates. Seedlings treated with 50 μM BFA for (a) 1 hr or (b) 3 hr, respectively, were used for the following immunolocalisation studies: (a) AP1M2 vs γCOP, AP1M2 vs SYP61, PIN1; (b) KNOLLE vs Tubulin, KNOLLE vs PIN1, H4::RFP-PEN1 vs GFP-KN and KN::Myc-SYP132 vs KN. Incubation was stopped by fixation with 4% paraformaldehyde in MTSB. Immunofluorescence staining was performed as described (***Lauber et al., 1997***) or with an InsituPro machine (Intavis, Cologne, Germany) (***Müller et al., 1998***).

Antibodies used: mouse anti-MYC (Santa Cruz Biotechnology, Heidelberg, Germany) 1:600, mouse anti-HA 1:1000 (BAbCO, Richmond, CA, USA), rat anti-tubulin 1:600 (Abcam, Cambridge, UK), rabbit anti-PIN1 1:1000 (***Geldner et al., 2001***), rabbit anti-γCOP 1:1000 (Agrisera, Vännäs, Sweden), rabbit anti-KNOLLE 1:2000 (***Reichardt et al., 2007***) and rabbit anti-SYP61 1:700 (***Park et al., 2013***). Alexa-488 or Cy3-conjugated secondary antibodies (Dianova, Hamburg, Germany) were diluted 1:600.

Live-cell imaging was performed with 2 μM FM4-64 or FM1-43 (Invitrogen, Molecular Probes) or propidium iodide (10 μg/ml).

Estradiol induction was performed using 10 or 20 μM estradiol. BFA incubation (25 μM) was done together with estradiol for 6 hr.

Heat-shock inducible secGFP (HS::secGFP) lines were first incubated for 30 min at 37°C in MS at pH8.1. BFA treatment (50 μM) in MS at pH8.1 followed for 4 hr at plant room conditions.

Analysis of BOR1 degradation was performed according to ***Takano et al. (2005)*** . In addition, we treated the seedlings with BFA, 5 μM, for 1 hr together with boron.

Electron microscopy

For ultrastructural analysis, root tips were high-pressure frozen (Bal-Tec HPM010; Balzers) in hexadecene (Merck Sharp and Dohme, Haar, Germany), freeze-substituted in acetone containing 2.5% osmium tetroxide, washed at 0°C with acetone, and embedded in Epon. For immunogold labeling of ultrathin thawed cryosections, root tips were fixed with 8% formaldehyde (2 hr), embedded in gelatin, and infiltrated with 2.1 M sucrose in PBS as previously described (***Dettmer et al., 2006***). Thawed ultrathin sections were labeled with rabbit anti-GFP antibodies (1:300; Abcam) and silver-enhanced (HQ Silver, 8 min; Nanoprobes, Yaphank, NY, USA) goat anti-rabbit IgG coupled to Nanogold (no. 2004; Nanoprobes). Antibodies and markers were diluted in blocking buffer (PBS supplemented with 0.5% BSA and 1% milk powder).

Acquisition and processing of fluorescence images

Fluorescence images were acquired at 512 × 512 or 512 × 256 pixels with the confocal laser scanning microscope TCS-SP2 or TCS-SP8 from Leica, using the 63x water-immersion objective and Leica software. All images were processed with Adobe Photoshop CS3 only for adjustment of contrast and brightness. Intensity line profile was performed with Leica software.

Pollen germination

Pollen medium was prepared as described (***Boavida and McCormick, 2007***). Pollen germinated over night or for 5 hr before microscopic analysis.

Physiological tests

To investigate primary root growth, 5–6 days old seedlings were transferred to plates with 10 μM BFA and analysed after 5–7 additional days using ImageJ. DR5::NLS-GFP expressing seedlings analysed for lateral root formation were treated with 5 μM NAA or 5 μM NAA plus 10 μM BFA over night. Roots were cleared according to ***Geldner et al. (2004)***. Gravitropic response was investigated by transferring 5 days old seedlings, expressing DR5::NLS-GFP, to BFA plates (5 μM). Seedlings were grown vertically for 1 hr on BFA plates before rotated by 135° for 4 hr.

For analysis of seed germination, seeds were sown out on MS medium containing 5 μM BFA. Images were taken after 5 days of growth.

Phylogenetic tree

Full-length protein sequence of BIG3 was used to search for related sequences from different plant species with sequenced genomes that are available at the phytozome homepage (http://www.phytozome.net/). ARF-GEFs from different species were aligned by ClustalW (www.ebi.ac.uk/clustalw) and the phylogenetic tree was drawn with Dendroscope (***Huson et al., 2007***).

Acknowledgements

We thank Lukas Sonnenberg and Marlene Ballbach for technical assistance, Toru Fujiwara, Niko Geldner, Christopher Grefen, Ueli Grossniklaus, Sumie Ishiguru, Peter Pimpl, Masao H. Sato and Karin Schumacher for sharing published materials, Joop Vermeer (Univ. Lausanne) for cloning vector pUC57L4, and NASC for T-DNA insertion lines. We also thank Martin Bayer, Niko Geldner, Christopher Grefen, Michael Hothorn and Steffen Lau for critical reading of the manuscript.

Additional information

Funding

Funder	Grant reference number	Author
German Research Foundation (DFG)	SFB446/TP A9	Gerd Jürgens
German Research Foundation (DFG)	JU 179/18-1	Gerd Jürgens
Carlsberg Foundation	2011_01_0789	Mads Eggert Nielsen

The funders had no role in study design, data collection and interpretation, or the decision to submit the work for publication.

Author contributions

SR, Conception and design, Acquisition of data, Analysis and interpretation of data, Drafting or revising the article; MK, MEN, MP, RG, CK, UV, HB, UM, Y-DS, Acquisition of data, Analysis and interpretation of data; SB, Analysis and interpretation of data, Drafting or revising the article; GJ, Conception and design, Analysis and interpretation of data, Drafting or revising the article

Additional files

Supplementary files

• Supplementary file 1. Localization of vesicle trafficking markers. This table summarizes the localization of different vesicle trafficking markers without BFA (1th column) and with BFA in wild-type (Col; 2th column), *big3* (3th column), BFA-resistant GNOM (GN^R; 4th column) and BFA-resistant GNOM in *big3* mutant background (GN^R *big3*; 5th column). Abbreviations: PM, plasma membrane; CP, cell plate; BFA-comp., BFA-compartment.

DOI: 10.7554/eLife.02131.016

References

Boavida LC, McCormick S. 2007. Temperature as a determinant factor for increased and reproducible in vitro pollen germination in *Arabidopsis thaliana*. *Plant Journal* **52**:570–582. doi: 10.1111/j.1365-313X.2007.03248.x.

Casanova JE. 2007. Regulation of Arf activation: the Sec7 family of guanine nucleotide exchange factors. *Traffic* **8**:1476–1485. doi: 10.1111/j.1600-0854.2007.00634.x.

Collins NC, Thordal-Christensen H, Lipka V, Bau S, Kombrink E, Qiu JL, Hückelhoven R, Stein M, Freialdenhoven A, Somerville SC, Schulze-Lefert P. 2003. SNARE-protein-mediated disease resistance at the plant cell wall. *Nature* **425**:973–977. doi: 10.1038/nature02076.

Cox R, Mason-Gamer RJ, Jackson CL, Segev N. 2004. Phylogenetic analysis of Sec7-domain-containing Arf nucleotide exchangers. *Molecular Biology of the Cell* **15**:1487–1505. doi: 10.1091/mbc.E03-06-0443.

Curtis MD, Grossniklaus U. 2003. A gateway cloning vector set for high-throughput functional analysis of genes in planta. *Plant Physiology* **133**:462–469. doi: 10.1104/pp.103.027979.

Dettmer J, Hong-Hermesdorf A, Stierhof YD, Schumacher K. 2006. Vacuolar H^+-ATPase activity is required for endocytic and secretory trafficking in Arabidopsis. *Plant Cell* **18**:715–730. doi: 10.1105/tpc.105.037978.

Geldner N, Anders N, Wolters H, Keicher J, Kornberger W, Muller P, Delbarre A, Ueda T, Nakano A, Jürgens G. 2003. The Arabidopsis GNOM ARF-GEF mediates endosomal recycling, auxin transport, and auxin-dependent plant growth. *Cell* **112**:219–230. doi: 10.1016/S0092-8674(03)00003-5.

Geldner N, Dénervaud-Tendon V, Hyman DL, Mayer U, Stierhof YD, Chory J. 2009. Rapid, combinatorial analysis of membrane compartments in intact plants with a multicolor marker set. *Plant Journal* **59**:169–178. doi: 10.1111/j.1365-313X.2009.03851.x.

Geldner N, Friml J, Stierhof YD, Jürgens G, Palme K. 2001. Auxin transport inhibitors block PIN1 cycling and vesicle trafficking. *Nature* **413**:425–428. doi: 10.1038/35096571.

Geldner N, Richter S, Vieten A, Marquardt S, Torres-Ruiz RA, Mayer U, Jürgens G. 2004. Partial loss-of-function alleles reveal a role for GNOM in auxin transport-related, post-embryonic development of Arabidopsis. *Development* **131**:389–400. doi: 10.1242/dev.00926.

Grefen C, Donald N, Hashimoto K, Kudla J, Schumacher K, Blatt MR. 2010. A ubiquitin-10 promoter-based vector set for fluorescent protein tagging facilitates temporal stability and native protein distribution in transient and stable expression studies. *Plant Journal* **64**:355–365. doi: 10.1111/j.1365-313X.2010.04322.x.

Huson DH, Richter DC, Rausch C, Dezulian T, Franz M, Rupp R. 2007. Dendroscope: an interactive viewer for large phylogenetic trees. *BMC Bioinformatics* **8**:460. doi: 10.1186/1471-2105-8-460.

Lauber MH, Waizenegger I, Steinmann T, Schwarz H, Mayer U, Hwang I, Lukowitz W, Jürgens G. 1997. The Arabidopsis KNOLLE protein is a cytokinesis-specific syntaxin. *Journal of Cell Biology* **139**:1485–1493. doi: 10.1083/jcb.139.6.1485.

Men S, Boutté Y, Ikeda Y, Li X, Palme K, Stierhof YD, Hartmann MA, Moritz T, Grebe M. 2008. Sterol-dependent endocytosis mediates post-cytokinetic acquisition of PIN2 auxin efflux carrier polarity. *Nature Cell Biology* **10**:237–244. doi: 10.1038/ncb1686.

Movafeghi A, Happel N, Pimpl P, Tai GH, Robinson DG. 1999. Arabidopsis Sec21p and Sec23p homologs. Probable coat proteins of plant COP-coated vesicles. *Plant Physiol* **119**:1437–1446. doi: 10.1104/pp.119.4.1437.

Müller A, Guan C, Gälweiler L, Tänzler P, Huijser P, Marchant A, Parry G, Bennett M, Wisman E, Palme K. 1998. AtPIN2 defines a locus of Arabidopsis for root gravitropism control. *The EMBO Journal* **17**:6903–6911. doi: 10.1093/emboj/17.23.6903.

Nakagawa T, Nakamura S, Tanaka K, Kawamukai M, Suzuki T, Nakamura K, Kimura T, Ishiguro S. 2008. Development of R4 gateway binary vectors (R4pGWB) enabling high-throughput promoter swapping for plant research. *Bioscience Biotechnology and Biochemistry* **72**:624–629. doi: 10.1271/bbb.70678.

Nielsen M, Albrethsen J, Larsen F, Skriver K. 2006. The Arabidopsis ADP-ribosylation factor (ARF) and ARF-like (ARL) system and its regulation by BIG2, a large ARF-GEF. *Plant Science* **171**:707–717. doi: 10.1016/j.plantsci.2006.07.002.

Nielsen ME, Feechan A, Bohlenius H, Ueda T, Thordal-Christensen H. 2012. Arabidopsis ARF-GTP exchange factor, GNOM, mediates transport required for innate immunity and focal accumulation of syntaxin PEN1. *Proceedings of the National Academy of Sciences of the United States of America* **109**:11443–11448. doi: 10.1073/pnas.1117596109.

Nomura K, Debroy S, Lee YH, Pumplin N, Jones J, He SY. 2006. A bacterial virulence protein suppresses host innate immunity to cause plant disease. *Science* **313**:220–223. doi: 10.1126/science.1129523.

Nomura K, Mecey C, Lee YN, Imboden LA, Chang JH, He SY. 2011. Effector-triggered immunity blocks pathogen degradation of an immunity-associated vesicle traffic regulator in Arabidopsis. *Proceedings of the National Academy of Sciences of the United States of America* **108**:10774–10779. doi: 10.1073/pnas.1103338108.

Park M, Song K, Reichardt I, Kim H, Mayer U, Stierhof YD, Hwang I, Jürgens G. 2013. Arabidopsis mu-adaptin subunit AP1M of adaptor protein complex 1 mediates late secretory and vacuolar traffic and is required for growth. *Proceedings of the National Academy of Sciences of the United States of America* **110**:10318–10323. doi: 10.1073/pnas.1300460110.

Reichardt I, Slane D, El Kasmi F, Knöll C, Fuchs R, Mayer U, Lipka V, Jürgens G. 2011. Mechanisms of functional specificity among plasma-membrane syntaxins in Arabidopsis. *Traffic* **12**:1269–1280. doi: 10.1111/j.1600-0854.2011.01222.x.

Reichardt I, Stierhof YD, Mayer U, Richter S, Schwarz H, Schumacher K, Jürgens G. 2007. Plant cytokinesis requires de novo secretory trafficking but not endocytosis. *Current Biology* **17**:2047–2053. doi: 10.1016/j.cub.2007.10.040.

Reyes FC, Buono R, Otegui MS. 2011. Plant endosomal trafficking pathways. *Current Opinion In Cell Biology* **14**:666–673. doi: 10.1016/j.pbi.2011.07.009.

Richter S, Geldner N, Schrader J, Wolters H, Stierhof YD, Rios G, Koncz C, Robinson DG, Jürgens G. 2007. Functional diversification of closely related ARF-GEFs in protein secretion and recycling. *Nature* **448**:488–492. doi: 10.1038/nature05967.

Richter S, Müller LM, Stierhof YD, Mayer U, Takada N, Kost B, Vieten A, Geldner N, Koncz C, Jürgens G. 2012. Polarized cell growth in Arabidopsis requires endosomal recycling mediated by GBF1-related ARF exchange factors. *Nature Cell Biology* **14**:80–86. doi: 10.1038/ncb2389.

Robinson MS. 2004. Adaptable adaptors for coated vesicles. *Trends in Cell Biology* **14**:167–174. doi: 10.1016/j.tcb.2004.02.002.

Samuels AL, Giddings TH Jnr, Staehelin LA. 1995. Cytokinesis in tobacco BY-2 and root tip cells: a new model of cell plate formation in higher plants. *Journal of Cell Biology* **130**:1345–1357. doi: 10.1083/jcb.130.6.1345.

Scheuring D, Viotti C, Krüger F, Künzl F, Sturm S, Bubeck J, Hillmer S, Frigerio L, Robinson DG, Pimpl P, Schumacher K. 2011. Multivesicular bodies mature from the trans-Golgi network/early endosome in Arabidopsis. *Plant Cell* **23**:3463–3481. doi: 10.1105/tpc.111.086918.

Schiel JA, Prekeris R. 2013. Membrane dynamics during cytokinesis. *Current Opinion In Cell Biology* **25**:92–98. doi: 10.1016/j.ceb.2012.10.012.

Schmid M, Davison TS, Henz SR, Pape UJ, Demar M, Vingron M, Schölkopf B, Weigel D, Lohmann JU. 2005. A gene expression map of *Arabidopsis thaliana* development. *Nature Genetics* **37**:501–506. doi: 10.1038/ng1543.

Stierhof YD, El Kasmi F. 2010. Strategies to improve the antigenicity, ultrastructure preservation and visibility of trafficking compartments in Arabidopsis tissue. *European Journal of Cell Biology* **89**:285–297. doi: 10.1016/j.ejcb.2009.12.003.

Surpin M, Raikhel N. 2004. Traffic jams affect plant development and signal transduction. *Nature Reviews Molecular Cell Biology* **5**:100–109. doi: 10.1038/nrm1311.

Tanaka H, Kitakura S, De Rycke R, De Groodt R, Friml J. 2009. Fluorescence imaging-based screen identifies ARF GEF component of early endosomal trafficking. *Current Biology* **19**:391–397. doi: 10.1016/j.cub.2009.01.057.

Tanaka H, Kitakura S, Rakusová H, Uemura T, Feraru MI, De Rycke R, Robert S, Kakimoto T, Friml J. 2013. Cell polarity and patterning by PIN trafficking through early endosomal compartments in *Arabidopsis thaliana*. *PLOS Genetics* **9**:e1003540. doi: 10.1371/journal.pgen.1003540.

Takano J, Miwa K, Yuan L, von Wiren N, Fujiwara T. 2005. Endocytosis and degradation of BOR1, a boron transporter of *Arabidopsis thaliana*, regulated by boron availability. *Proceedings of the National Academy of Sciences of the United States of America* **102**:12276–12281. doi: 10.1073/pnas.0502060102.

Teh OK, Moore I. 2007. An ARF-GEF acting at the Golgi and in selective endocytosis in polarized plant cells. *Nature* **448**:493–496. doi: 10.1038/nature06023.

Teh OK, Shimono Y, Shirakawa M, Fukao Y, Tamura K, Shimada T, Hara-Nishimura I. 2013. The AP-1 mu adaptin is required for KNOLLE localization at the cell plate to mediate cytokinesis in Arabidopsis. *Plant and Cell Physiology* **54**:838–847. doi: 10.1093/pcp/pct048.

Ueda T, Yamaguchi M, Uchimiya H, Nakano A. 2001. Ara6, a plant-unique novel type Rab GTPase, functions in the endocytic pathway of *Arabidopsis thaliana*. *The EMBO Journal* **20**:4730–4741. doi: 10.1093/emboj/20.17.4730.

Viotti C, Bubeck J, Stierhof YD, Krebs M, Langhans M, van den Berg W, van Dongen W, Richter S, Geldner N, Takano J, Jürgens G, de Vries SC, Robinson DG, Schumacher K. 2010. Endocytic and secretory traffic in Arabidopsis merge in the trans-Golgi network/early endosome, an independent and highly dynamic organelle. *Plant Cell* **22**:1344–1357. doi: 10.1105/tpc.109.072637.

Wang JG, Li S, Zhao XY, Zhou LZ, Huang GQ, Feng C, Zhang Y. 2013. HAPLESS13, the Arabidopsis mu1 adaptin, is essential for protein sorting at the trans-Golgi Network/early endosome. *Plant Physiology* **162**:1897–1910. doi: 10.1104/pp.113.221051.

Weijers D, Schlereth A, Ehrismann JS, Schwank G, Kientz M, Jürgens G. 2006. Auxin triggers transient local signaling for cell specification in *Arabidopsis embryogenesis*. *Developmental Cell* **10**:265–270. doi: 10.1016/j.devcel.2005.12.001.

Marker	- BFA	Col + BFA	*big3* + BFA	GN^R + BFA	GN^R *big3* + BFA
HS::secGFP	apoplast (Viotti et al., 2010)	apoplast	intracellular aggregate	-	-
Est>>YFP-SYP132	PM (this study)	PM	intracellular aggregate	-	-
Est>>AFVY-RFP	vacuole (this study)	vacuole	intracellular aggregate	-	-
BOR1-GFP	PM (Takano et al., 2005)	PM + BFA-comp.	intracellular aggregate	-	-
AP1M2-3xHA	TGN (Park et al., 2013)	BFA-comp.	cytosolic	-	-
γCOP	Golgi (Richter at al., 2007)	Golgi	Golgi	-	-
PIN1 (interphase)	basal PM (Geldner at al., 2001)	PM + BFA-comp.	PM + BFA-comp.	basal PM	basal PM
PIN1 (cytokinesis)	basal PM+CP (Geldner at al., 2001)	PM + CP+BFA-comp.	PM+intracellular aggegate	PM + CP+BFA-comp.	PM+intracellular aggegate
Est>>PIN1-RFP	basal PM (this study)	PM + BFA-comp.	intracellular aggregate	basal PM	intracellular aggregate
KNOLLE	CP (Lauber at al., 1997)	CP + BFA-comp.	intracellular aggregate	CP + BFA-comp.	intracellular aggregate
H4::RFP-PEN1	PM+CP (Reichardt et al., 2011)	PM+CP+BFA-comp.	PM+intracellular aggegate	-	-
KN::MYC-SYP132	PM+CP (Reichardt et al., 2011)	PM+CP	PM+intracellular aggegate	-	-

Supplementary Table 1. Localization of vesicle trafficking markers.
This table summarizes the localization of different vesicle trafficking markers without BFA (1th column) and with BFA in wild-type (Col; 2th column), *big3* (3th column), BFA-resistant GNOM (GN^R; 4th column) and BFA-resistant GNOM in *big3* mutant background (GN^R *big3*; 5th column). Abbreviations: PM, plasma membrane; CP, cell plate; BFA-comp., BFA-compartment.

6.2. Singh et al., 2014

Protein Delivery to Vacuole Requires SAND Protein-Dependent Rab GTPase Conversion for MVB-Vacuole Fusion

Manoj K. Singh, Falco Krüger, Hauke Beckmann, **Sabine Brumm**, Joop E.M.Vermeer, Teun Munnik, Ulrike Mayer, York-Dieter Stierhof, Christopher Grefen, Karin Schumacher und Gerd Jürgens

Current Biology *24*, 1383-1389

2014

Current Biology *24*, 1383–1389, June 16, 2014 http://dx.doi.org/10.1016/j.cub.2014.05.005

Report

Protein Delivery to Vacuole Requires SAND Protein-Dependent Rab GTPase Conversion for MVB-Vacuole Fusion

Manoj K. Singh,[1] Falco Krüger,[2] Hauke Beckmann,[1] Sabine Brumm,[1] Joop E.M. Vermeer,[3,5] Teun Munnik,[3] Ulrike Mayer,[4] York-Dieter Stierhof,[4] Christopher Grefen,[1] Karin Schumacher,[2] and Gerd Jürgens[1,*]

[1]Center for Plant Molecular Biology (ZMBP), Developmental Genetics, University of Tübingen, Auf der Morgenstelle 32, 72076 Tübingen, Germany

[2]Center for Organismal Studies (COS), University of Heidelberg, 69120 Heidelberg, Germany

[3]Section Plant Physiology, University of Amsterdam, Swammerdam Institute for Life Sciences, 1098 SM, Amsterdam, the Netherlands

[4]Center for Plant Molecular Biology (ZMBP), Microscopy, University of Tübingen, 72076 Tübingen, Germany

Summary

Plasma-membrane proteins such as ligand-binding receptor kinases, ion channels, or nutrient transporters are turned over by targeting to a lytic compartment—lysosome or vacuole—for degradation. After their internalization, these proteins arrive at an early endosome, which then matures into a late endosome with intraluminal vesicles (multivesicular body, MVB) before fusing with the lysosome/vacuole in animals or yeast [1, 2]. The endosomal maturation step involves a SAND family protein mediating Rab5-to-Rab7 GTPase conversion [3]. Vacuolar trafficking is much less well understood in plants [4–6]. Here we analyze the role of the single-copy *SAND* gene of *Arabidopsis*. In contrast to its animal or yeast counterpart, *Arabidopsis* SAND protein is not required for early-to-late endosomal maturation, although its role in mediating Rab5-to-Rab7 conversion is conserved. Instead, *Arabidopsis* SAND protein is essential for the subsequent fusion of MVBs with the vacuole. The inability of *sand* mutant to mediate MVB-vacuole fusion is not caused by the continued Rab5 activity but rather reflects the failure to activate Rab7. In conclusion, regarding the endosomal passage of cargo proteins for degradation, a major difference between plants and nonplant organisms might result from the relative timing of endosomal maturation and SAND-dependent Rab GTPase conversion as a prerequisite for the fusion of late endosomes/MVBs with the lysosome/vacuole.

Results and Discussion

Endocytosis is crucial in controlling the plasma-membrane protein repertoire in all eukaryotic cells. Membrane proteins such as cell-surface receptors are delivered to the lumen of the lytic compartment (lysosome or vacuole) for degradation. On their way, proteins endocytosed from the plasma membrane successively pass through the early endosome (EE) and the late endosome (LE) before reaching the lytic compartment (vacuole/lysosome). Recent evidence suggests that early endosomes mature into late endosomes containing intraluminal vesicles—so-called multivesicular bodies (MVBs)—through a process of Rab GTPase conversion [7]. This process involves Mon1/SAND protein, which together with CCZ1 acts as a guanine-nucleotide exchange factor (GEF) on Rab7-type GTPases that also inactivates Rab5-type GTPases [1, 3, 8, 9].

The lack of an independent early endosome (EE) is a distinguishing feature of the plant endomembrane system [10, 11]. In plants, the trans-Golgi network (TGN) is the first compartment reached by endocytic cargo and is thus at the crossroads of the secretory and endocytic routes [12]. Importantly, Rab5-like GTPases as well as phosphatidylinositol-3-phosphate (PI3P), hallmarks of yeast and animal early endosomes, are largely absent from the plant TGN/EE [13, 14]. Nevertheless, it has recently been proposed that MVBs mature from the TGN/EE [15] and we have thus investigated whether the single-copy *Arabidopsis SAND* gene is involved in TGN/EE-to-MVB maturation and/or whether it plays a role in mediating Rab5-to-Rab7 conversion.

Endosomal maturation from TGN/EE to MVB was examined in *Arabidopsis* seedling root cells, via pairwise colabeling of three marker proteins: TGN/EE-localized subunit a1 of V-ATPase (VHA-a1) [10], Rab5-like GTPase ARA7 (aka RABF2b) [13], and the fluorescent PI3P sensor YFP-2xFYVE [14]. In line with previous findings, colocalization between VHA-a1 and ARA7 was generally low as ARA7 mostly accumulated at the MVB [10, 16]. However, ARA7 also marked a subdomain of the VHA-a1-positive TGN/EE (Figure 1A). The dual localization of ARA7 to TGN/EE and MVB has also been observed in EM images of immunolabeled cryosections [13]. In contrast, 2xFYVE was separate from, but often abutted, the TGN/EE (Figure 1B). ARA7 was mostly colocalized with 2xFYVE, which labeled an additional subpopulation of endosomes devoid of ARA7 (Figure 1C). Upon BFA treatment, which causes aggregation of TGN/EEs into "BFA compartments" that do not include MVBs [16], some ARA7 colocalized with VHA-a1 in BFA compartments although the majority of the ARA7 signal still gave a distinct punctate pattern (Figure 1D). In contrast, the 2xFYVE signal was not altered such that the BFA compartments were exclusively ARA7 positive in double-labeled root cells (Figure 1E). Taken together, these results suggest that endosomal maturation in *Arabidopsis* appears to originate in a subdomain of the TGN/EE that recruits Rab5-like ARA7 and subsequently matures into an MVB, and this transition is accompanied by the accumulation of PI3P (Figure 1F). This conclusion is supported by ultrastructural studies indicating MVB formation on Golgi-associated tubular-vesicular structures, the local presence of ESCRT proteins on TGN/EE, and the strong reduction in the number of MVBs observed after inhibition of the V-ATPase in the TGN/EE [15].

The *Arabidopsis* genome harbors a single-copy *SAND* gene encoding a member of the eukaryotic SAND/Mon1 protein family and this gene appears to be expressed at moderate level throughout development (Figures S1A and S1B available online). Two mutant alleles, *sand-1* and *sand-2*, caused by T-DNA insertional gene inactivation (Figures S1C and S1D), impaired seed germination, seedling root growth, and plant growth but had almost no adverse effect on gametophyte

[5]Present address: Department of Plant Molecular Biology (DBMV), University of Lausanne, UNIL-Sorge, 1015 Lausanne, Switzerland

*Correspondence: gerd.juergens@zmbp.uni-tuebingen.de

Current Biology Vol 24 No 12
1384

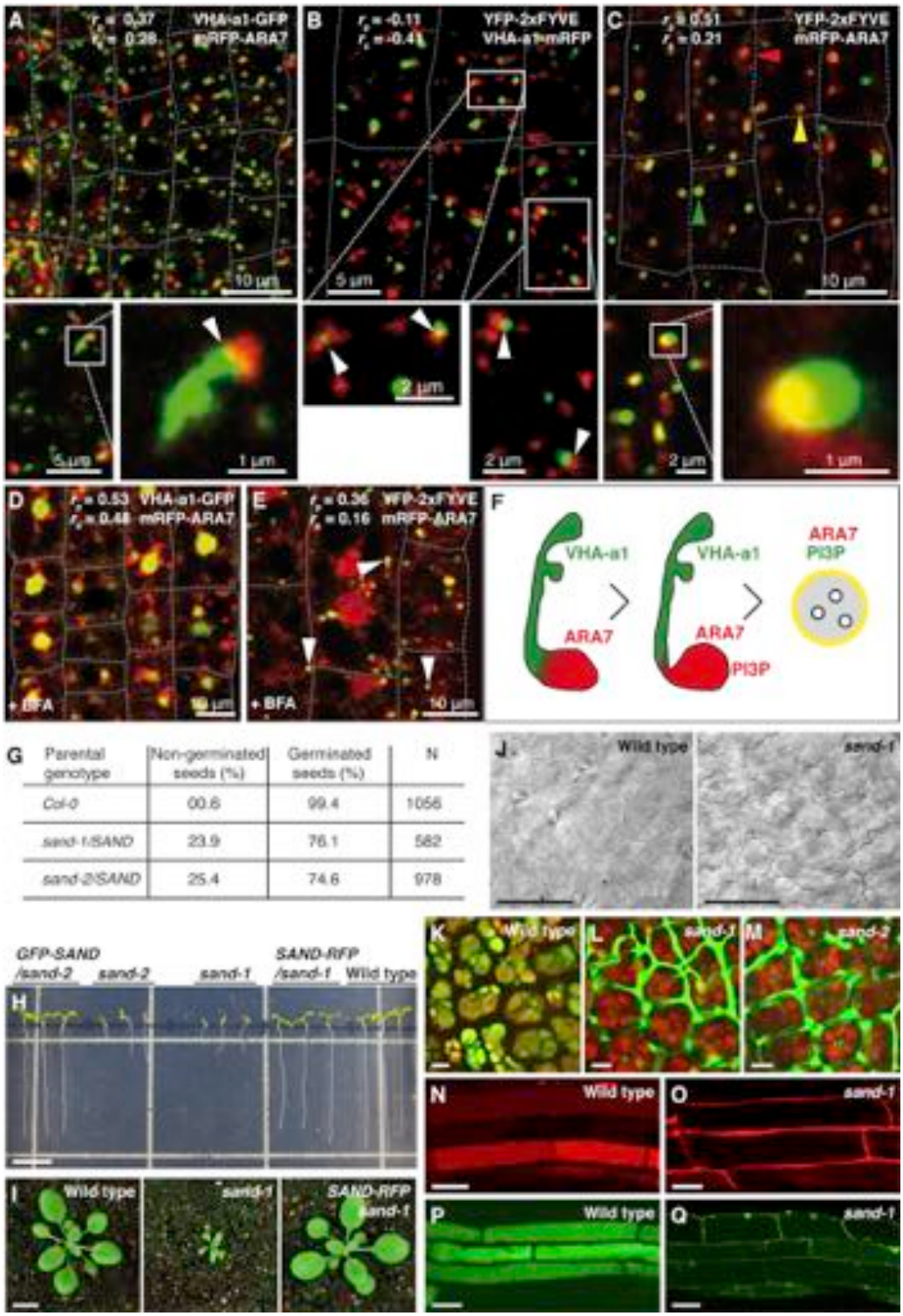

Figure 1. Spatial Relationship of TGN and MVB Markers, *sand* Mutant Phenotype, and Membrane Trafficking Defects

(A) Localization of VHA-a1-GFP and mRFP-ARA7. The lower panels show both proteins at a higher magnification, revealing a subdomain of mRFP the VHA-a1-GFP-labeled TGN. Fluorescence in lower panel was recorded with a pinhole diameter of 0.37 AU.

(B) Localization of YFP-2xFYVE and VHA-a1-mRFP. The lower panels show corresponding close-up views where small areas of overlap are vis images were obtained with a pinhole diameter of 0.37 AU.

(legend continued on n

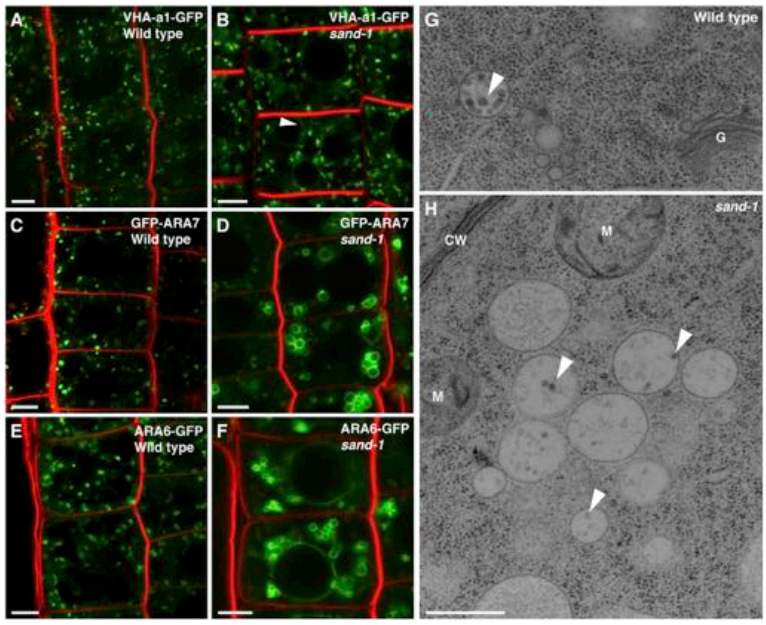

Figure 2. SAND Protein Acts at MVBs

(A and B) Localization of TGN-resident VHA-a1-GFP in wild-type and *sand-1*. Note additional faint labeling of vacuolar membrane in *sand-1* (B; arrowheads).

(C and D) ARA7-positive organelles are enlarged and clustered in *sand-1* (D).

(E and F) ARA6-positive organelles are enlarged and clustered in *sand-1* (F). In addition, ARA6 labeling of vacuolar membrane is also observed (F).

(G and H) Electron micrographs of clusters of enlarged MVBs in *sand-1* (H) as compared to wild-type (G). Note the presence of intraluminal vesicles in MVB clusters in *sand-1* similar to wild-type (arrowheads). CW, cell wall; G, Golgi stack; M, mitochondrion.

Scale bars represent 5 μm (A–F); 500 nm (G, H). See also Figure S2.

development or function (Figures 1G–1I and S1E–S1J). In addition, the pavement cells of the cotyledon epidermis were much less lobed in *sand-1* than in wild-type (Figure 1J). Similarly, cell sizes and cell shapes in the seedling root appeared abnormal (Figure S1G). These defects were abolished by expression of N-terminally GFP-tagged SAND driven by *UBQ10* promoter or C-terminally mRFP-tagged SAND under the control of *RPS5A* promoter, indicating that SAND protein is required in all those developmental contexts (Figures 1H, 1I, and S1).

To identify the trafficking pathway(s) in which SAND acts, we analyzed the subcellular localization of pathway-specific markers (Figures 1K–1Q and S2). Vacuolar marker proteins comprised fluorescent protein fusions of sorting signals from two storage proteins, α′-subunit of β-conglycinin (CT24) [17] and phaseolin (AFVY) [15], and the soluble protease aleurain fused to GFP [18], normally being delivered to the protein storage vacuole or the lytic vacuole, respectively. Rather than being delivered to the vacuole, all three soluble marker proteins for vacuolar trafficking were secreted from the cell (Figures 1K–1Q). These trafficking defects impair storage protein accumulation and vacuolar protein breakdown, limiting nutrients for growth, and might thus explain the developmental defects described above (see Figures 1K–1Q). In contrast, there was no detectable effect on secretory or recycling post-Golgi trafficking pathways. Cytokinesis-specific syntaxin KNOLLE [19] accumulated at the cell plate as in wild-type (Figures S2A and S2B), auxin efflux carrier PIN1 [20] was localized at the basal plasma membrane (Figures S2C and S2D), and PIN2 [21] accumulated at the apical end of epidermal cells (Figures S2E and S2F). The steady-state accumulation of the two PIN proteins at the plasma membrane results from their continuous cycling through endosomes [20, 21]. However, some aberrant endosomal localization of PIN2, but not PIN1, was detected (Figures S2E and S2F), which might suggest that vacuolar trafficking of PIN2 is impaired, consistent with the higher turnover of PIN2 as compared to PIN1 [21]. Thus, late secretory and recycling traffic from the TGN to the plasma membrane or the cell division plane does not require SAND function and SAND appears to be specifically required for protein delivery to the vacuole.

To delineate the site of action of SAND protein, we analyzed the subcellular localization of TGN and MVB markers in both wild-type and *sand-1* mutant seedling roots (Figure 2).

(C) Overview of YFP-2xFYVE and mRFP-ARA7 showing independent green and red signals together with compartments of merged fluorescence, marked with color-coded arrowheads. The close-up views reveal that some of these compartments display a gradual fluorescence distribution.

(D) VHA-a1GFP and mRFP-ARA7 after BFA treatment (50 μM, 30 min).

(E) YFP-2xFYVE and mRFP-ARA7 after BFA treatment (50 μM, 30 min). Note that some ring-like signals of YFP-2xFYVE still colocalize with mRFP-ARA7 on MVB (arrowheads).

(F) Schematic diagram showing spatial relationship between VHA-a1, ARA7, and PI3P. A subdomain of a TGN undergoing maturation becomes enriched with ARA7 and subsequently with PI3-kinases, generating a membrane domain positive for both ARA7 and PI3P. Once an MVB is pinched off from the TGN, its surface is covered with both PI3P and ARA7.

(G) Germination defect in *sand* mutant seeds. Homozygous mutant progeny (25% expected) from *sand-1*/SAND and *sand-2/SAND* mother plants often fail to germinate.

(H) Root growth of *sand* mutant seedlings is impaired. The growth of *sand-1* and *sand-2,* complemented by transgene is similar to that of wild-type.

(I) Homozygous *sand-1* showed severe dwarf phenotype on soil. The growth defects of *sand-1* plants expressing SAND-RFP were fully rescued.

(J) Reduced lobing of epidermal pavement cells in *sand-1* cotyledons.

(K–M) Storage vacuole marker GFP-CT24 delivered to the storage vacuole (red) in developing seeds of wild-type (K) but secreted from the cell in *sand-1* (L) and *sand-2* (M).

(N–Q) Phaseolin vacuolar targeting sequence AFVY fused to RFP (N, O) and lytic-vacuole marker aleurain fused to GFP (P, Q) secreted from the cell in *sand-1* (O, Q). Cell boundaries in (A)–(E) are shown with the dotted lines. The values of Pearson (r_p) and Spearman (r_s) correlation coefficients represent the extent of colocalization between the two proteins. The values range between +1, indicating a positive correlation, and −1 for a negative correlation. Scale bars represent 1 cm (H, I); 100 μm (J); 5 μm (K–M); 20 μm (N–Q). See also Figures S1 and S2.

Current Biology Vol 24 No 12
1386

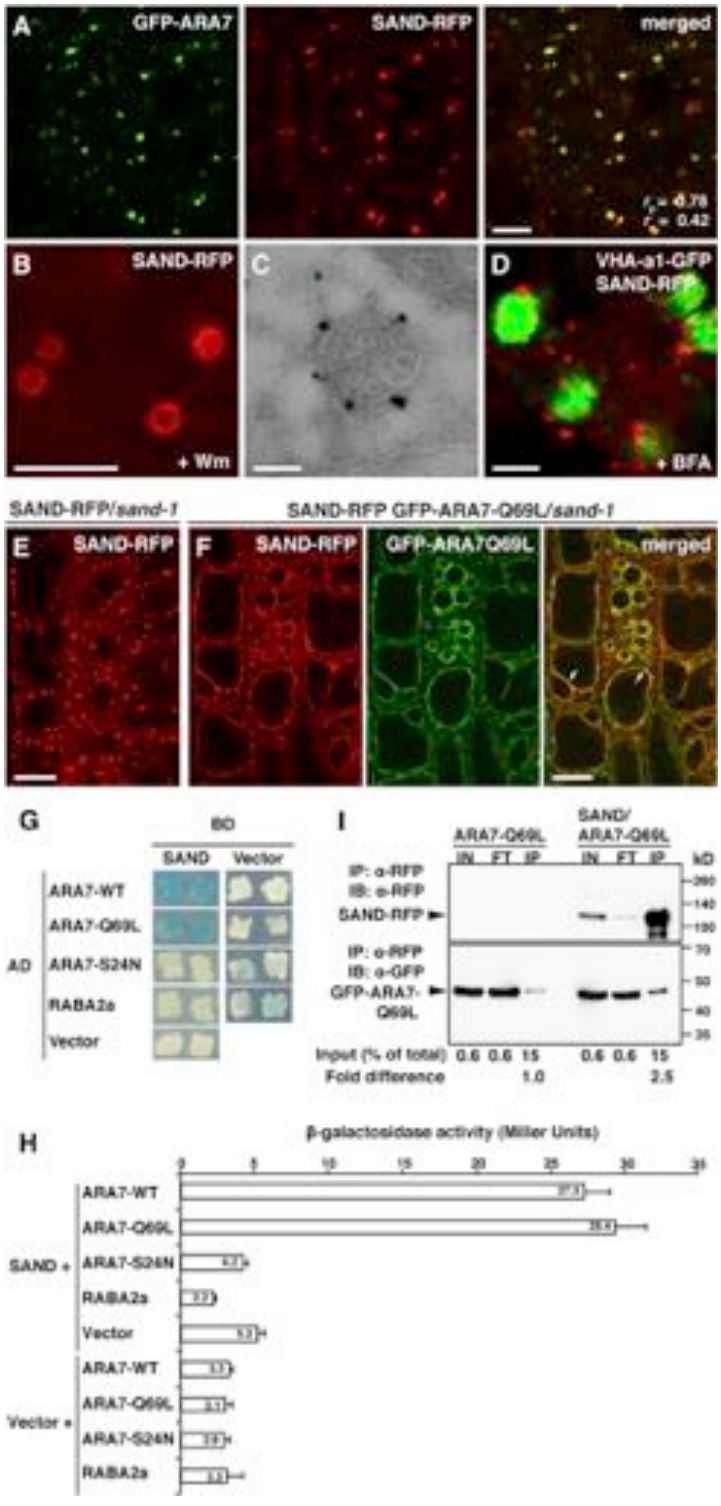

Figure 3. SAND Protein Localization and Interaction with Rab5-like ARA7

(A) Colocalization of SAND-RFP with GFP-ARA7. The values of Pearson (r_p) and Spearman (r_s) correlation coefficients represent the extent of colocalization between the two proteins. The values range between +1, indicating a positive correlation, and −1 for a negative correlation. See also Figure S3A.

(B) Enlarged ring-shaped signals of SAND-RFP in response to wortmannin treatment.

(C) Immuno-gold localization of SAND-RFP on limiting membrane of MVB.

(D) Double-labeling of TGN-localized VHA-a1-GFP and SAND-RFP in BFA-treated root cells. Note the close association of SAND signal (red) with VHA-a1-positive BFA compartment (green).

(E) SAND localization in rescued *sand-1* mutant.

(F) Double labeling of GFP-ARA7-Q69L (GTP-locked form) and SAND in rescued *sand-1* mutant. Note the colocalization of the two proteins in the vacuolar membrane (arrows).

(G) Yeast two-hybrid interaction analysis of SAND with ARA7 wild-type (WT), GTP-locked (Q69L), GDP-locked (S24N) forms, and RABA2a (TGN-localized; contr).

(H) Quantitation of SAND-ARA7 interaction strength in yeast, using β-galactosidase activity. Data shown as means ± SE; n = 5.

(I) Coimmunoprecipitation of ARA7-Q69L with SAND. *Arabidopsis* seedlings stably expressing both SAND-RFP and GFP-ARA7-Q69L, in *sand-1* background, were used for precipitation with anti-RFP antibody-linked agarose beads. Seedlings expressing only GFP-ARA7-Q69L were used as control. Upper half of the membrane was detected with anti-RFP antibody whereas lower half was used for anti-GFP antibody detection. The signal intensity of GFP-ARA7-QL band in IP relative to their respective inputs was used to calculate fold change. IN, input; FL, flow-through; IP, immunoprecipitate; IB, immunoblot; kD, kilodalton. Input (%) represents loading volume relative to the total volume used for IP.

Scale bars represent 5 μm (A, B, D); 100 nm (C); 10 μm (E, F). See also Figures S3 and S4.

TGN-localized VHA-a1 was largely unaffected. However, the vacuolar membrane was faintly labeled in *sand-1*, in addition to the exclusive labeling of the TGN in wild-type (Figures 2A and 2B). In contrast, two Rab5-like GTPases, ARA6 (aka RABF1) [22] and ARA7 (aka RABF2b), labeled clusters of abnormally shaped endosomal structures, which ultrastructural analysis identified as clusters of enlarged MVBs containing intraluminal vesicles (Figures 2C–2H). The mutant MVBs were approximately 60% larger than wild-type MVBs in diameter and had slightly fewer intraluminal vesicles (Figures 2G, 2H, and S2I). Interestingly, ARA6 (RABF1) and YFP-2xFYVE labeled the vacuolar membrane in *sand-1* mutants (Figures 2E, 2F, S2G, and S2H, arrowhead). Thus, SAND appears to act at the MVB.

SAND colocalized with ARA7 (RABF2b) and, like ARA7, was responsive to the PI3-kinase inhibitor wortmannin [23], yielding ring-shaped signals (Figures 3A, 3B, and S3A). Consistent with these findings, SAND localized to the limiting membrane of MVBs by immunogold labeling of ultrastructural sections (Figure 3C). Furthermore, the SAND-positive compartment did not respond to BFA treatment (Figure 3D). SAND also did not colocalize with TGN-resident VHA-a1 but largely colocalized

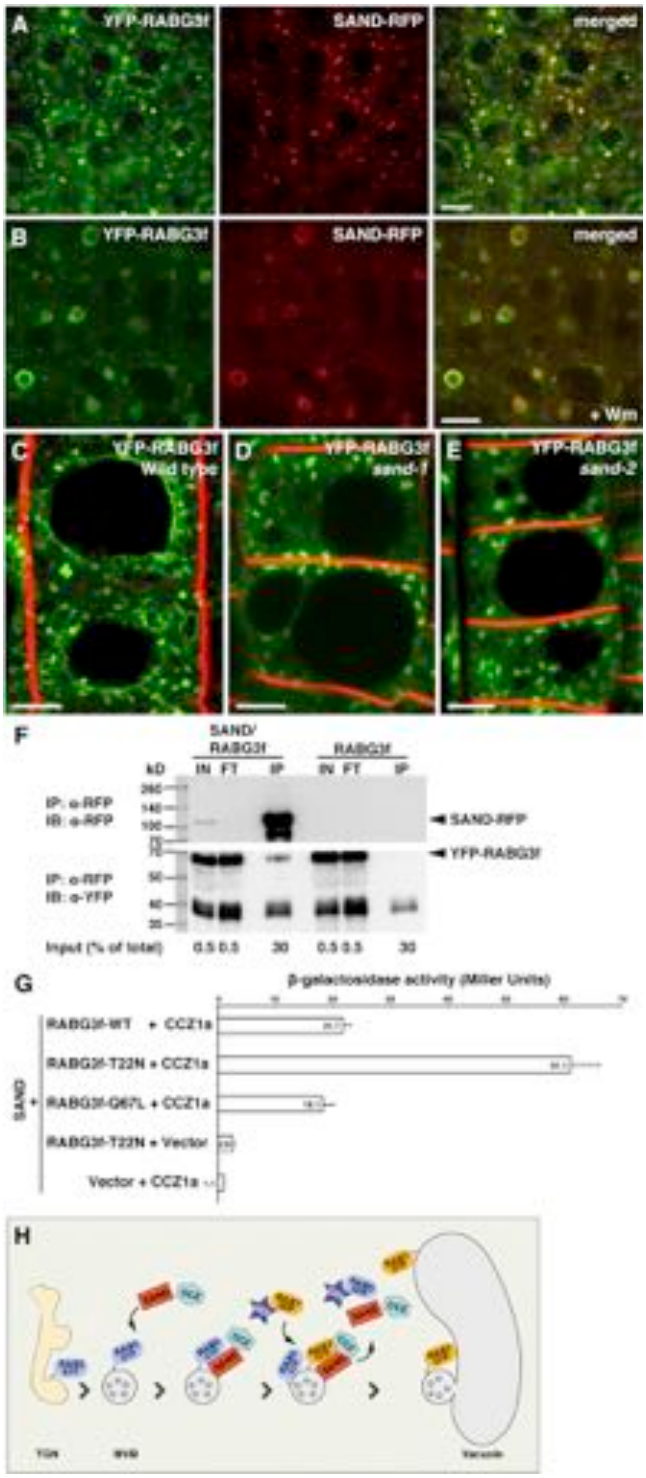

Figure 4. Role of SAND in Localization of Rab7-like RABG3f and Interaction of SAND-CCZ1 with Its GDP-Locked Isoform

(A) Colocalization of SAND-RFP and RabG3f in punctate structures.

(B) Colocalization of SAND-RFP and RabG3f in enlarged ring-shaped structures in wortmannin (Wm)-treated root cells.

(C) RabG3f localized to punctate structures and vacuolar membrane in wild-type.

(D and E) RabG3f localized to punctate structures and in the cytosol but not at the vacuolar membrane in *sand-1* (D) and *sand-2* (E).

(F) Coimmunoprecipitation of RABG3f with SAND. Immunoprecipitation was performed with transgenic line expressing both SAND-RFP and YFP-RABG3f and anti-RFP antibody-linked agarose beads. Seedlings expressing only YFP-RABG3f were used as control. Upper part of the membrane was developed with anti-RFP antibody and lower part was visualized with anti-YFP antibody. IN, input; FL, flow-through; IP, immunoprecipitate; IB, immunoblot; kD, kilodalton. Input (%) represents loading volume relative to the total volume used for IP.

(G) Quantitation of interaction strength between SAND (fused to binding domain) and wild-type (WT), GTP-locked (Q67L), or GDP-locked (T22N) isoforms of RABG3f (fused to activation domain) in presence or absence of CCZ1 protein in yeast three-hybrid assay using β-galactosidase reporter activity. Data shown as means ± SE; n = 5.

(H) Model of SAND protein action in vacuolar trafficking. RAB5 (ARA7) is recruited at the TGN and remains bound to the limiting membrane of newly formed MVB where it recruits SAND protein. Once present on MVB, SAND together with CCZ1 protein leads to the activation of RAB7 (RABG3f) on MVB and its fusion with vacuole.

Scale bars represent 5 μm (A–E). See also Figure S4.

with the PI3P sensor 2xFYVE and Rab5-like ARA6 (Figure S3). Constitutive activity of ARA7-Q69L [24, 25] (GTP-locked form) resulted in its vacuolar membrane localization (Figure 3F). Interestingly, in the presence of constitutively active ARA7, SAND was also detected on the enlarged MVBs and at the vacuolar membrane (Figures 3E and 3F). To examine whether SAND interacts with ARA7 directly, yeast two-hybrid interaction assays were performed. Both the wild-type form of ARA7 and the GTP-locked form (ARA-Q69L) interacted with SAND whereas the GDP-locked form (ARA7-S24N) did not (Figures 3G, 3H, S4A, and S4B). Interaction of SAND-RFP with GFP-tagged ARA7-Q69L was also detected by coimmunoprecipitation in extracts of transgenic *Arabidopsis* seedlings (Figure 3I). Thus, SAND appears to be an effector of GTP-bound ARA7.

In yeast, SAND/Mon1 forms a heterodimer with CCZ1 that acts as a guanine-nucleotide exchange factor (GEF) of late-endosomal/vacuolar Rab7-like Ypt7 [8]. In *Arabidopsis*, there are eight Rab7-like GTPases including RABG3f, which has been localized to MVBs and the vacuole [26, 27]. RABG3f colocalized with SAND protein both in untreated and in wortmannin-treated seedling roots, displaying ring-shaped signals upon wortmannin treatment (Figures 4A and 4B). Furthermore, YFP-tagged RABG3f localized to MVBs and the vacuolar membrane in wild-type roots (Figure 4C). In contrast, no YFP signal was detected on the vacuolar membrane in *sand-1* mutant seedling roots. Instead, RABG3f was present in punctae and in the cytosol (Figures 4D, 4E, and S4E). These punctate structures did not respond to wortmannin in *sand-1*, in contrast to wild-type, suggesting that they are not MVBs (Figure S4E). Thus, SAND is required for the correct localization of

Current Biology Vol 24 No 12
1388

RABG3f including its accumulation on the vacuolar membrane, which is similar to the dependence of Rab7-like Ypt7 on Mon1/SAND in yeast [28]. These data suggested that SAND, directly or indirectly, might interact with RABG3f. Indeed, interaction was detected in coimmunoprecipitation assays via extracts of transgenic plants that expressed SAND-RFP and YFP-tagged RABG3f (Figure 4F). We then employed yeast three-hybrid analysis involving CCZ1 as a bridging protein to characterize the potential interaction between SAND and RABG3f (Figures 4G, S4A, S4C, and S4D). In the presence of CCZ1, SAND interacted much more strongly with the GDP-locked form of RABG3f than with wild-type or the GTP-locked form, which would be consistent with a role for SAND-CCZ1 as RABG3f-GEF (see also the accompanying manuscript by Ebine et al [29]., which demonstrates RabG3f-GEF activity of SAND-CCZ1). Moreover, SAND alone did not interact with the GDP-locked form of RABG3f, suggesting that the coimmunoprecipitation of RABG3f with SAND from plant extracts actually involved the presence of the SAND-CCZ1 heterodimer.

Our results indicate that in plants, as has been described in nonplant organisms, protein trafficking to the vacuole for degradation involves endosomal maturation from early endosome to MVB and subsequent fusion of MVBs with the vacuole (see model in Figure 4H). In addition, the role of SAND protein in Rab5-to-Rab7 conversion appears to be evolutionarily conserved. Surprisingly, however, SAND-mediated Rab conversion is not required for MVB formation in *Arabidopsis*, as revealed by the presence of intraluminal vesicles in *sand* mutant plants, indicating that maturation of late endosomes from early endosomes takes place in the presence of Rab5 and the absence of Rab7. Instead, in plants Rab conversion by SAND is specifically required for the subsequent MVB-vacuole fusion. It is conceivable, though, that SAND-mediated Rab conversion might also play a role in MVB-vacuole/lysosome fusion in nonplant organisms, as suggested by the interaction of Rab7-like Ypt7 with the vacuolar HOPS complex [8]. However, this might not be readily apparent because of the earlier requirement of SAND protein in endosomal maturation such that functional MVBs are not generated in *sand* mutants. The underlying difference between plants and nonplant organisms thus relates to a difference in specific membrane recruitment and/or activation of Rab5-like GTPases, with ARA6 and ARA7 of *Arabidopsis* mainly associating with MVBs/LEs and Rab5 and yeast Vps21p associating with early endosomes [30]. It is tempting to speculate that the difference between plants and nonplant organisms observed in endosomal maturation and Rab conversion might result from the relative timing of two distinct processes: ESCRT-dependent formation of intraluminal vesicles, which transforms early into late endosomes, and Rab5-to-Rab7 conversion, which essentially prepares late endosomes/MVBs for their fusion with the lysosome/vacuole.

Supplemental Information

Supplemental Information includes four figures and Supplemental Experimental Procedures and can be found with this article online at http://dx.doi.org/10.1016/j.cub.2014.05.005.

Acknowledgments

We thank Niko Geldner, Ueli Grossniklaus, and Takashi Ueda for sharing published materials and Sacco de Vries for kindly providing anti-YFP antiserum and NASC for T-DNA insertion lines. This work was funded by DFG grant Ju179/18-1.

Received: February 12, 2014
Revised: April 7, 2014
Accepted: May 2, 2014
Published: May 29, 2014

References

1. Huotari, J., and Helenius, A. (2011). Endosome maturation. EMBO J. *30*, 3481–3500.
2. Henne, W.M., Buchkovich, N.J., and Emr, S.D. (2011). The ESCRT pathway. Dev. Cell *21*, 77–91.
3. Poteryaev, D., Datta, S., Ackema, K., Zerial, M., and Spang, A. (2010). Identification of the switch in early-to-late endosome transition. Cell *141*, 497–508.
4. Otegui, M.S., and Spitzer, C. (2008). Endosomal functions in plants. Traffic *9*, 1589–1598.
5. Richter, S., Voss, U., and Jürgens, G. (2009). Post-Golgi traffic in plants. Traffic *10*, 819–828.
6. Reyes, F.C., Buono, R., and Otegui, M.S. (2011). Plant endosomal trafficking pathways. Curr. Opin. Plant Biol. *14*, 666–673.
7. Rink, J., Ghigo, E., Kalaidzidis, Y., and Zerial, M. (2005). Rab conversion as a mechanism of progression from early to late endosomes. Cell *122*, 735–749.
8. Nordmann, M., Cabrera, M., Perz, A., Bröcker, C., Ostrowicz, C., Engelbrecht-Vandré, S., and Ungermann, C. (2010). The Mon1-Ccz1 complex is the GEF of the late endosomal Rab7 homolog Ypt7. Curr. Biol. *20*, 1654–1659.
9. Kinchen, J.M., and Ravichandran, K.S. (2010). Identification of two evolutionarily conserved genes regulating processing of engulfed apoptotic cells. Nature *464*, 778–782.
10. Dettmer, J., Hong-Hermesdorf, A., Stierhof, Y.D., and Schumacher, K. (2006). Vacuolar H+-ATPase activity is required for endocytic and secretory trafficking in *Arabidopsis*. Plant Cell *18*, 715–730.
11. Contento, A.L., and Bassham, D.C. (2012). Structure and function of endosomes in plant cells. J. Cell Sci. *125*, 3511–3518.
12. Viotti, C., Bubeck, J., Stierhof, Y.D., Krebs, M., Langhans, M., van den Berg, W., van Dongen, W., Richter, S., Geldner, N., Takano, J., et al. (2010). Endocytic and secretory traffic in *Arabidopsis* merge in the trans-Golgi network/early endosome, an independent and highly dynamic organelle. Plant Cell *22*, 1344–1357.
13. Stierhof, Y.D., and El Kasmi, F. (2010). Strategies to improve the antigenicity, ultrastructure preservation and visibility of trafficking compartments in *Arabidopsis* tissue. Eur. J. Cell Biol. *89*, 285–297.
14. Vermeer, J.E., van Leeuwen, W., Tobeña-Santamaria, R., Laxalt, A.M., Jones, D.R., Divecha, N., Gadella, T.W., Jr., and Munnik, T. (2006). Visualization of PtdIns3P dynamics in living plant cells. Plant J. *47*, 687–700.
15. Scheuring, D., Viotti, C., Krüger, F., Künzl, F., Sturm, S., Bubeck, J., Hillmer, S., Frigerio, L., Robinson, D.G., Pimpl, P., and Schumacher, K. (2011). Multivesicular bodies mature from the trans-Golgi network/early endosome in *Arabidopsis*. Plant Cell *23*, 3463–3481.
16. Robinson, D.G., Jiang, L., and Schumacher, K. (2008). The endosomal system of plants: charting new and familiar territories. Plant Physiol. *147*, 1482–1492.
17. Fuji, K., Shimada, T., Takahashi, H., Tamura, K., Koumoto, Y., Utsumi, S., Nishizawa, K., Maruyama, N., and Hara-Nishimura, I. (2007). *Arabidopsis* vacuolar sorting mutants (green fluorescent seed) can be identified efficiently by secretion of vacuole-targeted green fluorescent protein in their seeds. Plant Cell *19*, 597–609.
18. Sohn, E.J., Kim, E.S., Zhao, M., Kim, S.J., Kim, H., Kim, Y.W., Lee, Y.J., Hillmer, S., Sohn, U., Jiang, L., and Hwang, I. (2003). Rha1, an *Arabidopsis* Rab5 homolog, plays a critical role in the vacuolar trafficking of soluble cargo proteins. Plant Cell *15*, 1057–1070.
19. Reichardt, I., Stierhof, Y.D., Mayer, U., Richter, S., Schwarz, H., Schumacher, K., and Jürgens, G. (2007). Plant cytokinesis requires de novo secretory trafficking but not endocytosis. Curr. Biol. *17*, 2047–2053.
20. Geldner, N., Friml, J., Stierhof, Y.D., Jürgens, G., and Palme, K. (2001). Auxin transport inhibitors block PIN1 cycling and vesicle trafficking. Nature *413*, 425–428.

21. Abas, L., Benjamins, R., Malenica, N., Paciorek, T., Wiśniewska, J., Moulinier-Anzola, J.C., Sieberer, T., Friml, J., and Luschnig, C. (2006). Intracellular trafficking and proteolysis of the *Arabidopsis* auxin-efflux facilitator PIN2 are involved in root gravitropism. Nat. Cell Biol. *8*, 249–256.
22. Ebine, K., Fujimoto, M., Okatani, Y., Nishiyama, T., Goh, T., Ito, E., Dainobu, T., Nishitani, A., Uemura, T., Sato, M.H., et al. (2011). A membrane trafficking pathway regulated by the plant-specific RAB GTPase ARA6. Nat. Cell Biol. *13*, 853–859.
23. Takáč, T., Pechan, T., Samajová, O., Ovečka, M., Richter, H., Eck, C., Niehaus, K., and Samaj, J. (2012). Wortmannin treatment induces changes in *Arabidopsis* root proteome and post-Golgi compartments. J. Proteome Res. *11*, 3127–3142.
24. Ueda, T., Yamaguchi, M., Uchimiya, H., and Nakano, A. (2001). Ara6, a plant-unique novel type Rab GTPase, functions in the endocytic pathway of *Arabidopsis thaliana*. EMBO J. *20*, 4730–4741.
25. Jia, T., Gao, C., Cui, Y., Wang, J., Ding, Y., Cai, Y., Ueda, T., Nakano, A., and Jiang, L. (2013). ARA7(Q69L) expression in transgenic *Arabidopsis* cells induces the formation of enlarged multivesicular bodies. J. Exp. Bot. *64*, 2817–2829.
26. Rutherford, S., and Moore, I. (2002). The *Arabidopsis* Rab GTPase family: another enigma variation. Curr. Opin. Plant Biol. *5*, 518–528.
27. Geldner, N., Dénervaud-Tendon, V., Hyman, D.L., Mayer, U., Stierhof, Y.D., and Chory, J. (2009). Rapid, combinatorial analysis of membrane compartments in intact plants with a multicolor marker set. Plant J. *59*, 169–178.
28. Cabrera, M., and Ungermann, C. (2013). Guanine nucleotide exchange factors (GEFs) have a critical but not exclusive role in organelle localization of Rab GTPases. J. Biol. Chem. *288*, 28704–28712.
29. Ebine, K., Inoue, T., Ito, J., Ito, E., Uemura, T., Goh, T., Abe, H., Sato, K., Nakano, A., and Ueda, T. (2014). Plant vacuolar trafficking occurs through distinctly regulated pathways. Curr. Biol. *24*, this issue.
30. Markgraf, D.F., Peplowska, K., and Ungermann, C. (2007). Rab cascades and tethering factors in the endomembrane system. FEBS Lett. *581*, 2125–2130.

Note Added in Proof

An independent analysis of MON1, which is allelic to SAND, was recently reported (Cui et al., *The Plant Cell*, in press). Although Cui and colleagues used a different mutant allele and different trafficking markers, their study yielded essentially the same conclusion.

Current Biology, Volume *24*

Supplemental Information

Protein Delivery to Vacuole Requires SAND Protein-Dependent Rab GTPase Conversion for MVB-Vacuole Fusion

Manoj K. Singh, Falco Krüger, Hauke Beckmann, Sabine Brumm, Joop E.M. Vermeer, Teun Munnik, Ulrike Mayer, York-Dieter Stierhof, Christopher Grefen, Karin Schumacher, and Gerd Jürgens

Figure S1

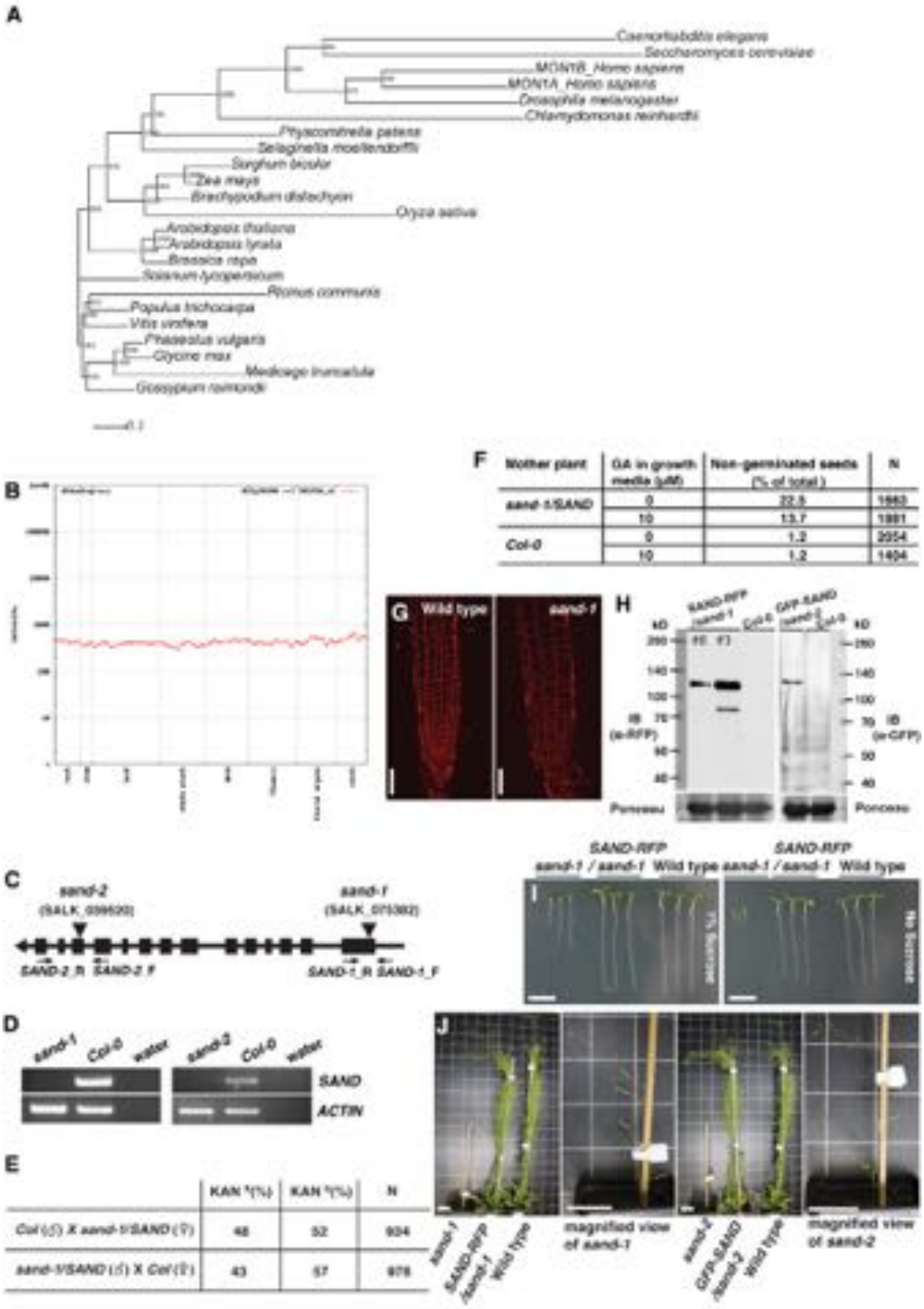

Figure S1, Related to Figure 1. *SAND* gene and mutant phenotypes
(A) Phylogenetic tree of SAND orthologs in various monocot and dicot plants, yeast, algae and animals. Following sequences were used for construction of the tree:

Chlamydomonas reinhardtii (Cre03.g154500.t1.2); *Saccharomyces cerevisiae* (NP_011391.2); *Caenorhabditis elegans* (NP_500791.2); *Homo sapiens* MON1B (NP_055755.1); *Homo sapiens* MON1A (Q86VX9.2); *Drosophila melanogaster* (NP_608868.1); *Physcomitrella patens* (Pp1s452_21V6); *Selaginella moellendorffii* (EFJ23517.1); *Sorghum bicolor* (XP_002459184.1); *Zea mays* (NP_001149118.1); *Brachypodium distachyon* (XP_003567548.1); *Oryza sativa* (Os01g74460.2); *Arabidopsis thaliana* (At2g28390); *Arabidopsis lyrata* (EFH55358.1); *Brassica rapa* (Bra000494); *Solanum lycopersicum* (XP_004235972.1); *Ricinus communis* (EEF27973.1); *Populus trichocarpa* (POPTR_0004s22080); *Vitis vinifera* (XP_002285170.1); *Phaseolus vulgaris* (Phvul.005G134800.1); *Glycine max* (Glyma12g29450.1); *Gossypium raimondii* (Gorai.003G141900.1); *Medicago truncatula* (AES67499.1)
(B) Expression profile of Arabidopsis *SAND* gene (At2g28390). Expression data was obtained using AtGenExpress Visualisation Tool
(http://www.weigelworld.org/resources/microarray/AtGenExpress; ref. [S1])
(C) Schematic diagram of *SAND gene* indicating position of T-DNA insertions and primers used for RT PCR analysis. (D) RT-PCR analysis of *sand-1* and *sand-2*. (E) Reciprocal crosses. Loss of *SAND* has no effect on gametophytic transmission. (F) Effect of Gibberellic acid (GA) on germination of *sand-1.* Seeds from *Col-0* and *sand-1/SAND* mother plants were germinated on growth media with or without GA. Data presented is from one representative experiment. (G) Abnormal cell shapes and sizes in *sand-1* seedling root. (H) Western blot showing expression of SAND-RFP and GFP-SAND in complemented *sand-1* and *sand-2* mutants. #3 and #8 are two independent rescued *sand-1* mutant lines expressing different levels of SAND-RFP. Col-0, non-transgenic wild type control; IB, Immunoblot; kD, kilodalton. (I) *sand-1* phenotype is aggravated by growth on medium lacking sucrose. (J) Rescue of *sand-1* and *sand-2* phenotype by expression of SAND-RFP and GFP-SAND, respectively.
Scale bar represents 50 µm in (G); 1 cm in (H); 3 cm in (I).

Figure S2

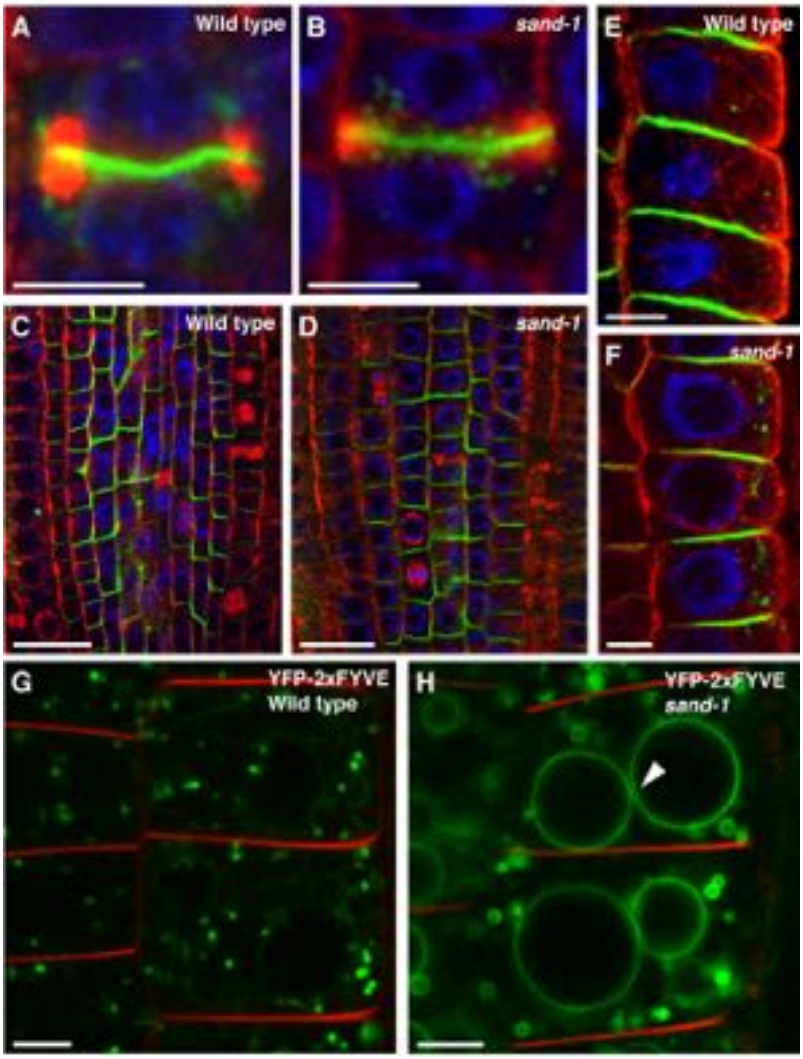

I

Genotype	Average diameter of MVB (in nm)	Average number of intraluminal vesicles (per MVB)	N
Wild type	229.55 ± 68.52	5.45 ± 3.36	29
sand-1	381.13 ± 119.74	3.11 ± 3.62	63

Figure S2, Related to Figure 1 and Figure 2. Secretory pathway and recycling is unaffected in *sand* mutants

(A, B) KNOLLE localisation at the cell plate. (C, D) Polar PIN1 localisation in inner cells. (E, F) Apical localisation of PIN2 in epidermal cells. Note the accumulation of PIN2 in punctate (endosomal) compartments (F). (G, H) YFP-2xFYVE localisation in wild type (G) and *sand-1* (H). Note the strong labeling of vacuolar membrane in *sand-1* (H; arrowhead) compared to wild type (G) where the signal was mainly on MVBs. (I) Quantitation of average MVB size and number of intraluminal vesicles in wild type and *sand-1* mutant. N, total number of MVBs used for analysis. Data shown as means ± SD.

Scale bar represents 5 µm in (A)(B)(E)-(H); 20µm in (C)(D).

Figure S3

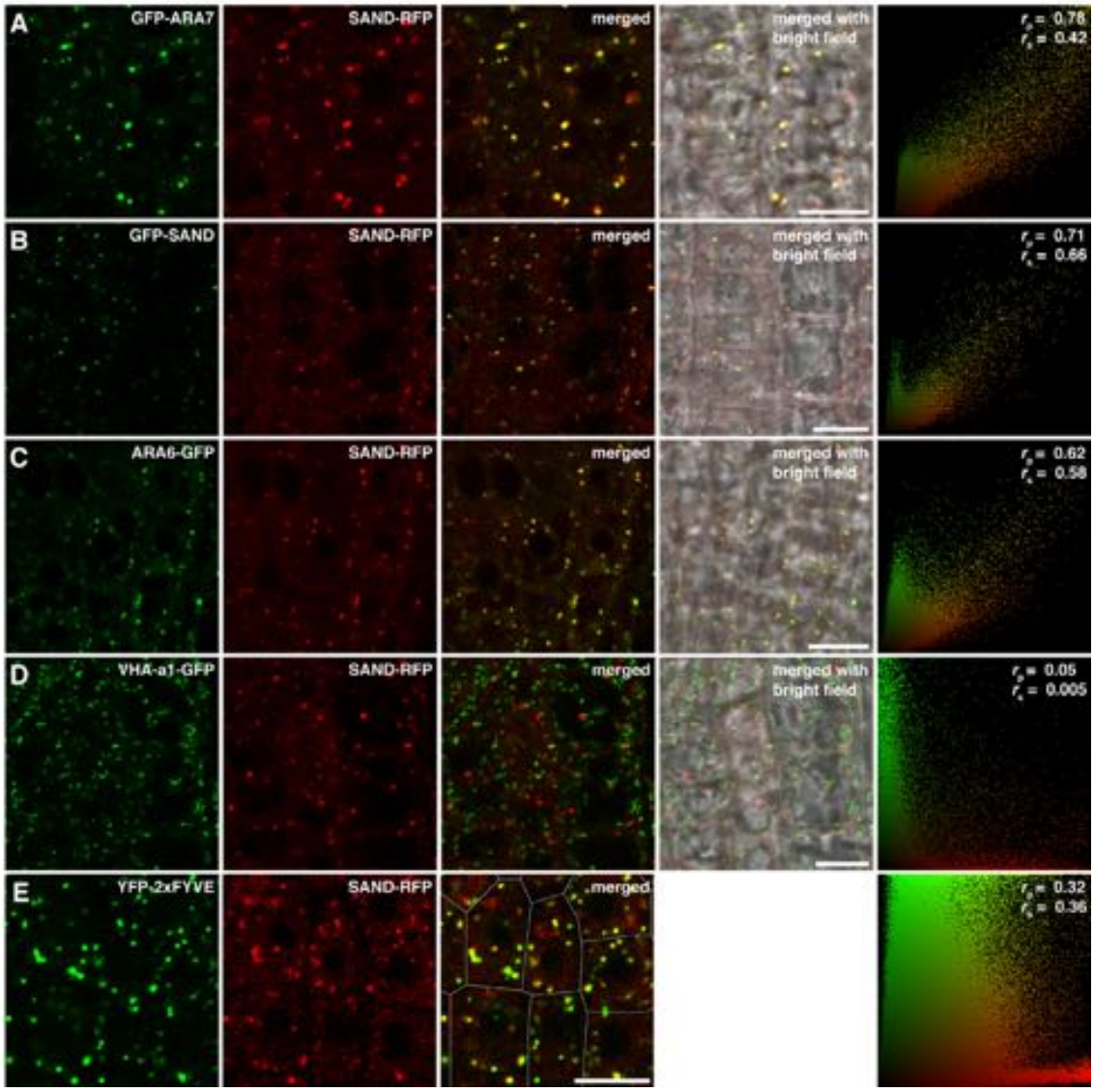

Figure S3, Related to Figure 3. Co-localisation of SAND-RFP with various subcellular markers

(A) GFP-ARA7 and SAND-RFP (same as in Fig. 3A). (B) GFP-SAND and SAND-RFP. (C) MVB marker ARA6-GFP and SAND-RFP. (D) VHA-a1-GFP and SAND-RFP. (E) YFP-2xFYVE and SAND-RFP. Cell boundaries in (E) are shown with dotted lines. Co-localisation analysis was performed using PSC plugin for ImageJ [S19] from a minimum of five independent seedling root images. Pearson (r_p) and Spearman (r_s) correlation coefficients and the scatter plots are shown in the right panels. The extent of co-localisation ranges between +1, indicating a positive correlation, and -1 for a negative correlation. Scale bar, 10 µm.

Figure S4

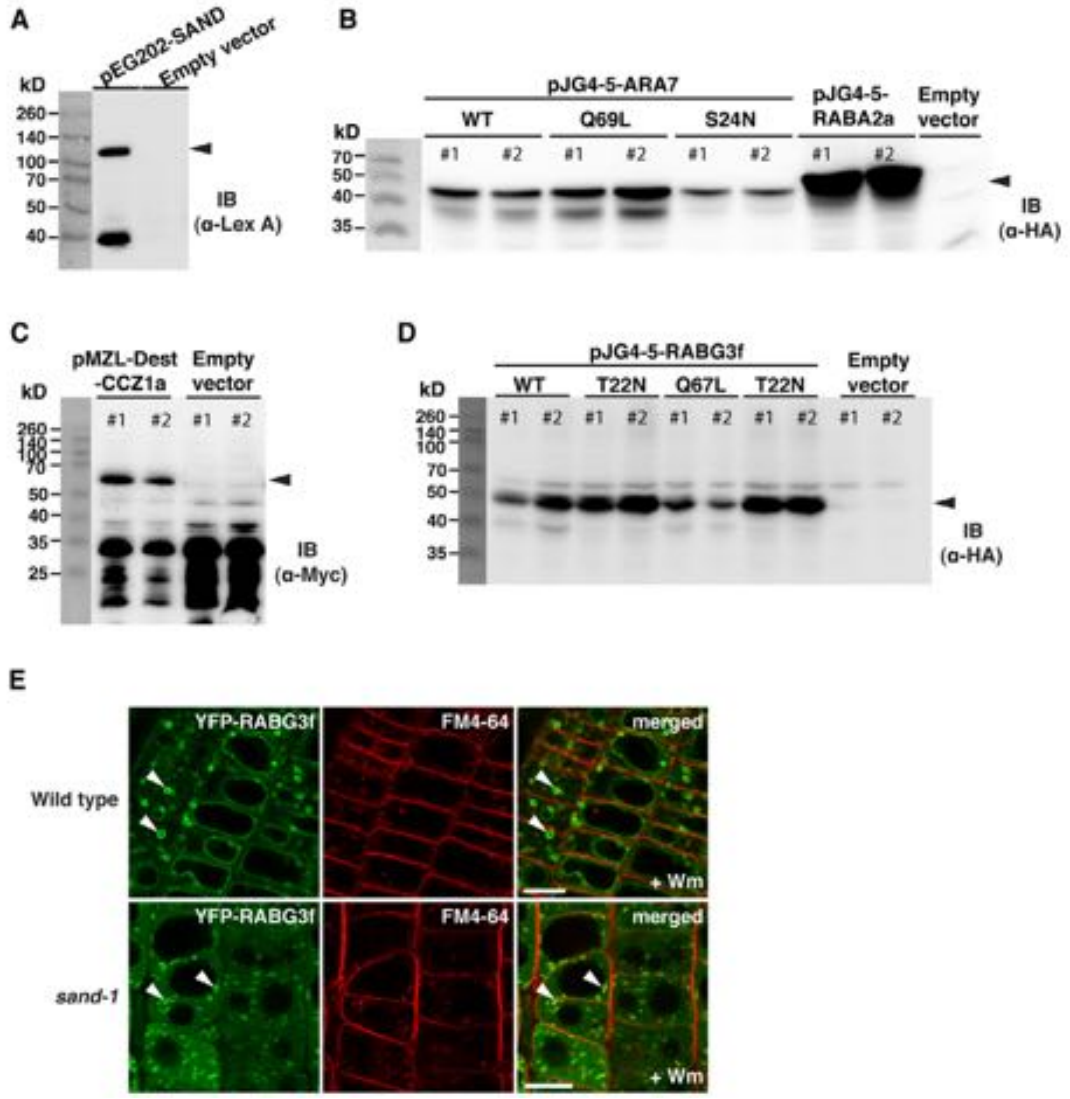

Figure S4, Related to Figure 3 and Figure 4. Yeast two-hybrid and three-hybrid protein expression and differential wortmannin sensitivity of RABG3f in wild type and *sand-1* mutant.

(A-D) Western blots showing expression of different constructs in yeast. Protein bands of LexA-SAND (90kD) in (A), HA-tagged wild type (WT) and mutant forms (Q69L, S24N) of ARA7 (35kD) and RABA2a (36kD) in (B), Myc-CCZ1a (60kD) in (C) and HA-tagged RABG3f isoforms (WT, Q67L and T22N) (35kD) in (D) are marked with arrowheads. #1 and #2 represent two independent yeast colonies. IB, Immunoblot; kD, kilodalton.

(E) Effect of Wortmannin (Wm) treatment on YFP-RABG3f in wild type and *sand-1* background. Note that punctate signals (arrowheads) do not form ring-shaped structures in *sand-1*, in contrast to wild type (arrowheads). Scale bar, 10 µm.

Supplemental Experimental Procedures

Plant Material and growth conditions

Arabidopsis thaliana wild type (ecotype Col-0) and transgenic lines, after surface sterilisation, were grown on Murashige and Skoog (MS) medium containing 1%(w/v) sucrose (if not stated otherwise) and 0.8% (w/v) agar in continuous light at 24^0C.

For seed germination in presence of gibberellic acid (GA), MS medium was supplemented with 10μM GA (GA_{4+7}, Sigma). Seedlings were transferred to soil 8-10 days after germination and grown in same conditions.

Seed germination assay

Seeds obtained from wild type and *sand* heterozygous plants were sown on MS medium supplemented with or without GA. After stratification for 3 nights at 4^0C in dark, plates were transferred to growth chamber. Germinated seeds were counted 4-days after transfer to plant growth chamber.

Isolation of *sand* mutants

SALK T-DNA lines carrying insertion in *SAND* gene (in Col-0 ecotype) were purchased from Nottingham Arabidopsis Stock Centre (NASC). The *sand-1* (SALK_075382) and *sand-2* (SALK_039520) insertions are located in the first and 12^{th} exon, respectively. Genotyping of *sand-1* insertion line was performed using SALK_075382_LP (5´-CGGTTTGCCTGAGTTACTCAG-3´), SALK_075382_RP (5´-AAAAGCCCAACAATATGGGTC-3´) and LBb1.3 (5´-ATTTTGCCGATTTCGGAAC-3´) primers. The *sand-2* insertion line was genotyped using SALK_039520_LP (5´-CAACCAACTCTCGTCTCCATC-3)´, SALK_039520_RP (5´-ATGCGTTCCATCATCTCAAAG-3´) and LBb1.3 primers. *SAND* transcript in mutants was analysed using following primers: *SAND1_F* (5´-ACACGTCTTGCCATTAGAGGA-3), *SAND1_R* (5´-CTTCACCTGCTTCCATTTCC-3), *SAND2_F* (5´-TGGACTTTGGCATTTCATGT-3´), *SAND2_R* (5´-CTTTTACCCTTTGGCACACC-3´).

RNA isolation, cloning and transgenic plants

Total RNA was isolated from seedlings using Trizol® (Invitrogen). After DNAse I (Fermentas) digestion, cDNA was synthesised using RevertAid H Minus First Strand cDNA Synthesis Kit (Thermo scientific).

For generation of transgenic lines expressing SAND-RFP, coding sequence (CDS) of *SAND* was amplified from a cDNA library derived from *Col-0*, cloned upstream of *mRFP* into pGrIIKRPS5a-tNOS vector [S2] and transformed into *sand-1*/*SAND* plants. To generate *GFP-SAND* lines, *SAND* CDS was cloned downstream of *GFP* in pUGT2Kan vector and transformed in *sand-2/SAND* plants. AFVY-RFP and Aleurain (Aleu)-GFP were amplified from existing templates [S3, S4] and cloned, using GATEWAY® (Life Technologies) method, in pMDC7 [S5] vector for generation of estradiol inducible Arabidopsis lines. UBQ10::YFP-2X FYVE was generated by cloning 2xFYVE [S6] into pUNI51 and recombined into pNIGEL07 using the CRE/lox system as described [S7]. Transgenic marker lines expressing YFP-RABG3f [S7], ARA6-GFP [S8], GFP-ARA7Q69L [S8], GFP-ARA7 [S9], mRFP-ARA7 [S10], GFP-CT24 [S11], VHA-a1-mRFP [S12] and VHA-a1-GFP [S12] were described earlier.

Yeast hybrid-protein interaction analysis

For yeast two-hybrid analysis, yeast (EGY48 strain) was transformed with following plasmids: pSH18-34, pEG202-SAND and pJG4-5 carrying either RABA2a or ARA7 isoforms (wild type, Q69L and S24N). The interaction assay was performed as reported previously [S13, S14].

For yeast three-hybrid assay, SAND and RABG3f isoforms (wild type, Q67L and T22N) were expressed using pEG202 and pJG4-5 vector, respectively. CCZ1a (At1g16020) was expressed under ADH promoter and with addition of an N-terminal Myc-tag using the Gateway-compatible yeast expression vector pMZL-Dest. This vector derives from vector pMZU-Dest [S15], the URA3 auxotrophy marker being replaced with LEU2 (sequence information available upon request). The assay was performed similar to two-hybrid assay.

Immunoprecipitation

Arabidopsis seedlings (3.0-3.5g) were ground thoroughly in liquid nitrogen and suspended in lysis buffer (50mM Tris pH 7.5, 150mM NaCl) containing 1%(v/v) Triton X-100 and protease inhibitor cocktail (cOmplete EDTA-free®, Roche). After 30 min incubation on ice, cell debris was removed by centrifugation at 10,000 x g for 30 min at 4^0C. The supernatant was filtered through Miracloth (Calbiochem) and incubated with anti-RFP beads (RFP-Trap®, Chromotek) for 4 hour with end-to-end rotation in the cold room. Beads were washed twice with lysis buffer containing 0.1% Triton, followed by 3 washes with buffer lacking Triton (for SAND-RABG3f coIP studies) or once with lysis buffer containing 0.5% Triton, twice with buffer containing 0.1% Triton followed by two washes using buffer without Triton (for SAND-ARA7Q69L coIP studies). After the last wash, beads were boiled in 2x Laemmli buffer.

Western blotting

Proteins were resolved on SDS-PAGE and immuno-detected using one of the following antibodies: anti-RFP (rat, 1:1,000, chromotek), anti-GFP (mouse 1:1,000, Roche), anti-YFP (rabbit, 1:1,000, a gift from S. de Vries), anti-LexA (mouse, 1: 1000, Santa Cruz Biotechnology), POD-conjugated anti-HA (1:1000, Roche).

Immunofluorescence and microscopy

5-day-old *Arabidopsis* seedlings were fixed in MTSB solution containing 4% paraformaldehyde. The immunostaining was performed as previously reported [S16]. The following antibodies were used for immunolocalisation in this study: rabbit anti-KNOLLE, 1:3,000 [S16]; rabbit anti-PIN1, 1:200 [S17]; rabbit anti-PIN2, 1:500 [S18] and rat anti-Tubulin 1:600 (abcam). Secondary antibodies conjugated with Alexa-488® (Invitrogen) and Cy3 (Dianova) were used at 1:600 dilution.

Live-cell imaging was performed using 4 to 5-day-old seedlings in liquid MS medium. FM4-64 was used at 2 µM final concentration. For induction of AFVY-RFP expression, seedlings were transferred to liquid MS medium (pH 5.8) containing 10 µM β-Estradiol (Sigma) and

kept in dark for 48 hr at 24^0C. Aleurain-GFP induction was, similarly, carried out in liquid MS medium of pH 8.1. For Wortmannin treatments, a final concentration of 33 µM was used for for 1 hr. BFA treatment was performed at a final concentration of 50 µM for 1 hr, unless indicated otherwise. Confocal images were obtained using Leica TCS SP8 microscope. For co-localisation studies, images were acquired using sequential scan mode.

For light microscopy of cotyledon pavement cells, cells were cleared using chloral hydrate (Sigma) solution and images were taken using Zeiss Axiophot microscope.

Immunogold labeling and ultra structural analysis

Immunogold labeling and ultra structural analyses were performed as reported previously [S9].

Co-localisation analysis

Confocal laser scanning microscope (CLSM) images from five independent seedling root images, showing a minimum of 8 cells in each image, were obtained using hybrid detectors (HyDs) of Leica TCS SP8 microscope and processed uniformly using smooth tool of ImageJ. Co-localisation analysis was done by calculating Pearson and Spearman correlation coefficients using PSC colocalization plugin of ImageJ according to the instructions of French et al. [S19] with a background level setting of 3.

Phylogenetic analysis

Full length SAND protein sequences from different organisms were aligned using CLC DNA Workbench 6 and a phylogenetic tree was generated using neighbor-joining algorithm with a bootstrap of 100 replicates. The tree was optimised using Dendroscope (version 2.5) program.

Softwares

CLC DNA Workbench 6 was used for DNA sequences analysis. Signal intensity of bands in western blot was quantified using ImageJ (NIH). For image processing Adobe Photoshop CS3 and Adobe Illustrator CS3 were used.

Supplemental References

S1. Schmid, M., Davison, T.S., Henz, S.R., Pape, U.J., Demar, M., Vingron, M., Scholkopf, B., Weigel, D., and Lohmann, J.U. (2005). A gene expression map of Arabidopsis thaliana development. Nat Genet *37*, 501-506.

S2. Weijers, D., Van Hamburg, J.P., Van Rijn, E., Hooykaas, P.J., and Offringa, R. (2003). Diphtheria toxin-mediated cell ablation reveals interregional communication during Arabidopsis seed development. Plant Physiol *133*, 1882-1892.

S3. Scheuring, D., Viotti, C., Krüger, F., Künzl, F., Sturm, S., Bubeck, J., Hillmer, S., Frigerio, L., Robinson, D.G., Pimpl, P., et al. (2011). Multivesicular bodies mature from the trans-Golgi network/early endosome in Arabidopsis. Plant Cell *23*, 3463-3481.

S4. Sohn, E.J., Kim, E.S., Zhao, M., Kim, S.J., Kim, H., Kim, Y.W., Lee, Y.J., Hillmer, S., Sohn, U., Jiang, L., et al. (2003). Rha1, an Arabidopsis Rab5 homolog, plays a critical role in the vacuolar trafficking of soluble cargo proteins. Plant Cell *15*, 1057-1070.

S5. Curtis, M.D., and Grossniklaus, U. (2003). A gateway cloning vector set for high-throughput functional analysis of genes in planta. Plant Physiol *133*, 462-469.

S6. Vermeer, J.E., van Leeuwen, W., Tobena-Santamaria, R., Laxalt, A.M., Jones, D.R., Divecha, N., Gadella, T.W., Jr., and Munnik, T. (2006). Visualization of PtdIns3P dynamics in living plant cells. Plant J *47*, 687-700.

S7. Geldner, N., Denervaud-Tendon, V., Hyman, D.L., Mayer, U., Stierhof, Y.D., and Chory, J. (2009). Rapid, combinatorial analysis of membrane compartments in intact plants with a multicolor marker set. Plant J *59*, 169-178.

S8. Ebine, K., Fujimoto, M., Okatani, Y., Nishiyama, T., Goh, T., Ito, E., Dainobu, T., Nishitani, A., Uemura, T., Sato, M.H., et al. (2011). A membrane trafficking pathway regulated by the plant-specific RAB GTPase ARA6. Nat Cell Biol *13*, 853-859.

S9. Richter, S., Geldner, N., Schrader, J., Wolters, H., Stierhof, Y.D., Rios, G., Koncz, C., Robinson, D.G., and Jürgens, G. (2007). Functional diversification of closely related ARF-GEFs in protein secretion and recycling. Nature *448*, 488-492.

S10. Beck, M., Zhou, J., Faulkner, C., MacLean, D., and Robatzek, S. (2012). Spatio-temporal cellular dynamics of the Arabidopsis flagellin receptor reveal activation status-dependent endosomal sorting. Plant Cell *24*, 4205-4219.

S11. Fuji, K., Shimada, T., Takahashi, H., Tamura, K., Koumoto, Y., Utsumi, S., Nishizawa, K., Maruyama, N., and Hara-Nishimura, I. (2007). Arabidopsis vacuolar sorting mutants (green fluorescent seed) can be identified efficiently by secretion of vacuole-targeted green fluorescent protein in their seeds. Plant Cell *19*, 597-609.

S12. Dettmer, J., Hong-Hermesdorf, A., Stierhof, Y.D., and Schumacher, K. (2006). Vacuolar H+-ATPase activity is required for endocytic and secretory trafficking in Arabidopsis. Plant Cell *18*, 715-730.

S13. Anders, N., Nielsen, M., Keicher, J., Stierhof, Y.D., Furutani, M., Tasaka, M., Skriver, K., and Jürgens, G. (2008). Membrane association of the Arabidopsis ARF exchange factor GNOM involves interaction of conserved domains. Plant Cell *20*, 142-151.

S14. Park, M., Touihri, S., Muller, I., Mayer, U., and Jürgens, G. (2012). Sec1/Munc18 protein stabilizes fusion-competent syntaxin for membrane fusion in Arabidopsis cytokinesis. Dev Cell *22*, 989-1000.

S15. Grefen, C., and Blatt, M.R. (2012). Do calcineurin B-like proteins interact independently of the serine threonine kinase CIPK23 with the K+ channel AKT1? Lessons learned from a menage a trois. Plant Physiol *159*, 915-919.

S16. Lauber, M.H., Waizenegger, I., Steinmann, T., Schwarz, H., Mayer, U., Hwang, I., Lukowitz, W., and Jürgens, G. (1997). The Arabidopsis KNOLLE protein is a cytokinesis-specific syntaxin. J Cell Biol *139*, 1485-1493.

S17. Vieten, A., Vanneste, S., Wisniewska, J., Benkova, E., Benjamins, R., Beeckman, T., Luschnig, C., and Friml, J. (2005). Functional redundancy of PIN proteins is

accompanied by auxindependent cross-regulation of PIN expression. Development *132*, 4521-4531.

S18. Abas, L., Benjamins, R., Malenica, N., Paciorek, T., Wisniewska, J., Moulinier-Anzola, J.C., Sieberer, T., Friml, J., and Luschnig, C. (2006). Intracellular trafficking and proteolysis of the Arabidopsis auxin-efflux facilitator PIN2 are involved in root gravitropism. Nat Cell Biol *8*, 249-256.

S19. French, A.P., Mills, S., Swarup, R., Bennett, M.J., and Pridmore, T.P. (2008). Colocalization of fluorescent markers in confocal microscope images of plant cells. Nature protocols *3*, 619-628.

6.3. Manuscript Brumm et al.

ARF1 dimerization through cooperative high-affinity binding by *Arabidopsis* ARF-GEF GNOM dimer

Sabine Brumm, Mads Eggert Nielsen, Sandra Richter, Hauke Beckmann, York-Dieter Stierhof, Manoj K. Singh, Angela-Melanie Fischer, Venkatesan Sundaresan and Gerd Jürgens

Membrane vesicle formation requires ARF GTPase activation by SEC7 domain of ARF guanine-nucleotide exchange factors (ARF-GEFs), resulting in the recruitment of coat proteins by GTP-bound ARFs. ARF-GEFs form dimers but their biological significance is unknown. Here we propose that ARF-GEF dimers mediate ARF1 dimer formation and we show that ARF1 dimers are required for membrane trafficking. Mutational disruption of ARF1 dimers interfered with ARF1-dependent trafficking but not coat protein recruitment. Mutations disrupting simultaneous binding of two ARF1•GDPs by the two SEC7 domains of ARF-GEF dimer prevented stable interaction of ARF1 with ARF-GEF and thus, efficient ARF1 activation. Our results suggest a model of activation-dependent dimerization of membrane-inserted ARF•GTP molecules required for coated membrane vesicle formation.

Activation of small GTPase ARF1 by guanine-nucleotide exchange factors (ARF-GEFs) plays a pivotal role in membrane traffic across the eukaryotes (Donaldson and Jackson, 2011). GDP-bound ARF1 interacts with the catalytic SEC7 domain of ARF-GEFs on donor membranes, resulting in GDP-GTP exchange on ARF1 and membrane insertion of its myristoylated N-terminal hasp (Casanova, 2007; Anders and Jürgens, 2008; Bui et al., 2009). GTP-bound ARF1 interacts with coat proteins involved in vesicle formation and cargo recruitment (D'Souza-Schorey and Chavrier, 2006; Gillingham and Munro, 2007; Singh and Jürgens, 2018). ARF1•GTP forms dimers in vitro, which are required for scission of membrane vesicles from donor membrane (Beck et al., 2008, 2011). ARF1 dimer formation is disrupted by a $Y_{35}A$ mutation, which reduces the yield of vesicles dramatically in vitro and fails to complement the lethality of *arf1 arf2* mutant yeast (Beck et al., 2008). How ARF1 dimers form under physiological conditions has not been addressed but might be related to ARF-GEF action. Eukaryotically conserved large ARF-GEFs such as human GBF1 or Arabidopsis GNOM have a stereotypic domain organization including an N-terminal dimerization (DCB) domain (Casanova, 2007; Anders and Jürgens, 2008; Bui et al., 2009). The DCB domain can interact with another DCB domain and with at least one other ARF-GEF domain (Grebe et al., 2000; Ramaen et al., 2007; Anders et al., 2008). Although conserved across the eukaryotes, the biological significance of ARF-GEF dimerization is not known. Our results presented here suggest that ARF-GEF dimers generate ARF1•GTP dimers during the activation process.

To address the issue of ARF1 dimerization, we tested ARF1 wild-type and two variants – activation-deficient ARF1-T_{31}N and hydrolysis-deficient ARF1-Q_{71}L (Dascher and Balch, 1994; Singh and Richter et al., 2018) – for interaction by co-immunoprecipitation. Both ARF1-T_{31}N and ARF1-Q_{71}L interacted with endogenous ARF1, although ARF1 wild-type failed to interact with itself (Figure 1A; Suppl. Figure S1A). However, ARF1-T_{31}N strongly interacted with ARF-GEF GNOM whereas ARF1-Q_{71}L did not, suggesting that ARF1•GDPs might be bridged by ARF-GEF dimer whereas ARF1•GTPs might display interaction independently of ARF-GEF. To test this idea, we made use of the putatively dimerization-deficient ARF1-Y_{35}A mutant (Beck et al., 2008). We generated transgenic Arabidopsis lines that inducibly co-expressed either ARF1-Y_{35}A,Q_{71}L-GFP and ARF1-Y_{35}A,Q_{71}L-RFP or ARF1-Q_{71}L-GFP and ARF1-Q_{71}L-RFP. FRET-FLIM measurements revealed interaction between ARF1-Q_{71}L proteins in seedling root cells, which was prevented by the additional Y_{35}A mutation (Figure 1B). These data suggest that membrane-bound ARF1•GTP molecules form dimers by direct physical interaction. To examine the biological significance of ARF1 dimers, we analyzed the ability of ARF1-Y_{35}A to rescue the secretion of alpha-amylase from tobacco protoplasts inhibited by ARF1-T_{31}N expression (Figure 2A, B; Suppl. Figure S1B, C). Rising concentrations of co-expressed wild-type form of ARF1 overcame the inhibition by ARF1-T_{31}N. In contrast, co-expression of comparable concentrations of ARF1-Y_{35}A failed to restore alpha-amylase secretion (Figure 2A). In addition, strong expression of ARF1-Y_{35}A also interfered with alpha-amylase secretion on its own (Figure 2B). Thus, ARF1 dimerization is required for ARF1-dependent membrane trafficking. We also analyzed the consequences of ARF1-Y_{35}A overexpression in seedling root cells at the ultrastructural level (Figure 2C, D). ARF1-Y_{35}A disrupted Golgi organization, resulting in strings of interconnected membrane vesicles, whereas overexpression of ARF1 wild-type protein only caused slight bending of the Golgi stacks. However, overexpression of ARF1-Y_{35}A did not interfere with membrane recruitment of γCOP (Suppl. Figure S2). Thus, ARF1 dimerization is essential for membrane trafficking.

How could ARF1 dimer formation be regulated? One candidate is the activating ARF-GEF which itself forms dimers (Ramaen et al., 2007; Anders et al., 2008). ARF1•GDP binding by ARF-GEF involves the C-terminal loop after helix J (loop>J) of the SEC7 domain of human GBF1, as demonstrated by specific mutations that interfere with

ARF1 binding (Lowery et al., 2011). We introduced homologous mutations into Arabidopsis GNOM to generate GN-loop>J(3A) mutant protein (Suppl. Figure S3A). ARF1-YFP was co-immunoprecipitated with Myc-tagged GNOM wild-type protein but not with Myc-tagged GN-loop>J(3A) mutant protein, using anti-YFP or anti-Myc beads (Figure 3A,B; Suppl. Figure S4A,B). The compromised interaction between GN-loop>J(3A) and ARF1•GDP resulted in a mutant phenotype corresponding to low level of ARF-GEF activity of GNOM (Suppl. Figure S3B-G). The residual activity of GN-loop>J(3A) mutant protein as evidenced by incomplete rescue of *gnom-sgt* deletion suggested low-affinity interaction of the mutant ARF-GEF with ARF1, which appeared to be below the detection limit. We thus stabilized the presumed interaction of the mutant ARF-GEF with ARF1 by estradiol-induced expression of activation-deficient ARF1-T_{31}N-YFP, which revealed co-immunoprecipitation (Figure 3C; Suppl. Figure S4C). This result suggested that ARF1 binding was impaired but the GN-loop>J(3A) protein was still able to carry out the GDP-GTP exchange, consistent with the partial rescue of the *gnom-sgt* deletion.

The fungal toxin brefeldin A (BFA) inhibits the exchange reaction, thus stabilizing abortive complexes of ARF-GEF and ARF1•GDP on endomembranes (Mossessova et al., 2003; Renault et al., 2003; Geldner et al., 2003). Treating seedling roots with BFA resulted in co-localization of GNOM and ARF1 in endosomal membrane aggregates called BFA compartments (Figure 3D, panels a-d; Geldner et al., 2003). In contrast, co-localization of GN-loop>J(3A) with ARF1 in BFA compartments was strongly reduced, thus resembling the strongly reduced accumulation of engineered BFA-resistant GNOM in ARF1-positive BFA compartments (Figure 3D, compare panels e-h with panels i-l). This result left unanswered the question of whether membrane association of GN-loop>J(3A) was reduced or the reduced BFA sensitivity was due to reduced affinity of ARF1 binding. Membrane association of GNOM requires interaction of its DCB domain with the complementary fragment called ΔDCB, which is disrupted in the membrane-association-deficient mutant protein GNOM(B4049) (Anders et al., 2008). A yeast two-hybrid assay of DCB-ΔDCB interaction was positive for GN-loop>J(3A), like GNOM wild-type and in contrast to GNOM(B4049) (Suppl. Figure S5). Furthermore, cell fractionation of seedlings revealed that GN-loop>J(3A) mutant protein partitioned between cytosol and membrane fraction like GNOM wild-type

protein (Figure 3E, F). In conclusion, GN-loop>J(3A) has normal membrane-association activity and its BFA insensitivity is consistent with reduced ARF1 binding.

GNOM like other ARF-GEFs forms dimers (Grebe et al., 2000; Anders et al., 2008). Co-immunoprecipitation with anti-Myc or anti-GFP beads revealed that Myc-tagged GN-loop>J(3A) mutant protein was able to dimerize with GNOM-GFP wild-type protein (Figure 4A). However, endogenous ARF1 was only detected in the precipitate of anti-GFP beads, which suggested that ARF-GEF dimers consisting of GNOM wild-type protein and GN-loop>J(3A) mutant protein have the same low-affinity binding of ARF1 as GN-loop>J(3A) homodimers (Figure 4A, B; Suppl. Figure S6). This puzzling result is consistent with the observation that GN-loop>J(3A) failed to rescue both *gnom-emb30* and *gnom-B4049* mutants (Suppl. Figure S3E, panels e and f; see also Suppl. Figures S7-9). The GNOM(emb30) protein is deficient in GDP-GTP-exchange whereas the GNOM(B4049) protein fails to associate with membranes such that the two mutant proteins complement each other to give functional ARF-GEF dimers (Anders et al., 2008). These results suggest that high-affinity binding of ARF1 requires simultaneous interaction of two ARF1•GDP molecules with the two SEC7 domains of ARF-GEF dimers.

We propose the following model of how ARF1 dimers required for the scission of membrane vesicles are generated (Figure 4C). Cytosolic GDP-bound ARF1 molecules are monomeric. They interact with membrane-associated ARF-GEF dimers, with the loop after helix J of the SEC7 domain playing a critical role in ARF1 binding. High-affinity binding requires cooperativity, i.e. simultaneous interaction of two ARF1•GDP molecules with the two SEC7 domains of ARF-GEF dimers. As a consequence, two adjacent ARF1 molecules undergo conformational change, resulting in GDP-GTP exchange, membrane insertion of the myristoylated N-terminus, and direct physical interaction of the two adjacent ARF1•GTP molecules. Following vesicle scission, GAP-assisted hydrolysis of GTP would alter the conformation of ARF1, disrupting the dimer and releasing monomeric ARF1•GDP into the cytosol. Considering the conservation of the overall domain organization of large ARF-GEFs (Casanova et al., 2007; Bui et al., 2009), it is highly likely that cooperative ARF1 binding by ARF-GEF dimers as a mechanism of forming active ARF1 GTPase dimers on the donor membrane applies to eukaryotes in general.

Acknowledgements

We thank Inwhan Hwang for providing published materials and Martin Bayer, Jeff Dangl, Christopher Grefen, Niko Geldner, Ancilla Neu and Thorsten Nürnberger for discussion and critical reading of the manuscript.

Competing interests

No competing interests declared

Author contributions

Conceptualization: G.J.; Methodology: S.B., M.E.N, M.K.S., S.R., V.S.; Formal analysis: S.B., M.E.N., V.S. G.J.; Data curation: S.B.; Writing - original draft: G.J.; Writing - review & editing: S.B., M.E.N., S.R., V.S., G.J.; Funding acquisition: G.J., M.E.N.

Funding

This work was supported by the Deutsche Forschungsgemeinschaft (Ju 179/18-1 and SFB1101/A01 to G.J.) and a fellowship from the Carlsberg Foundation to M.E.N.

Figure legends

Figure 1. In-vivo interaction between ARF1•GTP molecules revealed by co-immunoprecipitation and FRET-FLIM analysis

(**A**) Estradiol-inducible (20µM 7h) expression of ARF1-YFP, activation-deficient ARF1-T_{31}N-YFP and hydrolysis-deficient ARF1-Q_{71}L-YFP, immunoprecipitation with anti-GFP beads from transgenic Arabidopsis seedling extracts, and immunoblotting of PAGE-separated precipitates with anti-SEC7(GNOM) and anti-ARF1 antisera. Antisera indicated on the right. T, total extract; IP, immunoprecipitate; M, molecular markers (sizes in kDa indicated on the left). Asterisk, ARF1-YFP fusion proteins; arrow, endogenous ARF1 (both detected with anti-ARF1 antiserum); SEC7, antiserum detecting SEC7 domain of GNOM.

(**B**) FRET-FLIM analysis of ARF1-ARF1 interaction in Arabidopsis seedling root cells after estradiol induction (20µM 4h). The life time of hydrolysis-deficient ARF1-Q_{71}L-YFP was reduced whereas ARF1-Q_{71}L-YFP bearing dimerization-disrupting Y_{35}A mutation showed normal FRET-FLIM ratios. For comparison, the life time of ARF1-YFP was slightly reduced. Box plots of donor life time in ns of at least 19 independent measurements for each sample (exact numbers are indicated by n). Medians are

represented by the center lines and notches indicate 95% confidence interval. Tukey whiskers extend to the 1.5xIQR and data points are plotted as bee swarm. Exemplary p values (two tailed t-test assuming equal variances, alpha=0.05) are indicated in the graph.

Figure 2. Biological consequences of dimerization-deficient ARF1 expression

(**A**, **B**) Secretion of alpha-amylase from tobacco protoplasts (A) inhibited by ARF1-T_{31}N (TN) was restored by overexpression of ARF1 (WT) but not ARF1-Y_{35}A (Y35A) and (B) impaired by ARF1-Y_{35}A (Y35A) compared to wild-type control. Bottom panels: ARF1 expression detected with anti-ARF1 antiserum.

(**C**, **D**) Ultrastructural analysis of epidermal cells at the upper end of the seedling root meristem expressing ARF1-YFP (C) or ARF1-Y_{35}A-YFP (D) in response to 10 µM estradiol for 4 h. Golgi stacks (arrowheads) were bent in (C) but replaced by clusters of interconnected membrane vesicles (asterisk) and Golgi remnants (arrows) in (D).

Figure 3. ARF-GEF GN-loop>J(3A) mutant protein: interaction with ARF1, subcellular localization and membrane association

(**A-C**) Co-immunoprecipitation from Arabidopsis seedling extracts. No detectable interaction of (A) endogenous ARF1 or (B) YFP-tagged ARF1 with GN-loop>J(3A)-Myc compared to GNOM-Myc wild-type control, following IP with (A) anti-Myc beads or (B) anti-GFP beads. (C) Activation-deficient ARF1-T_{31}N-YFP dramatically increased the co-IP signal of GN-loop>J(3A)-Myc; IP with anti-GFP beads. Col, Columbia wild-type control. T, total extract; IP, immunoprecipitate; M, molecular markers (sizes in kDa indicated on the left).

(**D**) Immunostainings of BFA-treated seedling roots. GNOM co-localized with ARF1 (**a**-**d**), GN-loop>J(3A) essentially behaved like engineered BFA-resistant GNOM (**e**-**h**), not accumulating on the ARF1-positive endomembrane (**i**-**l**). Panels d, h and l show line scans as indicated by green lines in panels c, g and k, respectively.

(**E**, **F**) Cell fractionation revealed comparable partitioning between cytosol and membrane of Myc-tagged GNOM wild-type and Myc-tagged GN-loop>J(3A) mutant protein. (E) Immunoblot with antisera indicated on the right (controls: calnexin, ER membrane protein; Huang et al., 1993; AALP, soluble vacuolar protein; Holwerda et al., 1990); M, molecular markers (sizes in kDa indicated on the left). (F) Quantitation of anti-Myc signal intensities; total extracts set at 1. T, total extract; S10 and P10,

supernatant and pellet of 10,000 *g* centrifugation; S100 and P100*, supernatant and washed pellet of 100,000 *g* centrifugation;

Figure 4.

(**A**) Co-immunoprecipitation of GNOM-GFP and GN-loop>J(3A)-MYC from Arabidopsis seedling extracts with either anti-GFP or anti-MYC beads, revealing interaction of GNOM wild-type with GN-loop>J(3A)-MYC mutant protein but no ARF1 binding by GNOM heterodimer. Precipitates were probed with anti-GFP, anti-ARF1 and anti-MYC antisera. T, total extract; FT, unbound; IP, immunoprecipitate; M, molecular markers (sizes in kDa indicated on the left).

(**B**) Diagram of expected co-immunoprecipitation results showing precipitated GNOM dimers and ARF1. Green tag, GNOM-GFP (wild-type); red tag, GN-loop>J(3A)-MYC (mutant); grey tag, GNOM-MYC (wild-type); no tag, endogenous GNOM.

(**C**) Model of how ARF1 dimers required for the scission of membrane vesicles are generated through simultaneous binding and activation by ARF-GEF dimers. (**a**) ARF1 dimer formation by wild-type ARF-GEF dimers during GDP-GTP exchange on membrane. (**b**) GN-loop>J(3A) mutant protein reduces efficiency of ARF1 dimer formation because of reduced ARF1 binding affinity. (**c**) Two ARF1-Y_{35}A proteins are each activated by ARF-GEF dimers but fail to interact with each other, interfering with vesicle scission.

(**d**) Activation-hydrolysis cycle. Two ARF•1GDP monomers are simultaneously activated by membrane-associated ARF-GEF dimer, resulting in ARF1•GTP dimer. GTP hydrolysis facilitated by GTPase-activating protein (GAP) releases ARF1•GDP monomers from the membrane into the cytosol; P_i, inorganic phosphate.

Materials and Methods

Plant material and growth conditions

Plants were grown under permanent light conditions (Osram L18W/840 cool white lamps) at 23°C and 40% humidity in growth chambers on soil or agar plates. Previously published lines that were used in this study: *b4049*, *emb30-1*, *b4049/emb30-1* (Busch et al., 1996b), *R5* (Geldner et al., 2004), GNOM-Myc, GN-ML-MYC and GNOM-GFP (Geldner et al., 2003), ARF1-YFP, ARF1-TN-YFP, ARF1-QL-YFP (Singh and Richter et al., 2018).

sgt mutant: The Ds-induced *sgt* allele was generated in an Ac-Ds mutagenesis experiment and isolated for its *gnom*-like mutant phenotype (Kumaran et al., 1999). The deletion on chromosome 1 covers a nine genes from At1g13940 (5' end of Ds) to At1g14020 (3'end of Ds) including *GNOM* At1g13980 (Suppl. Figure S2B). For genotyping the following primers were used (Suppl. Figure S2C, D):
heterozygosity:
(N.A. 212) In At1g13940-sense: 5’ GGGGGGAGGGTATAAGAG 3’
(N.A. 213) DS-element-5’-antisense: 5’ ACGGTCGGGAAACTAGCTCTAC 3’
(N.A. 210) DS-element-3’-sense: 5’ GGTTCCCGTCCGATTTCGACT 3’
(N.A. 211) In At1g14020-antisense: 5’ AAGACACATGAGTGATTC 3’
homozygosity:
(S.R.264) GNOM-over-tag-sense: 5’ GAAAGTGAAAGTAAGAGGC 3’
(S.R.263) GNOM-over-tag-antisense: 5’ CGTAGAGAGGTGTTACATAAG 3’

Binary vector constructs, generation of transgenic plants and crosses

To generate the loop>J(3A) mutation, the amino acids residues 744, 745 and 747 (EI(R)T) were changed to alanines (AARA) by site directed mutagenesis. Mutagenesis PCR was performed on the genomic fragment GNXbaI^{wt}-myc (Geldner et al., 2003) in pBlueScript using the following primers:
Loop>J(3A) sense: 5’ AATGCGGCCAGGGCTACTCCAGAACAAGGTGC 3’
Loop>J(3A) rev: 5’ AGTAGCCCTGGCCGCATTGTTGCAGATGGAGTG 3’
The GN::GNloop>J(3A)XbaI-myc fragment was cloned via XbaI into pGreenII(Bar) expression vector and transformed into *Arabidopsis thaliana* ecotype Col-0. T1 plants were selected using phosphinotricine. Four different transgenic lines showed decent expression and two of them were chosen for further analysis.
Loop>J(3A)-MYC#5 was crossed into *sgt*, *b4049*, *emb30-1* backgrounds and analyzed for complementation. Loop>J(3A)-MYC *sgt* and Loop>J(3A)-MYC *emb30-1* were crossed with each other. For co-immunoprecipitation analysis, Loop>J(3A)-MYC was crossed with ARF1-YFP and ARF1-TN-YFP and Loop>J(3A)-MYC *sgt* with GN-GFP.
To generate an estradiol inducible ARF1-YFP variant, site-directed mutagenesis was performed on pEntry-ARF1-TN-YFP (Singh and Richter et al., 2018) using the following primer combination:
ARFA1C-WT-MUT-S: 5’ [Phos]GCTGGTAAGAcgACTATCCTcTACAAGC 3’
ARFA1C-WT-MUT-AS: 5’ AGCATCGAGACCAACCATC 3’

The Y35A mutation was introduced into pEntry-ARF1-YFP, pEntry-ARF1-TN-YFP and ARF1-QL-YFP by site-directed mutagenesis using the following primers:
ARFA1C-Y35A-MUT-S:5'[Phos]TACTATCCTCgcaAAGCTCAAACTTGGAGAGATC3'
ARFA1C-Y35A-MUT-AS: 5' TTCTTACCAGCAGCATCG 3'

To generate RFP-tagged ARF1 variants, the CDS of RFP with a N-terminal AvrII restriction site was amplified and cloned into pDONR221 (Invitrogen) generating a pEntry clone. The RFP gene and part of the KAN resistance gene of the pEntry clone were then introduced via AvrII and SspI restrictions sites into the YFP tagged ARFA1c Entry clones mentioned above, thereby replacing the YFP tag. The different ARF1 fragments were then introduced into a modified ß-estradiol inducible pMDC7 vector by gateway LR reaction (Singh and Richter et al., 2018).

Cloning of constructs for transient expression in protoplasts

CDS of ARFA1C, ARFA1C-TN and ARFA1C-Y35A were amplified from pEntry-clones mentioned above by using Sense-Primers containing NheI restriction site and Antisense-Primers containing BamHI restriction site. Amplified ARF fragments were introduced in pFK059 (Singh and Richter et al, 2018) via NheI and BamHI restriction sites.
NheI-ARFA1C-S: 5' gatctcgctagcATGGGGTTGTCATTCGGAAAGTT 3'
BamHI-Stop-ARFA1C-AS: 5' ggcagtggatccCTATGCCTTGCTTGCGATGTTGT 3'

Physiological tests

For primary root growth assays, 50 five-days old seedlings were transferred to agar plates containing 10 μM BFA for 24h and seedling growth was analyzed using ImageJ software. Gravitropic response of 50 five-days old seedlings was measured by ImageJ software after transferring seedlings to 10 μM BFA plates and rotating them by 135° for 24h. Lateral root primordia formation was analyzed after transferring 7-day old seedlings for 3 days on 20 μM NAA-containing agar plates and clearing the roots according to Geldner et al. (2004). To examine the vasculature of 7 to 10-days old cotyledons, seedlings were shaken for several hours in 3:1 ethanol/acetic acid solution at room temperature according to (Geldner et al., 2004). Light microscopy images were

taken with Zeiss Axiophot microscope, Axiocam and AxioVision_4 Software. Image size, brightness and contrast were edited with Adobe Photoshope CS 3 Software.

Yeast two-hybrid interaction assays

Assay and constructs of GNOM-DCB (AA 1-246), GNOM-ΔDCB (AA 232-1451) and GNOM-ΔDCB(b4049) (AA 232-1451; G579R) were as described (Grebe et al., 2000; Anders et al., 2008). GNOM-ΔDCB(L>J) was generated by site-directed mutagenesis using primers mentioned above.

Quantitative transport assays

Protoplasts were prepared and electrotransfected as previously described (Künzl et al., 2016). Harvesting and analysis of medium and cell samples as well as calculation of the secretion index was performed as described (Bubeck et al., 2008).

Whole-mount immunofluorescence staining

Four to six-days old seedlings were incubated in 24-well cell-culture plates for 1 hour in 50 μM BFA (Invitrogen, Thermo Fisher Scientific) containing liquid growth medium (0.5x MS medium, 1% sucrose, pH 5.8) at 23°C and then fixed for 1 hour in 4% paraformaldehyde in MTSB at room temperature. Whole-mount immunofluorescence staining was performed manually as described (Lauber et al., 1997a) or with an InsituPro machine (Intavis) (Müller et al., 1998). All antibodies were diluted in 1x PBS buffer. The following antisera were used for immunofluorescence staining: mouse anti-c-Myc mAB 9E10 (Santa Cruz Biotechnology) diluted 1:600; rabbit anti-ARF1 (Agrisera) diluted 1:1000; rabbit anti-AtγCOP (Agrisera) diluted 1:1000; anti-mouse Alexa488 (Invitrogen) and anti-rabbit CY3 (Dianova)-conjugated secondary antibodies were diluted 1:600. Nuclei were stained with Dapi (1:600 dilution).

Confocal microscopy and processing of images

Fluorescence images were acquired with the confocal laser scanning microscope TCS-SP2 or SP8 from Leica and Zeiss Airy Scan, using a 63x water-immersion objective and Leica software. Overlays and contrast/brightness adjustments of images were performed with Adobe Photoshop CS3 software. Intensity line profiling was performed with Leica or Zeiss Software.

FRET-FLIM analysis

Four-to-five days old seedlings were incubated 4-6hours in liquid growth medium containing 20μM estradiol. For Image acquisition and FLIM measurements, the Leica TCS SP8 confocal microscope with a rapid FLIM unit (Pico Quant), the LAS X (Leica) and SymPhoTime 64 (from PicoQuant) softwares were used. Images were taken with a 63x water-immersion objective and 2x digital zoom. Measurements were taken from at least 5 different seedlings in epidermal cells near the differentiation zone of the root.

EM analysis

Four-to-five days old ARF1-YFP and ARF1-Y35A-YFP seedlings were incubated 4h in liquid growth medium containing 10μM estradiol. For ultrastructural analysis, 1 mm long seedling root tips were high-pressure frozen, fixed and cut in 70 nm thin sections. Sections were stained and viewed in a Jeol JEM-1400plus TEM at 120 kV accelerating voltage. For more information, see Singh & Richter et al. (2018).

Subcellular fractionation

2g of plant material were ground in liquid nitrogen and suspended in 1:1 extraction buffer (50mM Tris pH 7.5, 150mM NaCl, 1mM EDTA, 1mM PMSF) supplemented with protease inhibitors (cOmplete EDTA-free®, Roche). Of cell lysates, 100 µl were taken as total fraction (T). Then cell lysates were cleared by centrifugation at 10,000 x g for 10 min at 4°C and 100 µl of supernatant (S10) were saved for further analysis. The pellet was dissolved in 1 ml extraction buffer and 100 µl were frozen (P10). After 1x 100.000g centrifugation at 4°C for 1h, 100 µl supernatant (S100) were stored and the pellet was dissolved in 200 µl extraction buffer of which 100 µl were stored (P100*). 25μl of 5x Lämmli buffer were added to 100 μl samples.

Co-immunoprecipitation analysis

Immunoprecipitation protocol was modified from Singh et al. (2014). 3-5g of 8 to 10-days old Arabidopsis seedlings were homogenized in 1:1 lysis buffer containing 1% Triton-X100. Seedlings bearing estradiol-inducible ARF1-TN-YFP were incubated in 20μM estradiol-containing liquid MS Media with sugar for 7h. For immunoprecipitation, anti-Myc-agarose beads (Sigma) or GFP-Trap beads (Chromotek) were incubated with the plant extracts for 2h at 4°C. Beads were then washed once with wash buffer containing 0.5% Triton-X100 and three times with 0.1% Triton-X100. Bound proteins

were eluted by boiling the beads in 2x Lämmli buffer at 95°C for 5min. Twice the usual amount of beads was used for immunoprecipitation involving GN-loop>J(3A)-Myc with anti-Myc beads or ARF1-YFP with anti-GFP beads.

SDS-PAGE and protein gel blotting

SDS-Pages and protein gel blotting with PVDF membranes (Millipore) were performed as described (Lauber et al., 1997). All antibodies were diluted in 5% milk/TBS-T solution. Antibodies and dilutions: mouse anti-c-Myc mAB 9E10 (Santa Cruz Biotechnology) 1:1000, mouse anti-GFP (Roche) 1:2500, rabbit anti-Calnexin (Agrisera) 1:2000, rabbit anti-AALP (Holwerda et al., 1990; a gift from Inhwan Hwang) 1:1000, rabbit anti-ARF1 (Agrisera) 1:2500, rabbit anti-SEC7 (Steinmann et al., 1999) 1:2500, mouse anti-LexA (Santa Cruz Biotechnology) 1:1000, POD-conjugated anti-HA (Roche) 1:4000, anti-mouse (Sigma) or anti-rabbit peroxidase-conjugated (Merck Millipore) or alkaline phosphatase-conjugated antibodies (Jackson Immuno Research) 1:10000. Detection was performed with the BM-chemiluminescence blotting substrate (Roche) and FusionFx7 imaging system (PeqLab). Image assembly was performed with Adobe Photoshop CS3, and ImageJ software was used for quantification of relative protein amounts.

References

N. Anders, G. Jürgens, Large ARF guanine nucleotide exchange factors in membrane trafficking. *Cell. Mol. Life Sci.* **65**, 3433-3445 (2008).

N. Anders, M. Nielsen, J. Keicher, Y.-D. Stierhof, M. Furutani, M. Tasaka, K. Skriver, G. Jürgens, Membrane association of the *Arabidopsis* ARF exchange factor GNOM involves interaction of conserved domains. *Plant Cell* **20**, 142-151 (2008).

R. Beck, Z. Sun, F. Adolf, C. Rutz, J. Bassler, K. Wild, I. Sinning, E. Hurt, B. Brügger, J. Béthune, F. Wieland, Membrane curvature induced by Arf1-GTP is essential for vesicle formation. *Proc. Natl. Acad. Sci. USA* **105**, 11731-11736 (2008).

R. Beck, S. Prinz, P. Diestelkötter-Bachert, S. Röhling, F. Adolf, K. Hoehner, S. Welsch, P. Ronchi, B. Brügger, J. A. Briggs, F. Wieland F, Coatomer and dimeric ADP ribosylation factor 1 promote distinct steps in membrane scission. *J. Cell Biol.* **194**, 765-777 (2011).

Q. T. Bui, M. P. Golinelli-Cohen, C. L. Jackson, Large Arf1 guanine nucleotide exchange factors: evolution, domain structure, and roles in membrane trafficking and human disease. *Mol. Genet. Genomics* **282**, 329-350 (2009).

M. Busch, U. Mayer, G. Jürgens, Molecular analysis of the Arabidopsis pattern formation of gene *GNOM*: gene structure and intragenic complementation. *Mol. Gen. Genet.* **250**, 681-691 (1996).

J. E. Casanova, Regulation of Arf activation: the Sec7 family of guanine nucleotide exchange factors. *Traffic* **8**, 1476-1485 (2007).

C. Dascher, W. E. Balch, Dominant inhibitory mutants of ARF1 block endoplasmic reticulum to Golgi transport and trigger disassembly of the Golgi apparatus. *J. Biol. Chem.* **269**, 1437-1448 (1994).

J. G. Donaldson, C. L. Jackson, ARF family G proteins and their regulators: roles in membrane transport, development and disease. *Nat. Rev. Mol. Cell Biol.* **12**, 362-375 (2011).

C. D'Souza-Schorey, P. Chavrier, ARF proteins: roles in membrane traffic and beyond. *Nat. Rev. Mol. Cell Biol.* **7**, 347-358 (2006).

N. Geldner, N. Anders, H. Wolters, J. Keicher, W. Kornberger, P. Muller, A. Delbarre, T. Ueda, A. Nakano, G. Jürgens, The Arabidopsis GNOM ARF-GEF mediates endosomal recycling, auxin transport, and auxin-dependent plant growth. *Cell* **112**, 219-230 (2003).

N. Geldner, S. Richter, A. Vieten, S. Marquardt, R. A. Torres-Ruiz, U. Mayer, G. Jürgens, Partial loss-of-function alleles reveal a role for *GNOM* in auxin transport-related, post-embryonic development of *Arabidopsis*. *Development* **131**, 389-400 (2004).

A. K. Gillingham, S. Munro, The small G proteins of the Arf family and their regulators. *Annu. Rev. Cell Dev. Biol.* **23**, 579-611 (2007).

M. Grebe, J. Gadea, T. Steinmann, M. Kientz, J.-U. Rahfeld, K. Salchert, C. Koncz, G. Jürgens, A conserved domain of the *Arabidopsis* GNOM protein mediates subunit interaction and cyclophilin 5 binding. *Plant Cell* 12, 343-356 (2000).

A. Hecker, N. Wallmeroth, S. Peter, M. R. Blatt, K. Harter, C. Grefen, Binary 2in1 vectors improve in planta (co)localization and dynamic protein interaction studies. *Plant Physiol.* **168**, 776-787 (2015).

B. C. Holwerda, N. J. Galvin, T. J. Baranski, J. C. Rogers, In vitro processing of aleurain, a barley vacuolar thiol protease. *Plant Cell* **2**, 1091-1106 (1990).

L. Huang, A. E. Franklin, N. E. Hoffman, Primary structure and characterization of an *Arabidopsis thaliana* calnexin-like protein. *J. Biol. Chem.* **268**, 6560-6566 (1993).

M. Kumaran, D. Ye, W.-C. Yang, V. Sundaresan, The *DIRECTIONLESS* mutation affects the pattern formation in Arabidopsis. *10th Int. Congr. Arab. Res., Abstract 8-24, Melbourne, July 1999* (1999).

F. Künzl, S. Früholz, F. Fäßler, B. Li, P. Pimpl, Receptor-mediated sorting of soluble vacuolar proteins ends at the trans-Golgi network/early endosome. *Nat. Plants* **2**, 16017 (2016).
M. H. Lauber, I. Waizenegger, T. Steinmann, H. Schwarz, U. Mayer, I. Hwang, W. Lukowitz, G. Jürgens, The Arabidopsis KNOLLE protein is a cytokinesis-specific syntaxin. *J. Cell Biol.* **139**, 1485-1493 (1997).

J. Lowery, T. Szul, J. Seetharaman, X. Jian, M. Su, F. Forouhar, R. Xiao, T. B. Acton, G. T. Montelione, H. Lin, J. W. Wright E. Lee Z. G. Holloway, P. A. Randazzo, L. Tong, E. Sztul, Novel C-terminal motif within Sec7 domain of guanine nucleotide exchange factors regulates ADP-ribosylation factor (ARF) binding and activation. *J. Biol. Chem.* **286**, 36898-36906 (2011).

U. Mayer, G. Büttner, G. Jürgens, Apical-basal pattern formation in the Arabidopsis embryo – Studies on the role of the *GNOM* gene. *Development* **117**, 149-162 (1993).

D. W. Meinke, Embryo-lethal mutants of *Arabidopsis thaliana*: analysis of mutants with a wide range of lethal phases. *Theor. Appl. Genet.* **69**, 543-552 (1985).

E. Mossessova, R. A. Corpina, J. Goldberg, Crystal structure of ARF1*Sec7 complexed with Brefeldin A and its implications for the guanine nucleotide exchange mechanism. *Mol. Cell* **12**, 1403-1411 (2003).

A. Müller, C. Guan, L. Gälweiler, P. Tänzler, P. Huijser, A. Marchant, G. Parry, M. Bennett, E. Wisman, K. Palme, AtPIN2 defines a locus of Arabidopsis for root gravitropism control. *EMBO J.* **17**, 6903-6911 (1998).

O. Ramaen, A. Joubert, P. Simister, N. Belgareh-Touzé, M. C. Olivares-Sanchez, J. C. Zeeh, S. Chantalat, M. P. Golinelli-Cohen, C. L. Jackson, V. Biou, J. Cherfils, Interactions between

conserved domains within homodimers in the BIG1, BIG2, and GBF1 Arf guanine nucleotide exchange factors. *J. Biol. Chem.* **282**, 28834-28842 (2007).

L. Renault, B. Guibert, J. Cherfils, Structural snapshots of the mechanism and inhibition of a guanine nucleotide exchange factor. *Nature* **426**, 525-530 (2003).

S. Richter, N. Geldner, J. Schrader, H. Wolters, Y.-D. Stierhof, G. Rios, C. Koncz, D. G. Robinson, G. Jürgens, Functional diversification of closely related ARF-GEFs in protein secretion and recycling. *Nature* **448**, 488-492 (2007).

D. E. Shevell, W. M. Leu, C. S. Gillmor, G. Xia, K. A. Feldmann, N. H. Chua, EMB30 is essential for normal cell division, cell expansion, and cell adhesion in Arabidopsis and encodes a protein that has similarity to Sec7. *Cell* **77**, 1051-1062 (1994).

M. K. Singh, G. Jürgens, Specificity of plant membrane trafficking - ARFs, regulators and coat proteins. *Semin. Cell Dev. Biol.* **80**, 85-93 (2018).

M. K. Singh, F. Krüger, H. Beckmann, S. Brumm, J. E. Vermeer, T. Munnik, U. Mayer, Y.-D. Stierhof, C. Grefen, K. Schumacher, G. Jürgens, Protein delivery to vacuole requires SAND protein-dependent Rab GTPase conversion for MVB-vacuole fusion. *Curr. Biol.* **24**, 1383-1389 (2014).

M. K. Singh, S. Richter, H. Beckmann, M. Kientz, Y.-D. Stierhof, N. Anders, F. Fässler, M. Nielsen, C. Knöll, A. Thomann, M. Franz-Wachtel, B. Macek, K. Skriver, P. Pimpl, G. Jürgens, A single class of ARF GTPase activated by several pathway-specific ARF-GEFs regulates membrane traffic in Arabidopsis. *PLoS Genet.* **14**, e1007795 (2018).

T. Steinmann, N. Geldner, M. Grebe, S. Mangold, C. L. Jackson, S. Paris, L. Gälweiler, K. Palme, G. Jürgens, Coordinated polar localization of auxin efflux carrier PIN1 by GNOM ARF GEF. *Science* **286**, 316-318 (1999).

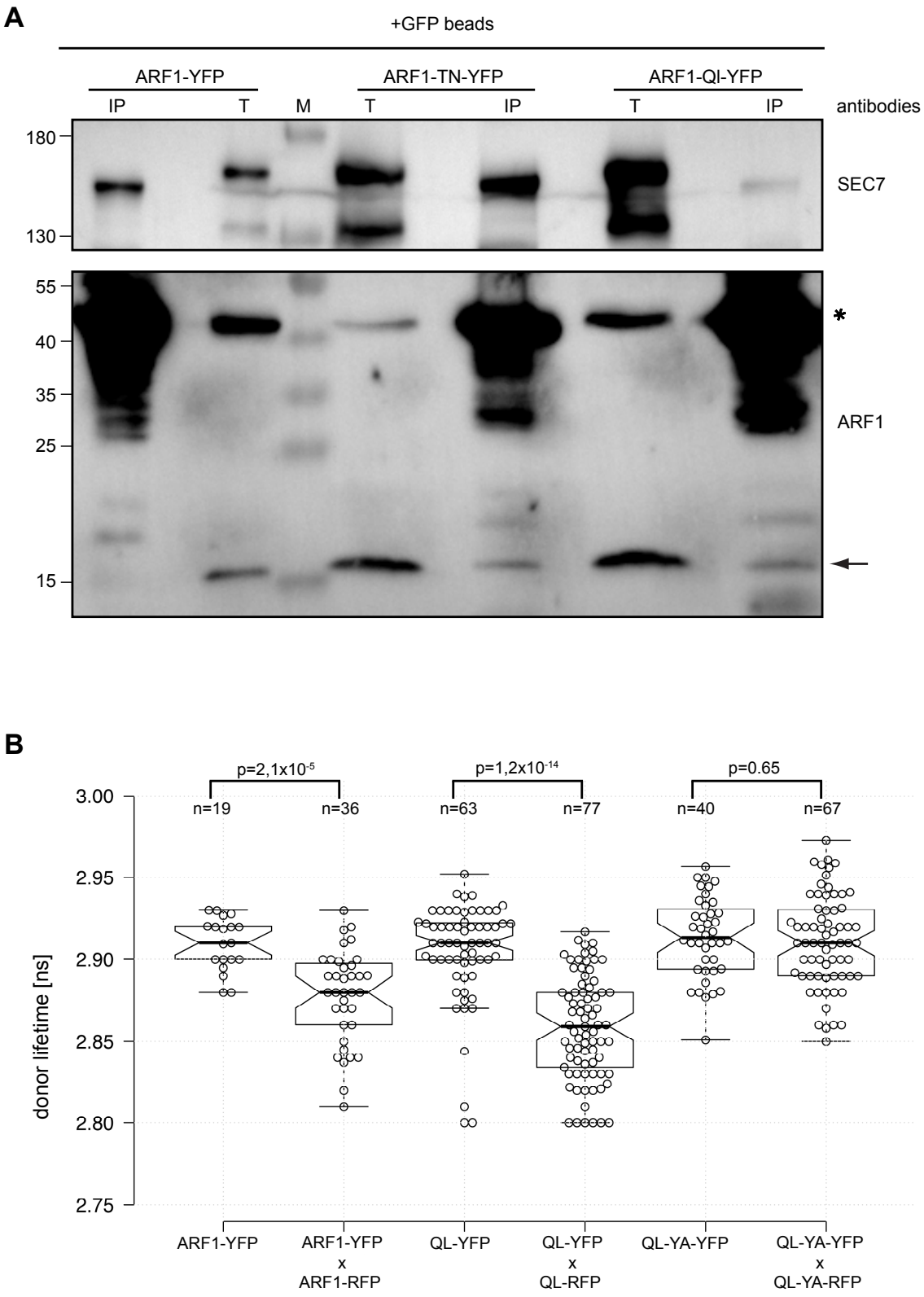

Brumm et al., Figure 1. In-vivo interaction between ARF1•GTP molecules revealed by co-immunoprecipitation and FRET-FLIM analysis

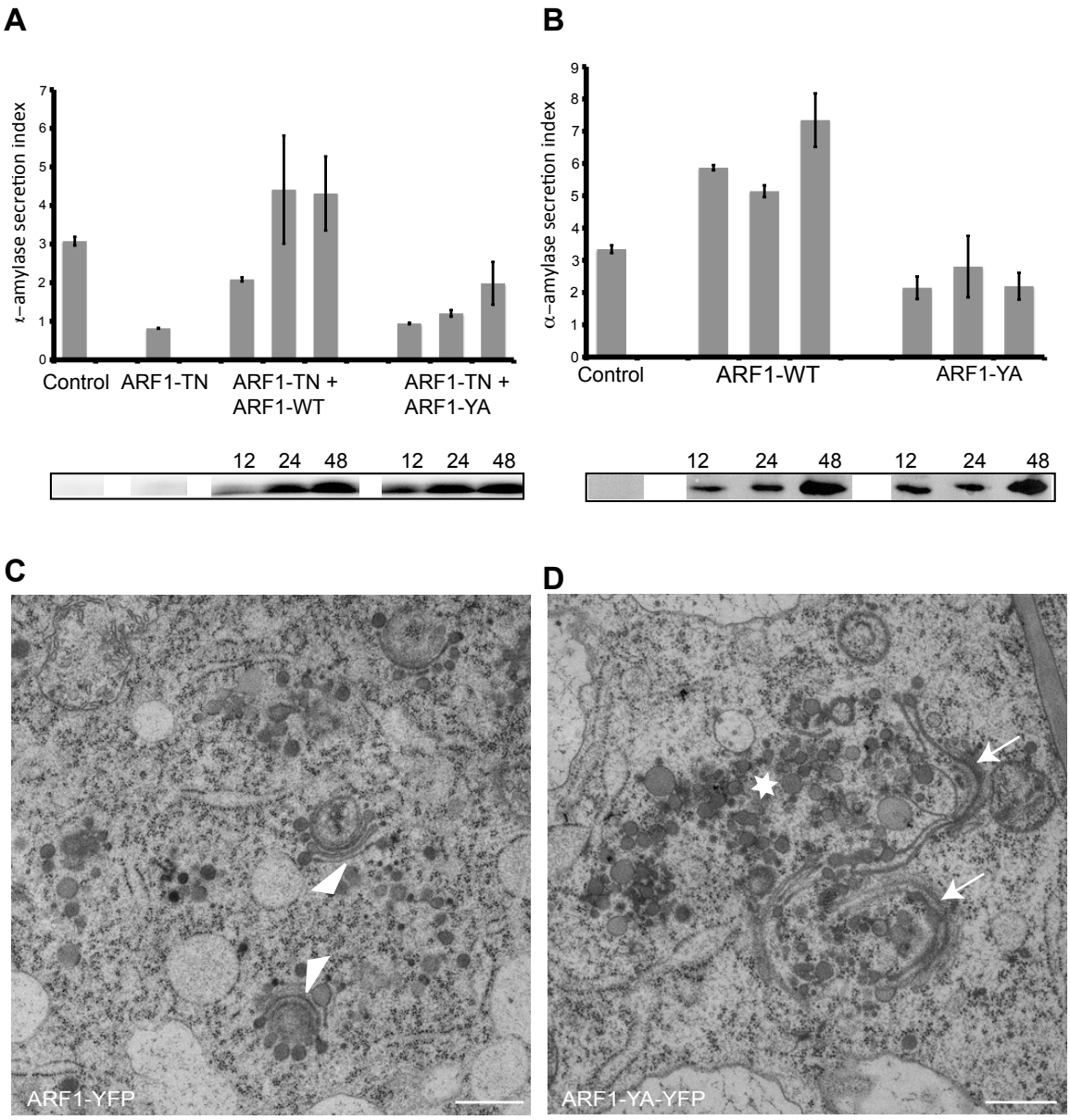

Brumm et al., Figure 2. Biological consequences of dimerization-deficient ARF1 expression

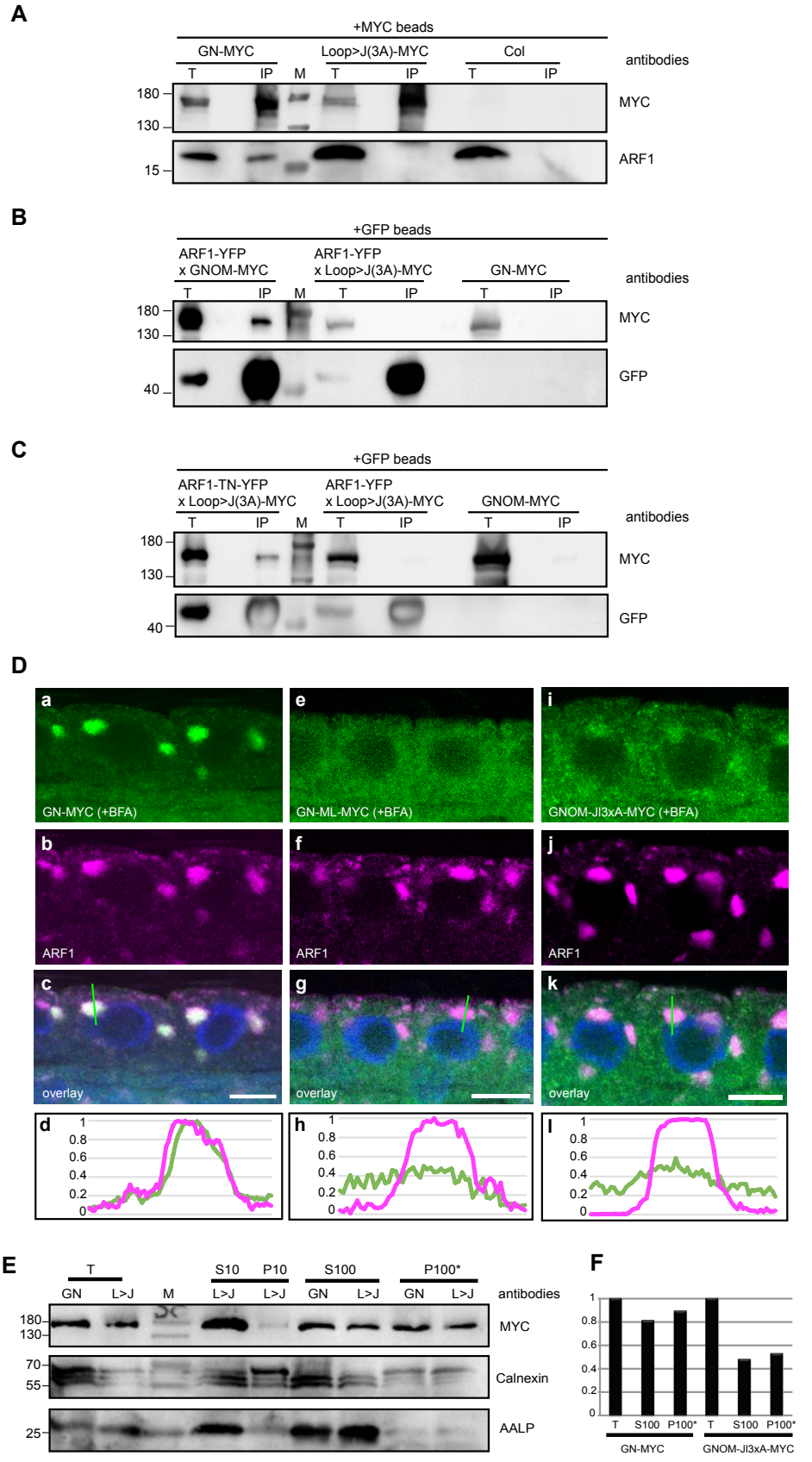

Brumm et al., Figure 3. ARF-GEF GN-loop>J(3A) mutant protein: interaction with ARF1, subcellular localization and membrane association

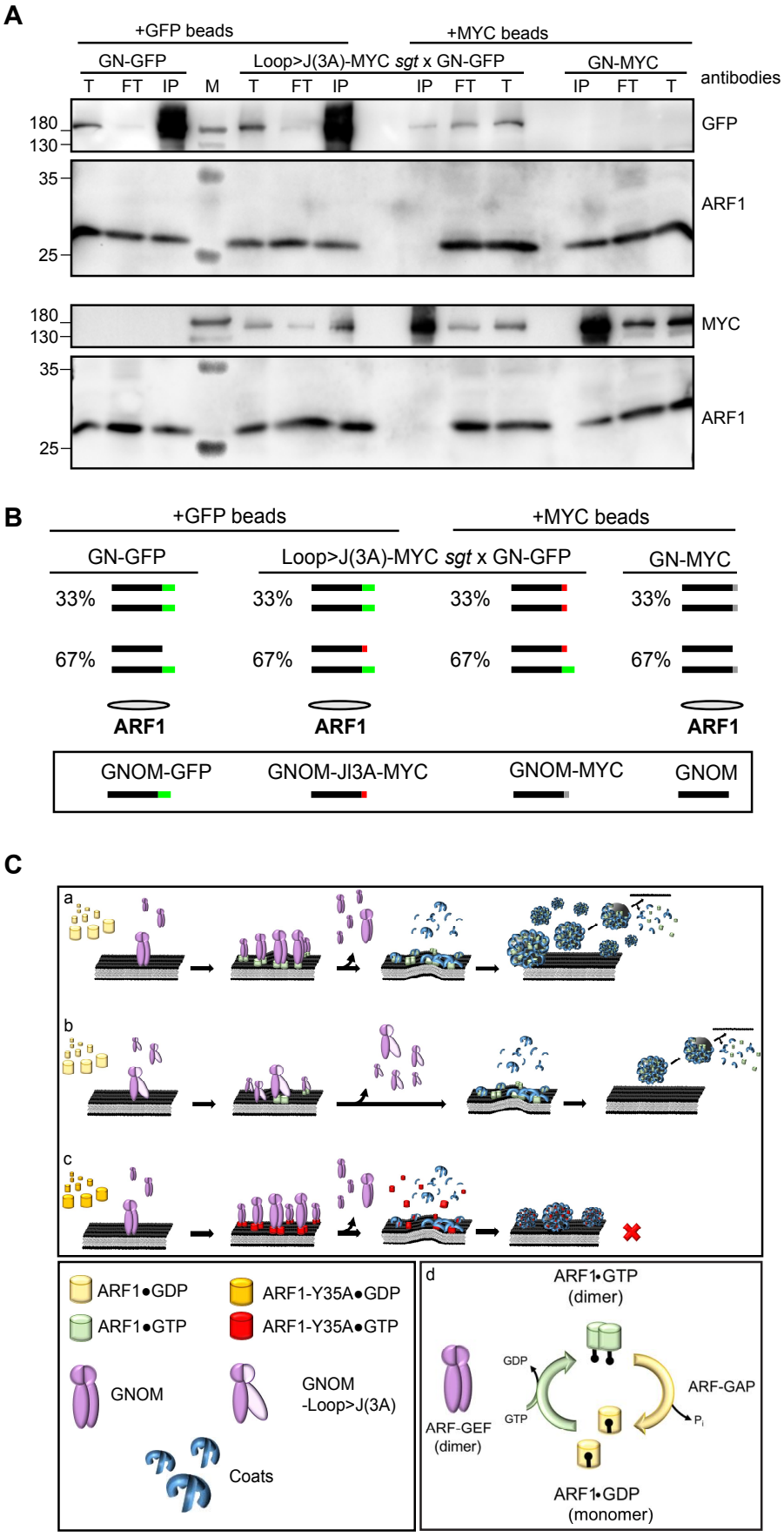

Brumm et al., Figure 4. ARF1 binding by ARF-GEF dimers and model of ARF1 dimer formation

Supplementary information

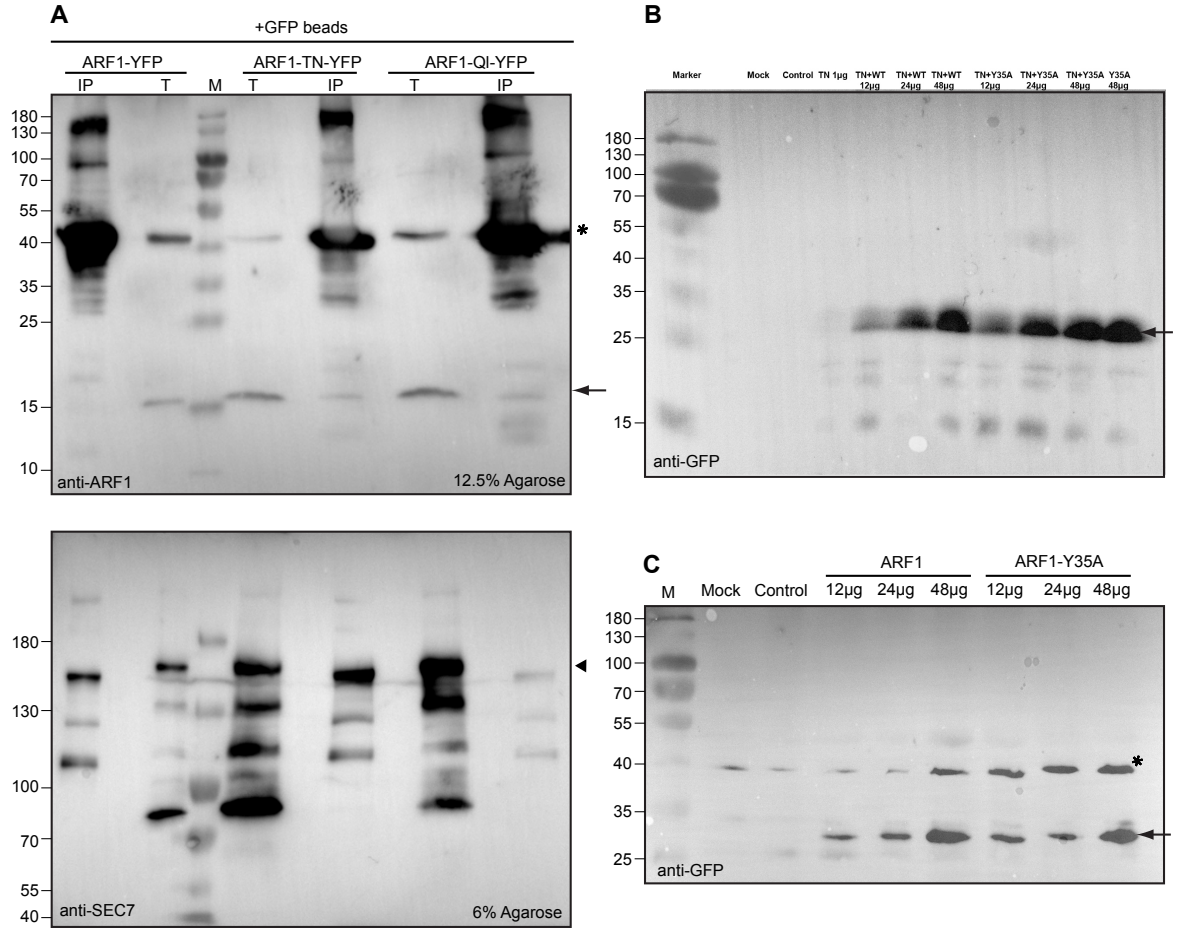

Brumm et al., Figure S1. Interaction of ARF1, ARF1-T_{31}N and ARF1-Q_{71}L protein with endogenous ARF1 and ARF-GEF GNOM

(**A**) Complete blots for main Figure 1(A). Estradiol-inducible (20µM 7h) expression of ARF1-YFP, activation-deficient ARF1-T_{31}N-YFP and hydrolysis-deficient ARF1-Q_{71}L-YFP, immunoprecipitation with anti-GFP beads from transgenic Arabidopsis seedling extracts, and immunoblotting of PAGE-separated precipitates with anti-SEC7(GNOM) and anti-ARF1 antisera. Antisera indicated on the right. T, total extract; IP, immunoprecipitate; M, molecular markers (sizes in kDa indicated on the left). Samples were run on 12.5% and 6% SDS-PAGE gels. Asterisk, ARF1-YFP fusion proteins; arrow, endogenous ARF1 (both detected with anti-ARF1 antiserum); SEC7, antiserum detecting SEC7 domain of GNOM. Arrowhead, endogenous GNOM

(B-C) Complete blots for main Figure 2(A) and (B). Western analysis of transgene expression in tobacco protoplasts. Immunoblotting with anti-GFP antiserum.; Arrow, mas promoter driven GFP expression; Asterisk, cross reaction of the GFP antiserum

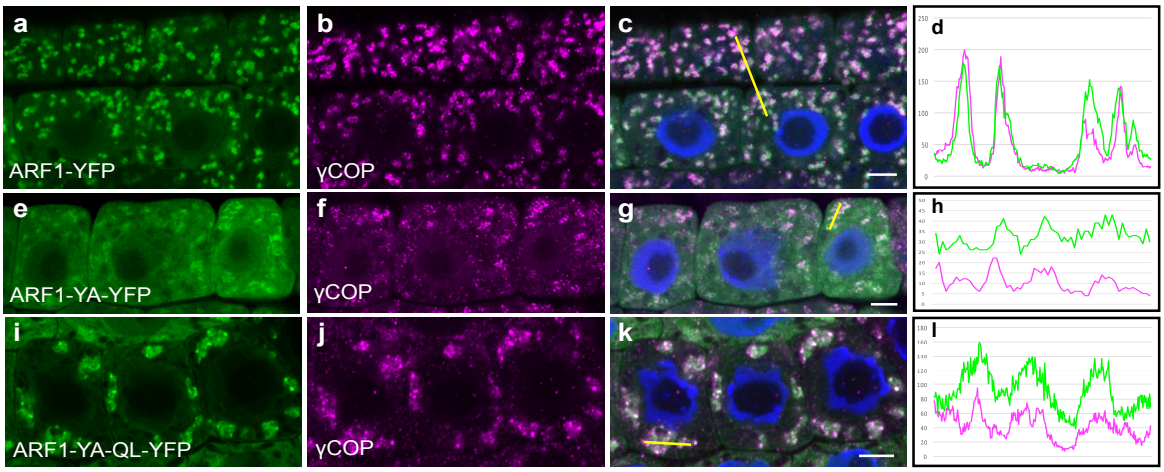

Brumm et al., Figure S2. Membrane association of COPI

Immunostaining of COPI subunit γCOP in seedling root cells expressing (**a-d**) ARF1-YFP, (**e-h**) ARF1-Y_{35}A-YFP or (**i-l**) ARF1-Y_{35}A,Q_{71}L-YFP in response to 20 µM estradiol for 4h. (**a,e,i**) ARF1 variant (green), (**bf,j**) γCOP (magenta), (**c,g,k**) merged images with DAPI-stained nuclei (blue), (**d,h,l**) Co-localization of ARF1 and γCOP in regions of interest (ROI) shown in line intensity profiles. Scale bar, 5 µm.

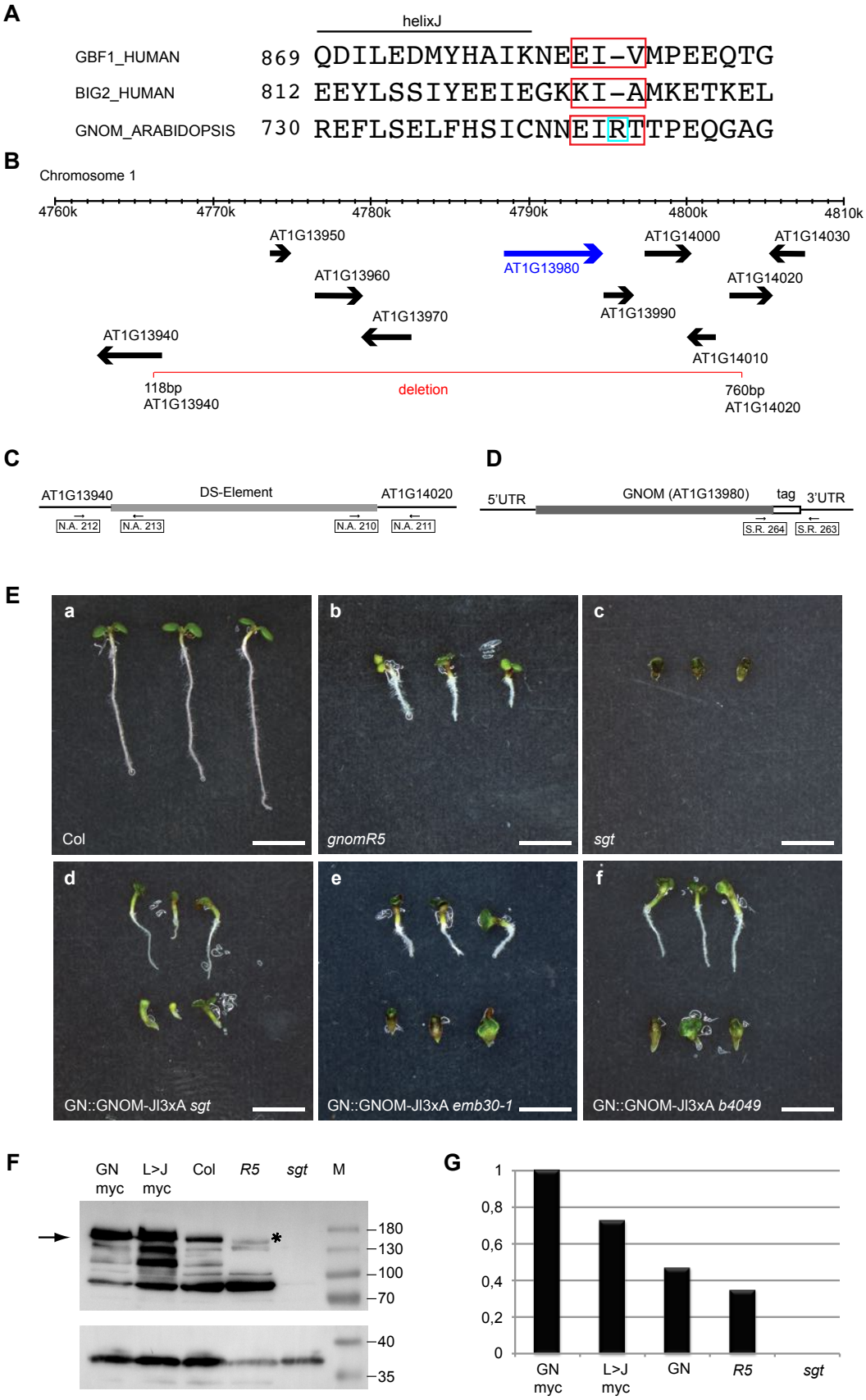

Brumm et al., Figure S3. Rescue activity of GN-loop>J(3A) in *gnom-sgt* deletion and other *gnom* mutants

(**A**) Alanine substitution sites (red boxes) in the loop after helix J (loop>J) of SEC7 domain of ARF-GEFs human GBF1, human BIG2 (Lowery et al., 2011) and Arabidopsis GNOM. In GN-loop>J(3A) mutant protein, amino acid residues 744 to 747 (EIRT) are replaced by AARA.

(**B**) Diagram of genomic segment of chromosome 1 displaying GNOM and adjacent genes. The *GNOM* gene is highlighted in blue. The straddling 37 kb deletion (named *gnom-sgt*) encompassing GNOM and 8 flanking genes is indicated by a red line (Kumaran et al., 1999).

(**C, D**) Primer combinations for genotyping seedlings to detect (C) the *gnom-sgt* deletion or (D) the endogenous *GNOM* gene and a *GNOM* transgene encoding a C-terminally tagged protein.

(**E**) Wild-type seedlings (Col, *a*), *gnom-sgt* deletion seedlings (*sgt*, *c*) and partially rescued *gnom-sgt* deletion seedlings bearing a *GNOM-loop>J(3A)-MYC* transgene (*d*); seedlings homozygous for the weak *gnom-R5* allele are shown for comparison (*b*). (*e, f*) Partial rescue of exchange-deficient *gnom* seedlings (*emb30*, *e*) or membrane-assocation-deficient *gnom* seedlings (*b4049*, *f*). Scale bars, 2.5 mm.

(**F, G**) GNOM protein expression levels of wild-type (Col), *gnom* mutant alleles (*R5*, *sgt*) and *GNOM* transgenes (*GN-myc*, *GN-loop>J(3A)*) detected by anti-SEC7 domain antiserum. Loading control: unstripped membrane re-probed with anti-SYP132 antiserum. (F) Immunoblot; M, marker lane; protein sizes in kDa on the right. Arrow, GNOM band at 165 kDa; asterisk, truncated GNOM protein of *gnom-R5* at 155 kDa. (G) Normalized expression levels; GNOM from *GN-myc* set at 1. GN, wild-type level of GNOM protein.Note that *gnom-sgt* deletion zygotes complete embryogenesis and give rise to highly abnormal seedlings because the retrograde COPI traffic from Golgi to ER is jointly mediated by GNOM and the paralogous ARF-GEF GNL1 whereas the GNOM-mediated polar recycling of auxin efflux carrier PIN1 from endosomes to the basal plasma membrane cannot be mediated by GNL1 (Richter et al., 2007).

Note also that the mutations *emb30* and *B4049* both reside in the SEC7 domain of GNOM. Allele *emb30* codes for a catalytically inactive $E_{658}K$ mutant protein, resulting in grossly abnormal seedlings (Meinke, 1985; Mayer et al., 1993; Shevell et al., 1994). *B4049* codes for a $G_{579}R$ mutant protein that is still catalytically active but fails to associate with endomembranes because the DCB-ΔDCB interaction is compromised (see Suppl. Figure S4), which also results in grossly abnormal seedlings (Busch et al., 1996; Anders et al., 2008).

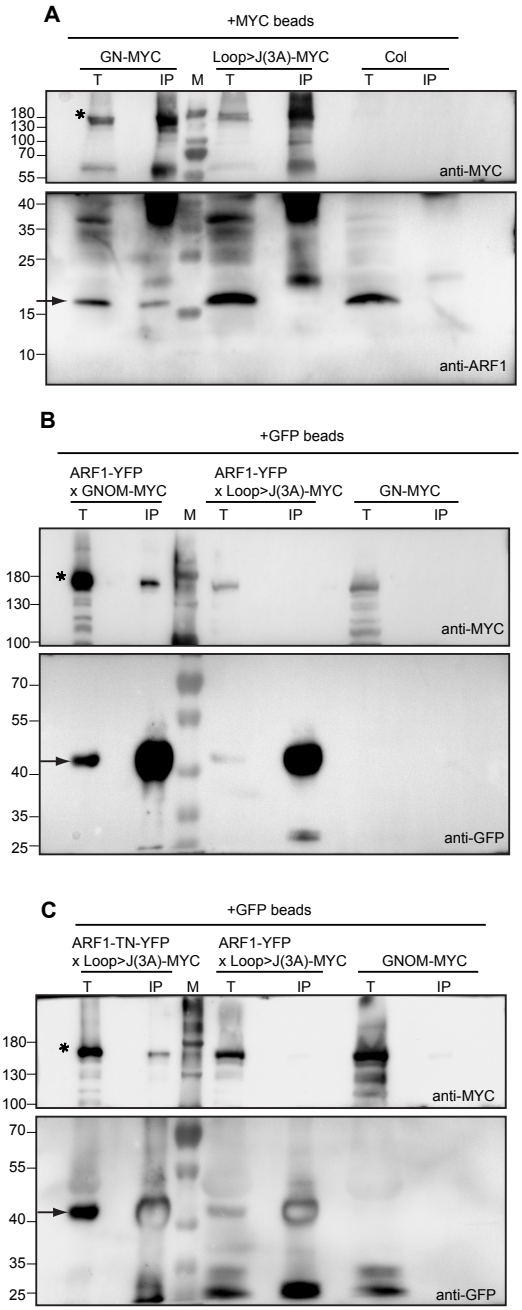

Brumm et al., Figure S4. Interaction of GN-L>J(3A) mutant protein with ARF1-T_{31}N protein but not ARF1 wild-type protein

(**A-C**) Co-immunoprecipitation from Arabidopsis seedling extracts. No detectable interaction of (A) endogenous ARF1 or (B) YFP-tagged ARF1 with GN-loop>J(3A)-Myc compared to GNOM-Myc wild-type control, following IP with (A) anti-Myc beads or (B) anti-GFP beads. (C) Activation-deficient ARF1-T_{31}N-YFP dramatically increased the co-IP signal of GN-loop>J(3A)-Myc; IP with anti-GFP beads. Col, Columbia wild-type control. T, total extract; IP, immunoprecipitate; M, molecular markers (sizes in kDa indicated on the left). Asterisks, GNOM-Myc or GN-loop>J(3A)-Myc bands; arrows, endogenous ARF1 (A), YFP-tagged ARF1 (B, C) or ARF1-T_{31}N (C).

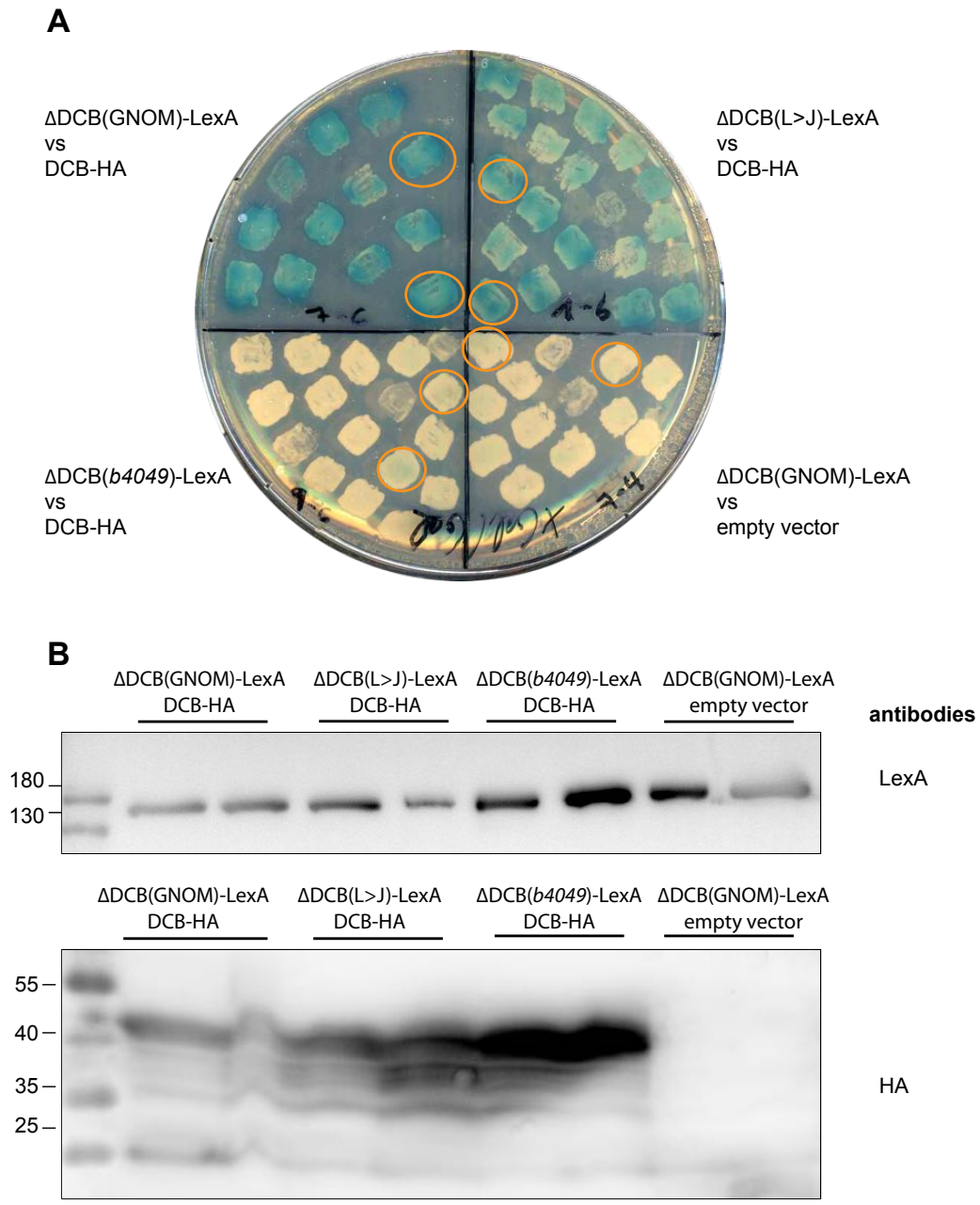

Brumm et al., Figure S5. Y2H assay for DCB-ΔDCB interaction of GN-loop>J(3A)

(**A**) ß-galactosidase activity stain. Unlike *gnom-B4049* (negative control, *lower left*), GN-loop>J(3A) displayed DCB-ΔDCB interaction (*upper right*). *Upper left*: GNOM wild-type, (positive control; *lower right*: empty-vector control. See also Grebe et al. (2000); Anders et al., 2008).

(**B, C**) Expression levels of constructs used for the interaction assay (protein extracts from circled colonies in A) detected by immunoblots with specific antisera indicated on the right: (B) LexA (DNA-binding domain) fused to ΔDCB domains of GNOM wild-type (GNOM) and mutant (L>J, GN-loop>J(3A); b4049, GNOM-B4049) proteins; (C) HA-tagged transactivation domain fused with DCB domain of GNOM (DCB-HA).

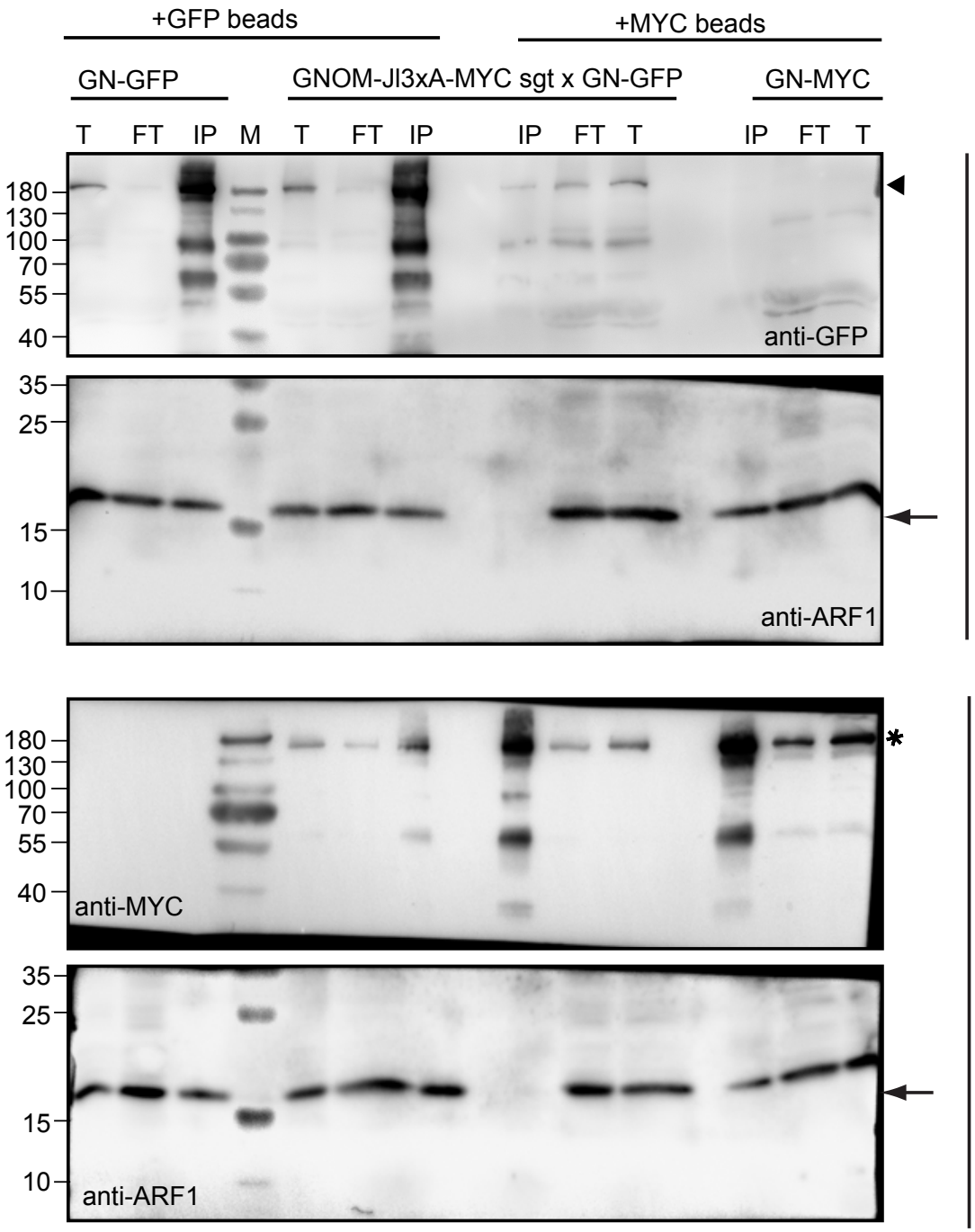

Brumm et al., Figure S6. Complete blots for main Figure 4A

Co-immunoprecipitation of GNOM-GFP and GN-loop>J(3A)-MYC from Arabidopsis seedling extracts with either anti-GFP or anti-MYC beads, revealing interaction of GNOM wild-type with GN-loop>J(3A)-MYC mutant protein but no ARF1 binding by GNOM heterodimer. Precipitates were probed with anti-GFP, anti-ARF1 and anti-MYC antisera. T, total extract; FT, unbound; IP, immunoprecipitate; M, molecular markers (sizes in kDa indicated on the left). Arrowhead, GFP-tagged GNOM; arrows, endogenous ARF1; asterisk, MYC-tagged GNOM or GNOM-loop>J(3A). Black lines on the right indicate membranes belonging together.

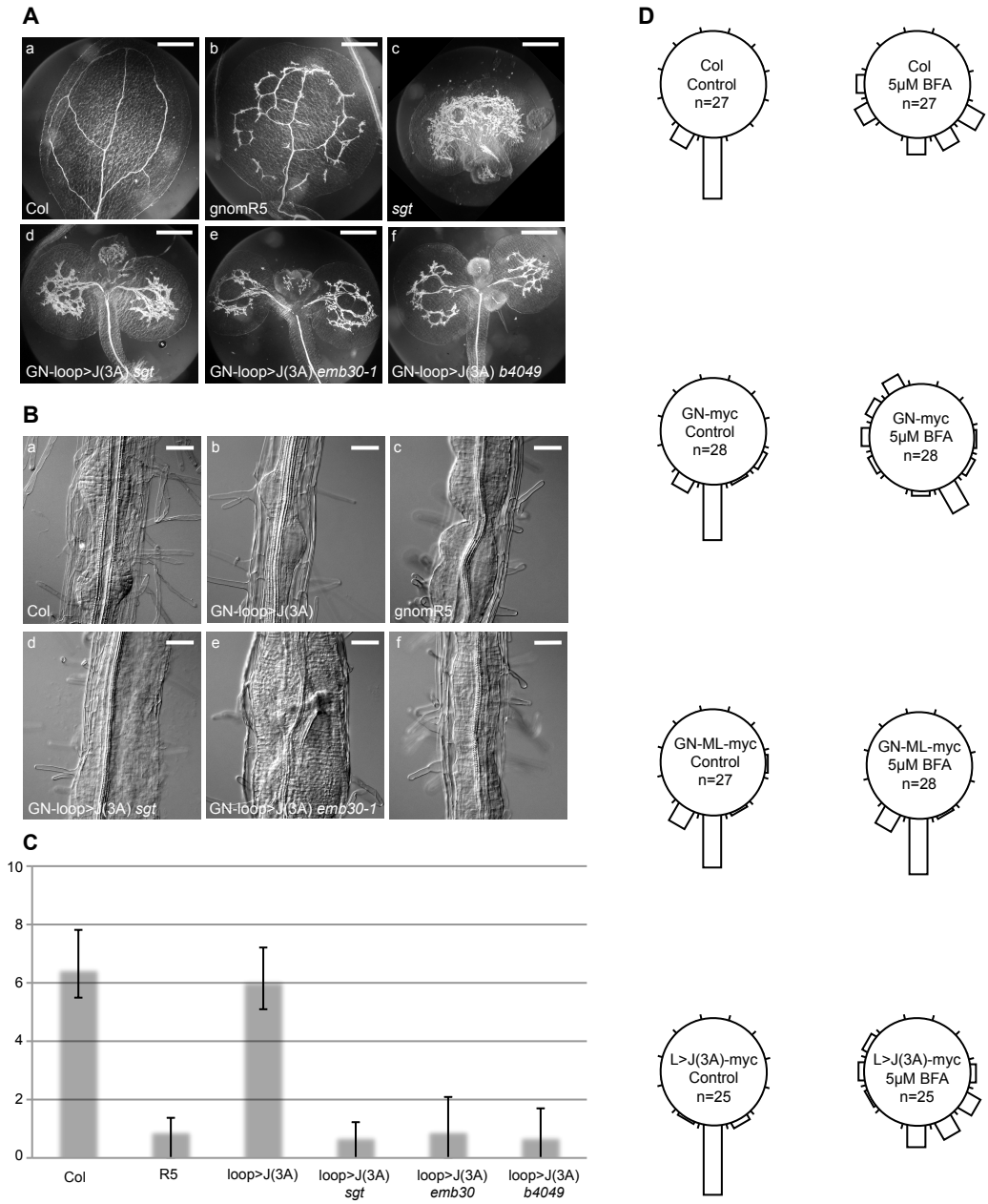

Brumm et al, Figure S7. Seedling phenotypes of *gnom* mutants rescued by *GN-loop>J(3A)* transgene

(A) Vascular tissue differentiation in cotyledon. Scale bars, 500 µm.

(B) Lateral root initiation. Scale bars, 50 µm.

(C) Primary root length (in mm).

(D) Root gravitropism in seedlings treated with 5 µM BFA and untreated control seedlings.

Col, wild-type; R5, gnom-R5; loop>J(3A), GN-loop>J(3A) in wild-type background; *sgt*, gnom-sgt deletion; *emb30*, catalytically defective gnom-emb30; *b4049*, membrane-association-defective gnom-B4049; *GN-myc*, *GN-myc* transgene; *GN-ML-myc*, engineered BFA-resistant GNOM; *L>J(3A)-myc*, *GN-loop>J(3A)-myc* transgene.

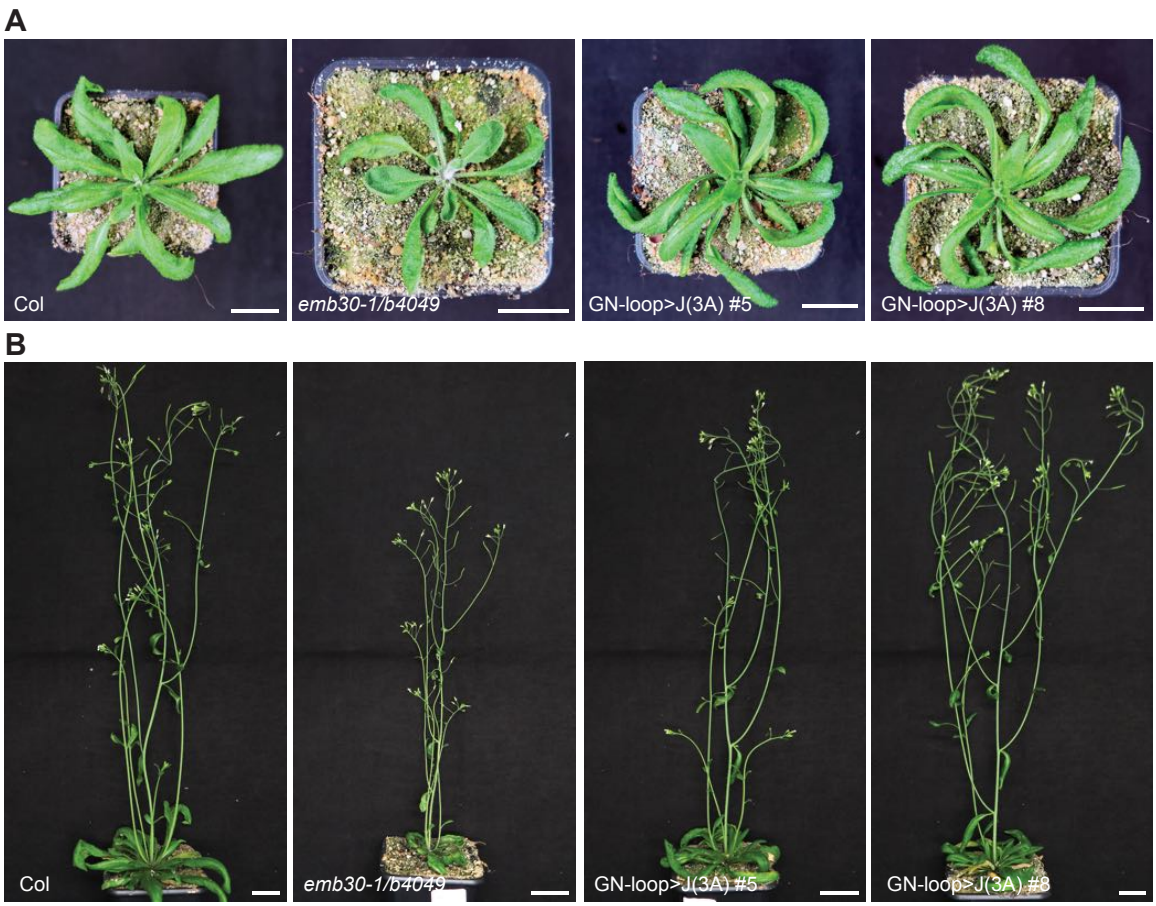

Brumm et al., Figure S8. Developmental phenotypes of wild-type plants expressing GN-loop>J(3A)

(**A**) Rosette stage. Col, wild-type. Note slightly twisted rosettes of *trans*-heterozygous plants bearing nearly fully complementing *gnom* alleles (*emb30-1/B4049*) and of *GN-loop>J(3A)* transgene in Col-0 (two transgenic lines #5, #8).

(**B**) Plants after the onset of flowering. Same genotypes as in (A). Note nearly normal stature of *GN-loop>J(3A)* transgenic plants.

Scale bars, 2 cm.

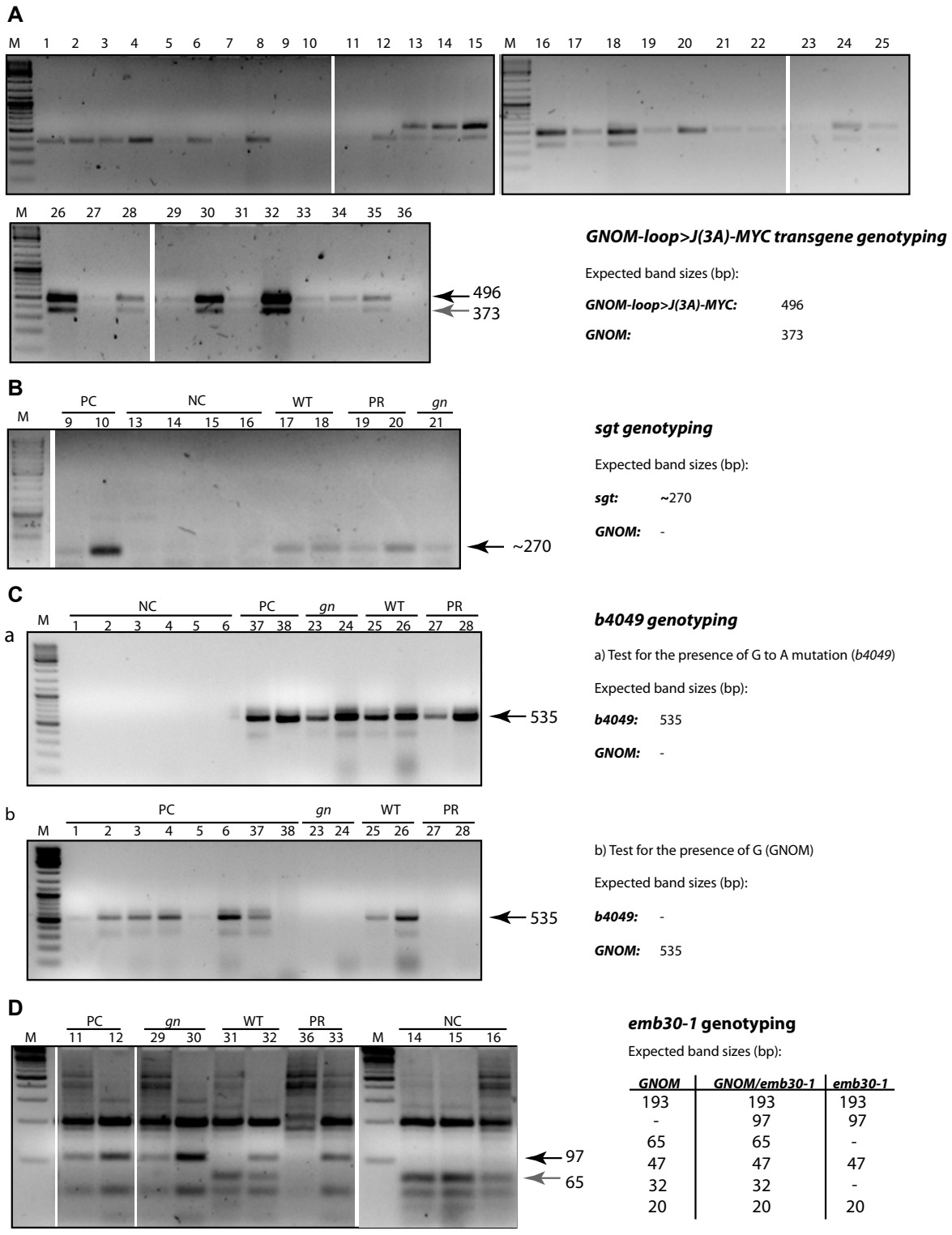

Brumm et al., Figure S9. PCR genotyping of endogenous *GNOM* alleles and transgenes

PCR genotyping was done with the primers shown in Suppl. Figure S2C, D.

gn, *gnom*; NC, negative control; PC, positive control; PR, partial rescue; WT, wild-type. The designations "WT", "PR" and "gn" refer to the seedling phenotypes in the segregating populations.

6.4. Manuscript Brumm et al.

Heterodimers of functionally divergent paralogues prevented by dimerisation domain

Sabine Brumm, Sandra Richter, Hauke Beckmann, Kerstin Huhn, Manoj Singh, Hanno Wolters, Shinobu Takada, Nadine Anders and Gerd Jürgens

Gene duplicates evolve to become functionally divergent, which often relates to changes in gene expression (Bland and Wolfe, 2004). Here, we address mechanisms that keep two functionally divergent paralogues separate within the same cell. The Arabidopsis ARF guanine-nucleotide exchange factor (ARF-GEF) GNOM mediates polar recycling of endocytosed auxin efflux regulator PIN1 from endosomes to the basal plasma membrane whereas its paralogue GNL1, together with GNOM, mediate COPI-coated vesicle formation in retrograde Golgi-ER traffic (Geldner et al., 2003; Richter et al., 2007). The paralogues each form homodimers but no heterodimers, although in both proteins an N-terminal dimerization (DCB) domain can interact with a complementary fragment (ΔDCB), which is required for membrane association (Anders et al., 2008). However, only the DCB domain of GNOM interacts with itself (Anders et al., 2008). The ΔDCB fragment of GNOM rescued the lethality caused by a large deletion of GNOM and flanking genes, which required interaction of ΔDCB(GNOM) with GNL1. Consequently, GNL1 localised to endosomal membranes, in contrast to its normal Golgi localization. However, physiological assays revealed quantitatively incomplete rescue of GNOM-dependent auxin-mediated processes, which would impair growth responses to changing environmental conditions. Our results suggest that prevention of heterodimer formation is an effective means to enable optimization of paralogues for different tasks within the same cell.

ARF guanine-nucleotide exchange factors (ARF-GEFs) mediate the formation of transport vesicles on endomembranes by catalyzing the GDP-GTP exchange of small ARF GTPases through their SEC7 domain (Anders and Jürgens, 2008). Plant genomes only encode large ARF-GEFs, which are evolutionarily conserved among eukaryotes and have a distinct domain organisation. In addition to the catalytic SEC7 domain, there are an N-terminal dimerisation (DCB) domain, a homology upstream of SEC7 (HUS) domain and three homology downstream of SEC7 (HDS1-3) domains (Mouratou et al., 2005; Anders and Jürgens, 2008). The DCB domain of several ARF-GEFs can interact with itself (Grebe et al., 2000; Ramaen et al., 2007;). Interaction between two DCB domains of GNOM yields functional heterodimers of mutant GNOM proteins of which one is catalytically inactive (GNOM-emb30, $GNOM^{E658K}$) and the other incompetent to associate with endomembranes (GNOM-B4049, $GNOM^{G579R}$) (Anders et al., 2008). In addition, the DCB domain interacts with at least one other

domain of the same ARF-GEF which is required for membrane association (Ramaen et al., 2007; Anders et al., 2008).

In Arabidopsis, there are three paralogues related to human GBF1. Like GBF1, GNOM and GNOM-LIKE 1 (GNL1) both mediate COPI traffic from the Golgi stacks to the ER whereas GNOM also mediates polar recycling of auxin efflux carrier PIN1 from endosomes to the basal plasma membrane (Steinmann et al., 1999; Geldner et al., 2003; Richter et al., 2007; Teh and Moore, 2007; Naramoto et al., 2010; Jelínková et al., 2015). The third paralogue GNL2 essentially behaves like GNOM but is only expressed and required in haploid pollen development (Richter et al., 2012). GNOM and GNL1 co-exist in virtually all tissues and yet only GNOM performs the task of polar recycling of PIN1. This is remarkable because GNOM and GNL1 are closely related by sequence, with 60% of their respective 1451 and 1443 amino acid residues being identical, and both paralogues mediate the formation of COPI-coated vesicles in retrograde Golgi-ER traffic. Their functional divergence suggests that GNOM and GNL1 are kept separate within the cell. This was tested by co-immunoprecipitation analysis of seedling extracts, using differently tagged proteins. As previously shown for GNOM (Anders et al., 2008), GNL1 formed homodimers but no heterodimers of GNL1 with GNOM were detected (Figure 1A).

To identify molecular mechanisms that keep GNOM and GNL1 separate, we initially tested by yeast two-hybrid assay whether the two proteins differ in the interactions of DCB domains and ΔDCB fragments (Figure 2). DCB(GNOM) interacted with itself but not with DCB(GNL1) nor did the latter interact with itself (Figure 2A). In contrast, both DCB(GNOM) and DCB(GNL1) interacted with the complementary fragments of their own protein and its paralogue but not with mutant ΔDCB(GNOM$^{HUS\text{-}BOX}$) or ΔDCB(GNOM-B4049) incapable of membrane association (Figure 2B; Anders et al., 2008;). The interaction platform for the DCB domain seems to consist of at least HUS, SEC7 and HDSI domain as DCB(GNL1) did not interact with a SEC7-HDSI (GNOM) fragment (Figure 2B). Since both, DCB(GNOM) and DCB(GNL1), interact with ΔDCB(GNOM), GNOM and GNL1 should in principle be able to form heterodimers by the simultaneous interaction of DCB(GNOM) or DCB(GNL1) with ΔDCB(GNOM). However, this is not the case *in planta*. One possible explanation would be that the

interaction of DCB(GNOM) with itself prevents heterotypic interaction of the two paralogues.

To explore the significance of DCB-DCB interaction for GNOM function in general we generated transgenic plants expressing a chimeric protein that had the DCB domain of GNL1 fused to the ΔDCB fragment of GNOM. This DCB(GNL1)-ΔDCB(GNOM) chimera rescued *gnom-sgt* deletion-mutant plants that lacked the *GNOM* gene and flanking genes on either side, suggesting that DCB-DCB interaction was not necessary for GNOM function (Suppl. Figure S1A,B). Interestingly, DCB(GNL1)-ΔDCB(GNOM) interacted with both paralogues, GNOM and GNL1, as assayed by co-immunoprecipitation from transgenic seedling extracts, and was able to rescue *sgt gnl1* double mutant gametophytes suggesting that the biological role of DCB-DCB interaction of GNOM might be to prevent the formation of GNOM-GNL1 heterodimers (Figure 1B, Suppl. Table S1A)). This idea was supported by the ability of ΔDCB(GNOM) lacking any DCB domain to interact with GNL1 (Figure 1C). Surprisingly, ΔDCB(GNOM) was able to rescue *gnom-sgt* deletion-mutant plants. *ΔDCB(GNOM) gnom-sgt* plants were nearly normal morphologically and fertile, resembling trans-heterozygous *gnom-B4049/gnom-emb30* plants in regard to leaf shape, delayed flowering and plant height (Suppl. Figure S1A,B). PCR Analysis of ΔDCB(GNOM) *sgt gnl1* progeny revealed that the interaction of ΔDCB(GNOM) with GNL1 was necessary for ΔDCB(GNOM) transgene rescuing activity. However, the mutant ΔDCB(GNOM-B4049) fragment, incapable of membrane association, did not rescue *gnom-sgt* deletion-mutant plants (Suppl. Table S1B). Thus, the rescuing activity of the *ΔDCB(GNOM)* transgene depended on the interaction of the GNL1 DCB domain with ΔDCB(GNOM) leading to the membrane association of the ΔDCB(GNOM) fragment.

If indeed GNL1 provided the missing DCB domain to ΔDCB(GNOM) this should be reflected in a changed subcellular localization of GNL1 (Figure 3). GNL1 normally localizes to Golgi stacks, which surround ARF1-positive endosomal BFA compartments in BFA-treated seedling root cells (Figure 3A-D). In contrast, GNL1 was relocated in *ΔDCB(GNOM) gnom-sgt* and, like GNOM, co-localised with ARF1 (Figure 3E-H, compare with Figure 3I-L). Recruitment of the COPI coat subunit γCOP to Golgi stacks was not impaired by the heterodimer formation of ΔDCB(GNOM) and GNL1-

YFP in *gnom-sgt* mutant background as probably enough GNL1 homodimers remain at the Golgi for proper ARF1 activation (Figure 3M-P, compare with Figure 3Q-T). In conclusion, ΔDCB(GNOM) forms a heterodimer with GNL1, which then associates with the endosomal target membrane of GNOM.

Our results show that the DCB domain of GNOM prevents the formation of GNOM-GNL1 heterodimers. The biological significance of this would seem unclear if these heterodimers were able to substitute for GNOM in PIN1 recycling. We therefore analysed GNOM-dependent auxin-mediated physiological processes such as gravitropic root growth and lateral root initiation to determine the activity of the GNL1-ΔDCB(GNOM) heterodimer relative to GNOM activity. Activity of the heterodimer was not sufficient for proper lateral root development (Suppl. Figure S2A). In a few cases emerging lateral root primordia were observed for *ΔDCB(GNOM)* in *gnom-sgt* but their development seemed to terminate in late stages (Suppl. Figure S2B). It may be necessary to prevent heterodimerization of GNOM and GNL1 during lateral root development since the formation of lateral roots requires on one hand proper auxin flux mediated by the PIN1 recycling activity of GNOM but also extensive secretory trafficking in dividing cells. Since GNL1, unlike GNOM, is naturally BFA-resistant we compared the effects of BFA treatment between wild-type, BFA-resistant GNOM and *ΔDCB(GNOM)-HA sgt* seedlings (Suppl. Figure S2C,D). The GNOM-dependent processes such as root gravitropism and cotyledon vasculature were incompletely BFA-insensitive in *sgt* seedlings rescued by *ΔDCB(GNOM)* (Suppl. Figure S2C,D), indicating that the PIN1-recycling activity of ΔDCB(GNOM) interacting with endogenous, BFA-resistant GNL1 was reduced as compared to BFA-resistant GNOM (Suppl. Figure S2D). However, BFA-treated roots of the DCB(GNL1)-ΔDCB(GNOM) chimera in *gnom-sgt* background were more BFA-sensitive as ΔDCB(GNOM) suggesting that the chimeric protein might have a higher preference for homodimerization with itself than heterodimerization with GNL1 whereas ΔDCB(GNOM) is non-functional without GNL1 (Suppl. Figure S2E).

Our results reveal an unexpected mechanism of keeping the closely related but functionally divergent ARF-GEFs GNOM and GNL1 separate within the same cell. The DCB domain interacts with the ΔDCB fragment for membrane association of ARF-GEFs. However, the DCB domain of GNOM prevents the heterodimerization of GNL1

with GNOM, presumably because the ΔDCB fragments direct GNOM and GNL1 to different membrane compartments. If DCB(GNOM) did not prevent heterodimerization there would be conflicting targeting such that not enough GNOM ARF-GEF would associate with endosomes to regulate the polar recycling of PIN1 and consequently, directional growth responses to gravity and other signals might be compromised. Furthermore, processes such as lateral root development and pollen tube growth with high demands of secretory trafficking and recycling at the same time might require the functional separation of the two paralogues to keep the system balanced.

Acknowledgements

We thank Christopher Grefen and Niko Geldner for discussion and critical reading of the manuscript

Competing interests

No competing interests declared

Author contributions

Conceptualization: G.J.; Methodology: S.B., S.R., H.B. ,K.H., M.K.S., S.R., H.W., S.T., N.A.; Formal analysis: S.B. H.B. ,K.H., M.K.S., G.J.; Data curation: S.B.; Writing - original draft: G.J.; Writing - review & editing: S.B., S.R., G.J.; Funding acquisition: G.J.

Funding

This work was supported by the Deutsche Forschungsgemeinschaft (Ju 179/18-1 and SFB1101/A01 to G.J.)

Figure legends

Figure 1. The DCB domain of GNOM promotes GNOM homodimerization but prevents heterodimerization of GNOM and GNL1 *in vivo*

(**A-C**) Co-immunoprecipitation from Arabidopsis seedling extracts. **(A)** No detectable interaction of BFA-sensitive GNL1-LM-MYC with GFP-tagged GNOM but homodimerization of BFA-sensitive GNL1-LM-MYC with YFP-tagged GNL1, following IP with anti-GFP beads. **(B)** In contrast, a MYC tagged chimeric GNOM protein composed of DCB (GNL1) and ΔDCB(GNOM) shows interaction with both, GFP-tagged GNOM and YFP-tagged GNL1 upon IP with anti-GFP beads. **(C)** Weak interaction HA-tagged ΔDCB(GNOM) with MYC-tagged GNL1 in comparison to the strong interaction of full length HA- and MYC-tagged GNOM, following IP with anti-HA beads. T, total extract; IP, immunoprecipitate; M, molecular markers (sizes in kDa indicated on the left). Membrane was first detected with anti-MYC and without stripping with anti-HA antibody

Figure 2. Interaction studies of GNOM and GNL1 DCB domains and Δ DCB fragments

(A) In contrast to DCB(GNL1), (DCB)GNOM forms homodimers in yeast two hybrid assays but DCB(GNOM) does not heterodimerize with DCB(GNL1) (left panel). Color assay: blue color indicates interaction. Expression of fusion proteins was tested by SDS-PAGE using anti-LexA and anti-HA antibodies (middle and right panel). **(B)** Quantification of ß-galactosidase activity (measured as Miller units) in yeast two-hybrid assay of DCB(GNL1) interactions with different GNOM fragments. A strong interaction of DCB(GNL1) and ΔDCB(GNOM), comparable to DCB(GNOM) and ΔDCB(GNOM), was detectable. No interaction was observed for DCB(GNL1) with ΔDCB(GNOM) fragments carrying mutations (G579R or HUS-BOX) already known to interfere with heterotypic interaction of DCB(GNOM) and ΔDCB(GNOM) (Anders et al., 2008) or the minimal SEC7-HDSI(GNOM) fragment. Data shown as means, n=5. Negative control, DCB(GNL1) with empty vector.

Figure 3. The heterodimer of ΔDCB(GNOM) and GNL1 associates with the endosomal target membrane of GNOM

Immunostainings of BFA-treated seedling roots. GNL1 localization in wild-type background was mainly visible at Golgi stacks surrounding the ARF1 positive labelled endomembranes in the BFA-compartment **(A-D)** while in *gnom-sgt* deletion-mutant background (with ΔDCB(GNOM) present) GNL1 relocated to the endosomes **(E-H)** resembling the localization of BFA-sensitive GNOM **(I-L)**. The COPI subunit γCOP colocalizes with GNL1 at Golgi stacks in wild-type background **(M-P)** and remains at Golgi in ΔDCB(GNOM) *sgt* mutant background (**Q-T**). **(A,E,M,Q)** GNL1-YFP (cyan), **(I)** GNOM-GFP (cyan), **(B,F,J)** ARF1 (magenta), **(N,R)** γCOP (magenta), **(C,G,K,O,S)** merged images with with regions of interest (ROIs) indicated as white strokes. Co-localization analysis of GNL1-YFP or GNOM-GFP and ARF1 **(D,H,L)** or of GNL1-YFP and γCOP **(P,T)** in ROIs shown in line intensity profiles. Scale bar, 10 µm.

Materials and Methods

Plant material and growth conditions

Plants were grown under permanent light conditions (Osram L18W/840 cool white lamps) at 23°C and 40% humidity in growth chambers on soil or agar plates. Previously published lines that were used in this study: *b4049/emb30-1* (Busch et al., 1996b), *gnom-sgt* (Brumm et al., unpublished manuscript),GN-ML-MYC, GNOM-GFP (Geldner et al., 2003), GN-HA x GN-MYC, XLIM-ΔDCB(GNOM-B4049)-MYC, ΔDCB(GNOM)-HA, ΔDCB(GNOM)-MYC (Anders et al., 2008), GNL1-YFP, GNL1-LM-MYC, GNL1-MYC, GNL1-YFP x GNL1-LM-MYC and GNOM-GFP x GNL1-LM-MYC (Richter et al., 2007).

Binary vector constructs, generation of transgenic plants and crosses

XLIM-ΔDCB(GNOM-B4049)-MYC, ΔDCB(GNOM)-HA, ΔDCB(GNOM)-MYC were crossed and/or transformed into heterozygous *gnom-sgt* and *sgt gnl1* double mutant and analyzed for complementation. Of three decent expressing, independent transgenic lines one was chosen for further analysis. For co-immunoprecipitation analysis and whole-mount immunofluorescence staining GNL1-MYC or GNL1-YFP were crossed with ΔDCB(GNOM)-HA in *gnom-sgt* mutant background. The DCB domain of GNL1 was amplified via primer extension PCR and via PmeI und SwaI restriction sites inserted into the genomic fragment GNXbaI^{wt}-myc (Geldner et al.,

2003) in pBlueScript. The GN::DCB(GNL1)-ΔDCB(GNOM)-MYC fragment was first inserted into an intermediate pBar vector via XbaI restriction sites and afterwards introduced into pGII(BAR) expression vector and transformed into Col-O background. T1 plants were selected using phosphinotricine. Decent expressing lines were crossed with heterozygous *sgt*, *gnl1* and *sgt gnl1* double mutants. For co-immunoprecipitation analysis GN::DCB(GNL1)-ΔDCB(GNOM)-MYC transgenic plants were crossed with GNOM-GFP and GNL1-YFP.

Physiological tests

For primary root growth assays, 50 five-days old seedlings were transferred to agar plates containing 10 μM BFA for 24h and seedling growth was analyzed using ImageJ software. Gravitropic response of 50 five-days old seedlings was measured by ImageJ software after transferring seedlings to 10 μM BFA plates and rotating them by 135° for 24h. Lateral root primordia formation was analyzed after transferring 7-day old seedlings for 3 days on 20 μM NAA-containing agar plates and clearing the roots according to Geldner et al. (2004). To examine the vasculature of 7 to 10-days old cotyledons, seedlings were shaken for several hours in 3:1 ethanol/acetic acid solution at room temperature according to (Geldner et al., 2004). Light microscopy images were taken with Zeiss Axiophot microscope, Axiocam and AxioVision_4 Software. Image size, brightness and contrast were edited with Adobe Photoshope CS 3 Software.

Yeast two-hybrid interaction assays

GNOM-DCB (AA 1-246), GNOM-ΔDCB (AA 232-1451), GNOM-ΔDCB^{G579R} (AA 232-1451) and GNOM-Δ$^{DCBHUS-BOX}$ (AA 232-1451; D468G) constructs and assay were as described (Grebe et al., 2000; Anders et al., 2008).

Whole-mount immunofluorescence staining

Four to six-days old seedlings were incubated in 24-well cell-culture plates for 1 hour in 50 μM BFA (Invitrogen, Thermo Fisher Scientific) containing liquid growth medium (0.5x MS medium, 1% sucrose, pH 5.8) at 23°C and then fixed for 1 hour in 4% paraformaldehyde in MTSB at room temperature. Whole-mount immunofluorescence staining was performed manually as described (Lauber et al., 1997a) or with an InsituPro machine (Intavis) (Müller et al., 1998). All antibodies were diluted in 1x PBS buffer. The following antisera were used for immunofluorescence staining: rabbit anti-

ARF1 (Agrisera) diluted 1:1000; rabbit anti-AtγCOP (Agrisera) diluted 1:1000; anti-rabbit CY3 (Dianova)-conjugated secondary antibodies were diluted 1:600. Nuclei were stained with Dapi (1:600 dilution).

Confocal microscopy and processing of images

Fluorescence images were acquired at the confocal laser scanning microscope TCS-SP8 from Leica or LSM880 from Zeiss, using a 63x water-immersion objective and Leica or Zeiss softwares. Overlays and contrast/brightness adjustments of images were performed with Adobe Photoshop CS3 software. Intensity line profiling was performed with Leica software.

Co-immunoprecipitation analysis

Immunoprecipitation protocol was modified from Singh et al. (2014). 0,5-3g of 8 to 10-days old Arabidopsis seedlings were homogenized in 1:1 lysis buffer containing 1% Triton-X100. For immunoprecipitation, anti-HA-agarose beads (Sigma) or GFP-Trap beads (Chromotek) were incubated with plant extracts for 2h30min at 4°C. Beads were then washed twice with wash buffer containing 0.1% Triton-X100 and twice without Triton-X100. Bound proteins were eluted by boiling the beads in 2x Lämmli buffer at 95°C for 5min.

SDS-PAGE and protein gel blotting

SDS-Pages and protein gel blotting with PVDF membranes (Millipore) were performed as described (Lauber et al., 1997). All antibodies were diluted in 5% milk/TBS-T solution. Antibodies and dilutions: mouse anti-c-Myc mAB 9E10 (Santa Cruz Biotechnology) 1:1000, mouse anti-GFP (Roche) 1:2500, mouse anti-LexA (Santa Cruz Biotechnology) 1:1000, POD-conjugated anti-HA (Roche) 1:4000, anti-mouse (Sigma) or anti-rabbit peroxidase-conjugated (Merck Millipore) or alkaline phosphatase-conjugated antibodies (Jackson Immuno Research) 1:10000. Detection was performed with the BM-chemiluminescence blotting substrate (Roche) and FusionFx7 imaging system (PeqLab). Image assembly was performed with Adobe Photoshop CS3.

References

Anders, N. & Jürgens, G. (2008). Large ARF guanine nucleotide exchange factors in membrane trafficking. *Cell. Mol. Life Sci.* **65**, 3433-3445

Anders, N. et al. Nielsen, J. Keicher, Y.-D. Stierhof, M. Furutani, M. Tasaka, K. Skriver, G. Jürgens, (2008). Membrane association of the Arabidopsis ARF exchange factor GNOM involves interaction of conserved domains. *Plant Cell* **20**, 142-151

Bhatt JM, Viktorova EG, Busby T, Wyrozumska P, Newman LE, Lin H, Lee E, Wright J, Belov GA, Kahn RA, Sztul E. (2016). Oligomerization of the Sec7 domain Arf guanine nucleotide exchange factor GBF1 is dispensable for Golgi localization and function but regulates degradation. *Am. J. Physiol. Cell Physiol*. **310**, C456-C469.

Blanc K and Wolfe KH (2004) Functional Divergence of Duplicated Genes Formed by Polyploidy during Arabidopsis Evolution. *The Plant Cell*, **16** (7) 1679-1691.

Bui QT, Golinelli-Cohen MP, Jackson CL. (2009). Large Arf1 guanine nucleotide exchange factors: evolution, domain structure, and roles in membrane trafficking and human disease. *Mol Genet Genomics* **282**, 329-350.

Cox R, Mason-Gamer RJ, Jackson CL, Segev N. (2004). Phylogenetic analysis of Sec7-domain-containing Arf nucleotide exchangers. *Mol Biol Cell* **15**, 1487-1505.

Doyle SM, Haeger A, Vain T, Rigal A, Viotti C, Łangowska M, Ma Q, Friml J, Raikhel NV, Hicks GR, Robert S. (2015). An early secretory pathway mediated by GNOM-LIKE 1 and GNOM is essential for basal polarity establishment in Arabidopsis thaliana. *Proc Natl Acad Sci USA* **112**, E806-815.

Geldner N, Anders N, Wolters H, Keicher J, Kornberger W, Muller P, Delbarre A, Ueda T, Nakano A, Jürgens G. (2003). The Arabidopsis GNOM ARF-GEF mediates endosomal recycling, auxin transport, and auxin-dependent plant growth. *Cell* **112**, 219-230.

Grebe M, Gadea J, Steinmann T, Kientz M, Rahfeld JU, Salchert K, Koncz C, Jürgens G. (2000). A conserved domain of the Arabidopsis GNOM protein mediates subunit interaction and cyclophilin 5 binding. *Plant Cell* **12**, 343-356.

Jelínková A, Müller K, Fílová-Pařezová M, Petrášek J. (2015). NtGNL1a ARF-GEF acts in endocytosis in tobacco cells. *BMC Plant Biol* **15**, 272.

M. H. Lauber, I. Waizenegger, T. Steinmann, H. Schwarz, U. Mayer, I. Hwang, W. Lukowitz, G. Jürgens, The Arabidopsis KNOLLE protein is a cytokinesis-specific syntaxin. *J. Cell Biol.* **139**, 1485-1493 (1997).

A. Müller, C. Guan, L. Gälweiler, P. Tänzler, P. Huijser, A. Marchant, G. Parry, M. Bennett, E. Wisman, K. Palme, AtPIN2 defines a locus of Arabidopsis for root gravitropism control. *EMBO J.* **17**, 6903-6911 (1998).

Mossessova E, Corpina RA, Goldberg J. (2003). Crystal structure of ARF1*Sec7 complexed with Brefeldin A and its implications for the guanine nucleotide exchange mechanism. *Mol Cell* **12**, 1403-1411.

Mouratou B, Biou V, Joubert A, Cohen J, Shields DJ, Geldner N, Jürgens G, Melançon P, Cherfils J. (2005). The domain architecture of large guanine nucleotide exchange factors for the small GTP-binding protein Arf. *BMC Genomics* **6**, 20.

Naramoto S, Otegui MS, Kutsuna N, de Rycke R, Dainobu T, Karampelias M, Fujimoto M, Feraru E, Miki D, Fukuda H, Nakano A, Friml J. (2014). Insights into the localization and function of the membrane trafficking regulator GNOM ARF-GEF at the Golgi apparatus in Arabidopsis*. Plant Cell* **26**, 3062-3076.

Naramoto S, Kleine-Vehn J, Robert S, Fujimoto M, Dainobu T, Paciorek T, Ueda T, Nakano A, Van Montagu MC, Fukuda H, Friml J. (2010). ADP-ribosylation factor machinery mediates endocytosis in plant cells. *Proc Natl Acad Sci USA* **107**, 21890-21895.

Ramaen O, Joubert A, Simister P, Belgareh-Touzé N, Olivares-Sanchez MC, Zeeh JC, Chantalat S, Golinelli-Cohen MP, Jackson CL, Biou V, Cherfils J. (2007). Interactions between conserved domains within homodimers in the BIG1, BIG2, and GBF1 Arf guanine nucleotide exchange factors. *J Biol Chem* **282**, 28834-28842.

Renault L, Guibert B, Cherfils J. (2003). Structural snapshots of the mechanism and inhibition of a guanine nucleotide exchange factor. *Nature* **426**, 525-530.

Richter S, Geldner N, Schrader J, Wolters H, Stierhof YD, Rios G, Koncz C, Robinson DG, Jürgens G. (2007). Functional diversification of closely related ARF-GEFs in protein secretion and recycling. *Nature* **448**, 488-492.

Richter S, Müller LM, Stierhof YD, Mayer U, Takada N, Kost B, Vieten A, Geldner N, Koncz C, Jürgens G. (2012). Polarized cell growth in Arabidopsis requires endosomal recycling mediated by GBF1-related ARF exchange factors. *Nat Cell Biol*. **14**, 80-86.

Steinmann T, Geldner N, Grebe M, Mangold S, Jackson CL, Paris S, Gälweiler L, Palme K, Jürgens G. (1999). Coordinated polar localization of auxin efflux carrier PIN1 by GNOM ARF GEF. *Science* **286**, 316-318.

Teh OK, Moore I. (2007). An ARF-GEF acting at the Golgi and in selective endocytosis in polarized plant cells. *Nature* **448**, 493-496.

Wright J, Kahn RA, Sztul E. (2014). Regulating the large Sec7 ARF guanine nucleotide exchange factors: the when, where and how of activation. *Cell Mol Life Sci*. **71**, 3419-3438.

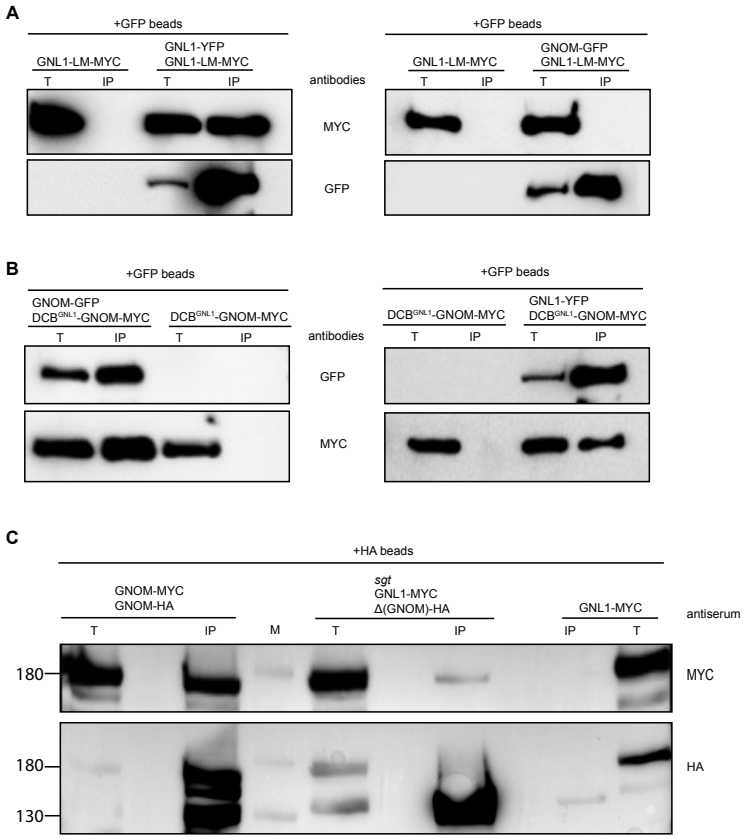

Brumm et al., Figure 1. The DCB domain of GNOM promotes GNOM homodimerization but prevents heterodimerization of GNOM and GNL1 *in vivo*

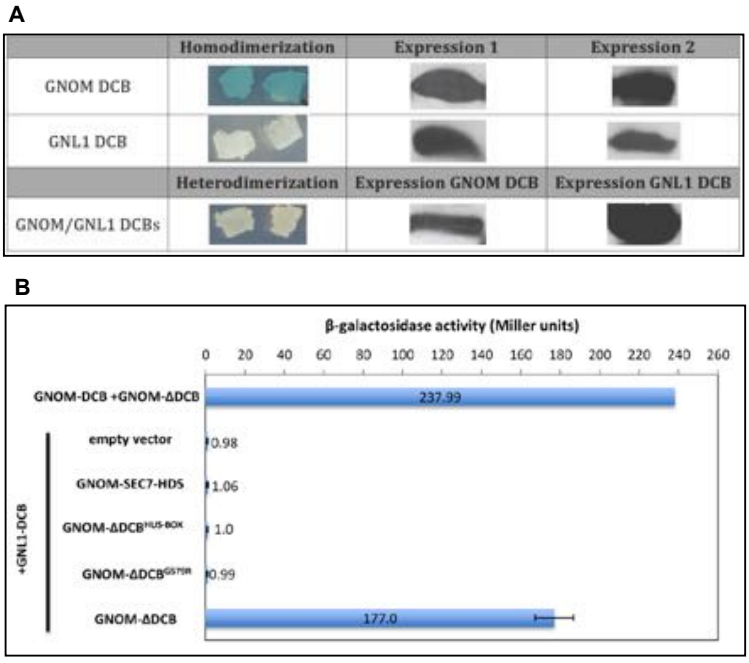

Brumm et al., Figure 2. Interaction studies of GNOM and GNL1 DCB domains and *Δ*DCB fragments

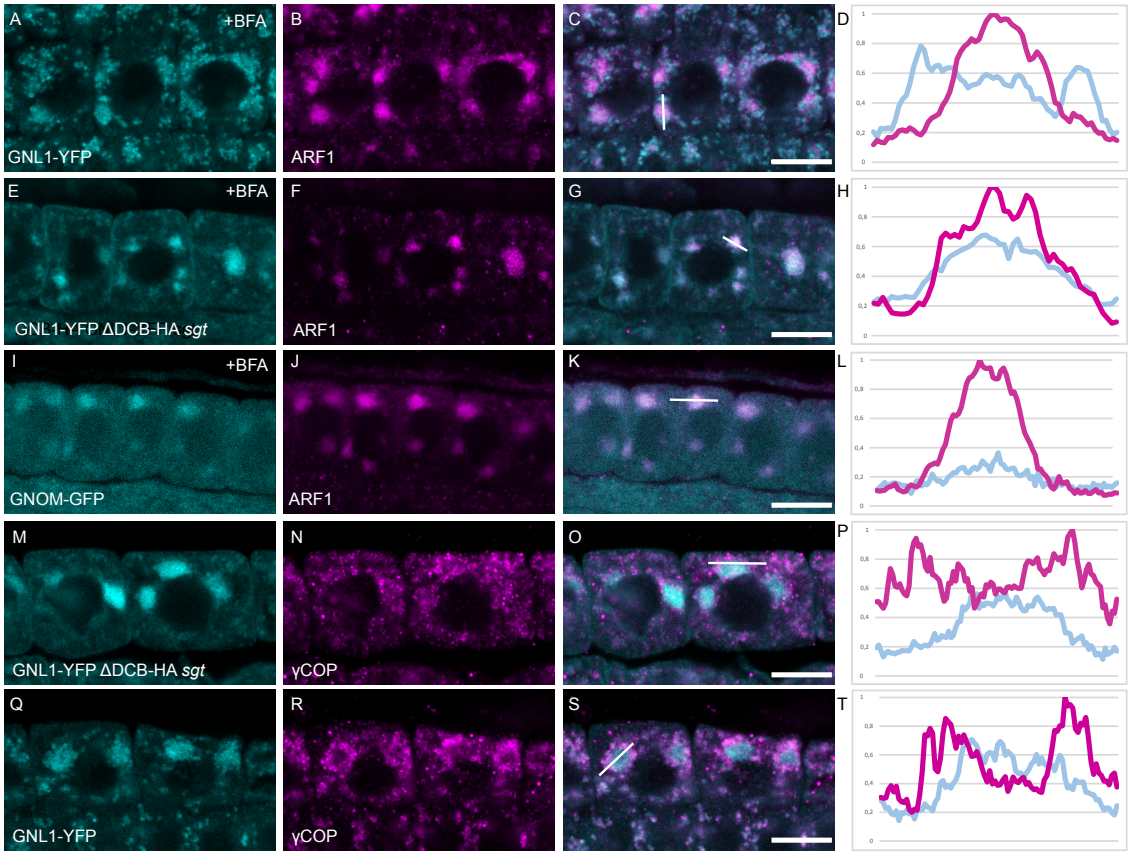

Brumm et al., Figure 3. The heterodimer of ΔDCB(GNOM) and GNL1 associates with the endosomal target membrane of GNOM

Supplementary informations

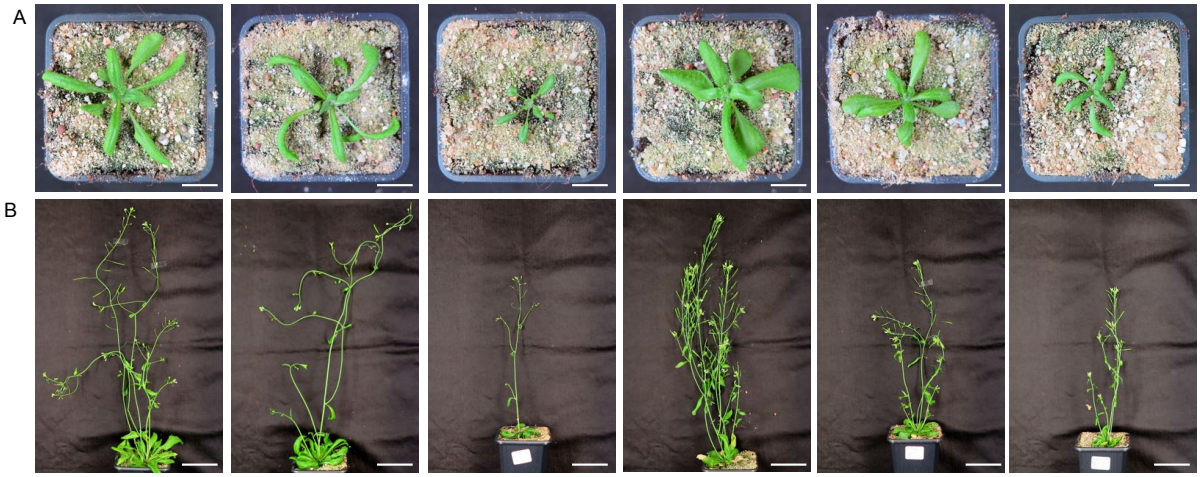

Brumm et al., Figure S1. Developmental phenotypes of *gnom-sgt* plants rescued by differently tagged ΔDCB(GNOM) or DCB(GNL1)-ΔDCB(GNOM) transgenes

(**A**) Rosette stage. Col and Ler, wild-type. Note slightly smaller rosettes of *trans*-heterozygous plants bearing nearly fully complementing *gnom* alleles (*emb30-1/B4049*) or ΔDCB(GNOM) or DCB(GNL1)-ΔDCB(GNOM) (DCB-Swap) in *sgt/GNOM* segregating Ler/Col-0 background. Scale bars, 1,6 cm.

(**B**) Plants after the onset of flowering. Same genotypes as in (A). Note slightly impaired fertility and smaller stature of ΔDCB(GNOM) sgt and DCB-Swap *sgt* transgenic plants. Scale bars, 5 cm.

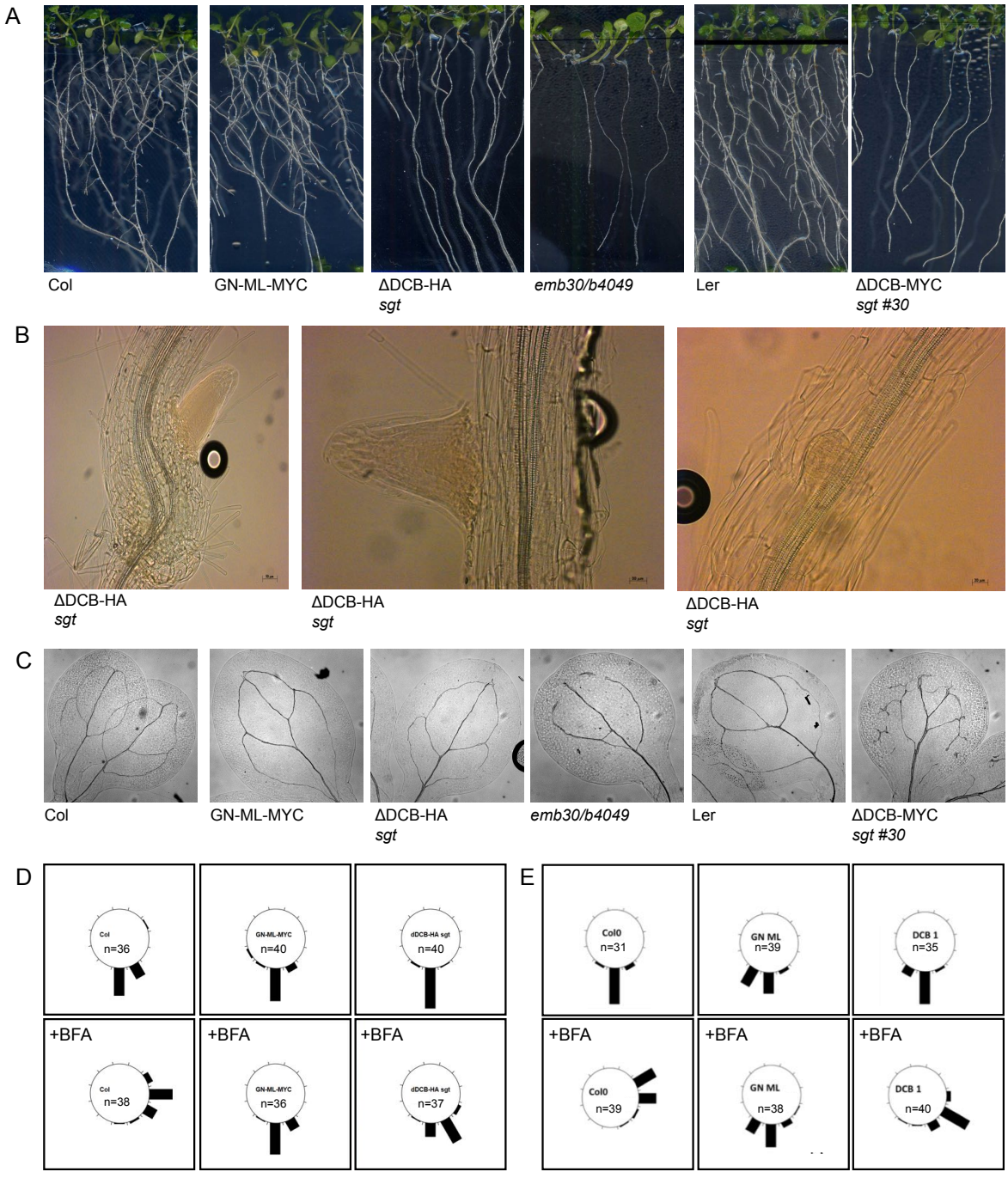

Brumm et al., Figure S2. Seedling phenotypes of rescued by differently tagged *Δ*DCB(GNOM) or DCB(GNL1)-ΔDCB(GNOM) transgenes

(A) Lateral root development 11dag. (B) Terminated lateral root primordia of sgt seedlings rescued by *Δ*DCB(GNOM)-HA transgene 11dag. **(C)** Vascular tissue differentiation in cotyledons **(D-E)** Root gravitropism in seedlings treated with 10 µM BFA and untreated control seedlings. Col, wild-type; *GN-ML-myc*, engineered BFA-resistant GNOM; *Δ*DCB(GNOM)-HA (D) or DCB(GNL1)-*Δ*DCB(GNOM)-HA (named DCB1) transgene in *sgt* background.

A) F1: Cross with Col ♀	**#**	**WT (%)**	***sgt* (%)**	***gnl1* (%)**	***gnl1 sgt* (%)**
DCB(GNL1)-ΔDCB(GNOM)-MYC$^{+/-}$ *sgt*$^{+/-}$ *gnl1*$^{+/-}$ ♂	15	27	-	60	13
ΔDCB(GNOM)-HA$^{+/-}$ *sgt*$^{+/-}$ *gnl1*$^{+/-}$ ♂	238	38,5	34,5	27	-
Expected values (rescue)		(25)	(25)	(25)	(25)
Expected values (no rescue)		(33,3)	(33,3)	(33,3)	-

B) F3: XLIM-ΔDCB(GNOM-B4049)-MYC$^{+/+}$ x *sgt*$^{+/-}$	**#**	**WT (%)**	***sgt* (%)**
Plant line #1	144	85	15
Plant line #2	114	71	29
Plant line #3	271	81	19
Expected values (rescue)		(100)	
Expected values (no rescue)		(75)	(25)

Brumm et al., Table S1. Segregation analyses

(A) Analysis of *DCB(GNL1)-ΔDCB(GNOM)-MYC* or *ΔDCB(GNOM)-HA sgt gnl1*mutant gametophyte viability. Backcross of heterozygous transgene pollen in heterozygous double mutant background with wild-type plants. By PCR analysis, no double heterozygous *sgt gnl1* mutant seedlings were identified in the case of *ΔDCB(GNOM)-HA sgt gnl1* whereas 13% of the ΔDCB(GNOM)-MYC *sgt gnl1* progeny were *sgt gnl1* heterozygous. **(B)** Phenotypes of three independent plant line seedling progenies of selfed *sgt/GNOM (KAN)* heterozygous plants that were homozygous for *XLIM-ΔDCB(GNOM-B4049)-MYC* transgene (PPT). Seedling were grown on phosphinotricine.

[a] Assuming independent segregation of the transgene.

7. Literature

Anders, N., and Jürgens, G. (2008). Large ARF guanine nucleotide exchange factors in membrane trafficking. Cellular and molecular life sciences : CMLS *65*, 3433-3445.

Anders, N., Nielsen, M., Keicher, J., Stierhof, Y.D., Furutani, M., Tasaka, M., Skriver, K., and Jürgens, G. (2008). Membrane association of the Arabidopsis ARF exchange factor GNOM involves interaction of conserved domains. The Plant cell *20*, 142-151.

Antonny, B., Beraud-Dufour, S., Chardin, P., and Chabre, M. (1997). N-terminal hydrophobic residues of the G-protein ADP-ribosylation factor-1 insert into membrane phospholipids upon GDP to GTP exchange. Biochemistry *36*, 4675-4684.

Beck, R., Prinz, S., Diestelkötter-Bachert, P., Röhling, S., Adolf, F., Hoehner, K., Welsch, S., Ronchi, P., Brügger, B., Briggs, J.A.G.*, et al.* (2011). Coatomer and dimeric ADP ribosylation factor 1 promote distinct steps in membrane scission. Journal of Cell Biology *194*, 765-777.

Beck, R., Sun, Z., Adolf, F., Rutz, C., Bassler, J., Wild, K., Sinning, I., Hurt, E., Brügger, B., Bethune, J.*, et al.* (2008). Membrane curvature induced by Arf1-GTP is essential for vesicle formation. P Natl Acad Sci USA *105*, 11731-11736.

Beraud-Dufour, S., Paris, S., Chabre, M., and Antonny, B. (1999). Dual interaction of ADP ribosylation factor 1 with Sec7 domain and with lipid membranes during catalysis of guanine nucleotide exchange. The Journal of biological chemistry *274*, 37629-37636.

Betz, S.F., Schnuchel, A., Wang, H., Olejnicak, E.T., Meadows, R.P., Lipsky, B.P., Harris, E.A.S., Staunton, D.E., and Fesik, S.W. (1998). Solution structure of the cytohesin-1 (B2-1) Sec7 domain and its interaction with the GTPase ADP ribosylation factor 1. P Natl Acad Sci USA *95*, 7909-7914.

Bhatt, J.M., Viktorova, E.G., Busby, T., Wyrozumska, P., Newman, L.E., Lin, H., Lee, E., Wright, J., Belov, G.A., Kahn, R.A.*, et al.* (2016). Oligomerization of the Sec7 domain Arf guanine nucleotide exchange factor GBF1 is dispensable for Golgi localization and function but regulates degradation. Am J Physiol-Cell Ph *310*, C456-C469.

Busch, M., Mayer, U., and Jürgens, G. (1996a). Molecular analysis of the Arabidopsis pattern formation gene GNOM: Gene structure and intragenic complementation. Mol Gen Genet *250*, 681-691.

Busch, M., Mayer, U., and Jürgens, G. (1996b). Molecular analysis of the Arabidopsis pattern formation of gene GNOM: gene structure and intragenic complementation. Mol Gen Genet *250*, 681-691.

Chen, X., Irani, N.G., and Friml, J. (2011). Clathrin-mediated endocytosis: the gateway into plant cells. Curr Opin Plant Biol *14*, 674-682.

Cherfils, J., Menetrey, J., Mathieu, M., Le Bras, G., Robineau, S., Beraud-Dufour, S., Antonny, B., and Chardin, P. (1998). Structure of the Sec7 domain of the Arf exchange factor ARNO. Nature *392*, 101-105.

Collins, N.C., Thordal-Christensen, H., Lipka, V., Bau, S., Kombrink, E., Qiu, J.L., Huckelhoven, R., Stein, M., Freialdenhoven, A., Somerville, S.C.*, et al.* (2003). SNARE-protein-mediated disease resistance at the plant cell wall. Nature *425*, 973-977.

Cui, Y., Zhao, Q., Gao, C.J., Ding, Y., Zeng, Y.L., Ueda, T., Nakano, A., and Jiang, L.W. (2014). Activation of the Rab7 GTPase by the MON1-CCZ1 Complex Is Essential for PVC-to-Vacuole Trafficking and Plant Growth in Arabidopsis. The Plant cell *26*, 2080-2097.

Dacks, J.B., and Robinson, M.S. (2017). Outerwear through the ages: evolutionary cell biology of vesicle coats. Curr Opin Cell Biol *47*, 108-116.

Dascher, C., and Balch, W.E. (1994). Dominant inhibitory mutants of ARF1 block endoplasmic reticulum to Golgi transport and trigger disassembly of the Golgi apparatus. The Journal of biological chemistry *269*, 1437-1448.

Deng, Y., Golinelli-Cohen, M.P., Smirnova, E., and Jackson, C.L. (2009). A COPI coat subunit interacts directly with an early-Golgi localized Arf exchange factor. EMBO reports *10*, 58-64.

Dettmer, J., Hong-Hermesdorf, A., Stierhof, Y.D., and Schumacher, K. (2006). Vacuolar H+-ATPase activity is required for endocytic and secretory trafficking in Arabidopsis. The Plant cell *18*, 715-730.

Donaldson, J.G., and Jackson, C.L. (2011). ARF family G proteins and their regulators: roles in membrane transport, development and disease. Nat Rev Mol Cell Biol *12*, 362-375.

Ebine, K., Inoue, T., Ito, J., Ito, E., Uemura, T., Goh, T., Abe, H., Sato, K., Nakano, A., and Ueda, T. (2014). Plant Vacuolar Trafficking Occurs through Distinctly Regulated Pathways. Current Biology *24*, 1375-1382.

Fan, L., Li, R., Pan, J., Ding, Z., and Lin, J. (2015). Endocytosis and its regulation in plants. Trends Plant Sci *20*, 388-397.

Friml, J., Vieten, A., Sauer, M., Weijers, D., Schwarz, H., Hamann, T., Offringa, R., and Jürgens, G. (2003). Efflux-dependent auxin gradients establish the apical-basal axis of Arabidopsis. Nature *426*, 147-153.

Früholz, S., Fässler, F., Kolukisaoglu, U., and Pimpl, P. (2018). Nanobody-triggered lockdown of VSRs reveals ligand reloading in the Golgi. Nat Commun *9*, 643.

Gälweiler, L., Guan, C., Müller, A., Wisman, E., Mendgen, K., Yephremov, A., and Palme, K. (1998). Regulation of polar auxin transport by AtPIN1 in Arabidopsis vascular tissue. Science *282*, 2226-2230.

Gebbie, L.K., Burn, J.E., Hocart, C.H., and Williamson, R.E. (2005). Genes encoding ADP-ribosylation factors in Arabidopsis thaliana L. Heyn.; genome analysis and antisense suppression. J Exp Bot *56*, 1079-1091.

Geldner, N., Anders, N., Wolters, H., Keicher, J., Kornberger, W., Muller, P., Delbarre, A., Ueda, T., Nakano, A., and Jürgens, G. (2003). The Arabidopsis GNOM ARF-GEF mediates endosomal recycling, auxin transport, and auxin-dependent plant growth. Cell *112*, 219-230.

Geldner, N., Denervaud-Tendon, V., Hyman, D.L., Mayer, U., Stierhof, Y.D., and Chory, J. (2009). Rapid, combinatorial analysis of membrane compartments in intact plants with a multicolor marker set. Plant J *59*, 169-178.

Geldner, N., Friml, J., Stierhof, Y.D., Jürgens, G., and Palme, K. (2001). Auxin transport inhibitors block PIN1 cycling and vesicle trafficking. Nature *413*, 425-428.

Geldner, N., Richter, S., Vieten, A., Marquardt, S., Torres-Ruiz, R.A., Mayer, U., and Jürgens, G. (2004). Partial loss-of-function alleles reveal a role for GNOM in auxin transport-related, post-embryonic development of Arabidopsis. Development *131*, 389-400.

Goldberg, J. (1998). Structural basis for activation of ARF GTPase: Mechanisms of guanine nucleotide exchange and GTP-myristoyl switching. Cell *95*, 237-248.

Grebe, M., Gadea, J., Steinmann, T., Kientz, M., Rahfeld, J.U., Salchert, K., Koncz, C., and Jürgens, G. (2000). A conserved domain of the arabidopsis GNOM protein mediates subunit interaction and cyclophilin 5 binding. The Plant cell *12*, 343-356.

Halaby, S.L., and Fromme, J.C. (2018). The HUS box is required for allosteric regulation of the Sec7 Arf-GEF. Journal of Biological Chemistry *293*, 6682-6691.

Hara-Nishimura, I., Shimada, T., Hatano, K., Takeuchi, Y., and Nishimura, M. (1998). Transport of storage proteins to protein storage vacuoles is mediated by large precursor-accumulating vesicles. The Plant cell *10*, 825-836.

Horiuchi, H., Lippe, R., McBride, H.M., Rubino, M., Woodman, P., Stenmark, H., Rybin, V., Wilm, M., Ashman, K., Mann, M*., et al.* (1997). A novel Rab5 GDP/GTP exchange factor complexed to Rabaptin-5 links nucleotide exchange to effector recruitment and function. Cell *90*, 1149-1159.

Huotari, J., and Helenius, A. (2011). Endosome maturation. EMBO J *30*, 3481-3500.

Ishizaki, R., Shin, H.W., Mitsuhashi, H., and Nakayama, K. (2008). Redundant roles of BIG2 and BIG1, guanine-nucleotide exchange factors for ADP-ribosylation factors in membrane traffic between the trans-Golgi network and endosomes. Mol Biol Cell *19*, 2650-2660.

Jackson, C.L., and Bouvet, S. (2014). Arfs at a glance. J Cell Sci *127*, 4103-4109.

Jürgens, G. (2004). Membrane trafficking in plants. Annu Rev Cell Dev Biol *20*, 481-504.

Jürgens, G. (2005). Cytokinesis in higher plants. Annu Rev Plant Biol *56*, 281-299.

Kahn, R.A., and Gilman, A.G. (1986). The protein cofactor necessary for ADP-ribosylation of Gs by cholera toxin is itself a GTP binding protein. The Journal of biological chemistry *261*, 7906-7911.

Kinchen, J.M., and Ravichandran, K.S. (2010). Identification of two evolutionarily conserved genes regulating processing of engulfed apoptotic cells. Nature *464*, 778-782.

Künzl, F., Früholz, S., Fässler, F., Li, B., and Pimpl, P. (2016). Receptor-mediated sorting of soluble vacuolar proteins ends at the trans-Golgi network/early endosome. Nat Plants *2*, 16017.

Kwon, C., Neu, C., Pajonk, S., Yun, H.S., Lipka, U., Humphry, M., Bau, S., Straus, M., Kwaaitaal, M., Rampelt, H.*, et al.* (2008). Co-option of a default secretory pathway for plant immune responses. Nature *451*, 835-840.

Lauber, M.H., Waizenegger, I., Steinmann, T., Schwarz, H., Mayer, U., Hwang, I., Lukowitz, W., and Jürgens, G. (1997a). The Arabidopsis KNOLLE protein is a cytokinesis-specific syntaxin. J Cell Biol *139*, 1485-1493.

Lauber, M.H., Waizenegger, I., Steinmann, T., Schwarz, H., Mayer, U., Hwang, I., Lukowitz, W., and Jürgens, G. (1997b). The Arabidopsis KNOLLE protein is a cytokinesis-specific syntaxin. Journal of Cell Biology *139*, 1485-1493.

Lee, M.H., Min, M.K., Lee, Y.J., Jin, J.B., Shin, D.H., Kim, D.H., Lee, K.H., and Hwang, I. (2002). ADP-ribosylation factor 1 of Arabidopsis plays a critical role in intracellular trafficking and maintenance of endoplasmic reticulum morphology in Arabidopsis. Plant Physiol *129*, 1507-1520.

Lippe, R., Miaczynska, M., Rybin, V., Runge, A., and Zerial, M. (2001). Functional synergy between Rab5 effector Rabaptin-5 and exchange factor Rabex-5 when physically associated in a complex. Mol Biol Cell *12*, 2219-2228.

Lowery, J., Szul, T., Seetharaman, J., Jian, X., Su, M., Forouhar, F., Xiao, R., Acton, T.B., Montelione, G.T., Lin, H.*, et al.* (2011). Novel C-terminal motif within Sec7 domain of guanine nucleotide exchange factors regulates ADP-ribosylation factor (ARF) binding and activation. The Journal of biological chemistry *286*, 36898-36906.

Lukowitz, W., Mayer, U., and Jürgens, G. (1996). Cytokinesis in the Arabidopsis embryo involves the syntaxin-related KNOLLE gene product. Cell *84*, 61-71.

Luo, Y., Scholl, S., Doering, A., Zhang, Y., Irani, N.G., Di Rubbo, S., Neumetzler, L., Krishnamoorthy, P., Van Houtte, I., Mylle, E.*, et al.* (2015). V-ATPase activity in the TGN/EE is required for exocytosis and recycling in Arabidopsis. Nat Plants *1*.

MacDonald, C., Buchkovich, N.J., Stringer, D.K., Emr, S.D., and Piper, R.C. (2012). Cargo ubiquitination is essential for multivesicular body intralumenal vesicle formation. EMBO reports *13*, 331-338.

Malhotra, V., and Mayor, S. (2006). Cell biology: the Golgi grows up. Nature *441*, 939-940.

Mallet, W.G., and Brodsky, F.M. (1996). A membrane-associated protein complex with selective binding to the clathrin coat adaptor AP1. Journal of Cell Science *109*, 3059-3068.

Martiniere, A., Bassil, E., Jublanc, E., Alcon, C., Reguera, M., Sentenac, H., Blumwald, E., and Paris, N. (2013). In Vivo Intracellular pH Measurements in Tobacco and Arabidopsis Reveal an Unexpected pH Gradient in the Endomembrane System. The Plant cell *25*, 4028-4043.

Marty, F. (1999). Plant vacuoles. The Plant cell *11*, 587-600.

Matheson, L.A., Suri, S.S., Hanton, S.L., Chatre, L., and Brandizzi, F. (2008). Correct targeting of plant ARF GTPases relies on distinct protein domains. Traffic *9*, 103-120.

Mattera, R., and Bonifacino, J.S. (2008). Ubiquitin binding and conjugation regulate the recruitment of Rabex-5 to early endosomes. EMBO J *27*, 2484-2494.

Mayer, U.B., G.; Jürgens, G. (1993). Apical-basal pattern formation in the Arabidopsis embryo: studies on the role of the gnom gene. Development *117*, 149-162.

Mayer, U.T.R., R.A.; Berleth, T.; Misera, S.; Jürgens, G. (1991). Mutations affecting body organization in the Arabidopsis embryo. Nature *353*, 402-407.

Mei, G., Di Venere, A., Rosato, N., and Finazzi-Agro, A. (2005). The importance of being dimeric. Febs J *272*, 16-27.

Mossessova, E., Corpina, R.A., and Goldberg, J. (2003). Crystal structure of ARF1*Sec7 complexed with Brefeldin A and its implications for the guanine nucleotide exchange mechanism. Mol Cell *12*, 1403-1411.

Mossessova, E., Gulbis, J.M., and Goldberg, J. (1998). Structure of the guanine nucleotide exchange factor Sec7 domain of human Arno and analysis of the interaction with ARF GTPase. Cell *92*, 415-423.

Müller, A., Guan, C., Gälweiler, L., Tänzler, P., Huijser, P., Marchant, A., Parry, G., Bennett, M., Wisman, E., and Palme, K. (1998). AtPIN2 defines a locus of Arabidopsis for root gravitropism control. EMBO J *17*, 6903-6911.

Müller, I., Wagner, W., Volker, A., Schellmann, S., Nacry, P., Kuttner, F., Schwarz-Sommer, Z., Mayer, U., and Jürgens, G. (2003). Syntaxin specificity of cytokinesis in Arabidopsis. Nat Cell Biol *5*, 531-534.

Munch, D., Teh, O.K., Malinovsky, F.G., Liu, Q., Vetukuri, R.R., El Kasmi, F., Brodersen, P., Hara-Nishimura, I., Dangl, J.L., Petersen, M.*, et al.* (2015). Retromer contributes to immunity-associated cell death in Arabidopsis. The Plant cell *27*, 463-479.

Myers, M.D., and Payne, G.S. (2013). Clathrin, adaptors and disease: insights from the yeast Saccharomyces cerevisiae. Front Biosci (Landmark Ed) *18*, 862-891.

Nielsen, E., Cheung, A.Y., and Ueda, T. (2008). The regulatory RAB and ARF GTPases for vesicular trafficking. Plant Physiol *147*, 1516-1526.

Niemes, S., Langhans, M., Viotti, C., Scheuring, D., San Wan Yan, M., Jiang, L., Hillmer, S., Robinson, D.G., and Pimpl, P. (2010). Retromer recycles vacuolar sorting receptors from the trans-Golgi network. Plant J *61*, 107-121.

Nilsson, T., and Warren, G. (1994). Retention and Retrieval in the Endoplasmic-Reticulum and the Golgi-Apparatus. Current Opinion in Cell Biology *6*, 517-521.

Nomura, K., Debroy, S., Lee, Y.H., Pumplin, N., Jones, J., and He, S.Y. (2006). A bacterial virulence protein suppresses host innate immunity to cause plant disease. Science *313*, 220-223.

Nomura, K., Mecey, C., Lee, Y.N., Imboden, L.A., Chang, J.H., and He, S.Y. (2011). Effector-triggered immunity blocks pathogen degradation of an immunity-associated vesicle traffic regulator in Arabidopsis. Proc Natl Acad Sci U S A *108*, 10774-10779.

Nordmann, M., Cabrera, M., Perz, A., Brocker, C., Ostrowicz, C., Engelbrecht-Vandre, S., and Ungermann, C. (2010). The Mon1-Ccz1 complex is the GEF of the late endosomal Rab7 homolog Ypt7. Curr Biol *20*, 1654-1659.

Park, M., Krause, C., Karnahl, M., Reichardt, I., El Kasmi, F., Mayer, U., Stierhof, Y.D., Hiller, U., Strompen, G., Bayer, M.*, et al.* (2018). Concerted Action of Evolutionarily Ancient and Novel SNARE Complexes in Flowering-Plant Cytokinesis. Dev Cell *44*, 500-+.

Park, M., Song, K., Reichardt, I., Kim, H., Mayer, U., Stierhof, Y.D., Hwang, I., and Jürgens, G. (2013). Arabidopsis mu-adaptin subunit AP1M of adaptor protein complex 1 mediates late secretory and vacuolar traffic and is required for growth. P Natl Acad Sci USA *110*, 10318-10323.

Paul, M.J., and Frigerio, L. (2007). Coated vesicles in plant cells. Seminars in Cell & Developmental Biology *18*, 471-478.

Pereira, C., Pereira, S., and Pissarra, J. (2014). Delivering of proteins to the plant vacuole--an update. Int J Mol Sci *15*, 7611-7623.

Peyroche, A., Antonny, B., Robineau, S., Acker, J., Cherfils, J., and Jackson, C.L. (1999). Brefeldin A acts to stabilize an abortive ARF-GDP-Sec7 domain protein complex: Involvement of specific residues of the Sec7 domain. Molecular Cell *3*, 275-285.

Pimpl, P., Hanton, S.L., Taylor, J.P., Pinto-daSilva, L.L., and Denecke, J. (2003). The GTPase ARF1p controls the sequence-specific vacuolar sorting route to the lytic vacuole. The Plant cell *15*, 1242-1256.

Poteryaev, D., Datta, S., Ackema, K., Zerial, M., and Spang, A. (2010). Identification of the switch in early-to-late endosome transition. Cell *141*, 497-508.

Ramaen, O., Joubert, A., Simister, P., Belgareh-Touze, N., Olivares-Sanchez, M.C., Zeeh, J.C., Chantalat, S., Golinelli-Cohen, M.P., Jackson, C.L., Biou, V.*, et al.* (2007). Interactions between conserved domains within homodimers in the BIG1, BIG2, and GBF1 Arf guanine nucleotide exchange factors. The Journal of biological chemistry *282*, 28834-28842.

Reichardt, I., Slane, D., El Kasmi, F., Knöll, C., Fuchs, R., Mayer, U., Lipka, V., and Jürgens, G. (2011). Mechanisms of Functional Specificity Among Plasma-Membrane Syntaxins in Arabidopsis. Traffic *12*, 1269-1280.

Reichardt, I., Stierhof, Y.D., Mayer, U., Richter, S., Schwarz, H., Schumacher, K., and Jürgens, G. (2007). Plant cytokinesis requires de novo secretory trafficking but not endocytosis. Curr Biol *17*, 2047-2053.

Renault, L., Guibert, B., and Cherfils, J. (2003). Structural snapshots of the mechanism and inhibition of a guanine nucleotide exchange factor. Nature *426*, 525-530.

Reyes, F.C., Buono, R., and Otegui, M.S. (2011). Plant endosomal trafficking pathways. Curr Opin Plant Biol *14*, 666-673.

Richardson, B.C., Halaby, S.L., Gustafson, M.A., and Fromme, J.C. (2016). The Sec7 N-terminal regulatory domains facilitate membrane-proximal activation of the Arf1 GTPase. Elife *5*.

Richter, S., Anders, N., Wolters, H., Beckmann, H., Thomann, A., Heinrich, R., Schrader, J., Singh, M.K., Geldner, N., Mayer, U.*, et al.* (2010). Role of the GNOM gene in Arabidopsis apical-basal patterning--From mutant phenotype to cellular mechanism of protein action. Eur J Cell Biol *89*, 138-144.

Richter, S., Geldner, N., Schrader, J., Wolters, H., Stierhof, Y.D., Rios, G., Koncz, C., Robinson, D.G., and Jürgens, G. (2007). Functional diversification of closely related ARF-GEFs in protein secretion and recycling. Nature *448*, 488-492.

Richter, S., Kientz, M., Brumm, S., Nielsen, M.E., Park, M., Gavidia, R., Krause, C., Voss, U., Beckmann, H., Mayer, U.*, et al.* (2014). Delivery of endocytosed proteins to the cell-division plane requires change of pathway from recycling to secretion. Elife *3*, e02131.

Richter, S., Müller, L.M., Stierhof, Y.D., Mayer, U., Takada, N., Kost, B., Vieten, A., Geldner, N., Koncz, C., and Jürgens, G. (2011). Polarized cell growth in Arabidopsis requires endosomal recycling mediated by GBF1-related ARF exchange factors. Nat Cell Biol *14*, 80-86.

Rink, J., Ghigo, E., Kalaidzidis, Y., and Zerial, M. (2005). Rab conversion as a mechanism of progression from early to late endosomes. Cell *122*, 735-749.

Robatzek, S., Chinchilla, D., and Boller, T. (2006). Ligand-induced endocytosis of the pattern recognition receptor FLS2 in Arabidopsis. Genes Dev *20*, 537-542.

Robinson, D.G. (2018). Retromer and VSR Recycling: A Red Herring? Plant Physiology *176*, 483-484.

Robinson, D.G., Jiang, L.W., and Schumacher, K. (2008). The endosomal system of plants: Charting new and familiar territories. Plant Physiology *147*, 1482-1492.

Robinson, D.G., and Neuhaus, J.M. (2016). Receptor-mediated sorting of soluble vacuolar proteins: myths, facts, and a new model. J Exp Bot *67*, 4435-4449.

Robinson, D.G., and Pimpl, P. (2014). Receptor-mediated transport of vacuolar proteins: a critical analysis and a new model. Protoplasma *251*, 247-264.

Robinson, M.S. (2004). Adaptable adaptors for coated vesicles. Trends Cell Biol *14*, 167-174.

Rodman, J.S., and Wandinger-Ness, A. (2000). Rab GTPases coordinate endocytosis - Commentary. Journal of Cell Science *113*, 183-192.

Rojas, R., van Vlijmen, T., Mardones, G.A., Prabhu, Y., Rojas, A.L., Mohammed, S., Heck, A.J., Raposo, G., van der Sluijs, P., and Bonifacino, J.S. (2008). Regulation of retromer recruitment to endosomes by sequential action of Rab5 and Rab7. J Cell Biol *183*, 513-526.

Russinova, E., Borst, J.W., Kwaaitaal, M., Cano-Delgado, A., Yin, Y., Chory, J., and de Vries, S.C. (2004). Heterodimerization and endocytosis of Arabidopsis brassinosteroid receptors BRI1 and AtSERK3 (BAK1). The Plant cell *16*, 3216-3229.

Rutherford, S., and Moore, I. (2002). The Arabidopsis Rab GTPase family: another enigma variation. Curr Opin Plant Biol *5*, 518-528.

Sata, M., Moss, J., and Vaughan, M. (1999). Structural basis for the inhibitory effect of brefeldin A on guanine nucleotide-exchange proteins for ADP-ribosylation factors. P Natl Acad Sci USA *96*, 2752-2757.

Satiat-Jeunemaitre, B., Cole, L., Bourett, T., Howard, R., and Hawes, C. (1996). Brefeldin A effects in plant and fungal cells: Something new about vesicle trafficking? J Microsc-Oxford *181*, 162-177.

Satiat-Jeunemaitre, B., and Hawes, C. (1992). Redistribution of a Golgi Glycoprotein in Plant-Cells Treated with Brefeldin-A. Journal of Cell Science *103*, 1153-1166.

Scheuring, D., Viotti, C., Kruger, F., Künzl, F., Sturm, S., Bubeck, J., Hillmer, S., Frigerio, L., Robinson, D.G., Pimpl, P.*, et al.* (2011). Multivesicular bodies mature from the trans-Golgi network/early endosome in Arabidopsis. The Plant cell *23*, 3463-3481.

Shen, J.B., Zeng, Y.L., Zhuang, X.H., Sun, L., Yao, X.Q., Pimpl, P., and Jiang, L.W. (2013). Organelle pH in the Arabidopsis Endomembrane System. Mol Plant *6*, 1419-1437.

Singh, M.K., and Jürgens, G. (2018). Specificity of plant membrane trafficking - ARFs, regulators and coat proteins. Semin Cell Dev Biol *80*, 85-93.

Singh, M.K., Krüger, F., Beckmann, H., Brumm, S., Vermeer, J.E.M., Munnik, T., Mayer, U., Stierhof, Y.D., Grefen, C., Schumacher, K.*, et al.* (2014). Protein Delivery to Vacuole Requires SAND Protein-Dependent Rab GTPase Conversion for MVB-Vacuole Fusion. Current Biology *24*, 1383-1389.

Singh, M.K., Richter, S., Beckmann, H., Kientz, M., Stierhof, Y.D., Anders, N., Fässler, F., Nielsen, M., Knoll, C., Thomann, A., Franz-Wachtel, M.*, et al.* (2018). A single class of ARF GTPase activated by several pathway-specific ARF-GEFs regulates essential membrane traffic in Arabidopsis. PLoS Genet *14*, e1007795.

Sohn, E.J., Kim, E.S., Zhao, M., Kim, S.J., Kim, H., Kim, Y.W., Lee, Y.J., Hillmer, S., Sohn, U., Jiang, L.*, et al.* (2003). Rha1, an Arabidopsis Rab5 homolog, plays a critical role in the vacuolar trafficking of soluble cargo proteins. The Plant cell *15*, 1057-1070.

Spang, A., Herrmann, J.M., Hamamoto, S., and Schekman, R. (2001). The ADP ribosylation factor-nucleotide exchange factors Gea1p and Gea2p have overlapping, but not redundant functions in retrograde transport from the Golgi to the endoplasmic reticulum. Mol Biol Cell *12*, 1035-1045.

Spang, A., Shiba, Y., and Randazzo, P.A. (2010). Arf GAPs: gatekeepers of vesicle generation. FEBS Lett *584*, 2646-2651.

Steinmann, T., Geldner, N., Grebe, M., Mangold, S., Jackson, C.L., Paris, S., Galweiler, L., Palme, K., and Jurgens, G. (1999). Coordinated polar localization of auxin efflux carrier PIN1 by GNOM ARF GEF. Science *286*, 316-318.

Stierhof, Y.D., and El Kasmi, F. (2010). Strategies to improve the antigenicity, ultrastructure preservation and visibility of trafficking compartments in Arabidopsis tissue. Eur J Cell Biol *89*, 285-297.

Stierhof, Y.D., Viotti, C., Scheuring, D., Sturm, S., and Robinson, D.G. (2013). Sorting nexins 1 and 2a locate mainly to the TGN. Protoplasma *250*, 235-240.

Takano, J., Tanaka, M., Toyoda, A., Miwa, K., Kasai, K., Fuji, K., Onouchi, H., Naito, S., and Fujiwara, T. (2010). Polar localization and degradation of Arabidopsis boron transporters through distinct trafficking pathways. Proc Natl Acad Sci U S A *107*, 5220-5225.

Takeuchi, M., Ueda, T., Yahara, N., and Nakano, A. (2002). Arf1 GTPase plays roles in the protein traffic between the endoplasmic reticulum and the Golgi apparatus in tobacco and Arabidopsis cultured cells. Plant J *31*, 499-515.

Tanaka, H., Kitakura, S., De Rycke, R., De Groodt, R., and Friml, J. (2009). Fluorescence imaging-based screen identifies ARF GEF component of early endosomal trafficking. Curr Biol *19*, 391-397.

Tanaka, H., Kitakura, S., Rakusova, H., Uemura, T., Feraru, M.I., De Rycke, R., Robert, S., Kakimoto, T., and Friml, J. (2013). Cell polarity and patterning by PIN trafficking through early endosomal compartments in Arabidopsis thaliana. PLoS Genet *9*, e1003540.

Tanaka, H., Nodzylski, T., Kitakura, S., Feraru, M.I., Sasabe, M., Ishikawa, T., Kleine-Vehn, J., Kakimoto, T., and Friml, J. (2014). BEX1/ARF1A1C is required for BFA-sensitive recycling of PIN auxin transporters and auxin-mediated development in Arabidopsis. Plant Cell Physiol *55*, 737-749.

Teh, O.K., and Moore, I. (2007). An ARF-GEF acting at the Golgi and in selective endocytosis in polarized plant cells. Nature *448*, 493-496.

Teh, O.K., Shimono, Y., Shirakawa, M., Fukao, Y., Tamura, K., Shimada, T., and Hara-Nishimura, I. (2013). The AP-1 mu Adaptin is Required for KNOLLE Localization at the Cell Plate to Mediate Cytokinesis in Arabidopsis. Plant Cell Physiol *54*, 838-847.

Trahey, M., and Hay, J.C. (2010). Transport vesicle uncoating: it's later than you think. F1000 Biol Rep *2*, 47.

Uemura, T., and Ueda, T. (2014). Plant vacuolar trafficking driven by RAB and SNARE proteins. Curr Opin Plant Biol *22*, 116-121.

Valencia, J.P., Goodman, K., and Otegui, M.S. (2016). Endocytosis and Endosomal Trafficking in Plants. Annu Rev Plant Biol *67*, 309-335.

van Ijzendoorn, S.C. (2006). Recycling endosomes. J Cell Sci *119*, 1679-1681.

Vermeer, J.E., van Leeuwen, W., Tobena-Santamaria, R., Laxalt, A.M., Jones, D.R., Divecha, N., Gadella, T.W., Jr., and Munnik, T. (2006). Visualization of PtdIns3P dynamics in living plant cells. Plant J *47*, 687-700.

Vernoud, V., Horton, A.C., Yang, Z., and Nielsen, E. (2003). Analysis of the small GTPase gene superfamily of Arabidopsis. Plant Physiol *131*, 1191-1208.

Viotti, C. (2014). ER and vacuoles: never been closer. Front Plant Sci *5*, 20.

Viotti, C., Bubeck, J., Stierhof, Y.D., Krebs, M., Langhans, M., van den Berg, W., van Dongen, W., Richter, S., Geldner, N., Takano, J.*, et al.* (2010). Endocytic and secretory traffic in Arabidopsis merge in the trans-Golgi network/early endosome, an independent and highly dynamic organelle. The Plant cell *22*, 1344-1357.

Vroemen, C.W., Langeveld, S., Mayer, U., Ripper, G., Jürgens, G., Van Kammen, A., and De Vries, S.C. (1996). Pattern Formation in the Arabidopsis Embryo Revealed by Position-Specific Lipid Transfer Protein Gene Expression. The Plant cell *8*, 783-791.

Vukasinovic, N., and Zarsky, V. (2016). Tethering Complexes in the Arabidopsis Endomembrane System. Front Cell Dev Biol *4*, 46.

Wang, J.G., Li, S., Zhao, X.Y., Zhou, L.Z., Huang, G.Q., Feng, C., and Zhang, Y. (2013). HAPLESS13, the Arabidopsis mu 1 Adaptin, Is Essential for Protein Sorting at the trans-Golgi Network/Early Endosome. Plant Physiology *162*, 1897-1910.

Xu, D., Tsai, C.J., and Nussinov, R. (1998). Mechanism and evolution of protein dimerization. Protein Sci *7*, 533-544.

Xu, J., and Scheres, B. (2005). Dissection of Arabidopsis ADP-RIBOSYLATION FACTOR 1 function in epidermal cell polarity. The Plant cell *17*, 525-536.

Zhang, C.H., Hicks, G.R., and Raikhel, N.V. (2014). Plant vacuole morphology and vacuolar trafficking. Front Plant Sci *5*.

Zhao, X., Claude, A., Chun, J., Shields, D.J., Presley, J.F., and Melancon, P. (2006). GBF1, a cis-Golgi and VTCs-localized ARF-GEF, is implicated in ER-to-Golgi protein traffic. J Cell Sci *119*, 3743-3753.

8. Appendices

8.1. Primers and oligonucleotides

Listed are primers and nucleotides used for cloning and genotyping in this work

Name	Sequence 5`to 3`	Remark
GN3A-rev-phos	[Phos]AGTAGCCCTGGCCGCATTGTTGCAGATGG AGTG	Site directed mutagenesis primers
GN3A-for	AATGCGGCCAGGGCTACTCCAGAACAAGGTGC	
GN3A-WT-rev	TCTGGAGTAGTCCTGATCTC	Genotyping of loop>J(3A)
GN3A-mut-rev	TGTTCTGGAGTAGCCCTGGC	
B4049-mut-for	TTAACAGGGATCCAAAGAATA	*b4049* genotyping
B4049-WT-for	TTAACAGGGATCCAAAGAATG	
emb30-Homo-AS	CTCACTTGTAAGGTCACGAACCAGTT	*emb30* genotyping, additional HinfI restriction digest
T391-S (emb30)	TTCAAGTTCTCAATGAGTTTGCT	
T391-AS (emb30)	CATTGTTGCAGATGGAGTGAA	
In AT1g13940 sense (*sgt*-sense)	GGGGGGAGGGTATAAGAG	*sgt* genotyping
DS5?-1a (*sgt* antisense)	ACGGTCGGGAAACTAGCTCTAC	
GN-overtag-S	GAAAGTGAAAGTAAGAGGC	*GNOM* genotyping
GN-overtag-AS	CGTAGAGAGGTGTTACATAAG	
FISH	CTGGGAATGGCGAAATCAAGGCAT	*gnl1* genotyping
GNL1-FOR	GATTGAGCCAAGAAGTTGGGGCGAG	
GNL1-overtag-S	CAAAAGCTCAAGACTCCAAA	*GNL1* genotyping
GNL1-overtag-AS	GGCGACGGGAGTTTTATTAC	
ARFA1C(ARF1)-Y35A-MUT-S	[Phos]TACTATCCTCgcaAGCTCAAACTTGGAGA GATC	Site directed mutagenesis primers
ARFA1C(ARF1)-Y35A-MUT-AS	TTCTTACCAGCAGCATCG	
ARFA1C-Y35A-test(BsrGI)-S	GGTTGGTCTCGATGCTGCTGGTAAGACGACTAT CCTg	Y35A genotyping; additional BsrGI restriction digest
ARFA1C-TN/YA-test-AS	TCAATTCATCCTCATTCAGC	
ARFA1C-WT-MUT-S	[Phos]GCTGGTAAGAcgACTATCCTcTACAAGC	Site directed mutagenesis primers
ARFA1C-WT-MUT-AS	AGCATCGAGACCAACCATC	
attB-AvrII-RFP-S	aaaaagcaggctCCTAGGATGGCCTCCTCCGAGGAC GTCA	Cloning of pEntry221-AvRII-RFP
RFP-attB-AS	agaaagctgggtcTTAGGCGCCGGTGGAGTGGCGGCCC	
AFVY-RFP-attB-S	aaaaagcaggctATGAAGACTAATCTTTTTCTCTTTC	Cloning of pEntry221-AFVY-RFP
RFP-attB-AS	agaaagctgggtcTTAGGCGCCGGTGGAGTGGCGGCCC	

PIN1-attB-S	aaaaagcaggctATGATTACGGCGGCGGACT	Cloning of pEntry221-PIN1-RFP
PIN1-attB-AS	agaaagctgggtcTCATAGACCCAAGAGAATGT	
Aleurain-attB-S	AAAAAGCAGGCTATGTCTGCGAAAACAATCCTATC	Cloning of pEntry221-Aleurain-GFP
GFP-attB-AS	agaaagctgggtcTTATTTGTATAGTTCATCCATGCC	
attB1-S	GGGGACAAGTTTGTACAAAAAAGCAGGCT	Adapter primers for 2. Gateway PCR
attB2-AS	GGGGACCACTTTGTACAAGAAAGCTGGGTC	
M13-S	GTTTTCCCAGTCACGAC	Sequencing of pEntry clones
M13-AS	CAGGAAACAGCTATGAC	
pMDC7-seq-S	GTGACTGGATATGTTGTA	Sequencing of pMDC7 clones
pMDC7-seq-AS	GATACGGACGAAAGCTGG	

8.2. DNA vector constructs

Listed are vector constructs generated for this work. All PCR products or pEntry clones used for cloning were sequenced beforehand.

	Construct name	**Resistance (E.coli/plant)**	**Cloning strategy**
1	pBlue-GNXbaI$^{Loop>J(3A)-}$myc	AMP	Site directed mutagenesis on pBlue-GNXbaI^{wt-}myc (Geldner et al., 2003)
2	pGII(Bar)-pGN::GN-loop>J(3A)-myc	KAN/PPT	XbaI fragment from construct (1) was inserted into pGreen Basta (pGII(Bar)) (www.pGREEN.AC.uk)
3	pDONR221-ARFA1C-YFP	KAN	A.M. Fischer performed site directed mutagenesis on pEntry-ARFA1C-TN-YFP (Singh and Richter et al., 2018)
4	pUBQ-pMDC7-ARFA1C-YFP	SPEC/HYG	A.M. Fischer performed Gateway LR reaction using construct (3) and modified pMDC7 vector (Singh and Richter et al., 2018)
5	pDONR221-ARFA1C-Y35A-YFP	KAN	A.M. Fischer performed site directed mutagenesis on construct (3)
6	pUBQ-pMDC7-ARFA1C-Y35A-YFP	SPEC/HYG	A.M. Fischer performed Gateway LR reaction using construct (5) and modified pMDC7 vector (Singh and Richter et al., 2018)
7	pEntry221-ARFA1C-Y35A-QL-YFP	KAN	Site directed mutagenesis on pEntry-ARFA1C-QL-YFP (Singh and Richter et al., 2018)
8	pUBQ-pMDC7-ARFA1C-Y35A-QL-YFP	SPEC/HYG	Gateway LR reaction using construct (7) and modified pMDC7 vector (Singh and Richter et al., 2018)
9	pEntry221-AvrII-RFP	KAN	RFP-CDS with N-terminal AvrII restriction site was amplified and via gateway BP-reaction introduced into pDONR221 (Invitrogen)
10	pEntry221-ARFA1C-Y35A-QL-RFP	KAN	AvrII/SspI fragment from construct (9) was inserted into construct (5) via AvrII/SspI restriction sites
11	pUBQ-pMDC7-ARFA1C-Y35A-QL-RFP	SPEC/HYG	Gateway LR reaction using construct (10) and modified pMDC7 vector (Singh and Richter et al., 2018)
12	pEntry221-ARFA1C-RFP	KAN	AvrII/SspI fragment from construct (9) was inserted into construct (3) via AvrII/SspI restriction sites

13	pUBQ-pMDC7-ARFA1C-RFP	SPEC/HYG	Gateway LR reaction using construct (12) and modified pMDC7 vector (Singh and Richter et al., 2018)
14	pEntry221-ARFA1C-QL-RFP	KAN	AvrII/SspI fragment from construct (9) was inserted into pEntry-ARFA1C-QL-YFP (Singh and Richter et al., 2018) via AvrII/SspI restriction sites
15	pUBQ-pMDC7-ARFA1C-RFP	SPEC/HYG	Gateway LR reaction using construct (14) and modified pMDC7 vector (Singh and Richter et al., 2018)
16	pFK059-ARFA1C(masGFP)	KAN	A.M. Fischer amplified ARFA1C CDS from construct (4) and inserted fragment in pFK059 (Singh and Richter et al., 2018) via NheI/BamHI restriction sites
17	pFK059-ARFA1C-TN(masGFP)	KAN	A.M. Fischer amplified ARFA1C-TN CDS from pEntry-ARFA1C-TN-YFP (Singh and Richter et al., 2018) and inserted fragment in pFK059 (Singh and Richter et al., 2018) via NheI/BamHI restriction sites
18	pFK059-ARFA1C-Y35A (masGFP)	KAN	A.M. Fischer amplified ARFA1C-Y35A CDS from construct (5) and inserted fragment in pFK059 (Singh and Richter et al., 2018) via NheI/BamHI restriction sites
19	pEG202-ΔDCB-GN3A(GN232-1451)	AMP	Site directed mutagenesis PCR on pEG202-ΔDCB(GN232-1451) (Anders et al., 2008)
20	pJG4-5-ΔDCB-GN3A(GN232-1451)	AMP	Site directed mutagenesis PCR on pJG4-5-ΔDCB(GN232-1451) (Anders et al., 2008)
21	pMH5-GNL1(1-1451)	AMP	GNL1-CDS from pGEM-GNL1 (Hauke Beckmann, unpublished material) was introduced in modified pJG4 vector (Grebe et al., 2000) via XagI/NcoI restrictions sites
22	pMH8-GNL1(1-1451)	AMP	GNL1-CDS from pGEM-GNL1 (Hauke Beckmann, unpublished material) was introduced in modified pEG202 vector (Grebe et al., 2000) via NotI/XhoI restricitons sites
23	pEntry221-AFVY-RFP	KAN	RFP CDS with N-terminal AFVY signal peptide was amplified from 35S::AFVY-RFP (Scheuring et al., 2011) and via gateway BP reaction introduced into pDONR221 (Invitrogen)

24	pMDC7-AFVY-RFP	SPEC/HYG	Gateway LR reaction using construct (23) and pMDC7 destination vector (Curtis and Grossniklaus, 2003)
25	pEntry221-PIN-RFP	KAN	PIN-RFP was amplified from pGem-PIN-RFP (Richter et al., 2014) and via gateway BP reaction introduced into pDONR221 (Invitrogen)
26	pMDC7-PIN-RFP	SPEC/HYG	Gateway LR reaction using construct (25) and pMDC7 destination vector (Curtis and Grossniklaus, 2003)
27	pEntry221-Aleurain-GFP	KAN	Aleurain-GFP was amplified from template (Sohn et al., 2003) and via gateway BP reaction introduced into pDONR221 (Invitrogen)
28	pMDC7-Aleurain-GFP	SPEC/HYG	Gateway LR reaction using construct (27) and pMDC7 destination vector (Curtis and Grossniklaus, 2003)

8.3. Plant lines

Listed are transgenic plant lines, T-DNA- insertion lines and mutants generated for this work

Name	Resistance	Remark
sgt	KAN	*gnom* deletion mutant in Landsberg (Ler) background
GNOM-loop>J(3A)-myc	PPT	Homozygous for pGN::GNOM-loop>J(3A) in Col-0 background
GNOM-loop>J(3A)-myc *sgt*	PPT/KAN	Homozygous for pGN::GNOM-loop>J(3A) in heterozygous *sgt* background
GNOM-loop>J(3A)-myc *b4049*	PPT	Homozygous for pGN::GNOM-loop>J(3A) in heterozygous *b4049* background
GNOM-loop>J(3A)-myc *emb30*	PPT	Homozygous for pGN::GNOM-loop>J(3A) in heterozygous *emb30* background
GNOM-loop>J(3A)-myc; GNOM-GFP *sgt*	PPT/KAN	Homozygous for both transgenes in homozygous *sgt* background
GNOM-loop>J(3A)-myc; ARF-YFP	PPT/HYG	Homozygous for pGN::GNOM-loop>J(3A) and RPS5A::ARFA1C-YFP (Singh and Richter et al. 2018) in Col-0 background
GNOM-loop>J(3A)-myc; ARF-TN-YFP	PPT/HYG	Homozygous for pGN::GNOM-loop>J(3A) and RPS5A::ARFA1C-TN-YFP (Singh and Richter et al. 2018) in Col-0 background
EST::ARF1-YFP	HYG	Homozygous for pUBQ-pMDC7::ARF1A1C-YFP in Col-0 background
EST::ARF1-TN-YFP	HYG	Homozygous for pUBQ-pMDC7::ARF1A1C-TN-YFP in Col-0 background (Singh and Richter et al., 2018)
EST::ARF1-QL-YFP	HYG	Homozygous for pUBQ-pMDC7::ARF1A1C-QL-YFP in Col-0 background (Singh and Richter et al., 2018)
EST::ARF1-Y35A-YFP	HYG	Homozygous for pUBQ-pMDC7::ARF1A1C-Y35A-YFP in Col-0 background
EST::ARF1-Y35A-QL-YFP	HYG	Homozygous for pUBQ-pMDC7::ARF1A1C-Y35A-QL-YFP in Col-0 background
EST::ARF1-YFP; EST::ARF1-RFP	HYG	Heterozygous F1 for both transgenes in Col-O background
EST::ARF1-QL-YFP; EST::ARF1-QL-RFP	HYG	Heterozygous F1 for both transgenes in Col-O background
EST::ARF1-QL-Y35A-YFP; EST::ARF1-QL-Y35A-RFP	HYG	Heterozygous F1 for both transgenes in Col-O background

ΔDCB(GNOM)-HA *sgt*	HYG/KAN	Homozygous for pGN::ΔDCB(GNOM)-HA (Anders et al., 2008) in homozygous *sgt* background (Col-0)
ΔDCB(GNOM)-MYC *sgt*	PPT/KAN	Homozygous for pGN::ΔDCB(GNOM)-MYC (Anders et al., 2008) in homozygous *sgt* background (Col-0 and Ler)
ΔDCB(GNOM)-HA *sgt gnl1*	HYG/KAN	Heterozygous F1
XLIM-ΔDCB(GNOM^{b4049})-MYC *sgt*	PPT/KAN	Homozygous for pGN::XLIM-ΔDCB(GNOM^{b4049})-MYC in heterozygous *sgt* background
ΔDCB(GNOM)-HA; GNL1-YFP *sgt*	HYG/KAN	Homozygous for pGN::ΔDCB(GNOM)-HA (Anders et al., 2008) and GNL1-YFP (Richter et al., 2007) in homozygous *sgt* background
ΔDCB(GNOM)-HA; GNL1-MYC *sgt*	HYG/PPT/ KAN	Homozygous for pGN::ΔDCB(GNOM)-HA (Anders et al., 2008) and GNL1-MYC (Richter et al., 2007) in homozygous *sgt* background
EST:: PIN-RFP	HYG	Homozygous for 35S-pMDC7::PIN1-RFP in Col-0 and homozygous *big3* background
EST:: AFVY-RFP	HYG	Homozygous for 35S-pMDC7::AFVY-RFP in Col-0 and homozygous *big3* background
EST::Aleurain-GFP	HYG	Homozygous for 35S-pMDC7::AFVY-GFP in Col-0 background

9. Darstellung des Eigenanteils an den Publikationen

9.1. Delivery of endocytosed proteins to the cell-division plane requires change of pathway from recycling to secretion. (eLife. 3, e02131)

Sandra Richter, Marika Kientz, **Sabine Brumm**, Mads E. Nielsen, Richard Gavidia, Cornelia Krause, Ute Voss, Hauke Beckmann, Ulrike Mayer, York-Dieter Stierhof and Gerd Jürgens

Ich klonierte die Est>>PIN1-RFP und Est>>AFVY-RFP Konstrukte und etablierte die entsprechenden transgenen Pflanzenlinien. Die ersten mikroskopische Analysen der Lokalisation der transgenen Fusionsproteine wurden von mir durchgeführt.

9.2. Protein delivery to vacuole requires SAND protein-dependent Rab GTPase conversion for MVB-vacuole fusion. (Curr Biol. 24 (12), 1383-1389)

Manoj K. Singh, Falco Krüger, Hauke Beckmann, **Sabine Brumm**, Joop E.M. Vermeer, Teun Munnik, Ulrike Mayer, York-Dieter Stierhof, Christopher Grefen, Karin Schumacher and Gerd Jürgens

Die Klonierung des EST>>Aleurain-GFP Konstrukts und Etablierung der transgenen Pflanzenlinie im Col-O Hintergrund wurden von mir durchgeführt. Außerdem analysierte ich die Lokalisation des transgenen Fusionsproteins im Col-O Hintergrund.

9.3. ARF1 dimerization through cooperative high-affinity binding by *Arabidopsis* ARF-GEF GNOM dimer (Manuscript)

Sabine Brumm, Mads Eggert Nielsen, Sandra Richter, Hauke Beckmann, Manoj K. Singh, Angela-Melanie Fischer, Matthias Herbst, Tobias Pazen, Venkatesan Sundaresan and Gerd Jürgens

Die experimentelle und wissenschaftliche Arbeit wurde zum größten Teil von Gerd Jürgens, Sandra Richter und mir geplant. Bis auf die Klonierung des GN::GNOM-Loop>J(3A)Konstrukts, Etablierung der transgenen Pflanzenlinie und den ersten Kreuzungen in die GNOM allele *sgt*, *b4049* und *emb30* durch Mads E. Nielsen, wurden alle phänotypischen Analysen, Yeast two-Hybdrid, Lokalisationsstudien (bis auf die ARF1-RFP Lokalisierung in ARF1-TN-YFP), Co-Immunoprezipitationsexperimente von mir durchgeführt. Die FRET-FLIM Ergebnisse enstanden in enger Zusammenarbeit von mir und Sandra Richter. Die Konstrukte für die Protoplasten-Sekretionsassays wurden von Angela Fischer kloniert und die Experimente von Hauke

Beckmann durchgeführt. Die Abbildungen dieser Publikation wurden größtenteils von mir zusammengestellt und das Manuskript entstand in enger Zusammenarbeit mit Gerd Jürgens.

9.4. Heterodimers of functionally divergent paralogues prevented by dimerization domain (Manuscript)

Sabine Brumm, Sandra Richter, Hauke Beckmann, Kerstin Huhn, Manoj Singh, Hanno Wolters, Shinobu Takada, Gerd Jürgens

Die Idee zu diesem Manuskript enstand auf Grund von mir durchgeführter und geplanter Rettungsexperimente der *sgt* Mutant mit ΔDCB-GNOM. Die anschließende wissenschaftliche und experimentelle Arbeit wurde zum größten Teil von Gerd Jürgens geplant. Ich kreuzte die ΔDCB-GNOM *sgt* Linien mit GNL1-YFP und der gnl1 Mutante und führte weitere Rettungs-, Lokalisations- und Co-Immunoprezipitationsexperimente durch. Die Figuren und das Manuskript entstanden in enger Zusammenarbeit aller Autor